EA4HP SH 2024

22ND MEETING OF THE EUROPEAN ASSOCIATION FOR HAEMATOPATHOLOGY

21–26 September 2024 | Dubrovnik, Croatia

ABSTRACT BOOK

www.ea4hp-sh2024.com

COMMITTEES

Local Organising Committee

Snjezana Dotlic, Croatia (Chair local organiser)
Margareta Radic Antolic, Croatia
Igor Aurer, Croatia
Slavko Gasparov, Croatia
Sandra Basic Kinda, Croatia
Velibor Puzovic, Croatia

Executive Committee

Leticia Quintanilla-Fend, Germany
Maurilio Ponzoni, Italy
Stefan Dirnhofer, Switzerland
Birgitta Sander, Sweden
John Goodlad, UK
Alexandra Traverse-Glehen, France
Snjezana Dotlic, Croatia
Livia Raso-Barnett, UK
Alexandar Tzankov, Switzerland
Jim Cook, USA
Lorenzo Leoncini, Italy
Thomas Tousseyn, Belgium
Patricia Groenen, The Netherlands
Socorro Maria Rodriguez-Pinilla, Spain
Alberto Zamo, Germany

Lymphoma Workshop Panel Members

Leticia Quintanilla-Fend, Germany
Stefan Dirnhofer, Switzerland
Ioannis Anagnostopoulos, Germany
James Cook, USA
Maurilio Ponzoni, Italy
Stefania Pittaluga, USA
Camille Laurent, France
Gorana Gasljevic, Slovenia
Michael van den Brand, The Netherlands
Birgitta Sander, Sweden
Olga Balague, Spain

Bone Marrow Workshop Panel Members

Alexandar Tzankov, Switzerland
Roos Leguit, The Netherlands
Olga Weinberg, USA
Alexandra Traverse-Glehen, France
Leonie Saft, Sweden
Anna Green, UK

LEGAL ORGANISER & PCO

MCI Deutschland GmbH
MCI | Germany – Berlin
Markgrafenstr. 56 | 10117 Berlin, Germany
T: +49 30 204590
F: +49 30 2045950
ea4hp-sh@wearemci.com

CONTENTS

Bone Marrow Abstracts Oral Presentations

EA4HP24-ABS-546	Responses to avapritinib in patients with advanced systemic mastocytosis (advsmSM histopathologic analyses from the explorer and pathfinder clinical studies
EA4HP24-ABS-505	Somatic mutations in FAS pathway increase hemophagocytic lymphohistiocytosis risk in T- and/or NK-cell lymphoma patients
EA4HP24-ABS-593	Acute myeloid leukemia with mixed phenotype is characterized by *RUNX1* mutations, stemness features and limited lineage plasticity
EA4HP24-ABS-509	Evidence that the NPM1 mutant can be expressed in the nucleus, lost during tumor differentiation and that mature macrophages belong to the leukemic clone
EA4HP24-ABS-523	Myeloid neoplasms with plasmacytoid dendritic cell proliferations: Morphologic, immunophenotypic, and genetic comparisons between major diagnostic entities
EA4HP24-ABS-487	*IKZF1* Deletion Status and Correlation with Cytogenetics and Measurable Residual Disease in Adult B Lineage Acute Lymphoblastic Leukemia.
EA4HP24-ABS-552	*MECOM* Copy Number Gain in Myeloid Neoplasms is Associated with Evi-1 Overexpression, *TP53* mutations, and Poor Survival

EA4HP24-ABS-546

RESPONSES TO AVAPRITINIB IN PATIENTS WITH ADVANCED SYSTEMIC MASTOCYTOSIS (AdvSM): HISTOPATHOLOGIC ANALYSES FROM THE EXPLORER AND PATHFINDER CLINICAL STUDIES

Tracy I. George[1], Anton Rets[1], Kristin H. Karner[1], Karen A. Moser[1], Jason Gotlib[2], Andreas Reiter[3], Deepti H. Radia[4], Michael Deininger[5], Hui-Min Lin[6], Guang Yang[6], Javier I. Muñoz-González[7], Saša Dimitrijević[7], Daniel DeAngelo[8]

[1] University of Utah School of Medicine, ARUP Laboratories, Department of Pathology, Salt Lake City, USA; [2] Stanford University School of Medicine, Stanford Cancer Institute, Stanford, USA; [3] University Hospital Mannheim, Heidelberg University, Department of Hematology and Oncology, Mannheim, Germany; [4] Guy's & St Thomas' NHS Foundation Trust, London, UK; [5] Versiti Blood Research Institute, Milwaukee, USA; [6] Blueprint Medicines Corporation, Cambridge, USA; [7] Blueprint Medicines Corporation, Zug, Switzerland; [8] Dana-Farber Cancer Institute, Department of Medical Oncology/Hematologic Malignancies, Boston, USA

Background

Systemic mastocytosis (SM) is a hematologic neoplasm driven by the *KIT* D816V mutation in ~95% of cases. In AdvSM, neoplastic mast cell (MC) proliferation and accumulation can cause life-threatening organ damage and debilitating symptoms. Avapritinib is a potent, selective KIT D816V inhibitor approved in the USA and Europe for adults with AdvSM based on phase 1 EXPLORER (NCT02561988) and phase 2 PATHFINDER (NCT03580655).

Principles/Methodology

Effects of avapritinib on bone marrow (BM) histopathology and peripheral blood (PB) in patients on these studies were evaluated. Patients aged ≥18 years with centrally confirmed AdvSM initiated <200 mg (n=11), 200 mg (n=125), or ≥300 mg (n=40) once-daily avapritinib. BM biopsies (BMBs), aspirates (BMAs), PB smears, and blood counts were done at screening and Week (Wk) 8, 24, 40, and 64. Standard Wright-Giemsa and H&E staining (BMAs) and IHC for CD25, CD30, and CD117 (BMBs) were done. MF score (European Consensus on BM fibrosis grading) and separate osteosclerosis grading were done.

Results

176 patients with AdvSM enrolled in EXPLORER (n=69) and PATHFINDER (n=107) were analyzed including aggressive SM (n=29), MC leukemia (MCL, n=28), and SM with an associated hematological neoplasm (SM-AHN, n=119). Median (range) age was 68 (31–88) years, 59% were male, and 95% had a *KIT* exon 17 mutation per central assay. In BMBs, 95% of patients had multifocal dense aggregates at screening and 36% at Wk 64; mean decreases from screening to Wk 64 in aberrant CD25+ and CD30+ MCs were 59.2% and 24.5%. CD117 expression in all MCs was unchanged. In BMAs, MC burden decreased from 11.8% to 2.2% at Wk 8 and maintained to Wk 64, with a decreased atypical MC proportion through Wk 40 (**Figure**). 8 of 9 patients (6 SM-AHN, 3 MCL) with PB MCs at screening and on-treatment samples had no detectable PB MCs by Wk 8. Cellularity in BMBs decreased through Wk 64 to normal levels. Patients with fibrosis and osteosclerosis Grades 2–3 decreased by 35% and 19% at Wk 40. PB white blood cells decreased from 11.5x10^9/L at screening to 5.9x10^9/L at Wk 40. Hemoglobin stayed relatively unchanged through Wk 40. Platelets were 173x10^9/L at screening and stayed above 160x10^9L at Wks 24 and 40.

Conclusion

Avapritinib showed rapid (Wk 8), marked, sustained (Wk 64) reductions in neoplastic BM MCs, return to normal MC phenotype and morphology, and decreased circulating MCs, accompanied by normalized BM cellularity and improved fibrosis. These data support efficacy of avapritinib on underlying pathology of AdvSM.

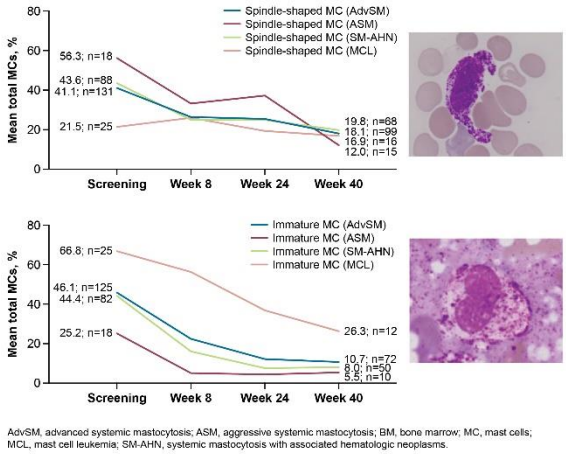

AdvSM, advanced systemic mastocytosis; ASM, aggressive systemic mastocytosis; BM, bone marrow; MC, mast cells; MCL, mast cell leukemia; SM-AHN, systemic mastocytosis with associated hematologic neoplasms.

Figure.
Avapritinib reduced atypical morphology in BM aspirate smears in all subtypes of AdvSM

EA4HP24-ABS-505

Somatic mutations in FAS pathway increase hemophagocytic lymphohistiocytosis risk in T- and/or NK-cell lymphoma patients

Dr. Ying Liu[1], Dr. Rohan Sardana[1], Dr. David Nemirovsky[2], Denise Frosina[1], Achim Jungbluth[1], Dr. William H. Johnson[3], Dr. Santosha Vardhana[3], Dr. Maria Arcila[1], Dr. Steven M. Horwitz[3], Dr. Andriy Derkach[2], Dr. Ahmet Dogan[1], Dr. Wenbin Xiao[1]

[1] MSKCC, Pathology and Laboratory Medicine, New York City, USA; [2] MSKCC, Epidemiology and Biostatistics, New York City, USA; [3] MSKCC, Lymphoma Service, Department of Medicine, New York City, USA

Background

While significant progress has been made in understanding the genetic basis of primary hemophagocytic lymphohistiocytosis (HLH), the pathogenesis of secondary HLH (sHLH) remains unclear. HLH in lymphoma patients (HLH-L) particularly T- and/or NK-cell (T/NK-cell) lymphomas, accounts for a substantial proportion of sHLH. As there is lack of studies on the association between somatic mutations and sHLH, we set out to investigate the frequency of somatic mutations in sHLH in T/NK-cell lymphomas patients.

Principles/Methodology

The study cohort included 433 patients with confirmed diagnosis of T/NK-cell lymphomas AND matched MSK-IMPACT analysis on neoplastic cells. 2004 criteria were used for HLH diagnosis. Associations between genetic and clinical characteristics and risk of HLH were assessed using cause-specific Cox proportional-hazard model. Overall survival (OS) was evaluated by Kaplan-Meier method.

Results

HLH was diagnosed in 29 patients (6.7%), including AITL (2/89, 2.2%), PTCL-NOS (13/78, 16.7%), ALCL (2/47, 4.3%), LGLL (3/46, 6.5%), ATLL (2/25, 8.0%), ENKTL (1/12, 8.3%), HSTCL (2/7, 28.6%), ANKCL (2/3, 66.7%), MF/SS (1/62, 1.6%) and other types of cutaneous T-cell lymphoma (1/19, 5.3%). Among all the patients undergoing HLH evaluation, an increased risk of HLH was seen in patients harbouring somatic mutations in *FAS* (HR: 4.24, 95%CI: 1.46-12.4, p=0.008), *CASP8* (HR: 13.4, 95%CI: 3.14-57. 5, p<0.001), *HLA-A* (HR: 5.71, 95%CI: 1.96-16.6, p=0.001), *CDNK1B* (HR: 19.2, 95%CI: 4.40-83.5, p<0.001), *STAT5B* (HR: 3.45, 95%CI: 1.19-10.0, p=0.022), *TNFAIP3* (HR: 5.20, 95%CI: 1.56-17.4, p=0.007), and *RARA* (HR: 6.72, 95%CI: 1.58-28.6, p=0.010). The presence of at least 1 mutation involving FAS pathway (*FAS*, *CASP8* and *TNFAIP3*) was independently associated with increased HLH risk (HR: 3.56, 95%CI: 1.44-8.77, p=0.006) when stratified by lymphoma subgroups (indolent T-cell lymphoma, AITL, PTCL-NOS, aggressive T-cell lymphoma). Importantly, the presence of at least 1 mutation in FAS pathway genes was significantly associated with inferior OS in multivariable model (HR: 1.91, 95%CI: 1.10-3.34, *p*=0.022); however, the association was lost when stratified by HLH, further validating the close interaction between FAS pathway mutations and HLH.

Conclusion

We identified a 3-time higher frequency of mutations in FAS pathway in patients with HLH-L. Patients harbouring these mutations had a significantly increased HLH-L risk. These mutations were independently associated with inferior outcome.

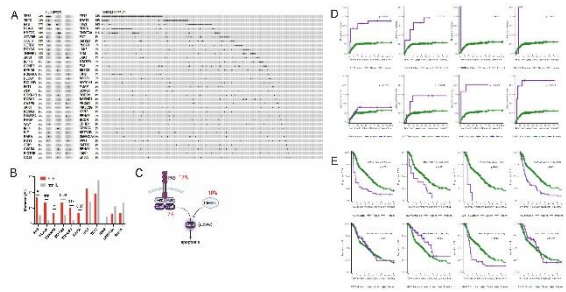

Figure 1
A. Mutational profiles between patients with and without HLH. B. Bar plots showing the comparison of mutations in various genes. C. Illustration of mutations in FAS pathway. D. Association between HLH risk and mutations of *FAS*, *CASP8*. *HLA-A*, *CDKN1B*, *TP53*, *TNFA1P3*, *RARA* and *STAT5B*. E. Association between OS and mutations of selected genes.

Characteristics		N	Event N	HR	95% CI	p-value
FAS mutation	Absent	405	24	Ref.	Ref.	
	Present	37	4	2.35	0.76, 7.22	0.14
HLA-A mutation	Absent	417	24	Ref.	Ref.	
	Present	15	4	4.35	0.88, 3.78	0.012
CDKN1B mutation	Absent	425	26	Ref.	Ref.	
	Present	3	2	59.2	7.27, 389	<0.001
CASP8 mutation	Absent	427	26	Ref.	Ref.	
	Present	5	2	7.78	1.57, 38.6	0.012
TP53 mutation	Absent	365	22	Ref.	Ref.	
	Present	64	6	1.26	0.47, 3.33	0.6
TET2 mutation	Absent	314	22	Ref.	Ref.	
	Present	116	6	1.16	0.40, 3.43	0.8
STAT3 mutation	Absent	369	24	Ref.	Ref.	
	Present	63	4	1.17	0.38, 3.59	0.8
STAT5B mutation	Absent	405	24	Ref.	Ref.	
	Present	27	4	2.57	0.82, 8.07	0.11
ROHA mutation	Absent	374	26	Ref.	Ref.	
	Present	58	2	1.58	0.24, 12.4	0.6
RARA mutation	Absent	425	28	Ref.	Ref.	
	Present	7	2	2.25	0.49, 12.3	0.3
TNFAIP3 mutation	Absent	418	25	Ref.	Ref.	
	Present	14	3	5.43	1.52, 12.4	0.009
KMT2D mutation	Absent	395	24	Ref.	Ref.	
	Present	37	4	1.36	0.45, 4.17	0.5
DNMT3A mutation	Absent	384	26	Ref.	Ref.	
	Present	48	2	0.67	0.15, 2.96	0.6
Any mutations involving FAS, CASP8, TNFAIP3	Absent	388	21	Ref.	Ref.	
	Present	43	7	3.56	1.44, 8.77	0.006
Number of mutations involving FAS, CASP8, TNFAIP3	0	388	21	Ref.	Ref.	
	1	40	5	2.91	1.06, 8.04	0.039
	2	3	2	9.17	1.70, 49.4	0.010

Table 1
Multivariable Cause-Specific Time-to-HLH for Each Mutation Stratified by Specific T-Cell Malignancy, Adjusting for Age and Sex.

Abbreviations: HR: Hazard Ratio, CI: Confidence Interval. One HLH patient was excluded from the analysis as the event of HLH (date of diagnosis) occurred before the patient entered the risk set (date of first MSK visit).

EA4HP24-ABS-593

Acute myeloid leukemia with mixed phenotype is characterized by *RUNX1* mutations, stemness features and limited lineage plasticity

Dr. Pallavi K. Galera, Deepika Dilip, Dr. Andriy Derkach, Dr. Alexander Chan, Dr. Yanming Zhang, Dr. Ying Liu, Dr. Ahmet Dogan, Dr. Mikhail Roshal, Dr. Jacob Glass, Dr. Wenbin Xiao

Memorial Sloan Kettering Cancer Center, New York, USA

Background

Mixed phenotype (MP) in acute leukemias poses unique classification & management dilemmas and can be seen in entities other than de novo mixed phenotype acute leukemia (MPAL). Although WHO recommends excluding AML with myelodysplasia related changes & therapy related AML (t-AML) with mixed phenotype (AML-MP) from MPAL, studies investigating their clinical & biologic features are lacking.

Principles/Methodology

55 AML-MP & 45 MPAL cases were retrieved from MSKCC database (Fig1A). A cohort of 100 patients diagnosed as AML-MRC (63) or t-AML (37) without MP was included for comparison.

Results

Table1 describes the 3 cohorts. Both AML cohorts (with & without MP) were significantly older, had fewer peripheral/bone marrow blasts but more severe leukopenia & thrombocytopenia than MPAL.

Genomic studies (Fig1B) revealed that *TP53* and MR genes (*SRSF2*, *U2AF1*, *BCOR*, *EZH2*, *STAG2* and *SETBP1*), while variably common in both AML cohorts, were notably absent from MPAL. Conversely, MPAL was enriched for *PHF6* mutations & various fusions. *RUNX1* mutations were significantly more frequent in AML-MP in comparison to both AML without MP and MPAL.

The AML-MP overall survival (OS) was inferior in comparison to MPAL but comparable to AML without MP (Fig1C). A subset of patients exhibited lineage shift from diagnosis either post-therapy/at relapse, with MPAL patients frequently shifting to lymphoid-only blasts. Expression of transcription factors critical for lymphoid differentiation were upregulated only in MPAL cases (Fig1D).

Gene-expression analysis performed on flow sorted myeloid- vs T-lineage leukemic blasts using RNA-seq revealed 2 distinct lineage-based groups: one primarily of MPAL samples and the other with both AML without MP and AML-MP (Fig1E). Pathway & enrichment analysis performed to determine the specific lineage features separating MPAL from AML-MP using custom hematopoietic lineage gene sets revealed a significant HSC gene set enrichment in the AML-MP compared to MPAL in both myeloid and T blasts (Fig1F).

Conclusion

AML-MP & AML without MP are clinically similar and have biological overlaps with frequent mutations in *TP53*, chromatin modifying genes and spliceosome-complex genes, which is different from MPAL. However, the frequency of *RUNX1* mutation is higher in AML-MP than AML without MP suggesting its role in lineage infidelity. RNA-seq data demonstrates a stemlike signature in AML-MP and AML without MP compared to MPAL. Together, these data support the designation of AML-MP as a diagnosis distinct from MPAL.

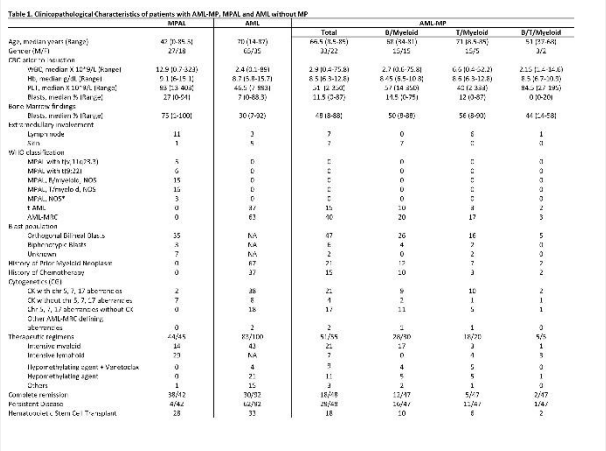

Table 1.
Clinicopathological Characteristics of patients with AML-MP, MPAL and AML without MP

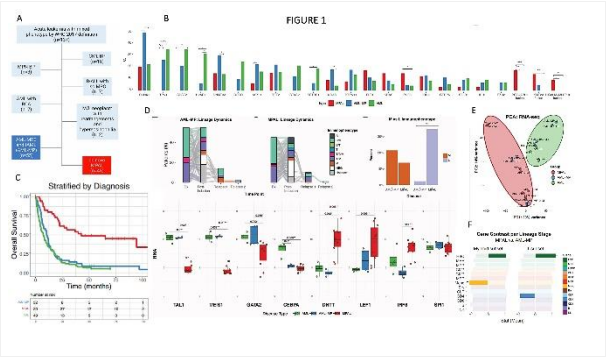

Figure 1

EA4HP24-ABS-509

Evidence that the NPM1 mutant can be expressed in the nucleus, lost during tumor differentiation and that mature macrophages belong to the leukemic clone

Prof. Brunangelo Falini[1], Prof. Teresa Marafioti[2], Prof. Fabio Facchetti[3], Dr. Daniele Sorcini[1], Dr. Vincenzo Perriello[1], Dr. Andrea Marra[1], Prof. Enrico Tiacci[1], Prof. Paolo Sportoletti[1], Prof. Bjørn T. Gjertsen[4], Dr. Vibeke Andresen[4]

[1] Institute of Hematology and CREO, University and Hospital of Perugia, Perugia, Italy; [2] University College, London, UK; [3] University of Brescia School of Medicine, Brescia, Italy; [4] Centre for Cancer Biomarkers (CCBIO), Department of Clinical Science, University of Bergen, Bergen, Norway

Background

NPM1-mutated AML is a distinct ICC and WHO entity showing unique clinical and molecular features (*Falini B, NEJM 352(3):254-266, 2005; Falini B, Blood, 136(15):1707-1721, 2020*), including cytoplasmic expression of NPM1 mutant, that is critical for leukemogenesis and is detectable by immunohistochemistry (*Falini B, Blood Cancer Discov 5(1):8-20, 2024*).

Principles/Methodology

Aims

We generated a specific monoclonal antibody (mAb) UBE recognizing the NPM1 mutant A to study its expression at subcellular level and during maturation of leukemic clone.

Methods

Single and double immunostainings with the UBE mAb were performed according to standard procedures.

Results

The NPM1 mutant was consistently and strongly expressed in the cytoplasmic of leukemic cells but 40-50% *NPM1*-mutated AML cases showed also nuclear positivity that was mainly found in the nucleoli (more strongly in leukemic proerythroblasts). The UBE antibody was tumor specific since did not react with any normal human tissue.

Immunostaining of 75 *NPM1*-mutated AML of M4-M5 FAB subtype (Figure 1 A,B) showed that the NPM1 mutant expression was lost in the terminal phases of tumor differentiation (Figure 1D, arrow), whilst that of residual NPM1 wild-type was retained (Figure 1 C, arrows), suggesting that the NPM1 mutant may be degraded during maturation more rapidly than the NPM1 wild-type protein. A percentage of leukemic cells showed nuclear-restricted positivity for the NPM1 mutant, suggesting that the mutant may have relocated from the cytoplasm to the nucleus by the residual NPM1 wild-type (higher NPM1 wild-type to mutant ratio).

Because the NPM1 mutant protein is not expressed in the most mature cells (including starry sky macrophages), this probe cannot be used to establish whether they belong or not to the leukemic clone. To track clonality, we analyzed AML cases co-mutated for *NPM1* and *IDH1* R132H. Immunostaining, with a specific anti-IDH1 R132H mAb revealed strong positivity of NPM1-mutant negative mature macrophages for the IDH1 mutant (Figure E, F, arrows and G), clearly demonstrating for the first time that these cells belong to the leukemic clone.

Conclusion

We demonstrate for the first time the presence of the NPM1 mutant in the nucleolus of leukemic cells and the loss or nuclear relocation of the NPM1 mutant during tumor maturation and provide evidence that mature macrophages may belong to the leukemic clone. These findings have implications for the pathogenesis of *NPM1*-mutated AML.

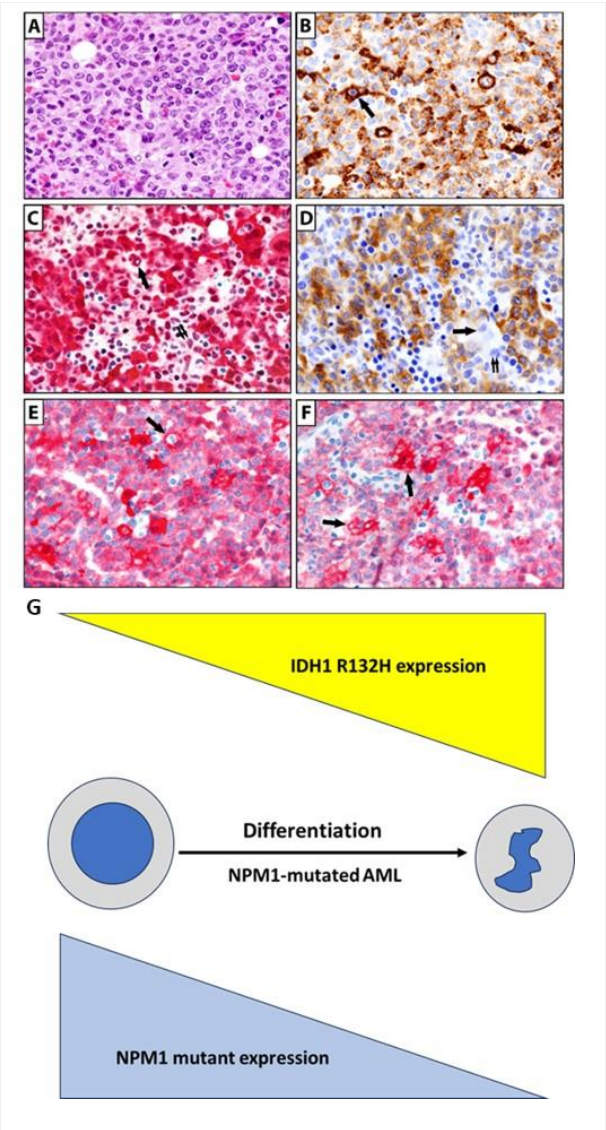

Figure 1

EA4HP24-ABS-523

Myeloid neoplasms with plasmacytoid dendritic cell proliferations: Morphologic, immunophenotypic, and genetic comparisons between major diagnostic entities

Dr. Alexander Chan, Dr. Liam Donnelly, Dr. Mikhail Roshal, Dr. Ying Liu, Dr. Wenbin Xiao

Memorial Sloan Kettering Cancer Center, Department of Pathology, NEW YORK, USA

Background

Plasmacytoid dendritic cells (pDCs) are stem-cell derived, interferon producing cells that can be increased in myeloid neoplasms (MNs). Blastic plasmacytoid dendritic cell neoplasm (BPDCN) is defined by proliferation of immature pDCs. PDC proliferations also occur in acute myeloid leukemia (AML) with increased pDCs (pDC-AML) and chronic myelomonocytic leukemia (CMML) can also show increased pDCs (pDC-CMML). Comparison between these 3 entities is lacking, and as they can overlap in clinicopathologic features, this benefits hematopathology evaluation.

Principles/Methodology

We searched our archives from 1/1/2015 through 4/30/2024 for cases of MNs with >2% pDCs in the bone marrow (BM) detected by flow cytometry (FC) using a 28-color immunophenotyping panel. We compared BM biopsy and aspirate morphology, immunohistochemical and FC immunophenotype, and genetic features between pDC-AML, pDC-CMML, and BPDCN.

Results

We identified 67 patients with pDC-AML, 19 with pDC-CMML, and 12 with BPDCN (summarized in Table 1). There were expected significant differences in extramedullary disease, presenting CBC, and BM pathologic features between the 3 entities. Morphologically, BPDCN was significantly more likely to show sheets of immature pDCs than other entities. All 3 had nodules of pDCs in a subset of cases (Figure 1A-J). There were differences in FC immunophenotype of pDCs between entities, with BPDCN expressing more CD56 and TCL1, and less CD34 and CD303. CD2 expression in pDCs was more common in pDC-CMML. There were no differences in TdT expression by FC. Mutational testing (Figure 1K) of BPDCN showed increased *TET2* mutations compared to pDC-AML and pDC-CMML. As previously described, pDC-AML had increased *RUNX1* mutations. PDC-CMML carried significantly more *RAS* and *CBL* mutations than pDC-AML but not when compared with BPDCN. Interestingly, 2 of 3 patients with a history of CMML who developed pDC-AML carried *RUNX1* mutations and no *RAS* mutations, while 2 of 3 patients with a history of CMML who developed BPDCN carried *RAS* mutations and no *RUNX1* mutations.

Conclusion

The 3 major disease entities which show pDC proliferations show differences in morphology, FC immunophenotypes, genetic features. However, the 3 entities also overlap substantially, especially pDC-CMML and BPDCNs, particularly when BPDCN shows only partial BM involvement. This emphasizes the need for accurate clinical information and pDC immunophenotyping when reviewing BM samples with increased pDCs.

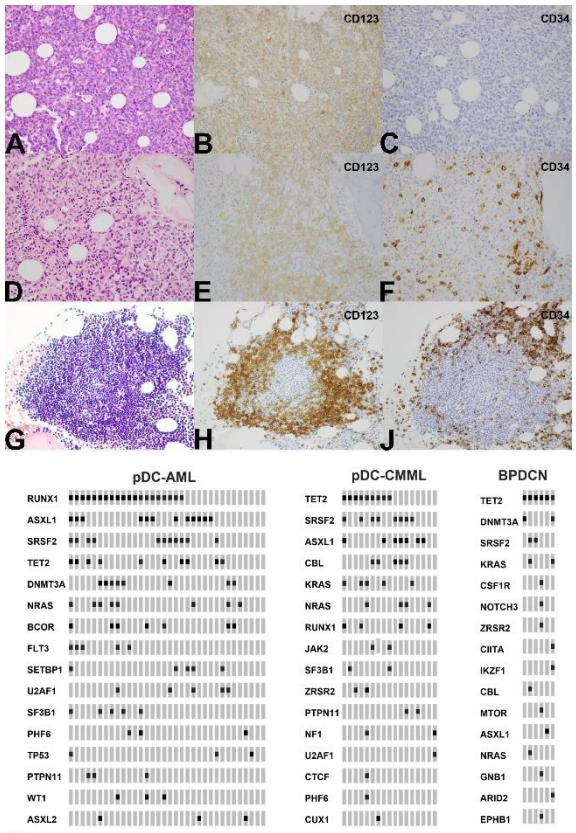

Figure 1
A-J. Comparison of morphology and immunohistochemical findings in BPDCN, PDC-CMML, and PDC-AMML. A. BPDCN morphology (H&E, 400x magnification). B. BPDCN shows sheets of CD123 positive pDCs (IHC, 400x magnification). C. BPDCN shows lack of CD34 expression. D-F. PDC-CMML demonstrating a nodule of PDCs that are CD123 positive and CD34 negative. G-J. PDC-AML demonstrating a nodule of PDCs that are CD123 positive and CD34 engative. K. Oncoprint diagram demonstrating mutational profiles of BPDCN, PDC-CMML, and PDC-AML.

	pDC-AML (n=67)	pDC-CMML (n = 19)	BPDCN (n = 12)
Age, median (IQR)	70 (60-77)	69 (60-74)	70 (65-81)
Sex (M/F)	48/17	11/8	10/1
History of MDS	32.3%	n/a	0%
History of CMML	4.6%	n/a	27%
Any prior cytotoxic therapy	36.9%	27.8%	9%
Any extramedullary disease	13.4%	36.8%	82%
Lymph node involvement	3%	21%[A]	18%
Skin involvement	10%	5.3%	82%[B,C]
CBC at diagnosis			
WBC, median x10⁹/L (IQR)	2.6 (1.2-6.6)[A]	6.6 (3.7-13.9)	5.6 (4.3-6.8)
ANC, median x10⁹/L (IQR)	0.5 (0.2-2.4)[A,B]	3.3 (0.8-6.7)	2.0 (1.7-3.9)
Percent monocytes, median % (IQR)	10% (0-22%)	23% (17-28%)[A,C]	8.3% (3.4-14.1%)
AMC, median x10⁹/L (IQR)	0.3 (0-1.2)	1.4 (1.0-2.4)[A,C]	0.5 (0.2-0.8)
Hb, median g/dL (IQR)	8.4 (7.6-10)[B]	9.3 (8.4-11.2)[C]	13.8 (11.6-14)
PLT, median x10⁹/L (IQR)	69 (35-114)[B]	80 (39-170)	121 (98-186)
Blasts, median % (IQR)	2% (0-12%)	0% (0-0%)	0% (0-0%)
BM morphology			
BM blasts/blast equivalents, median % (IQR)	37% (21-60%)[A]	6% (4-11%)	23% (12-65%)[C]
BM pDC distribution			
Nodules or aggregates	25%	57%	18%
Sheets	0%	0%	64%[B,C]
Genetic Features			
Complex Karyotype	3.1% (2/65)	5.6% (1/18)	25% (3/12)[B]
***RUNX1* mutation**	56.9% (37/65)[A,D]	22.2% (4/18)	0% (0/11)
Combined *RAS* mutations	20% (13/65)	50% (9/18)[A]	27% (3/11)
***KRAS* mutations**	3% (2/65)	28% (5/18)[A]	18% (2/11)
***NRAS* mutations**	17% (11/65)	28% (5/18)	9% (1/11)
***CBL* mutations**	3.2% (2/63)	33.3% (6/18)[A]	0% (0/11)
***TET2* mutations**	19% (12/63)	44.4% (8/18)	100% (8/8)[B,C]

[A]: P < 0.05 (comparison between AML and CMML)
[B]: P < 0.05 (comparison between AML and BPDCN)
[C]: P < 0.05 (comparison between CMML and BPDCN)

Table 1
Clinicopathologic comparison between PDC-AML, PDC-CMML, and BPDCN, including clinical features, CBC features, BM morphologic features, and genetic features.

EA4HP24-ABS-487

IKZF1 Deletion Status and Correlation with Cytogenetics and Measurable Residual Disease in Adult B Lineage Acute Lymphoblastic Leukemia.

Dr. Sreejesh Sreedharanunni[1], M.Sc./M.A. Prabhjot Kaur[1], M.Sc./M.A. Sudhanshi Raina[1], Anand Balakrishnan[1], M.Sc./M.A. Shailja Rathore[1], M.Sc./M.A. Anshu Anshu[1], Dr. Praveen Sharma[1], Pramod Kumar[1], M.Sc./M.A. Parveen Bose[1], Dr. Arihant Jain[2], Prof. Shano Naseem[1], Prof. Alka Khadwal[2], Prof. Man Updesh S. Sachdeva[1], Prof. Reena Das[1], Prof. Pankaj Malhotra[2]

[1] *Postgraduate Institute of Medical Education and Research, Hematology, Chandigarh, India;* [2] *Postgraduate Institute of Medical Education and Research, Clinical Hematology and Medical Oncology, Chandigarh, India*

Background

IKZF1-deletion/*IKZF1*^{del} is recognized as a poor-risk genetic abnormality in pediatric B-lineage acute lymphoblastic leukemia (B-ALL), but its influence in adult B-ALL is not entirely understood. We report the association of *IKZF1*^{del} and *IKZF1*^{plus} status with cytogenetic abnormalities/CG and measurable residual disease/MRD in a cohort of adult-B-ALL.

Principles/Methodology

Multiplex ligation-dependent probe amplification/MLPA (MRC, Holland) was used to study the copy number variations/CNV in 94 consecutive cases of adult-B-ALL. Final probe ratios of 0, 0.40-0.65, 1.3-1.65, and 1.75-2.15 were used to detect homozygous deletion, heterozygous deletion, heterozygous gain, triplication/homozygous gain, respectively, with a focus on *IKZF1* gene. *IKZF1*^{plus} was diagnosed if *IKZF1*^{del} was associated with the deletion of one or more of *CDKN2A/B, PAX,* or *PAR1*. The findings were correlated with CG abnormalities and flow-cytometry-based MRD status.

Results

The demographic profile of patients is summarized in Table 1. Overall, *IKZF1*^{del} was seen in 32/94(34%) cases, being more frequent in *BCR::ABL1*-positive (15/35;42%) than *BCR::ABL1*-negative 17/59 (28.8%) patients. However, *IKZF1*^{plus}was diagnosed in 15 (15.9%) patients more frequently in *BCR::ABL1*-negative cases [10 (16.9%) vs. 5 (14.2%)] especially in diploid/low-hyperdiploid cases (8/42;19%). None of the high-hyperdiploid (n=3)/near-triploid (n=3)/high-hypodiploid (n=1) B-ALLs showed *IKZF1*^{del}. The most frequent associated deletions in *IKZF1*^{del}were *CDKN2A*^{del}*+CDKN2B*^{del}(n=5). *IKZF1*^{del} were more frequent in MRD-positive cohort (33.3% vs. 26.6%) especially in *BCR::ABL1*-negative patients (36.3% vs. 10.5%). The frequency of *IKZF1*^{plus}was significantly higher in *BCR::ABL1*-negative MRD-positive patients compared to *BCR::ABL1*-negative MRD-negative patients (36.2% vs. 5.2%; p=0.047).

Conclusion

There are limited studies on the role of *IKZF1*^{del} and *IKZF1*^{plus} in adult B-ALLs compared to pediatric B-ALL. Our research reveals that among *BCR::ABL1*-negative adult B-ALLs, 28.8% exhibit *IKZF1*^{del}, while 15.9% display *IKZF1*^{plus} .In *BCR::ABL1* positive cases, the frequencies are 42% and 16.9%, respectively. Among *BCR::ABL1*-negative patients, *IKZF1*^{plus}was significantly more frequent in MRD-positive compared to the negative group. Our findings suggest testing for *IKZF1*^{del} in adult B-ALLs, especially *BCR::ABL1*-negative cases.

Table 1: Demographic profile and laboratory findings of patients (n=94)		
Age – median (Inter-quartile range) years	26 (17-40)	
Males: Females	55:39	
Hemoglobin (g/dL) median (Inter-quartile range)	7.3 (5.6-8.9)	
Total leukocyte count (x10^9/L) median (Inter-quartile range)	19.05 (6.57-99.05)	
Platelet counts (x10^9/L) median (Inter-quartile range)	28.5 (15.5-75.2)	
Cytogenetics (n;%)		
BCR::ABL1	35 (37.2%)	
Low hyperdiploidy	16 (17%)	
High Hyperdiploidy	3 (3.1%)	
Near triploidy	3 (3.2%)	
TCF3::PBX1	3 (3.2%)	
PR2Y8::CRLF2	2 (2.1%)	
MEF2D rearrangement	1 (1.1%)	
High hypodiploidy	1 (1.1%)	
IGH::CRLF2	1 (1.1%)	
Genetic abnormality in MLPA	n (%)	
IKZF1 deletions in the whole cohort	32 (34%)	
Type and distribution of *IKZF1* deletion		
Deletion Exons 4-7	8 (25%)	
Deletion Exons 2-7	7 (21.8%)	
Deletion Exons 1-8	4 (12.5%)	
Deletion Exons 5-7	2 (6.25%)	
Deletion Exons 4-5	2 (6.25%)	
Deletion Exons 1-2	2 (6.5%)	
Others	6 (18.7%)	
Monoallelic versus Biallelic	20 (62.5%) and 12 (37.5%)	
IKZF1 deletions in the subgroups	n (%)	
IKZF1 deletions in *BCR::ABL1* positive cohort	15/35 (42%)	P=0.17
IKZF1 deletions in *BCR::ABL1* negative cohort	17/59 (28%)	
$IKZF1^{plus}$ in the whole cohort	15 (15.9%)	
$IKZF1^{plus}$ in the subgroups		
$IKZF1^{del}$+$CDKN2A^{del}$+$CDKN2B^{del}$	5 (33.3%)	
$IKZF1^{del}$+$CDKN2A^{del}$+$CDKN2B^{del}$+$PAX5^{del}$	4 (26.6%)	
$IKZF1^{del}$+$CDKN2A^{del}$	2 (13.3%)	
$IKZF1^{del}$+PAR^{del}	2(13.3%)	
$IKZF1^{del}$+PAX^{del}	1 (6.6%)	
$IKZF1^{del}$+$CDKN2A^{del}$+$CDKN2B^{del}$+$PAX5^{del}$+PAR^{del}	1 (6.6%)	
$IKZF1^{plus}$ in BCR::ABL1 positive cohort	5 (14.2%)	*P*=1.0
$IKZF1^{plus}$ in BCR::ABL1 negative cohort	10 (16.9%)	
Measurable residual disease/MRD in the whole cohort (n=48)		
Positive	18 (37.5%)	
Negative	30 (62.5%)	
IKZF1 deletions in MRD positive cohort (n=18)	6 (33.3%)	*P*=0.75
IKZF1 deletions in MRD negative cohort (n=30)	8 (26.6%)	
IKZF1 deletions in BCR::ABL1 negative MRD positive cohort (n=11)	4 (36.3%)	*P*=0.15
IKZF1 deletions in BCR::ABL1 negative MRD negative cohort (n=19)	2 (10.5%)	
$IKZF1^{plus}$ in BCR::ABL1 negative MRD positive cohort (n=11)	4 (36.3%)	*P*=0.047
$IKZF1^{plus}$ in BCR::ABL1 negative MRD negative cohort (n=19)	1 (5.2%)	

Table 1
Demographic profile and laboratory findings of adult B-ALL patients in the cohort (n=94)

EA4HP24-ABS-552

MECOM Copy Number Gain in Myeloid Neoplasms is Associated with Evi-1 Overexpression, *TP53*mutations, and Poor Survival

Dr. Nandan Padmanabha[1], Dr. Katelynn M. Wilton[2], Dr. Phillip D. Michaels[2]

[1] *Beth Israel Deaconess Medical Center, Harvard Medical School, Pathology, Boston, USA;* [2] *Brigham and Women's Hospital, Harvard Medical School, Pathology, Boston, USA*

Background

MECOM/3q26.2 rearrangements occur in 1-2% of myelodysplastic neoplasms (MDS) and acute myeloid leukemias (AML) and confer an aggressive clinical course; however, *MECOM* copy number gains/amplifications are an exceedingly rare event in MDS and AML that are associated with a similarly poor outcome. To date, their genetic and clinicopathologic characteristics have not been characterized. Herein, we assessed the genetic profile, Evi-1 expression pattern, and clinicopathologic features to gain deeper understanding of this rare event in MDS and AML.

Principles/Methodology

Pathology records from 2015-2023 were reviewed for cases that had *MECOM* fluorescence in situ hybridization (FISH) performed for a diagnosis of MDS or AML. Additional medical and pathology records were reviewed for associated clinical outcomes, karyotype, next-generation sequencing results, and histopathologic findings. Evi-1 expression was assessed via immunohistochemistry on archival bone marrow biopsies. Statistical analysis was performed via Chi-square with Yates correction and Kaplan-Meier evaluation.

Results

Fifty-two cases were identified with an altered *MECOM* FISH pattern; comprising of 11 with a *MECOM* copy number gain/amplification and 41 with a *MECOM* rearrangement. Kaplan-Meier analysis revealed no difference in overall survival between the groups (p=0.51). *MECOM* rearranged cases less frequently had a complex karyotype compared to *MECOM* copy number gain cases (p=0.06). Cases with a *MECOM* copy number gain revealed enrichment for *TP53* mutations ($p < 0.0001$), while cases with a *MECOM* rearrangement were enriched for *DNMT3A, TET2,* and *ASXL1* mutations (p=0.05, fig. 1). Sixteen archived trephine bone marrow biopsies were available for immunohistochemical analysis, consisting of 10 with *MECOM* rearrangements and 6 with *MECOM* copy number gains. Evi-1 overexpression was uniformly identified across all cases with equal intensity (fig. 2).

Conclusion

Akin to *MECOM* rearrangements, copy number gains/amplifications of *MECOM* confer a similarly poor overall survival in MDS and AML. Although there is a shared phenotype of Evi-1 overexpression suggesting that *MECOM* copy number gain may be an alternative mechanism leading to its overexpression, there were molecular and cytogenetic differences between the two groups, particularly *TP53* mutational status and complex karyotype. As *MECOM* copy number gain/amplification is an exceedingly rare event, this is the first study to date to characterize the genotypic and phenotypic features of this phenomenon.

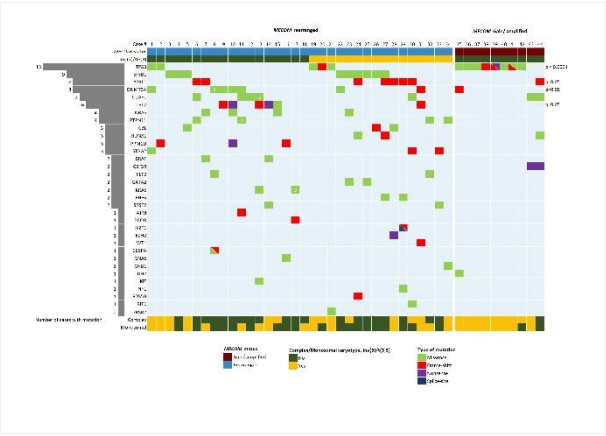

Figure 1.
Mutational and cytogenetic heatmap of *MECOM* rearranged and *MECOM* copy number gain/amplified cases.

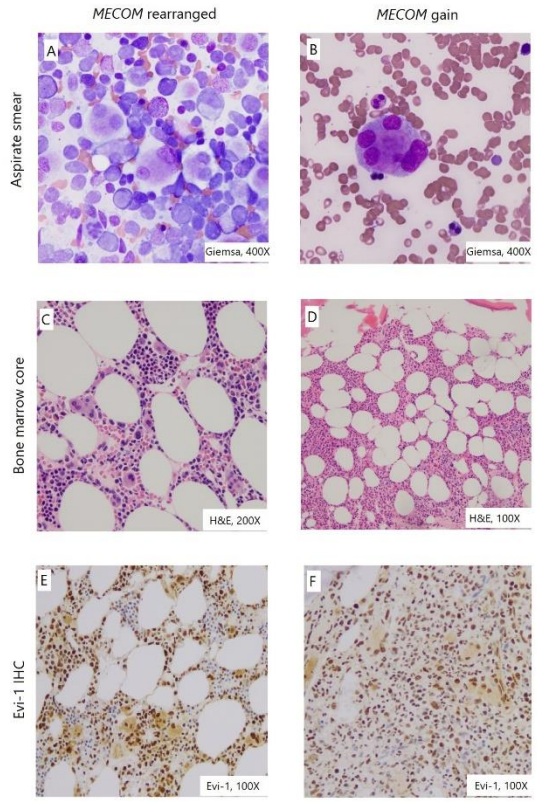

Figure 2.
A-B. Megakaryocytic dysplasia in *MECOM* rearranged and *MECOM* copy number gained cases of AML, respectively (Giemsa, 400x).

C-D. Cellular bone marrows revealing altered topography and dyspoiesis (H&E, 200x and 100x).
E-F. Evi-1 overexpression present in a *MECOM* rearranged case and *MECOM* copy number gained case of AML, respectively (200x).

Bone Marrow Abstracts Poster

EA4HP24-ABS-502	Gene variants linked to familial hemophagocytic lymphohistiocytosis(HLH) present in lymphoma-associated adult HLH
EA4HP24-ABS-521	Pseudoglandular histiocytic proliferation with myelofibrosis and bone marrow necrosis: a rare mimicker of two neoplasms in a benign disease
EA4HP24-ABS-534	Hemophagocytic Lymphohistiocytosis with neuroinflammatory disease, a rare presentation at adult onset.
EA4HP24-ABS-535	Evaluation of the bone marrow microenvironment in hemophagocytic lymphohistiocytosis
EA4HP24-ABS-547	Significantly Increased Expression of CD95 (Fas) by Immunohistochemistry in Idiopathic Aplastic Anemia Bone Marrow Core Biopsies
EA4HP24-ABS-599	Megakaryocytic changes and reticulin fibrosis, mimicking myeloproliferative neoplasm, in bone marrow biopsies of patients with immune thrombocytopenia, treated with thrombopoietin receptor agonists.
EA4HP24-ABS-622	Secondary Hemophagocytosis: Challenges in Identifying Underlying Disease
EA4HP24-ABS-484	Short Term Myeloid Leukemic Transformation in Triple Negative ET: Case report
EA4HP24-ABS-510	Immunohistochemical patterns, molecular features and outcome of extramedullary disease in *NPM1*-mutated AML
EA4HP24-ABS-514	Starry sky pattern predicts RAS pathway activation in *NPM1*-mutated AML
EA4HP24-ABS-556	Chronic myeloid leukemia (CML) evolving from a JAK2 V617-mutated myeloproliferative neoplasm.
EA4HP24-ABS-587	Deciphering the Prognostic Significance and Molecular Role of SLC40A1 in Acute Myeloid Leukemia
EA4HP24-ABS-600	VEXAS Syndrome: Contemporary Diagnostic Evaluation and Management
EA4HP24-ABS-613	Lymphadenopathy as presenting feature of a Myeloid/lymphoid neoplasm with PDGFRA rearrangement.
EA4HP24-ABS-629	Philadelphia chromosome-positive acute leukemia with cells harboring *BCR::ABL* discordantly higher than blast count may represent de novo blast phase of chronic myeloid leukemia with silenced chronic phase
EA4HP24-ABS-665	Acute erythroid leukemia post chemo-radiotherapy and autologous stem cell transplantation due to multiple myeloma
EA4HP24-ABS-669	Determination of IgG4 myeloma in IgG myeloma cases and analysis of morphological, immunohistochemical, clinical and prognostic features
EA4HP24-ABS-670	The molecular landscape of acute myeloid leukemia with *KMT2A* / *MECOM* / *NUP98* rearrangement diagnosed by RNA sequencing – a single center experience.
EA4HP24-ABS-486	Tackling the problem of a small divergent aberrant clone in predominant AML or ALL cases?
EA4HP24-ABS-516	B-cell antigen expression in acute leukemia with *MECOM* gene rearrangement

EA4HP24-ABS-517	Acute Undifferentiated Leukemia, am I a real entity? What's the best treatment approach?
EA4HP24-ABS-526	Shades of ERG: Strong, vascular-like ERG expression may help differentiate Histiocytic Sarcoma from Myeloid Sarcoma with Monocytic/Monoblastic differentiation.
EA4HP24-ABS-533	SLC38A1 A potential prognostic factor in Acute Lymphoblastic Leukemia
EA4HP24-ABS-548	An AI-Driven Software Tool for Diagnosing Myeloid and Lymphoid Neoplasms
EA4HP24-ABS-558	Mixed phenotype acute leukemia with higher levels of eosinophils: a case report
EA4HP24-ABS-560	CD142 is Overexpressed in Acute Promyelocytic Leukemia: A Study of 80 Cases by Immunohistochemistry
EA4HP24-ABS-572	Acute Lymphoblastic Leukemia with T- and B- Lineage Defining Markers
EA4HP24-ABS-597	BCR::ABL-1 positive Early T- cell precursor lymphoblastic leukemia/lymphoma (ETP-ALL): case report and awareness of a rare acute leukemia with unique genetic findings.
EA4HP24-ABS-631	ERG/CD117 Double-Staining May Help Avoid Overcounting Myeloblasts in Specific Scenarios
EA4HP24-ABS-668	The use of deep learning neural networks in analysis and differentiation of cells in bone marrow aspirate from patients with hematological diseases

EA4HP24-ABS-502

Gene variants linked to familial hemophagocytic lymphohistiocytosis(HLH) present in lymphoma-associated adult HLH

Dr. Chih-Yi Hsu, Dr. Ching-Fen Yang

Taipei Veterans General Hospital, Department of Pathology and Laboratory Medicine, Taipei, Taiwan

Background

Secondary hemophagocytic lymphohistiocytosis (HLH) manifests clinically similarly to primary HLH but is absence of a family history or associated genetic mutations. It arises from triggering factors such as infections, malignancies, and autoimmune disorders, resulting in hyperinflammatory states. Secondary HLH is an uncommon and life-threatening condition. Unlike primary HLH, the precise pathological pathways underlying secondary HLH remain incompletely elucidated, and limited research on its genetic features.

Principles/Methodology

The bone marrow cell pellets after conventional cytogenetic studies were collected from 18 adult patients when presented HLH. Next-generation sequencing (NGS) whole exome sequencing had been conducted. Agilent SureSelect XT Reagent kit protocol was followed to generate Illumina Hiseq paired-end sequencing libraries (catalog #G9611A). These libraries were constructed using the SureSelect XT Clinical Research Exome Version 2 probe set, covering 67.3 Mb of the genome. All samples underwent sequencing on an Illumina Sequencer using the 150PE protocol. For variant analysis, qualified read data underwent genomic alignment against the Ensembl database using the Burrows-Wheeler Aligner to extract basic sequence information. Variant calling and annotations were conducted employing the Genome Analysis Toolkit and Variant Effect Predictor. Variants with a Global Minor Allele Frequency of < 1% were classified as rare variants.

Results

None had a familial history of HLH.

The male/female was 8/10, and the median age was 59 years (range, 22-88 years).

17/ 18 patients who died from HLH were associated with lymphoma, Including 12 cases of large B-cell lymphoma (8 primary bone marrow large B-cell lymphoma, 3 diffuse large B-cell lymphoma, not otherwise specified, with marrow involvement, and 1 EBV-positive diffuse large B-cell lymphoma) and 5 cases of T-cell lymphoma (2 primary bone marrow ALK-negative anaplastic large cell lymphoma, 1 EBV-positive nodal peripheral T-cell lymphoma, 1 hepatosplenic T-cell lymphoma, and 1 nodal T-follicular helper cell lymphoma). The only one who survived was suspected to be associated with subcutaenous panniculitis T-cell lymphoma but without pathology proof.

The mutation variants in genes associated with primary HLH can be detected in 44% cases. The most common one is STXBP2(8/18), and followed by AP3B1(6/18).

Conclusion

Primary HLH-related gene variants may be one of the key components to contribute the lymphoma associated HLH.

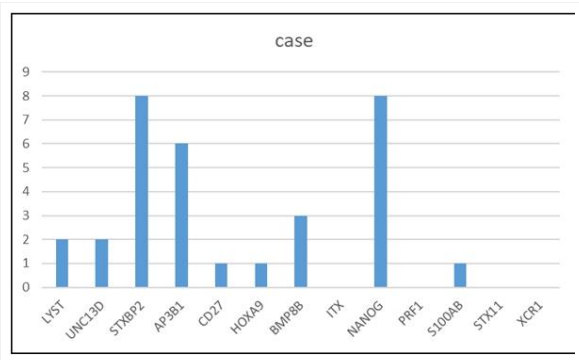

Distribution of primary HLH related gene variants

EA4HP24-ABS-521

Pseudoglandular histiocytic proliferation with myelofibrosis and bone marrow necrosis: a rare mimicker of two neoplasms in a benign disease

Dr. Vidya Nagrale[2], Dr. Jerry Wong[2], Dr. Jayalakshmi Balakrishna[2], **Dr. Mihai Merzianu**[2]

[1] Roswell Park, Pathology, Buffalo, USA; [2] Roswell Park Comprehensive Cancer Center, Department of Pathology, Buffalo, USA

Background

Bone marrow necrosis (BMN) is a rare antemortem diagnosis and may be fatal, occurring in hemoglobinopathies such as sickle cell disease (SCD) and in various primary and metastatic hematolymphoid or solid tumors, due to ischemia and malignant cell necrosis. We report an unusual case of BMN with extensive multinucleated giant cells (MGC) with pseudoglandular appearance and associated myelofibrosis, mimicking primary myelofibrosis and metastatic adenocarcinoma (ACA). We surveyed a patient cohort with BMN for comparison.

Principles/Methodology

Clinicopathological findings of the index case and 20 samples with BMN were included. The type and extent of necrosis, viable tumor cells, residual hematopoiesis, osteonecrosis, fibrosis, and histiocytic component were recorded.

Results

A 51-year-old man with SC/Beta thalassemia with recent history of SC crisis underwent a BM biopsy for progressive pancytopenia. A core biopsy revealed extensive BMN (~50%) with numerous ghost cells and no residual hematopoiesis. The increased MGCs had pseudoglandular appearance (Fig. 1), were positive for CD68 and CD163, negative for cytokeratin, and surrounded by reticulin and collagen fibers (Fig.2). No polarizable material or organisms were detected. All 20 samples with neoplastic disease had variable necrosis extent (mean, 82%; range, 20%-100%), including 16 acute leukemias (9 myeloid, 7 lymphoblastic), 1 myelodysplastic syndrome, 2 metastatic ACA and 1 lymphoma; most (17 of 20) received prior chemotherapy. Cytopenia was seen in 19 of 20, BMN was present at the initial diagnosis in 9 and found in serial samples in 10 patients. BMN was associated with ghost cells, an amorphous appearance, or both. Osteonecrosis was seen in 17 of 20 and fibrosis in 7 of 20 cases, none with circumferential

pattern. A histiocytic component was seen in 12 cases, but MGCs were present only in 2, none with pseudoglandular morphology.

Conclusion

We describe an unusual MGC reaction, heretofore not reported, associated with BMN which posed a diagnostic challenge. No similar findings were seen in the samples with malignant BMN. This peculiar pattern of MGC reaction is likely due to recent or remote ischemia, vaguely resembling fat necrosis seen in other organs. While histiocytes were common in neoplastic BMN, no pseudoglandular pattern was seen even when BMN was persistent, suggesting this may be limited to non-neoplastic diseases with high risk for multiple ischemic events, such as SCD.

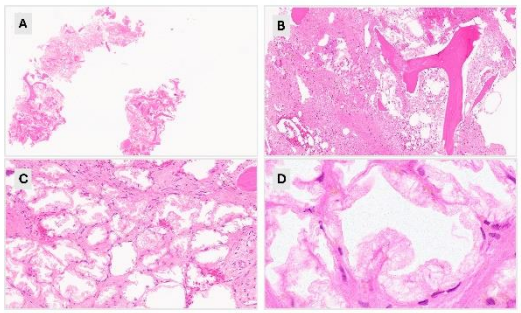

Bone marrow necrosis, fibrosis and pseudoglandular giant cells

Figure 1. A. Core biopsy showed marrow space necrosis (lower fragment) and decreased hematopoiesis (H&E, 1x). B. Extensive bone marrow necrosis, hemorrhage and osteonecrosis lacking hematopoietic elements (H&E, 10x). C.-D. Glandlike structures with foamy cytoplasm, papillary infoldings, central space resembling a lumen and scant nuclei, suggesting necrotic adenocarcinoma. These findings can be seen in fat necrosis at other sites (H&E, 10x and 60x)

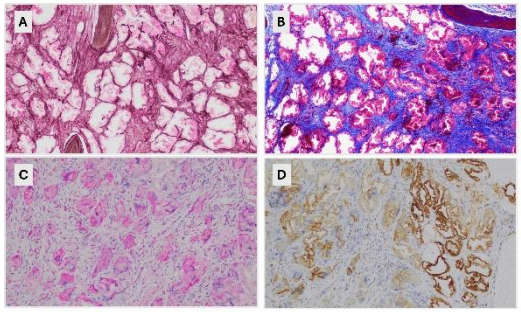

Multinucleated giant cells immunophenotype and surrounding fibrosis

Figure 2. Extensive reticulin (A) and collagen fibers (B) encircled the glandlike structures (reticulin and trichrome stains, both 10x). The multinucleated giant cells identity was confirmed by CD68 and lysozyme (10x). Only rare cells showed the typical multinucleation.

EA4HP24-ABS-534

Hemophagocytic Lymphohistiocytosis with neuroinflammatory disease, a rare presentation at adult onset.

Dr. Ana C. de Brito Lyra, Dr. Jackson A. Barbosa, Dr. Denise D.C. Pasqualin, Dr. Aline Ueda

Hospital Israelita Albert Einstein, Anatomia patológica, São Paulo, Brazil

Background

Hemophagocytic lymphohistiocytosis is a rare disease caused by an inappropriate immune activation syndrome manifesting as hematological disorder encompassed by an array of pathological findings and various physical and laboratory abnormalities. Primary HLH is autosomal recessive/ familial, usually diagnosed within the first 2 years of life, although adult onset primary HLH has also been reported rarely. Central nervous system presentation with neuroinflammatory manifestations is not so common.

Here we describe a case of a 56-year man, who had fever, asthenia, ataxia, fecal retention, nocturia, gait disturbance and thrombocytopenia after an acute Epstein-Barr infection associated with a hypogammaglobulinemia in blood tests. Brain MRI showed a diagnosis of encephalitis. The results of several exams were of bone marrow presenting some rare figures of hemophagocytosis with multiple reactional lymphoid aggregates and a recessive gene STXBP2 mutation which is linked to the development of familial HLH type 5. After corticosteroid and Immunoglobulin therapy the patient is evolving well, waiting for a bone marrow transplant.

Principles/Methodology

The diagnosis was performed only after clinical, pathological and molecular correlations. Neuroinflammatory manifestations are unusual and brain MRI may show nonspecific white-matter signal abnormalities, that could be misdiagnosed with other autoimmune or infectious diseases.

Results

STXBP2 mutation encodes syntaxin-binding protein (Munc18-2). This protein plays a major role in the regulation of intracellular granule trafficking in epithelial cells, neutrophils, and mast cells. Patients demonstrate variable hematological and gastrointestinal symptoms. Chronic diarrhea, hypogammaglobulinemia and other atypical features, including sensorineural hearing loss and abnormal bleeding. These defects also can affect the platelets function and secretion, with persistent thrombocytopenia. The clinical symptoms resulting from hypogammaglobulinemia can also be confused with a condition of a primary immunodeficiency as common variable immunodeficiency.

Conclusion

HLH common findings in bone marrow biopsy evaluation usually demonstrate hemophagocytic activity. Here we report a case that the bone marrow biopsy showed mild findings of hemophagocytosis and exuberant lymphoid aggregates that could be associated with the hypogammaglobinemia presentation. Central nervous system inflammation is part of this systemic disease and has an important impact on long-term prognosis.

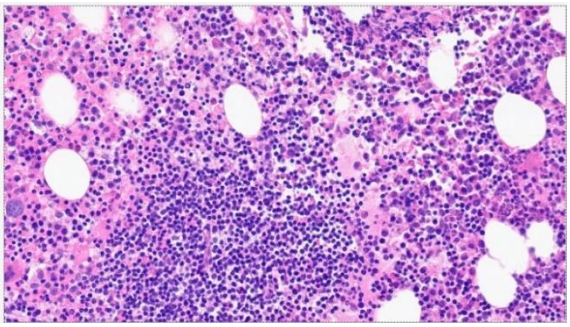

Lymphoid aggregates

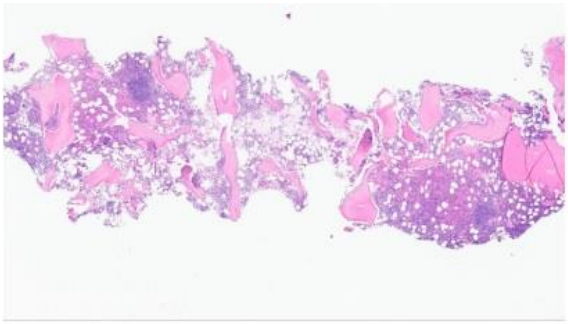

Panoramic view bone marrow

EA4HP24-ABS-535

Evaluation of the bone marrow microenvironment in hemophagocytic lymphohistiocytosis

Priv.-Doz. Thomas Menter[1], M.Sc./M.A. Manuel Trebo[2], Dr. Josia Fauser[2], Dr. Lena Horvath[2], Prof. Andreas Pircher[2], Dr. Beate Posch[2], Prof. Michael Medinger[3], Dr. Claire Seydoux[3], Prof. Sieghart Sopper[2], Prof. Dominik Wolf[2], Prof. Alexandar Tzankov[1]

[1] University Hospital Basel, Pathology, Institute of Medical Genetics and Pathology, Basel, Switzerland; [2] Medical University of Innsbruck, Department of Internal Medicine V, Haematology & Oncology, Comprehensive Cancer Center Innsbruck (CCCI) and Tyrolean Cancer Research Institute (TKFI), Innsbruck, Austria; [3] University Hospital Basel, Division of Hematology, Basel, Switzerland

Background

Hemophagocytic lymphohistiocytosis (HLH) is a severe and potentially life-threatening disease resulting from an uncontrolled activation of macrophages. HLH has various etiologies and in many cases a distinct genetic predisposition. However, the role of crucial immune regulators and checkpoints have not been completely elucidated yet.

Principles/Methodology

We analyzed bone marrow (BM) trephine biopsies of 37 clinically well-documented patients with confirmed HLH according to current standards (at least 5/8 HLH-defining symptoms and HLH-score >150) by immunohistochemistry for selected immune checkpoint markers (CD40, CD47, CD200, LILRB1, PD1, PDL1, SIRPα, TIM4). 11 BM biopsies of healthy individuals were used as a control.

Results

Causes for HLH were categorized as genetic, autoinflammatory, infectious, neoplastic and a combination of infectious and neoplastic. The age of the patients significantly differed between genetic and neoplasm-associated subgroups (median age 28 versus 60 years, respectively).

We found a positive correlation in the HLH cohort between the number of PDL1-positive cells and those expressing LILRB1 (Leukocyte Immunoglobulin Like Receptor B1) (ρ=0.709, p=0.015), which is an important gatekeeper regarding the stimulation of the immune system. PD1 and PDL1 only correlated in the control group indicating potential disturbances in PD1-PDL1 intercellular signaling in HLH (ρ=0.674, p=0.023). SIRPα (Signal Regulatory Protein α), which inhibits macrophage function via CD47 engagement, was significantly less prevalent in the HLH versus the control group (19/37 vs 10/11, p=0.013). Presence of CD40-positive cells positively correlated with increased amounts of PDL1 and CD47-positive cells (ρ=0.743 and 0.506, respectively, p<0.001, each). Epstein-Barr-virus (EBV) positive cells could only be detected in male patients (9/24 vs. 0/13, p=0.011), but this did not affect the expression of the proteins investigated.

Conclusion

Our research reveals disruptions in immune pathway homeostasis in HLH patients, linked to altered expression of immune checkpoint proteins. Detailed analysis of SIRPα, a potential therapeutic target, is crucial to address the disturbed immunologic microenvironment in HLH and develop effective treatments.

EA4HP24-ABS-547

Significantly Increased Expression of CD95 (Fas) by Immunohistochemistry in Idiopathic Aplastic Anemia Bone Marrow Core Biopsies

Dr. Collin Klonk, PhD/MD Joseph Rohr

University of California, San Francisco, Department of Laboratory Medicine, San Francsico, USA

Background

Aplastic anemia (AA) is a syndrome of chronic primary haematopoietic failure leading to reduced haematopoietic precursors and attendant pancytopenia. This syndrome is associated with numerous etiologies, including heritable, environmental, or neoplastic. However, many AA cases have no known insult, termed idiopathic (IAA), which is associated with increased CD95 (Fas) expression in flow cytometry studies.

Principles/Methodology

We investigated the utility of CD95 immunohistochemical staining in primary human bone marrow biopsies undergoing standard clinical processing. We searched our institution's pathology database, with IRB approval, for cases in which the clinicopathologic diagnosis of IAA was made. Twenty-four unique cases were found, of which 20 ultimately had sufficient tissue available for evaluation after staining with anti-human CD95 (Abcam, Cambridge, UK) on an autostainer using standard methodologies. Four hypocellular marrows of known etiology (short telomere syndrome, hypoplastic MDS, infectious; “IAA mimic” marrows) and three "normal" marrows were also included. In addition, all specimens were stained for CD3, CD4, CD8, CD20, and CD34. H-scoring of the CD95-stained slides was performed; separate H-scores were generated for lymphocytes, myeloid cells, erythroid cells, and adipocytes, as permitted, for each biopsy. Approximate percentages of each cell type were assigned an intensity score of 0-3. Data were analyzed using unpaired t- and Mann-Whitney tests, as appropriate.

Results

IAA marrows contained a significantly greater proportion of lymphocytes than non-IAA marrows (P=2.2x10E-5) driven by CD3+ and CD8+ cells (P=1.2x10E-5 and 3.9x10E-5, respectively; Figure 1). There was no significant difference in CD20+ B cells, CD4+ lymphocytes, or CD34+ cells. Significant differences in lymphocyte scoring for CD95 expression were identified between IAA and non-IAA marrows (Figure 2: H-score 1.026 vs. 0.500, respectively; P=0.034). There was no significant difference for CD95 expression identified in myeloid, erythroid, or adipocytic elements.

Conclusion

There is a significant increase in lymphocyte staining for CD95 in IAA cases relative to non-IAA cases. These findings suggest potential utility of CD95 immunohistochemical staining as an adjunct to clinical practice in AA diagnosis. Further investigation in IAA and mimics may be beneficial.

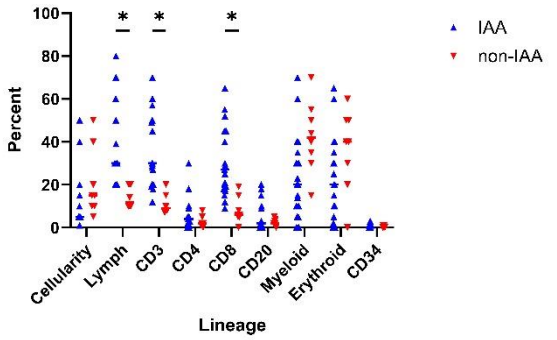

Figure 1. Assayed Characteristics of Idiopathic Aplastic Anemia (IAA) and non-IAA Bone Marrows
Specimens were evaluated on H&E for cellularity and proportion of lymphocytes, myeloid cells, and erythroid cells, as well as by immunohistochemistry for T cells (CD3) and subsets (CD4, CD8), B cells (CD20), and myeloblasts (CD34). There was a significantly greater proportion of lymphocytes in IAA marrows (P=2.2x10E-5), which were comprised primarily of CD3+ (P=1.2x10E-5) and CD8+ (P= 3.9x10E-5) cells. There was no significant difference in cellularity, or proportion of other cells.

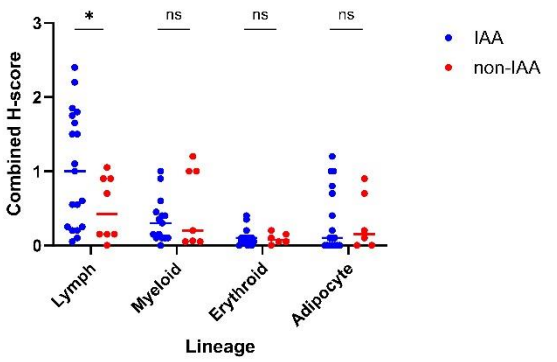

Figure 2. H-score for CD95 in IAA and non-IAA Bone Marrows
Immunohistochemistry for CD95 (Fas) was scored by proportion of total cellularity and intensity of staining on a four-tier scale (0-3). The sums for each lineage assessed by H&E (lymphocytes "lymph"), myeloid, and erythroid elements, as well as staining in background adipocytes, were recorded. Lymphocytes in IAA marrows had a significantly higher total H-score than lymphocytes in non-IAA marrows (P=0.034) which was not found for the other assessed lineages.

EA4HP24-ABS-599

Megakaryocytic changes and reticulin fibrosis, mimicking myeloproliferative neoplasm, in bone marrow biopsies of patients with immune thrombocytopenia, treated with thrombopoietin receptor agonists.

Dr. Christos Masaoutis[1], Dr. Leonidas Marinos[1], Dr. Anna Kolovou[2], Dr. Dimitra Liapi[3], Dr. Niki Rougkala[4], Prof. Kostas Liapis[5], Dr. Emily Stavroulaki[3], Dr. Goni Mitsiou[4], Dr. Asimina Papanikolaou[1], **Dr. George Kanellis**[1]

[1] Evaggelismos Hospital, Hematopathology, Athens, Greece; [2] Chania Hosptial "Agios Georgios", Hematology, Chania, Greece; [3] Venizelio Hospital, Hematology, Heraklion, Greece; [4] Sismanoglio Hospital, Hematology, Athens, Greece; [5] University Hospital of Alexandroupoli, Hematology, Alexandroupoli, Greece

Background

Thrombopoietin receptor agonists (TPO-RAs)are used to treat persistent, chronic and refractory immune thrombocytopenia (ITP). Relatively recent literature correlates TPO-RA administration with morphologic alterations of megakaryocytes and bone marrow fibrosis. The aim of this study is to describe these alterations on bone marrow biopsy specimens and highlight the differential diagnostic considerations that may arise in the distinction from myeloproliferative neoplasms (MPNs).

Principles/Methodology

We searched the histopathology reports archive of our laboratory (Hematopathology Laboratory, Evaggelismos General Hospital of Athens) with the keywords “ITP” and “TPO-RA.” Cases describing MPN-like megakaryocytic alterations were selected. Megakaryocyte morphology was evaluated on H&E and LAT-immunostained slides. Reticulin fibers were semi-quantitatively evaluated according to the European Consensus (scale 0-3).

Results

Thirteen (13) cases were found over the last six years (2018-2024), among which 8 females και 5 males, 53 – 87 years old. Persistent thrombocytopenia led to revaluation in most cases (12/13) and anemia in one. Histologically, megakaryocytes were characterized by pleiomorphism with frequent presence of large forms, occasionally hyperlobulated. All cases showed age-adjusted hypercellularity (mild: 5/13, moderate: 5/13, severe: 3/13) and increase in megakaryocyte numbers (moderate: 5/13, severe: 8/13). In most cases at least some megakaryocytic aggregates were noted (11/13) and/or at least mild reticulin fibrosis (9/13), either intertrabecular (7/13) or paratrabecular (2/13). In four cases (4/13) reticulin fibrosis was moderate MF-2; megakaryocytic pleiomorphism and aggregates were also present mimicking primary myelofibrosis.

Conclusion

Thrombopoietin receptor agonists, administered to ITP patients, may induce MPN-mimicking changes, in terms of megakaryocytic numbers, morphology and topography, as well as reticulin fibrosis. These histomorphological parameters are included among the diagnostic criteria of primary myelofibrosis and essential thrombocythemia. Therefore, awareness of these therapy-induced changes and of the patient’s clinical and medication history is vital to avoid diagnostic errors.

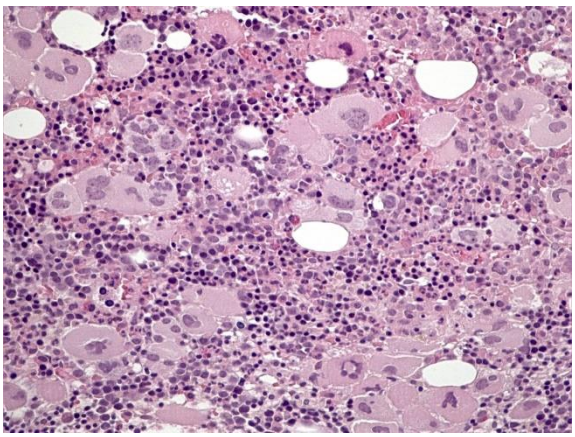

Bone marrow of ITP patient on TPO-RA
82-year-old female on TPO-RA for ITP showing striking hypercellularity, conspicuous megakaryocytic hyperplasia and pleiomorphism with giant forms coalescing in large (>7 cells), tight aggregates. These findings mimic pre-fibrotic primary myelofibrosis.

EA4HP24-ABS-622

Secondary Hemophagocytosis: Challenges in Identifying Underlying Disease

Dr. Megan O. Nakashima, Dr. Marcello Toscano

Cleveland Clinic, Pathology and Laboratory Medicine, Cleveland, USA

Background

Hemophagocytic lymphohistiocytosis (HLH) is a left-threatening condition of immune dysregulation which can arise either due to underlying mutation or as a response to infection, malignancy, and autoimmune disease. While general treatment protocols are available, optimal therapy targets the underlying cause, thus establishing the associated infection, malignancy, or autoimmune disorders in secondary cases is crucial. This may be difficult in acute illness, especially in the case of bone marrow-based disease where the diagnostic findings may be obscured by the hemophagocytosis and reactive changes.

Principles/Methodology

Cases were identified by searching our bone marrow biopsy/aspirate report archives for “hemophagocytic” or “hemophagocytosis.” Only cases clinically considered to represent HLH were included. The medical records were searched to identify the underlying cause of HLH including whether or not patients were tested for gene mutations associated with primary HLH and the number of biopsies/excisions required to identify the underlying malignancy in malignancy-associated cases.

Results

200 adult patients had bone marrow cases with slides available for review were identified between 2009 and 2022, 60 of which were clinically considered to be HLH. 23 cases were thought to be secondary to malignancy,12 infectious, and 27 with unknown etiology. The underlying malignancies were all hematolymphoid, including 1 AML, 10 B-cell, 3 NK cell, 8 T-cell, and one patient with both myelodysplasia and a B-cell neoplasm. The underlying malignancy was diagnosed in the same bone marrow as the HLH in 13 cases (56.5%), however the remaining cases (10, 43.5%) needed an additional one to four tissue samples (average 2.2) including additional bone marrow biopsies and samples from liver, lymph node, spleen, and soft tissue masses.

Conclusion

In 45% of our HLH cases, an underlying cause was not able to be documented, which may have led to less-than-optimal treatment. Malignancy-associated cases accounted for 38% of cases compared to infection-related (20%), consistent with previous reports from the United States and Europe. Although the underlying malignancy was also able to be diagnosed in the HLH-diagnostic marrow in over 50% of cases, additional tissue sampling was often needed, as many as four times, to reach the ultimate diagnosis.

EA4HP24-ABS-484

Short Term Myeloid Leukemic Transformation in Triple Negative ET: Case report

Prof. Nahla A. Ibrahim

NCI, CAIRO, Egypt

Background

Essential thrombocythemia (ET) is an uncommon a BCR-ABL negative myeloproliferative disorder involving hemopoietic stem cell especially megakaryocytic lineage marked by increase in platelets count. Haemorrhage and thrombosis are the main clinical manifestation due to increased number of functionally abnormal platelets. ET can progress to acute myeloid leukaemia and post ET Myelofibrosis with or without antecedent myelodysplastic syndrome. The rate of blast transformation is very low compared with that in chronic myeloid leukaemia, idiopathic Myelofibrosis and polycythemia Vera. The risk of leukemic transformation has been variable in several studies ranging from 1- 4% during median follow up of seven to ten years.

Principles/Methodology

we herein present a female diagnosed as ET October 2020,, with elevated platelet count of 1449x109/L, increased megakaryopoiesis with large hyperlobulated forms, and occasional hyperchromatic forms.No increase in bone marrow reticulin fibrosis. At this point, chromosomal analysis revealed no abnormalities,BCR/ABL translocation (9; 22) not detected.In addition, her molecular workup was normal,and her MPN NGS was negative.The platelet count was controlled using HU 500mg daily and aspirin with maximum platelet count she reached was 600 -700x109/L during these three years.

Results

Later on September 2023, she presented to ER with fever,dry cough,fatigue,and hepatosplenomegaly.In the ER her CBC showed leukocytosis and thrombocytopenia with presence of blasts, full hematological work up including CBC with manual differential count, bone marrow aspiration /biopsy, flow cytometry analysis, conventional chromosome and FISH analysis, and molecular testing.Based on all investigations the case diagnosed as ET transformed into acute myeloid leukemia with monocytic component, without antecedent Myelofibrosis.
Induction chemotherapy with 3+7 was performed .she achieved remission and planed for bone marrow transplantation until that she is maintained on Azacytidine andventoclax

Conclusion

Essential thrombocythemia is a myeloproliferative disorder that is rarely have leukemic transformation. Any eligible patients should be treated with AML-induction chemotherapy followed by allogeneic stem cell transplantation for long-term disease control.

EA4HP24-ABS-510

Immunohistochemical patterns, molecular features and outcome of extramedullary disease in *NPM1*-mutated AML

Prof. Brunangelo Falini[1], Dr. Alessandra Venanzi[1], Prof. Bjørn T. Gjertsen[2], Dr. Vibeke Andresen[2], Dr. Vincenzo Perriello[1], Dr. Andrea Marra[1], Prof. Elena Sabattini[3], Prof. Sarah Bertoli[4], Prof. Andrè Pigneux[5], Prof. Pierre-Yves Dumas[5], Prof. Christian Recher[4]

[1] Institute of Hematology and CREO, University and Hospital of Perugia, Perugia, Italy; [2] Centre for Cancer Biomarkers (CCBIO), Department of Clinical Science, Bergen, Norway; [3] S.Orsola Malpighi Hospital, Bologna, Italy; [4] Centre Hospitalier Universitaire de Toulouse, Institut Universitaire du Cancer de Toulouse Oncopole, Toulouse, France; [5] Centre Hospitalier Universitaire de Bordeaux, Bordeaux, France

Background

Despite a great bulk of information is now available on *NPM1*-mutated AML, (*Falini B, NEJM 352(3):254-266, 2005; Falini B Blood, 136(15):1707-1721, 2020*), little is known about the characteristics of extramedullary disease occurring in patients affected by this leukemia entity

Principles/Methodology

Myeloid sarcomas (MS) (n=56) observed during 2002-2020 were retrieved from the archive of Hematopathology, Institute of Hematology, Perugia University. Ten NPMc+ (cytoplasmic-positive) MS from the Hematopathology Unit, S. Orsola Hospital, were also available for study. All cases were investigated by immunohistochemistry (IHC) for cytoplasmic expression of nucleophosmin that is predictive of *NPM1* mutation *(Falini B et al, Blood, 108(6):1999-2005, 2006*). Seven cases of NPMc+ MS for which adequate material was available were subjected to targeted sequencing and the results compared to those obtained in bone marrow. Impact of extramedullary disease on survival was investigated in 734 *NPM1*-mutated AML patients from the Toulouse-Bordeaux AML database (DATAML), observed in the period 2000-2020 and treated with intensive chemotherapy.

Results

Twenty-three out of the 56 MS (41.07%) expressed cytoplasmic NPM1 mutant at IHC. The most frequently involved extramedullary site was skin but other sites, including lymph nodes, testicle, kidney, and pharynx were affected. The anti-N terminus NPM1 monoclonal antibody labelled both the nucleus and cytoplasm of the tumor cells whilst the antibody specific for NPM1 mutant A labelled exclusively the cytoplasm of leukemic cells and was tumor specific. Targeted sequencing of seven extramedullary sites and paired bone marrow samples showed, with minimal variations, an overlapping mutational profile between extramedullary and medullary disease. No impact of extramedullary disease on survival was observed (no EMD: median OS 77 months vs EMD: 49 months, P=0.08). 3y and 5y OS was 61% and 53% in the no EMD group vs 53% and 49% in the EMD group.

Conclusion

theNPM1c+ (mutated) genotype was frequent (41,07%) among MS in our series. IHC is an ideal technique for diagnosing these cases, for which only a small amount of material is often available (especially skin biopsies). Molecular studies point to a stability of the mutational profile among medullary and extramedullary sites. This genetic stability may account for the lack of negative impact on survival of the extramedullary involvement in *NPM1*-mutated AML.

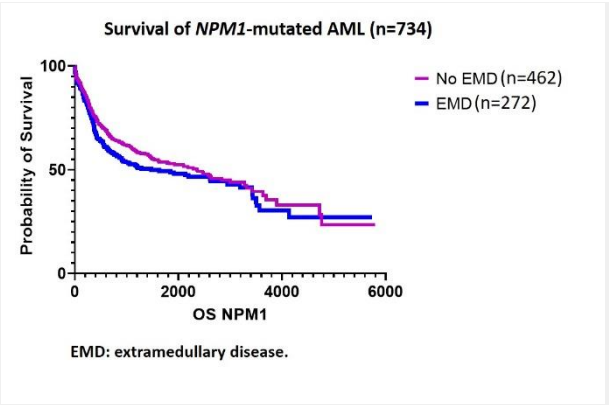

Figure 1

EA4HP24-ABS-514

Starry sky pattern predicts RAS pathway activation in *NPM1*-mutated AML

Prof. Brunangelo Falini[1], Dr. Alessandra Venanzi[1], Dr. Vincenzo Perriello[1], Dr. Valeria Cardinali[1], Dr. Francesco Albano[2], Dr. Gaetano Cimino[1], Dr. Giovanni Martino[1], Dr. Andrea Marra[1], Prof. Paolo Sportoletti[1], Dr. Vibeke Andresen[3], Prof. Bjørn T. Gjertsen[3], Prof. Simona Sica[4,5], Dr. Patrizia Chiusolo[4,5], Prof. Maria P. Martelli[1], Prof. Enrico Tiacci[1]

[1] Institute of Hematology, Centro Ricerche Emato-Oncologiche (CREO), Ospedale S. Maria della Misericordia, University of Perugia, Perugia, Italy; [2] Hematology and Stem Cell Transplantation Unit, Department of Precision and Regenerative medicine and Ionian Area (DiMePRe-J), University of Bari "Aldo Moro", Bari, Italy; [3] Centre for Cancer Biomarkers (CCBIO), Department of Clinical Science, University of Bergen, Bergen, Norway; [4] Fondazione Policlinico Universitario A. Gemelli IRCCS, Dipartimento di Scienze di Laboratorio ed Ematologiche, Rome, Italy; [5] Università Cattolica del Sacro Cuore, Sezione di Ematologia, Dipartimento di Scienze Radiologiche ed Ematologiche, Rome, Italy

Background

NPM1-mutated AML shows peculiar molecular and clinico-pathological features and represents a distinct leukemia entity in the ICC and WHO classifications (*Falini B Blood, 136(15):1707-1721, 2020*). *NPM1*-mutated AML exhibits a wide morphological spectrum including multilineage involvement and cup-like nuclei, but whether morphological features are predictive of mutational profile has been never investigated.

Principles/Methodology

we reviewed the bone marrow (BM) biopsies from 450 *NPM1*-mutated AML. M4 and M5 were the most common FAB categories and multilineage involvement was seen in about 25% of cases. Notably, we observed 5 cases with a “starry sky pattern” resembling that seen in Burkitt-lymphoma/L3-acute lymphoblastic leukemia. All cases were extensively investigated by immunohistochemistry (IHC) and targeted sequencing for commonly myeloid mutated genes.

Results

BM biopsies from all cases showed diffuse infiltration by blasts with myeloid (M1-M2), myelomonocytic (M4) or monoblastic (M5) appearance. Tingible body macrophages were dramatically increased and imparted to the histological picture a starry sky pattern, consistent with the high proliferative index of leukemic cells. At IHC, the anti-N terminus NPM1 monoclonal antibody labelled both the nucleus and

cytoplasm of tumor cells, whilst the tingible body macrophages showed a nucleus-restricted NPM1 expression. The antibody specific for NPM1 mutant A labelled exclusively the cytoplasm of the leukemic cells but not the tangible body macrophages. Targeted sequencing revealed mutations activating the RAS pathway in all cases (Table 1 1). In particular, one patient harbored a missense mutation in the RING domain of CBL (R420Q; VAF 40.7%, hence possibly hemizygous or homozygous). This mutation disrupts the CBL ubiquitin ligase activity interfering with wild-type CBL and leading to activation of FLT3 signaling (*Sargin B et al, Blood 110(3):1004-1012, 2007*). Two cases were triple mutated for *NPM1/FLT3-ITD/DNMT3A* that associates with worse prognosis. All patients presented with high blood cell count (usually >100.000/µl) and increased LDH (Table 1).

Conclusion

NPM1-mutated AML with starry sky pattern is a distinctive morphological variant that predicts co-mutations leading to RAS pathway activation. Whether tingible body macrophages are reactive or belong to the leukemic clone remains unclear. Allogeneic transplant was curative in the two patients with *NPM1/FLT3-ITD/DNMT3A* mutated AML.

Table 1

Table 1. Clinical, morphological and molecular features of *NPM1*-mutated AML with starry sky pattern.

Case	Age/Sex	WBC count	BM pattern	FAB	Karyotype	Mutations	Out came
1.	66/M	123.000/µl	Diffuse infiltration by AML cells with "starry sky" pattern	M5a	n.a.*	*NPM1* W288C (VAF: 25.1%) *NPM1* W290RfsTer10 (VAF: 20.7%) *CBL* R420Q (VAF:40.7%)	Died
2.	67/M	87.740/ µl	Diffuse infiltration by AML cells with "starry sky" pattern + focal metastatic carcinoma	M2	47XY, +8, der (11) (p15) (3 met) 47, idem, +1, der (1) (1;15) (q10;p10) (7Met)	*NPM1* W288C fsTer12 (VAF:11%) *NRAS* G12D (VAF:36%) *KRAS* G13D (VAF:24.4%) *TP53* G244V (VAF:12.4%) *ZRSR2* C181Y (VAF:11.8%)	Died
3.	52/F	180.000/ µl	Diffuse infiltration by AML cells with "starry sky" pattern	M1	46XX	*NPM1* W288CfsTer12 (VAF:37.5%) *FLT3*-ITD (AR:0.63) *DNMT3A* R882H (VAF:49.7%) *KRAS* G12D (VAF:1.6%)	Alive post allo-HSCT
4.	73/F	147.000/ µl	Diffuse infiltration** by AML cells with "starry sky" pattern + lymphoplasmocytic lymphoma	M3	46XX	*NPM1* W288CfsTer12 (VAF:30.6%) *FLT3-ITD* (AR:0.34)	Died
5.	45/F	147.900/ µl	Diffuse infiltration** by AML cells with "starry sky" pattern	M4	Aneuploidy (43%) 46XX (57%)	*NPM1* (VAF:52%) *FLT3ITD* (AR:0.39) *DNMT3A* R882H (VAF:40%)	Alive post allo-HSCT

*No methaphases available for analysis; ** Skin involvement by *NPM1*-mutated AML was also documented.

EA4HP24-ABS-556

Chronic myeloid leukemia (CML) evolving from a JAK2 V617-mutated myeloproliferative neoplasm.

Dr. Lucas Brammar, Josh Willoughby, Dr. Sebastian Francis, **Dr. Malee Fernando**

Sheffield Teaching Hospitals NHS Trust, Haemato-Oncology Diagnostic Service, Sheffield, UK

Background

Myeloproliferative neoplasms (MPNs) are a heterogeneous group of hematologic diseases. The ICC and WHO classification divides MPNs based on the presence of an underlying genetic abnormality. Whilst the BCR::ABL1 fusion is essential for diagnosis of CML, JAK2 V617F mutations are reported in polycythaemia vera, primary myelofibrosis and essential thrombocythemia (ET) and the JAK2 V617F mutation and BCR::ABL1 translocation are considered mutually exclusive.

Principles/Methodology

We report on a 80year old male who presented from 10y ago with multiple reactive nodal biopsies done to investigate unexplained cervical lymphadenopathy with a partial temporary response to steroids. In 2021 a JAK2 V617F mutation was detected when investigating for rising thrombocytosis (560 to 699 x10^9/L over 2 months) whilst other indices were within normal range. A diagnosis of ET was made. The blood indices remained normal until December 2023 on Hydroxycarbamide. He then developed an unexplained increase of WBC (31.6 x10^9/L) with a basophilia, mild anaemia and 15cm splenomegaly. Bone marrow examination was done 2 months later when the WBC increased to 62.4 x10^9/l with a basophilia, neutrophil leukocytosis, thrombocytosis and leukoerythroblastic blood film. A concomitant CML (with a e14a2 transcript) and persistent ET (JAK2 V617F VAF 51%) with grade 2 fibrosis was diagnosed. Karyotyping showed a three-way translocation as opposed to the standard t(9;22) and that there were no additional cytogenetic abnormalities.

Results

With the addition of a TKI, the WBC and then platelet count reduced to current respective14.7 & 406 x10^9/l within a month. The symptoms of nights sweats, fevers and fatigue improved dramatically.

Conclusion

Development of CML needs consideration when CML-like features appear in a JAK2+ MPN years after clinical stability. The clinical course of the disease in our patient reflects what is reported in the literature, ie when MPN precedes CML the mean time interval between the diagnoses is 10.6y, and reported more in males. The frequency of this “dual disease” is unknown, but is likely under-diagnosed.It is currently unknown whether the JAK2V617F and BCR::ABL1 clones are related at the molecular level and despite multiple reports detailing an increasing degree of clonal heterogeneity in MPNs, the coexistence of multiple genetic abnormalities in a single patient has not been addressed by the last ICC and WHO classifications.

EA4HP24-ABS-587

Deciphering the Prognostic Significance and Molecular Role of SLC40A1 in Acute Myeloid Leukemia

Dr. Pranay Tanwar[1], PhD/MD student Harsh Goel[1], Dr. Anita Chopra[1], Dr. Amar Ranjan[1], Dr. Jagdish P. Meena[2], Dr. Aditya K. Gupta[2], Dr. Ganesh K. Viswanathan[3], Dr. Sameer Bakhshi[4], Dr. Maroof A. Khan[5]

[1] All India Institute of Medical Sciences, Laboratory Oncology Unit, Dr. B.R.A. Institute Rotary Cancer Hospital, New Delhi, India; [2] All India Institute of Medical Sciences, Division of Pediatric Oncology, Department of Pediatrics, New Delhi, India; [3] All India Institute of Medical Sciences, Department of Hematology, New Delhi, India; [4] All India Institute of Medical Sciences, Department of Medical Oncology, Dr. B.R.A. Institute Rotary Cancer Hospital, New Delhi, India; [5] All India Institute of Medical Sciences, Department of Biostatistics, New Delhi, India

Background

Acute myeloid leukemia (AML) is a genetically diverse hematological disorder characterized by abnormal differentiation and clonal proliferation of myeloid progenitor cells in the bone marrow. While iron metabolism alterations are observed in various cancers, the role of iron metabolism in AML remains unclear. Ferroportin, encoded by the SLC40A1 gene, is the sole protein responsible for cellular

iron export. This study aimed to elucidate the molecular functions, clinical relevance, and prognostic value of the SLC40A1 gene in AML.

Principles/Methodology

We examined the SLC40A1 gene expression in 173 AML cases and 70 controls. Correlation analysis was conducted using the Linked Omics database to identify genes associated with SLC40A1 expression. Prognostic significance was assessed via Kaplan-Meier survival estimation using the Kaplan Meier plotter. The DNA methylation status of SLC40A1 was evaluated using the MEXPRESS database. Gene set enrichment analysis (GSEA) was performed to explore the molecular mechanisms of SLC40A1 in AML. Additionally, the relationship between SLC40A1 expression and immune checkpoints was analyzed using the SANGER Box 3.0 database.

Results

SLC40A1 mRNA was significantly overexpressed in AML cases compared to controls and was associated with poor overall survival ($P < 0.05$). Correlation analysis revealed that SLC40A1 was positively correlated with genes including DNAJC6, CD59, PLS1, GCLM, and CAPRIN2, and negatively correlated with MSLN, MYH11, DAGLB, ST18, and PLCD3 (PCC < 0.80). Lower methylation levels of the SLC40A1 gene were observed in AML, which were inversely related to its expression. GSEA indicated that SLC40A1 is involved in processes such as lymphocyte homeostasis, endothelium development, spleen development, cell communication, and differentiation. Molecular function enrichment highlighted roles in iron ion transmembrane transport, protein and metal cluster binding, growth factor binding, and catalytic activity. KEGG pathway enrichment showed SLC40A1 involvement in hematopoietic stem cell differentiation, ferroptosis, mRNA surveillance, autophagy, TGF-beta signaling, and pathways regulating stem cell pluripotency. Additionally, SLC40A1 was positively correlated with immune checkpoints including CD160, CD274, CD40, CD44, and CD80.

Conclusion

SLC40A1 is crucial in AML progression and may serve as a prognostic biomarker and therapeutic target for AML management.

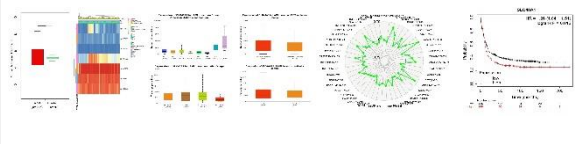

Figure 1. Expression, Methylation, Survival, and Clinical Correlation of SLC40A1 Gene in Acute Myelo

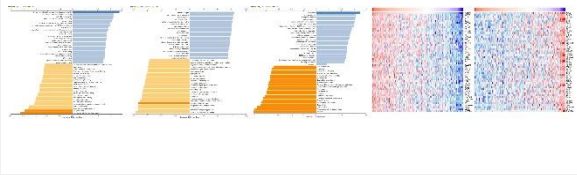

Figure 2. Gene Correlation and Molecular Mechanisms Associated with SLC40A1 Expression in AML

EA4HP24-ABS-600

VEXAS Syndrome: Contemporary Diagnostic Evaluation and Management

Dr. Ashley Hagiya[1], Dr. Imran Siddiqi[1], Dr. Endi Wang[1], **Dr. Chuanyi M. Lu**[2]

[1] University of Southern California, Pathology, Los Angeles, USA; [2] University of California, San Francisco, Laboratory Medicine, San Francisco, USA

BackgroundVEXAS syndrome (vacuoles, E1 enzyme, X-linked, autoinflammatory, somatic) is a newly discovered, adult-onset and progressive systemic inflammatory disorder with overlapping rheumatologic and hematologic manifestations, including an increased risk for myelodysplastic neoplasms. The aim of this presentation is to comprehensively review VEXAS syndrome, including its clinical and pathologic features, diagnostic challenges, contemporary diagnostic approach, and management.

Principles/Methodology

A clinical case-based approach and pertinent literature review are used to highlight the features of VEXAS syndrome, how to make the diagnosis, and available therapies.

Results

VEXAS syndrome is associated with a somatic mutation of the X-linked *UBA1* gene involved in ubiquitylation, typically involving p.Met41; however, other *UBA1* mutations have been identified outside of this region. Patients often present with complex histories and are seen by physicians of multiple specialties prior to receiving the diagnosis, which is often delayed. Symptoms are related to inflammation, as well as peripheral cytopenias, particularly macrocytic anemia. Charactertic cytoplasmic vacuoles are present in myeloid (granulocytic, monocytic) and erythroid precursors in the vast majority of cases. Management is not yet standardized, and patients are often treatment refractory to therapies other than steroids. Allogeneic hematopoietic stem transplantation is the only potentially curative treatment at this time.

Conclusion

VEXAS syndrome can be challenging to diagnose and requires both clinicians and pathologists to be aware and vigilant of this entity. A diagnosis of VEXAS syndrome may be suspected by either clinician or pathologist depending on the clinical presentation and bone marrow findings. More studies are needed to further elucidate the pathophysiology and determine the best therapeutic options.

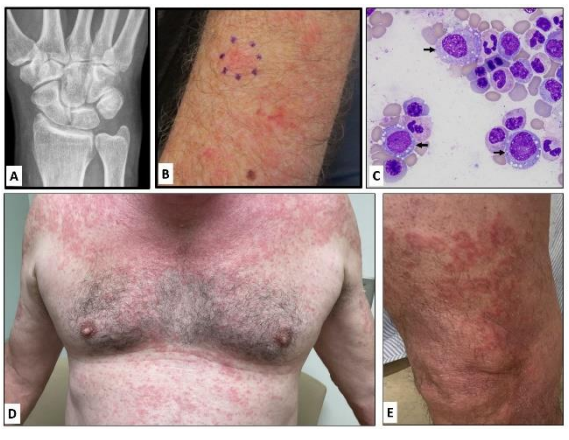

Clinical features of VEXAS syndrome
Selected clinical manifestations of the VEXAS syndrome.A, chondritis; B, urticarial hypersensitivity dermatitis and focal subepidermal vesiculation; C, small vacuoles in bone marrow myeloid precursor cells; D, intensely diffuse, erythematous and blanching rashes; E, serpiginous, non-blanching and livedo-like rashes.

EA4HP24-ABS-613

Lymphadenopathy as presenting feature of a Myeloid/lymphoid neoplasm with PDGFRA rearrangement.

Dr. Malee Fernando[1], Dr. Sebastian Francis[1], Dr. Lucas Brammar[1], Josh Willoughby[2], Dr. Rumana Rashid[5]

[1] Haemato-oncology Diagnostic Service, Laboratory Medicine, Sheffield Teaching Hospitals NHS Trust, Sheffield, UK; [2] North-East and Yorkshire Genomic laboratory Hub, Haem-onc geneomics, Sheffield, UK; [3] Haemato-oncology Diagnostic Service, Laboratory Medicine, Sheffield Teaching Hospitals NHS Trust, Sheffield, UK; [4] Haemato-oncology Diagnostic Service, Laboratory Medicine, Sheffield Teaching Hospitals NHS Trust, Sheffield, UK; [5] Barnsley Hospital NHS Foundation Trust, Department of Haematology, Barnsley, UK

Background

Myeloid/lymphoid neoplasms with eosinophilia and tyrosine kinase gene fusions (M/LN-Eo-TK) is a rare group of neoplasms with a broad range of clinical presentations. Lymph nodes are reported as a site of extramedullary involvement.

We discuss a 62y old male who presented in September 2020 with a left axillary mass. He was generally unwell with increasing tiredness, poor appetite, weight loss, dry cough, generalised pruritus, and drenching night sweats for a few months.

Principles/Methodology

On examination he looked unwell, had a left axillary lymph nodal mass and few small palpable groin nodes; no rashes or eosinophilia-related features.

Bloods demonstrated haemoglobin 115g/L, platelets 195 x10^9/L, WBC 30.8 (12.1 neutrophils & eosinophilia of 12.3) x10^9/L. He had normal LDH (178 U/L), elevated vitamin B12 (1798 pmol/L) & ferritin (359 ug/L), slightly elevated tryptase (14.8) and low folate (1.7).

Imaging showed 2 nodes in the left axilla (larger 22mm), a few small mediastinal nodes (largest 11mm) and a 15cm splenomegaly.

PB examination confirmed a PDGFRA-rearrangement (in 96% of cells scored) without a BCR::ABL1 or mutated JAK2 exon 14.

The nodal biopsy showed nodular aggregates of CD3+ CD4+ T-cells within expanded paracortical zones and background reactive follicles. There were no lymphoblasts or TFH markers (BCL6, CD10, PD1, ICOS). There were TCR gamma clonal products in a polyclonal background but no mutated RHOA G17V or B-cell clonality. FISH confirmed a PDGFRA-rearrangement in 84% of cells scored.

Bone marrow demonstrated myeloid proliferation (M:E ratio of 23:1) with 10% eosinophils and increased reticulin. Karyotype was normal and there was a *FIP1L1::PDGFRA* fusion, but no other mutations with HTS.

Results

On oral Imatinib 100g/day the cough, itching and sweats completely resolved within a week. WBC normalised within 2 weeks (13 x10^9 with Eo 0.2) and remains normal at 7.9 x10^9/L (Eo 0.36) at 36months.

Within 4 weeks he was feeling well with a 5.2kg weight increase and without lymphadenopathy.

The imaging at 5 months showed only a solitary 8mm node in axilla, calcification of the single mediastinal node and resolution of the splenomegaly.

Conclusion

He remains well on same dose of TKI with clinical and haematological response (Hb 155g/L, WBC 7.5, PLT 190, neut 5.2, eo 0.2 x10^9/L) and is currently awaiting PB results to assess continued complete molecular response.

We describe the first reported patient with a M/LN-Eo-TK presenting with mild lymphadenopathy.

EA4HP24-ABS-629

Philadelphia chromosome-positive acute leukemia with cells harboring *BCR::ABL* discordantly higher than blast count may represent de novo blast phase of chronic myeloid leukemia with silenced chronic phase

Dr. Yaping Ju[1], Dr. Sophie Stuart[1], Dr. Yue Zhao[2], Dr. Ashley Hagiya[1], Dr. Maria Vergara-Lluri[1], Dr. Eric Carlsen[3], Dr. Luis Carrillo[3], Dr. Imran Siddiqi[1], Dr. Mark Lu[4], Dr. Ling Zhang[5], **Dr. Endi Wang**[1]

[1] University of Southern California, Department of Pathology, Los Angeles, USA; [2] China Medical University, Department of Pathology, Shenyang, China; [3] Duke University, Depatment of Pathology and Laboratory Medicine, Durham, USA; [4] University of California San Francisco, Department of Laboratory Medicine, San Francisco, USA; [5] Moffitt Cancer Center, Department of Hematopathology, Tampa, USA

Background

Chronic myeloid leukemia (CML) typically presents at chronic phase and undergoes stepwise progression to blast phase. However, de novo blast phase without identifiable chronic phase has been reported

Principles/Methodology

Retrospective analysis of 10 cases of Ph+ acute leukemia with pathologic features suggestive of CML blast phase

Results

Seven patients were male and 3 were female. The median age was 67.5 years (range 31-85). Eight patients presented with leukocytosis with left-shifted neutrophilia and two presented with pancytopenia. Circulating blasts ranged from 1 to 88% (median=29%). Blasts in bone marrow ranged 20-90% (median=48.3%). While 7 cases showed myeloid phenotype in blasts, 3 cases exhibited B-lymphoblastic phenotype. Of 9 cases with karyotyping, 8 (88.9%) demonstrated abnormalities besides Ph chromosome. In the case without karyotyping, FISH revealed multiple changes suggestive of complex abnormalities. All cases had *BCR::ABL* fusion confirmed by FISH. Cells harboring *BCR::ABL* ranged 71.5-98.5% with a median of 95%. In each case, cells with *BCR::ABL* were higher than blast count with 8 cases showing a difference ≥18.5% and 2 cases showing a difference <10% due to very high blast counts (90%). Eight cases exhibited p210 fusion transcripts with IS consistent with FISH-*BCR::ABL* including 3 cases with B-lymphoblastic phenotype, while 2 cases showed equivocal results. Of 8 cases with next generation sequencing performed, seven had pathogenic mutations detected, including mutations in *TP53* (5), *RUNX1* (3), *IDH1* (1), *NRAS* (1), *ASXL1* (1) and *SRSF2* (1). After therapy, 4 cases showed evidence of reversing to chronic phase with persistently high cells harboring *BCR::ABL* in a context of low blast count. Of note, reversed chronic phase was seen in both cases with <10% difference between

FISH-*BCR::ABL* and blast count at diagnosis. Follow-up ranged 3-23 months (median=10) with 6 patients died. Median survival is estimated at 12.5 months (95% CI: 2.3-22.8)

Conclusion

Ph+ acute leukemia with *BCR::ABL*-positive cells discordantly higher than blast count suggests cells besides blasts harbor this hallmark fusion gene and implies neoplastic transformation involve multilineages or occur at the level of pluripotent stem cell. Cytogenetic profile and mutation landscape as well as clinical outcome in our cases resemble those reported in CML blast phase. Therefore, Ph+ acute leukemia with evidence of multilineage involvement may represent de novo blast phase of CML with silenced chronic phase

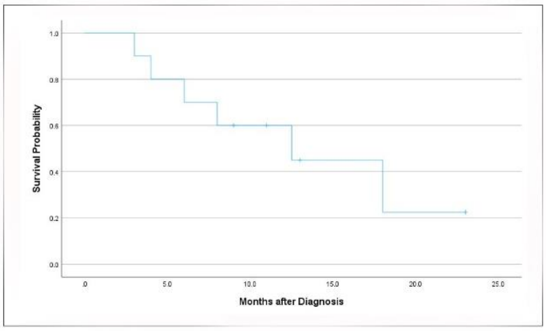

Figure 1.

Table 1.

Table 1. Clinicopathologic characteristics of 10 cases of de novo blast phase of chronic myeloid leukemia

Case #	1	2	3	4	5	6	7	8	9	10
Age/Sex	67/M	85/M	68/F	60/F	75/M	71/M	51/M	68/F	41/M	40/M
Present	Leukocytosis, weakness	Pancytopenia	Pancytopenia	Leukocytosis	Leukocytosis	Leukocytosis	Leukocytosis	Leukocytosis	Leukocytosis	Leukocytosis, splenomegaly
CBC	161.2/6.0/71,	3.6/7.4/56	4.2/7.2/32	46/9/14	263.2/11.2/56	66.1/13.1/104	45.6/8.7/ 46	94.92/61.5/108	55.6/8.4/150	120/10.2/78
Blood blasts	27%	41%	27%	1%	60%	10%	51%	17%	88%	51%
LN/Basophilia	Yes/No	Yes/yes	Yes/Yes	Yes/No	Yes/No	Yes/No	Yes/No	Yes/Yes	No/No	Yes/No
Marrow blasts	50%	20-25%	42%	90%	80%	15-20%	35%	46.5%	90%	52.2%
Marrow cellularity	95%	80%	95%	100%	80%	99%	100%	100%	90%	100%
Myeloid/megakaryocytes	Hyperplasia/normal	Decreased/few small forms	Decreased/decreased	Decreased/decreased	Decreased/decreased	Hyperplasia/hyperplasia	Hyperplasia/hyperplasia	Hyperplasia/hyperplasia	Decreased/atypia	Hyperplasia/normal
phenotype	B-lymphoblasts	Myeloblasts	Myeloblasts	Myeloblasts	Myeloblasts	Myeloblasts	Myeloblasts	Myeloblasts	lymphoblasts	Lymphoblasts
Cytogenetics	-7, Ph+	Complex, Ph+	Complex, Ph+	Complex, Ph+ (FISH)	Complex, Ph+	Ph+	der(19)t(17;19), Ph+	Complex, Ph+	Complex, Ph+	Complex, Ph+
FISH BCR::ABL	98.5%	71.5%	92% (blood)	96.5%	98.5%	95%	85%	95	98%	96%
RT-PCR for BCR-ABL	p210; IS % = 246.3283%.	P210, P190; IS% = 0.0071	p210; IS % = 126.8051	p210; IS % = 7.4620%.	p210; IS % = 96.2017%	p210; IS%= 75.6316%	p210; IS%= 53.2432.	p190 IS%=0.00987	P210; IS % = 100.000%	P210; NA
NGS mutation profile	No	TP53 (44.3%), TP53 (43.8%), SRSF2 (14.9%)	TP53 (70%), RUNX1 (35.9%)	TP53 (NA)	RUNX1 (NA)	RUNX1 (40.2%)	IDH1 (NA)	TP53 (91.3%), ASXL1 (56.7%), NRAS (46.2%)	NA	NA
Treatment	Dasatinib + chemotherapy	TKI + Azacitidine/ Venetoclax	Nilotinib + combination Chemotherapy	Dasatinib + combination Chemotherapy	Dasatinib + Decitabine	TKI + combination chemo (clinical trial)	Ponatinib + combination chemotherapy	TKI + combination chemotherapy	Dasatinib + combination chemotherapy	TKI + combination chemotherapy
Post induction CBC	-	0.5/8.1/81,	14.5/16.5/188	4.0/7.7/28	1.8/10.1/225	0.34/8/21	2.84/9/25	228.39/7.7/22	5.2/12.9/268	2.57/9.1/86
Blood blasts	-	0	0	0	0	0	0	48%	<1%	0
Marrow blasts	-	0	NA	1%	1%	4-5%	1%	40%	11%	<1%
Marrow cellularity	-	60%	NA	10%	50%	60%	65%	89%	50%	50%
Myeloid/megakaryocytes	-	Decreased/increased with small forms	NA	Decreased/decreased	Normal/normal	Normal/atypical	Normal/normal	Increased/increased with small forms	Normal/increased with small forms	Erythroid hyperplasia (67.5%)
Cytogenetics	-	NA	NA	46,XX[20]	46,XY[20]	46,XY[20]	46,XY[20]	NA	NA	NA
FISH BCR::ABL	-	73.5%	NA	17%	0	0	NA	93%	NA	85%
RT-PCR for BCR-ABL	-	NA	P210 IS % = 0.0739 (PB)	p210 IS % = 2.9994	p210 IS % = 0.1589	P210 IS% = 0.0695	P210 IS%= 0.1398	p190 IS% =0.00171	p210 IS % = 100.000%	P210 IS% = 12.8014
Subsequent treatment	-	Dasatininb	Nilotininb	Ponatinib	Dasatininb maintenance	HSCT	HSCT	HSCT	Plan for HSCT	Plan for HSCT
follow up (m)	4 months	8 months;	6 months	5 months	18 months	23 months	15 months	12.5 months	11 months	9 months
Outcome	Deceased	Comfort care; deceased.	CNS involvement; comfort care; deceased	Pleural myeloid Sarcoma; Comfort care; deceased	CNS relapse; Hospice; deceased	CR; alive	CR; alive	Deceased	Alive	Alive

M, male; F, female; CBC, complete blood cell count (leukocytes/hemoglobin/platelets) (leukocytes = $\times 10^3$/µl; hemoglobin = g/dL; Platelets = $\times 10^3$/µl); LN, left shifted neutrophilia; FISH Fluorescence in situ hybridization; RT-PCR, reverse transcription polymerase chain reaction; Ph+, Philadelphia chromosome; IS, International Scale; TKI, tyrosine kinase inhibitor; CNS, central nervous system; HSCT, hematopoietic stem cell transplant; NA, not available; CR, complete remission

EA4HP24-ABS-665

Acute erythroid leukemia post chemo-radiotherapy and autologous stem cell transplantation due to multiple myeloma

Prof. Gábor Méhes[1], Dr. Attila Mokánszki[2], Dr. Anikó Ujfalusi[3], Dr. Judit Bedekovics[4]

[1] University of Debrecen, Faculty of Medicine, Department of Pathology, Debrecen, Hungary; [2] University Of Debrecen, Faculty of Medicine, Department of Pathology, Debrecen, Hungary; [3] University Of Debrecen, Faculty of Medicine, Department of Laboratory Medicine, Debrecen, Hungary; [4] University Of Debrecen, Faculty of Medicine, Department of Pathology, Debrecen, Hungary

Background

The clinical impact of therapy related acute leukemias is increasing with the extension of cancer-related survival, however, its origins remain largely unknown. Acute erythroleukemia (AEL), a rare unfavorable type of myeloid neoplasia may also develop secondary to cytotoxic therapy. The disorder is featured by specific genetic alterations, most importantly multiple mutations of the *TP53* gene.

Principles/Methodology

We present two AEL cases arising after cytotoxic therapy and melphalan-based myeloablation/autologous peripheral stem cell transplantation (PSCT) due to multiple myeloma (MM). Potential mechanisms of leukemogenesis were investigated which include 1) the common origin of MM and AEL due preexisting preneoplastic hemopoetic stem cells (HSC), 2) the intramedullary survival of p53 deficient post-chemotherapy HSCs, 3) the reinoculation of mobilized autologous *TP53* mutated HSCs and 4) melphalan treatment-induced late onset myelodysplasia/leukemia with newly aquired *TP53* mutations.

Results

Preexisting MM bone marrow proved to be *TP53* wild-type configuration. The diagnosis of secondary AEL was suggested by masses of CD71+/E-cadherin+/CD34-/CD117- blast cell component and dysplastic morphology. Leukemic clones presented with complex karyotype and multiple *TP53* variants (three and two pathogenic variants per case). Only one archived autologous HSC sample (case 2) was available for retrospective NGS which lacked *TP53*-mutation.

Conclusion

After the exclusion of other major opportunities melphalan-based myeloablative cytotoxic therapy appeared to be the most likely inducer of secondary AEL diagnosed years after autologous PSCT of MM, the latter otherwise successfully treated.

EA4HP24-ABS-669

Determination of IgG4 myeloma in IgG myeloma cases and analysis of morphological, immunohistochemical, clinical and prognostic features

Dr. Zeycan Hacioglu[1], Dr. Betül K. Tüzün[2], Prof. Mine Hekimgil[1], PhD/MD Derya Demir[1], Nur Soyer[2], Prof. Nazan Ozsan[1]

[1] Ege University, Department of Clinical Pathology, Izmir, Turkey; [2] Ege University, Department of Haematology, Izmir, Turkey

Background

Multiple myeloma (MM) is a neoplasm characterized by multifocal infiltration of monotypic plasma cells in the bone marrow. IgG myelomas have 4 isoforms, G1, G2, G3 and G4. The rarest isoform is IgG4 myeloma. IgG4-related disease is a newly described entity. The manifestations of IgG4-related disease have been described in almost every organ system except bone marrow.

With this study, we aimed to define the characteristics of IgG4-secreting myelomas as a subgroup; we investigated the incidence of IgG4 myelomas among cases diagnosed as IgG myeloma; and searched for any association with IgG4-related disease.

Principles/Methodology

610 IgG MM cases diagnosed in Ege University Department of Pathology between 2010 and 2020 were reevaluated by immunohistochemical study (IHC) using IgG4 antibody. 20 cases (3.27%) were evaluated as IgG4 MM and we analyzed them in all aspects.

Results

In accordance with the literature, IgG4 myelomas were found to be more frequent in female patients; as 55% female and 45% male. Prior to MM diagnosis, 7% of IgG MM patients had been diagnosed to have 'plasmacytoma' and 11.1% of IgG myelomas had 'amyloidosis' either at the time of diagnosis or follow-up. Neither plasmacytoma nor amyloidosis were found in any of IgG4 MM patients. When compared to the given ratios for MM patients in literature, anemia (50%), myelofibrosis (5%), osteolytic bone lesions (65%) and C-myc positivity (5%) were found at low frequencies in IgG4 MM patients. Overall survival time for IgG4 MM according to gender was significantly different; with a 5-year overall survival of 80% for female and 20% for male patients. No clear relationship was found between IgG4-related disease and IgG4 myeloma.

Conclusion

When the results of 20 IgG4 MM patients were evaluated; none of them had plasmacytoma or amyloidosis prior to MM diagnosis at the time of diagnosis or during follow-up; the ratio of anemia, osteolytic bone lesions and myelofibrosis at the time of diagnosis were all at lower levels compared to given ratios for MM patients in the literature, and also the frequency of C-myc positivity by immunohistochemistry was low for IgG4 MM; with these results IgG4 MM cases may be considered to have better prognostic features; however, further studies including high number of IgG4 MM patients are needed for this conclusion.

EA4HP24-ABS-670

The molecular landscape of acute myeloid leukemia with *KMT2A* / *MECOM* / *NUP98* rearrangement diagnosed by RNA sequencing – a single center experience.

Dr. Martin Zacharias, Nikolaus Kratochwill, Dr. Fotini R. Vagena, Prof. Karl Kashofer, Prof. Gerald Hoefler

Medical University of Graz, Diagnostic and Research Institute of Pathology, Graz, Austria

Background

The latest WHO and ICC classifications for the first time recognize three AML types that are purely defined by rearrangements involving *KMT2A*, *MECOM*, or *NUP98*. Of note, these rearrangements tend to be cryptic on conventional karyotyping. Furthermore, the identification of fusion partners might provide valuable information for prognosis and disease monitoring. RNA sequencing should therefore be the gold standard for diagnosis but real-world data on the molecular landscape of these cases are still scarce due to their low incidence.

Principles/Methodology

We performed a retrospective single-center study including all AML cases with rearrangements involving *KMT2A*, *MECOM*, or *NUP98* diagnosed by RNA-based next-generation sequencing (NGS) between 2022 and 2024. RNA-based NGS was performed using the Archer FusionPlex Myeloid panel. Furthermore, DNA-based NGS was performed in all cases using an Ion Torrent Ampliseq panel that covers 49 genes relevant in myeloid neoplasms. Clinical and pathological metadata were retrospectively collected and correlated with sequencing results.

Results

We identified 11 consecutive AML cases with *KMT2A*, *MECOM*, or *NUP98* rearrangement (Table). 8/11 (72.7%) were men, 3/11 (27.3%) were women, and the median age was 52 years (range 6-85). The median blast count determined on bone marrow biopsy was 85% (range 25-98%). Bone marrow biopsy was also the most common specimen for molecular testing (7/11, 63.6%, both for RNA- and DNA-based NGS). The most commonly rearranged gene was *KMT2A* (7/11, 63.6%), followed by *MECOM* and *NUP98* (2/11, 18.2%, respectively), all of them showing a highly diverse repertoire of fusion partners. Intriguingly, one case harbored the *ZEB2::MECOM* fusion that has so far never been described in the literature. In 7/11 (63.6%) cases additional mutations could be detected by DNA-based NGS, comprising a plethora of different genes possibly influencing the biology and treatment of the disease.

Conclusion

Accurately diagnosing AML cases with defining rearrangements is clinically highly relevant but can be diagnostically challenging due to the rarity of these only recently defined entities and due to limitations of conventional karyotyping. Our real-world data indicate that RNA-based NGS can detect even exceedingly rare fusion events that might affect prognosis and treatment response. In addition to different fusion partners, the high diversity of co-mutations detected by concomitant DNA-based NGS might be an important factor to consider in future clinical trials.

Gender	Age	Diagnosis (WHO 2022)	Blast count (%, BM biopsy)	Specimen type for fusion testing	Fusion	Specimen type for mutation testing	Mutations
Female	61	AML with *KMT2A* rearrangement	70	BM biopsy	*KMT2A::MLLT1*	BM biopsy	No
Female	23	AML with *KMT2A* rearrangement	95	BM biopsy	*KMT2A::MLLT4*	BM biopsy	No
Female	38	AML with *KMT2A* rearrangement	95	BM biopsy	*KMT2A::MLLT3*	BM biopsy	*NRAS*, p.G12S (pathogenic), VAF: 2.81% / 2.54%
Male	63	AML with *KMT2A* rearrangement	80	BM biopsy	*KMT2A::MLLT3*	BM biopsy	*U2AF1*, p.Q157P (pathogenic), VAF: 20.62% / 20.85%
Female	52	AML with *KMT2A* rearrangement	90	BM biopsy	*KMT2A::SEPT11*	BM biopsy	*KRAS*, p.G13D (pathogenic), VAF: 43.28% / 45.75% *TET2*, p.I1340R (UV), VAF: 40.37% / 41.54% *FLT3*, p.Q575E (UV), VAF: 7.35% / 9.90%
Female	21	AML with *KMT2A* rearrangement	95	Blood	*KMT2A::AFF1*	Blood	No
Female	48	AML with *KMT2A* rearrangement	85	Blood	*KMT2A::MLLT3*	BM aspiration	No
Male	85	AML with *MECOM* rearrangement	25	Blood	*ZEB2::MECOM*	BM aspiration	*DNMT3A*, p.P904L (pathogenic), VAF: 48.04% / 46.54% *JAK2*, p.V617F (pathogenic), VAF: 96.71% / 96.94% *U2AF1*, p.Q157R (pathogenic), VAF: 44.82% / 46.01% *TET2*, p.Q1580* (likely pathogenic), VAF: 52.01% / 49.03%
Female	62	AML with *MECOM* rearrangement	25	BM biopsy	*ETV6::MECOM*	BM biopsy	*DNMT3A*, p.M403T (UV), VAF: 46.20% / 47.48%
Male	81	AML with *NUP98* rearrangement	80	BM aspiration	*NUP98::TNRC18*	BM aspiration	*IDH2*, p.R140Q (pathogenic), VAF: 43.72% / 45.31% *DNMT3A*, p.C532S (likely pathogenic), VAF: 46.35% / 40.27%
Female	6	AML with *NUP98* rearrangement	98	BM biopsy	*NSD1::NUP98*	BM biopsy	*WT1*, p.P377Rfs*7 (likely pathogenic), VAF: 20.15% / 34.63% *FLT3*, p.L601_K602insGYLYDL (pathogenic), VAF: 24.00% / 32.38%

Overview of AML cases with KMT2A / MECOM / NUP98 rearrangement

EA4HP24-ABS-486

Tackling the problem of a small divergent aberrant clone in predominant AML or ALL cases?

Barina Aqil, Kristy Wolniak, Yi-Hua Chen, Qing Chen, Juehua Gao

Northwestern University, Pathology, Chicago, USA

Background

Mixed Phenotype acute leukemia (MPAL) is characterized by >1 lineage marker on a single blast population (biphenotypic leukemia) or ≥2 lineage leukemic populations (bilineal leukemia). Apart from the requirement of total 20% blasts, the WHO classification does not provide reference on how to address very small aberrant clones (≤5%) identified in seemingly straightforward acute myeloid leukemia (AML) or acute lymphoblastic leukemia (ALL).

Principles/Methodology

Retrospective data search is performed from 2017 to 2024 and 36 cases of MPAL are identified. Comparison between two groups [MPAL with >5% (M>5%) and MPAL with ≤5% (M≤5%) two lineage blasts] is assessed based on clinical and genetic findings along with treatment and survival outcome.

Results

There are 27 MPAL-B/M, 6 MPAL-T/M and 2 MPAL-T/M/B. Among cases of MPAL-B/M, 4 cases have a predominant B-lymphoid blast population with a small (≤5%) myeloid blasts and 4 cases with mainly myeloid blast population and ≤5% B-lymphoblasts. There is no difference between the groups based on clinical parameters (age, gender, WBC, Hb, PLT counts) and genetic mutations. Somatic mutations found within the two groups are a mixture of those commonly seen in both AML and ALL, AML-associated genes (*FLT3, ASXL1, RUNX1, CSF3R, SETBP1, BCOR, SF3B1, TET2, JAK2, IDH2, TP53*) and the ALL-associated genes (*PHF6, CDKN2A*). T/myeloid MPAL cases show alterations in signaling pathways, including the RAS and JAK-STAT pathways (*NRAS, JAK1, JAK3*), transcription factors (*RUNX1*) and epigenetic regulators (*DNMT3A, IDH2*).

M>5% group has a more complex karyotype (25%) and *BCR::ABL1* fusion (25%) in comparison to M≤5% (13% and 13%) respectively. In our study no specific treatment approach was taken between the two groups and ranged from ALL, AML, and hybrid ALL-AML protocols (such as FALG plus idarubicin with vincristine and prednisone or hyper-CVAD regimens). Cases with MPAL with *BCR::ABL1* received a tyrosine kinase inhibitor. Disease relapse (20% vs 13%) is seen more frequently in M>5% vs M≤5% group. The survival outcome is not different between the groups.

Conclusion

Gene mutations found within the two groups of MPAL are a mixture of both AML and ALL and as such not helpful to define a lineage. Optimal therapy remains elusive. Given no different survival outcome, it is suggested that cases with aberrant clones representing <5%, require a diagnosis based on the major leukemic population with a descriptive modifier mentioning the small divergent clone till more data becomes available.

EA4HP24-ABS-516

B-cell antigen expression in acute leukemia with *MECOM* gene rearrangement

PhD/MD Alireza Torabi, PhD/MD David Gajzer, PhD/MD Jonathan Fromm, PhD/MD Sindhu Cherian

University of Washington, Hematopathology, Seattle, USA

Background

Rearrangement of *MDS1* and *EVI1* complex locus, is a defined genetic abnormality of acute myeloid leukemia (AML) based on the WHO and ICC classifications for hematolymphoid malignancies. The rearrangement is associated with a high-grade myeloid neoplasm/AML and often dysplastic megakaryocytes. Unlike AML with t(8;21), aberrant expression of B-cell antigens is not described as a characteristic of myeloid neoplasm with inv(3) and has been rarely reported. In this study, we report 5 cases of acute leukemia with expression of myeloid and B-cell antigens, raising the consideration of mixed phenotype acute leukemia (MPAL B/Myeloid) harboring the *MECOM* gene rearrangement.

Principles/Methodology

A search was conducted of the hematopathology database of the University of Washington for mixed phenotype acute leukemia cases. Five cases with *MECOM* gene rearrangement were identified. Demographic data, immunophenotype, cytogenetic and molecular findings, and response to treatment were evaluated.

Results

Demographic and cytogenetic findings of the patients are listed in table 1. Four patients were presented with leukocytosis, while one had leukopenia. While 3 patients had thrombocytopenia, one had a normal platelet count and one thrombocytosis. CD34-positive blast populations in the blood and/or bone marrow were between 17-92%. All 5 patients had dysplastic megakaryocytes in the bone marrow. Monosomy 7 was present in 4 cases. In all five cases, the CD34 expression on the blast population was bright with dim to negative CD38 expression, indicating a stem cell or primitive phenotype. Cytoplasmic MPO expression was very dim to negative in all cases, while expression of B-cell markers were more prominent, comprising from 10% to 77% of the blast population. TdT was positive in 3 cases and cCD3 expression was dim in only one case. Pax5 immunostain was performed on 2 cases and both highlight a subset of the blast population.

Conclusion

MECOM is a transcription factor that is involved in cell differentiation and proliferation. Its overexpression can skew differentiation of hematopoietic stem cells towards

megakaryocytes. Presence of *MECOM* gene rearrangement excludes the diagnosis of immature B or T lymphoid malignancies. CD7 expression can be frequently seen in this entity, while expression of B-cell antigens has rarely been reported. The significance of these observations is unclear and whether the *MECOM* gene rearrangement can also upregulate B-cell programing in the stem cell subset needs further studies.

Case	Sex/Age	WBC	Hgb/Plt	CD34+ blast %	Karyotype	NGS	Response to treatment
1	F/33	31k	8.5/242k	73.5%	inv(3), -7	*PTPN11* VAF39%, *WT1* VAF4%, *FLT3-TKD*	Alive/ Positive MRD / Refractory to multiple regimens
2	F/35	100k	8.4/37k	71.1%	46,XX,t(2,3)(p23;q27),der(7)del(7)(p11.1)del(7)(q11.1)[14]/46,XX,t(2;3)(p23;q27),-7[5]/46,XX[1]	*NRAS* VAF 43%	Alive/ positive MRD / Refractory to multiple regimens
3	M/41	84k	7/18k	92%	inv (3), -7	*FLT3-TKD* VAF45%	Alive (3 years post-transplant) Negative MRD
4	M/67	56.7k	6.8/727k	85%	46,XY,t(2;22)(q31;q12),inv(3)(q21q26.2)[20]	Negative for *NPM1, JAK2, BCR/ABL, FLT3, CEBPA* mutations	Died of disease
5	M/80	3.02k	8.8/126k	17%	44-46,X,-Y, t(3;3)(q21;q26.2), -7, del(12)(q24.1q24.3),del(15)(q15q22)[cp19]/46,XY[1]	None identified	Alive

Case	TdT/cCD3	CD5/CD7	CD19/CD79a	CD10/CD22	CD13/CD33	CD34/CD38	CD117/cMPO	Pax5
1	ND/Neg	Low/Low	Var/Var (20%)	Neg/Var	+/+	Inc/Dec	Var/dim	Pos
2	+/Neg	Low/Low	Var/Var (24%)	Var/Var	+/Dec	Inc/Dec	Var/dim	Pos/weak
3	+/Neg	Neg/Neg	Var/Var (77%)	Neg/Var	+/+	Inc/Dec	Var/dim	ND
4	Neg/Low	Inc/Low	Low/Var	Neg/Low	+/+	Inc/Dec	Dec/dim	ND
5	Dim/Neg	Low/subset	Var/Low	ND/Low	+/Dec	Inc/Dec	Inc/dim	ND

Table
Demographic, CBC, blast count and cytogenetic/next gene sequencing and immunophenotype of the blast population by flow cytometry. (MRD: minimal/measurable residual disease; ND: Not done, Var: variable, Dec: decreased, Inc: increased)

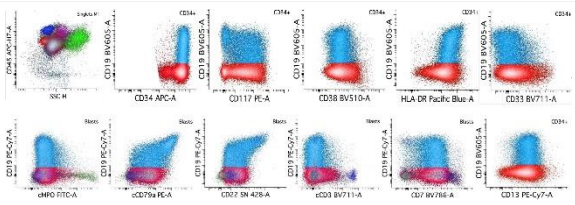

Figure
Peripheral blood flow cytometry (patient 2). Plots reflecting the blast gate (CD45/SSC low) and CD34+ gate. Note the bright expression of CD34 and low to negative expression of CD38.

EA4HP24-ABS-517

Acute Undifferentiated Leukemia, am I a real entity? What's the best treatment approach?

Barina Aqil

Northwestern University Feinberg School of Medicine, Pathology, Chicago, USA

Background
Acute undifferentiated leukemia (AUL) is a rare acute leukemia which is included in acute leukemia of ambiguous lineage in WHO. It is characterized by expression of stem cell markers (CD34, HLA-DR, TdT) with at least one myeloid-associated antigen (CD13, CD33, CD117) expression but lacks lineage-specific antigens (MPO, s/cyto CD3, CD19, CD10, CD79a, s/cyto CD22 and monocytic).
Principles/Methodology
Retrospective data search is performed for the past 5 years (2019-2024) along with immunophenotypic re-evaluation by flow cytometry/immunohistochemistry and 5 cases of AUL are identified. Clinical, cytogenetic and molecular data is collected along with survival outcome (OS).

Results

The study group consists of 3 males and 2 females with a mean age of 61 years (32-74 years) (Figure 1). All cases (100%) were CD34 positive and 4/5 (80%) cases showed TdT and CD7 expression. Cytogenetic analysis showed del 20q, trisomies of chromosomes 8, 10, 13 and one case of t(9;22). The somatic mutations include epigenetic regulators (*ASXL1, BCOR, IDH2, DNMT3A, TET2*), transcription factors (*RUNX1, IKZF1*), spliceosome (*SRSF2*) and signaling pathway (*FLT3*). 60% cases (3/5) received FLAG-IDA-Ven (fludarabine, cytarabine, granulocyte colony stimulating factor and venetoclax). 2 cases (67%) relapsed with mean progression free survival (PFS) of 344 days and one died (33%). Case with t(9;22) was treated with dasatinib (TKI) with clinical remission (CR) and is alive. Decitabine with venetoclax was given to one patient with multiple relapses but deceased. Out of the 3 alive patients 2 received stem cell transplant and are in CR. The mean OS for the group is 1215 days. 2/3 relapsed cases (67%) showed different phenotype, one with a subset of blasts expressing plasmacytoid dendritic cell (PDC) markers and the other with prior t(9;22) with B-cell antigens.

Conclusion

Due to the advancements in immunophenotyping, the incidence of AUL has decreased. Although this study has few cases but mostly demonstrate mutations associated with myeloid neoplasms. Only 1 case had *IKZF1* mutation which is seen in lymphoblastic leukemia. The study raises the point:can we combine immunophenotype with genetics for precise classification of this entity into myeloid or lymphoid lineage? In addition, AUL has no well-defined standard treatment ranging from AML or ALL protocols. The majority of patients in our study received AML regimen along with venetoclax. Targeted (TKI) and selected therapies (venetoclax) may show improvement in prognosis.

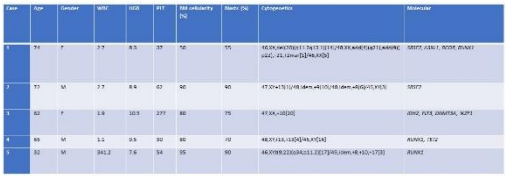

Table 1: Clinicopathologic parameters of the study group

EA4HP24-ABS-526

Shades of ERG: Strong, vascular-like ERG expression may help differentiate Histiocytic Sarcoma from Myeloid Sarcoma with Monocytic/Monoblastic differentiation.

Dr. Jackson A. Barbosa, Dr. Aline Ueda, Dr. Denise D.C. Pasqualin, Dr. Ana Carolina D.B. Lyra

Hospital Israelita Albert Einstein, Anatomia Patológica, São Paulo, Brazil

Background

ERG is a known marker of myeloid lineage. In the appropriate setting, strong, vascular-like ERG expression could be indicative of Myeloid Sarcoma and should prompt additional molecular

investigation. We report a case of Myeloid Sarcoma with Monocytic / Monoblastic Differentiation without peripheral blood or bone marrow involvement that illustrates this idea.

Principles/Methodology

In recent years, patterns of ERG expression have been characterized in hematolymphoid tissues. This marker is not totally specific for determining histogenesis as it is expressed in vascular neoplasms, in many types of carcinomas, in myeloid and even in some non-myeloid hematologic malignancies. In bone marrow, it is characteristically positive in the myeloid lineage and negative in the erythroid lineage. In our experience with clone EP111, we noticed not only this, but also consistent weak staining in megakaryocytes and macrophages.

Results

The case involves a toddler with a cervical mass. Clinically, it consisted of an isolated 4 cm cervical mass without systemic symptoms and without significant findings in peripheral blood and bone marrow. Histologically, the lesion consisted of sheets of round, atypical cells positive for CD45, CD4, CD14 (focal), CD163, CD68, and negative for MPO, that would fit the diagnosis of Histiocytic Sarcoma. However, weak CD34 positivity was noted in a few areas (which could have easily been missed in a core biopsy) together with a zonal pattern with negative CD14/high Ki67 in the periphery and positive CD14/low Ki67 in the center, consistent with monoblastic and monocytic components. Interestingly, strong, diffuse vascular-like ERG expression was observed in both regions. Additional molecular studies showed MLL-MLLT10 (AF10) fusion.

Conclusion

In some cases, distinguishing between Monoblastic/Monocytic Sarcoma and Histiocytic Sarcoma requires molecular studies. The presence of strong, endothelial-like ERG expression should raise a red flag for the possibility of Myeloid (Monoblastic/Monocytic) Sarcoma, even in the absence of peripheral blood or bone marrow disease. Additional studies are needed to explore the utility of ERG in such scenarios.

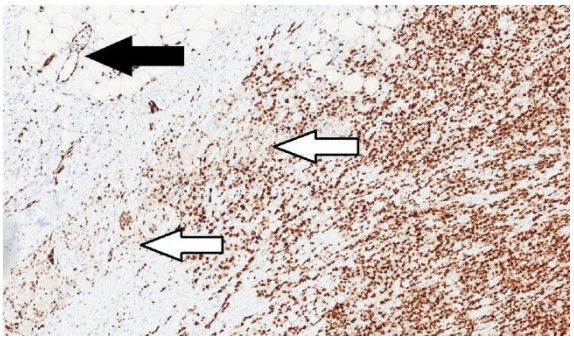

ERG expression nuances
Strong ERG expression in myeloid sarcoma (right half of the image) and in endothelial cells (black arrow). Weak ERG expression in reactive histiocytes / multinucleated giant cells (white arrows), which were prominent, as this specimen was obtained from a re-excision.

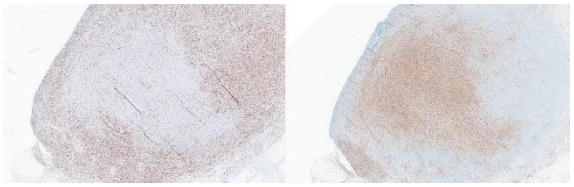

Monoblastic and Monocytic components
Ki67 (left) shows a high proliferation rate at the periphery and a low proliferation rate in the center, while CD14 (right) is negative at the periphery and positive in the center.

EA4HP24-ABS-533

SLC38A1 A potential prognostic factor in Acute Lymphoblastic Leukemia

Dr. Samaneh Boroumand Noughabi[1,2], M.Sc./M.A. Maryam Khajavi[1], Prof. Hossein Ayatollahi[1,2], Prof. Mohammad Reza Keramati[1,2], M.Sc./M.A. Arefeh Mazhari[1], M.Sc./M.A. Maryam Sheikhi[2], Prof. Habibollah Esmaily[3]

[1] Mashhad University of Medical Sciences, Hematology and Blood banking, Mashhad, Iran; [2] Mashhad University of Medical Sciences, Cancer Molecular Pathology Research Center, Mashhad, Iran; [3] Mashhad University of Medical Sciences, Social Determinants of Health Research Center, Mashhad, Iran

Background

Solute carrier family 38 member 1 (SLC38A1) is a principal glutamine transporter that is the main metabolic fuel and nitrogen source in tumor cells. Overexpression of SCL38A1 has been found in many solid tumors and was significantly linked to tumor metastasis and advanced disease stage. It has been rarely investigated in hematologic malignancies. Hence, this study aimed to assess the expression status and correlation of SLC38A1 with disease features and clinical outcomes in acute lymphoblastic leukemia (ALL) patients.

Principles/Methodology

This cross-sectional study included 70 newly diagnosed ALL cases and 30 age and sex matched control group. Quantitative real-time polymerase chain reaction (QRT-PCR) was used to evaluate the expression level of SLC38A1. Statistical analysis was done by IBM SPSS software version 20.

Results

ALL patients composed of 27 (38.6%) females and 43(61.4%) males with mean age of 6.8±5.6 years and in the control group, the mean age was 8.8 ± 8.3 years, and female/male ratio was 12/18. SLC38A1 was found to be overexpressed in ALL patients compared to controls (P=0.019) (Figure 1). According to median expression level of SLC38A1, ALL patients were stratified into high and low groups. Kaplan-Meier analysis indicated that patients with SLC38A1 ^{high} had shorter overall survival (OS) compared to SLC38A1 ^{low} patients (P=0.007) (Figure 2). The multivariate cox regression analysis demonstrated that age (HR=1.195, 95%-CI=1.100-1.299, P<0.001) and high SLC38A1 expression (HR=2.718, 95%-CI=1.086-6.797, P=0.03) were independent risk factors associated with shorter OS.

Conclusion

Our results indicated that SLC38A1 was upregulated in ALL patients and its high expression was an unfavorable prognostic factor for OS. It may indicate that SLC38A1 could serve as an independent biomarker of survival in ALL patients and may be used as a therapeutic target.

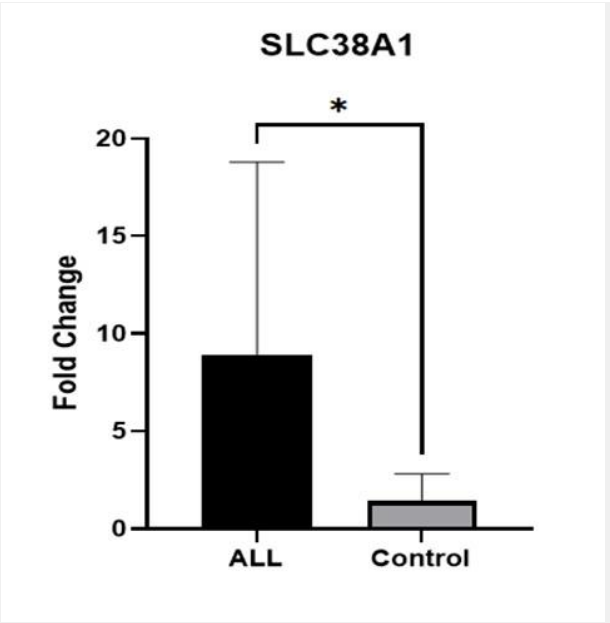

Figure 1
Expression of SLC38A1 in patients and controls. Expression of SLC38A1 in ALL patients is significantly higher compared with corresponding controls. **Abbreviations**: SLC38A1: Solute Carrier Family 38A1; ALL: Acute Lymphoblastic Leukemia.

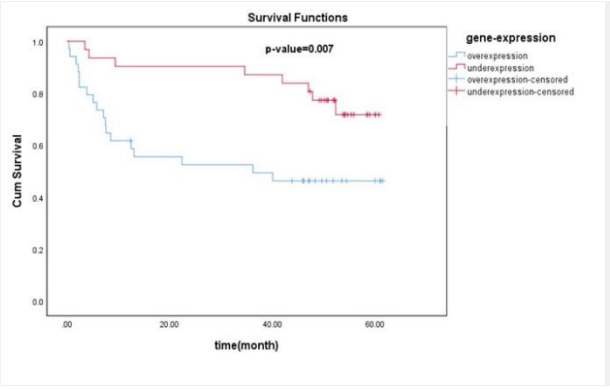

Figure 2
Kaplan-Meier curve according to SLC38A1 expression status for comparison of overall survival in ALL patients. Overall survival was compared between the two groups using the log-rank test. Survival analysis exhibits a lower overall survival in patients with high SLC38A1 expression compared to the SLC38A1 low-expressed group. **Abbreviations:** Cum: Cumulative; SLC38A1: Solute Carrier Family 38A1; OS: overall survival; ALL: Acute Lymphoblastic Leukemia.

EA4HP24-ABS-548

An AI-Driven Software Tool for Diagnosing Myeloid and Lymphoid Neoplasms

Dr. Kirill Karlin[1,2], **Dr. Ping Mao**[3,2]

[1] Beth Israel Deaconess Medical Center, Harvard Medical School, Department of Pathology, Boston, USA; [2] CertaintyDx, Boston, USA; [3] Brigham and Women's Hospital, Harvard Medical School, Department of Pathology, Boston, USA

Background

In the dynamic landscape of hematopathology, accurate classification of myeloid and lymphoid neoplasms and mixed phenotype acute leukemias often presents diagnostic challenges. Efficient integration of multi-modal, longitudinal data with the latest WHO and ICC classification systems and evolving risk prognostication scores remains a significant unmet need.

Principles/Methodology

We have developed an AI-powered software tool that employs advanced language models to interpret data from unstructured pathology reports. This tool utilizes a comprehensive data extraction pipeline

that integrates morphology, cytogenetics, NGS, flow cytometry phenotype, and IHC information across multiple time points. The system redacts protected health information (PHI), identifies key missing data, and consolidates the structured data for accurate diagnosis retrieval. This tool facilitates automated, precise differential diagnosis formulation and disease prognostication by embedding classification systems (WHO-HEME5 and ICC 2022) and risk stratification models into a vector database.

Results

Performance testing confirms that our software effectively extracts and synthesizes pertinent clinical and multi-modal pathology data from unstructured reports and interprets these data using the WHO and ICC classification systems to establish differential diagnoses. This tool markedly improves the speed and accuracy of generating diagnoses, especially for complex hematologic disorders.

Conclusion

Initial outcome data demonstrate that our software tool significantly enhances diagnostic accuracy and clinical workflow efficiency. We provide a user-friendly web interface that supports rapid, intuitive data upload and entry. We invite the hematopathology community to test this software further to validate its utility and robustness in real-world clinical scenarios.

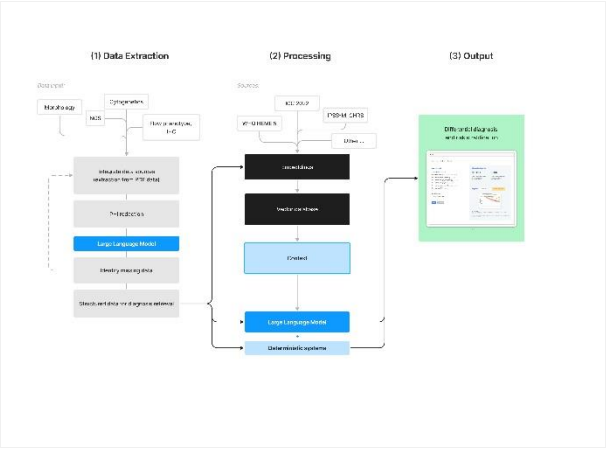

Workflow of an AI-Driven Diagnostic Tool for Myeloid and Lymphoid Neoplasms
The workflow of an AI-driven diagnostic tool for myeloid and lymphoid neoplasms is shown. It consists of three stages: data extraction, processing, and output. In the extraction stage, multimodal data from morphology, cytogenetics, NGS, flow phenotype, and IHC are integrated and structured. The processing stage uses embeddings and a vector database with different classification and prognostication systems supported by large language models and deterministic systems. The output stage delivers differential diagnosis and risk stratification for clinical decision-making.

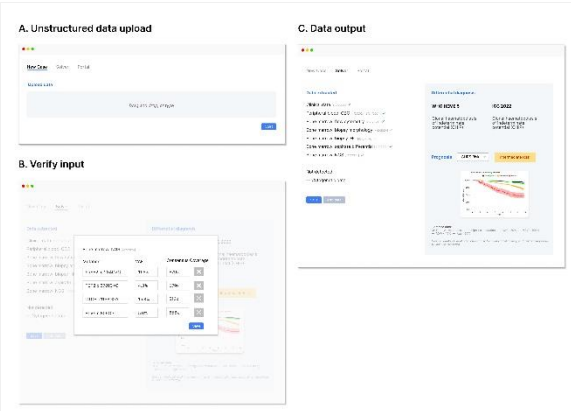

User Interface for AI-Driven Hematologic Diagnosis
User interface of an AI-driven diagnostic tool for hematologic neoplasms. A) Demonstrates the unstructured data upload feature, where users can drag and drop unstructured files. B) Highlights the input verification process. C) Details the final data output, including differential diagnosis and risk stratification based on WHO HEME 5 and ICC 2022 classifications, showing an example output with risk stratification. This interface streamlines data entry and verification and supports clinical decision-making.

EA4HP24-ABS-558

Mixed phenotype acute leukemia with higher levels of eosinophils: a case report

M.Sc./M.A. Xiaona Zuo[1], Jinlong Xu[2], Ting Zhang[1], Yijun Wang[1], M.Sc./M.A. Jing Deng[1], Dr. Jing Pan[2], Prof. Cuiling Liu[3], Prof. Zifen Gao[1,3], Prof. Yanrong Liu[1,4], Dr. Ligai Guo[1]

[1] Beijing GoBroad Hospital, GoBroad Diagnosis Center, Beijing, China; [2] Beijing GoBroad Hospital, Department of Hematological Tumor Immunotherapy, Beijing, China; [3] Peking University Third Hospital, Department of Pathology, Beijing, China; [4] Peking University People's Hospital, Institute of Hematology, Beijing, China

Background

A 20-year-old male presented to hospital with about 1-month history of low-grade fever, fatigue, multiple enlarged lymph nodes on clavicles (both left and right sides), and hepatosplenomegaly on 25th, April. Routine blood examine: white blood cell (WBC) count 13.29×10^9/L, eosinophil count 5.14×10^9/L (38.7%).

Principles/Methodology

Bone marrow smear and biospy.

Results

On bone marrow smear evaluation 32.5% eosinophil cells and 22.5% unclassified cells were detected.

Flow cytometry detected 6.51% abnormal cells, with large FSC, positive for CD7, CD13, CD19, CD33, CD38, CD79a, CD123, HLA-DR, $cMPO^{dim}$, negative for other makers, and diagnosed MPAL-B/My, also found 33.22% eosinophil cells. There were 4.15% abnormal cells and 42.21% eosinophil cells in blood, shared the same phenotype with bone marrow.

Bone marrow biopsy found more than 80% atypical cells, IHC showed positive for CD19, LMO2, PAX5, negative for CD34, CD117, TdT, CD20, MPO. Consided as B-ALL.

The bone marrow karyotype was normal. FISH tests were negative. No fusion gene was detected by NGS . PCR-TCR determine TCRG rearrangement.

The final diagnosis for this patient was B-ALL by the first hospital, and treated with VP regime, but the WBC got higher during chemotherapy (26.1×10^9/L, with 45.9% eosinophil cells). So, the patient went to our hospital with high fever. Routine blood examine: WBC 25.37×10^9/L, eosinophil count 10.28×10^9/L.

Bone marrow smear found 2.5% unclassified cells and 45% eosinophil cells, while in blood 1% unclassified cells and 28% eosinophil cells.

Flow cytometry found 2.96% abnormal cells, positive for CD7, CD13, CD19, CD33, CD38, $cMPO^{part}$, negative for others, 42.59% eosinophil cells also found, the diagnose was AML.Reviewed the bone marrow biopsy and added some markers, there were more than 80% atypical cells (Fig.1), IHC showed positive for CD7, CD19, CD38, LMO2, PAX5, negative for CD34, CD117, TdT, CD22, CD10, CD20, CD79a, CD79b, CD3, CD13, CD33, MPO.

Conclusion

The integrated diagnosis for this patient was: MPAL-B/My, but there are still different opinions among experts in flow cytometry and pathologist about the diagnosis of B-ALL.It's seldom to see MPAL with high level eosinophil cells, so we presented this case report and also want to discuss with other pathologists about the diagnosis.

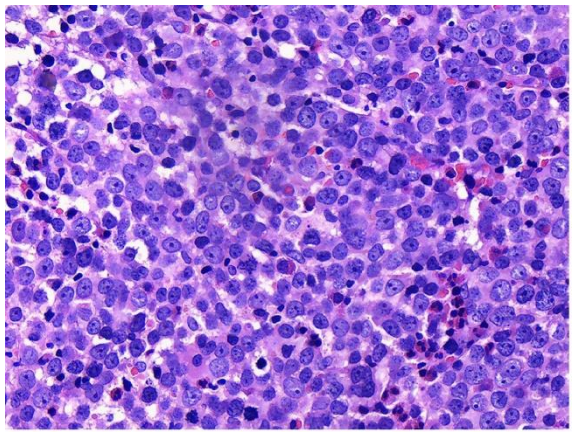

Fig.1 Bone marrow biopsy
HE×400

EA4HP24-ABS-560

CD142 is Overexpressed in Acute Promyelocytic Leukemia: A Study of 80 Cases by Immunohistochemistry

M.Sc./M.A. student Lana Koubaitary[1], Dr. Mohammad A. Al-zyoud[1], Dr. Maher Sughayer[2], Prof. Tariq N. Aladily[1]

[1] The University of Jordan, Department of Hematopathology, Amman, Jordan; [2] King Hussein Cancer Center, Department of Pathology, Amman, Jordan

Background

Acute promyelocytic leukemia (APL) is a subtype of acute myeloid leukemia (AML) characterized by t(15;17)(PML;RARA) mutation and a high incidence of disseminated intravascular coagulation (DIC). Several mechanisms were proposed to explain coagulopathy, among which is the secretion of tissue factor (TF) by leukemic cells. This study aims to survey the expression of CD142, or TF, on leukemic cells of APL by immunohistochemistry in comparidson with other types of AML.

Principles/Methodology

The archives of pathology at Jordan University Hospital and King Hussein Cancer Center were retrospectively searched for APL and AML cases. Formalin-fixed paraffin-embedded blocks were retrieved, cut and stained with CD142 (monoclonal antibody from Bio SB Inc, clone BSB-143). A cutoff of ≥1% membranous and/or cytoplasmic staining was considered positive, as normal bone marrow was consistently negative. The positive results were further divided to diffuse (>90%), and focal (1-90%). Relevant clinical data of patients' age, sex, DIC presence, and follow-up were collected. Fisher's exact test was used to examine the statistical difference. A P-value of 0.05 was set as significant.

Results

A total of 80 cases of APL and 40 cases of AML were included in the study. In APL, there were 39 (49%) male and 41 (51%) female patients, with a range of age from 3-76 years (mean: 37.5). CD142 was positive in 36 (45%) of APL cases, compared to only 1 (2.5%) of AML cases ($P < 0.00001$). In APL, the positivity was diffuse in 15 (42%) and focal in 21 (58%) of cases. Within APL, the expression of CD142 was correlated with the clinical evidence of DIC ($P = 0.003$).

Conclusion

CD142 is overexpressed in APL compared to other types of AML. This study provides morphologic evidence of the involvement of TF in APL-associated coagulopathy. Yet, other initiating factors may play a role in the emergence of coagulopathy in APL, as some CD142-negative cases developed DIC. A future study to examine the expression of other suspected factors such as annexin-II, tumor necrosis factor, interleukin-1 and platelets activating factor is recommended.

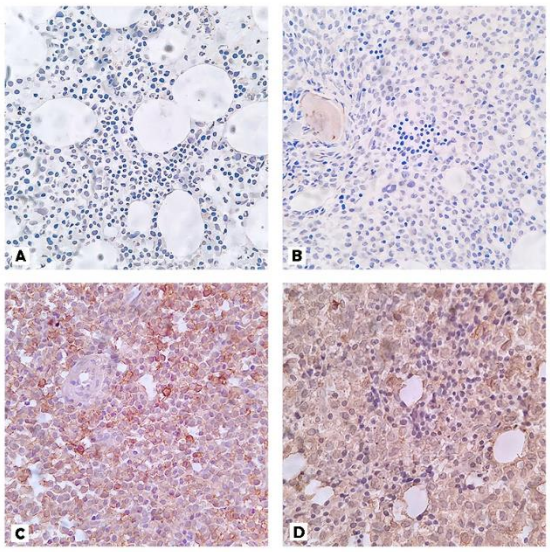

A comparison between positive and negative CD142 expression

(A) Normal hematopoietic cells are negative for CD142. (B) A case of APL that is negative for CD142. (C) A case of APL showing strong membranous and cytoplasmic positivity to CD142. (D) A single case of AML in our series that was positive to CD142.

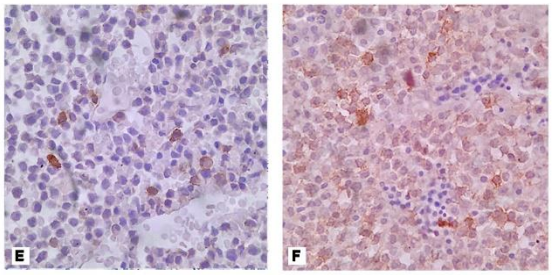

A comparison between focal and diffuse expression of CD142 in APL

(E) This case of APL shows positive expression in a few scattered leukemic cells only (Focal). (F) A case of APL showing diffuse positive expression, note the negative normal cells in the background.

EA4HP24-ABS-572

Acute Lymphoblastic Leukemia with T- and B- Lineage Defining Markers

Dr. Sa A. Wang, Dr. Shuyu E-Shuyu, Dr. Fatima Jelloul, Dr. Karen Nahmod, Dr. L. Jeffrey Medeiros

MD Anderson Cancer Center, Hematopathology, Houston, USA

Background

In the diagnosis of acute lymphoblastic leukemia (ALL), cytoplasmic CD3 defines T- lineage, and CD19 plus another B-cell marker (CD22, CD79a) defines B-lineage. However, some ALL cases express both B and T-lineage markers making it challenging to assign lineage.

Principles/Methodology

We screened all cCD3+ ALL and identified 23 cases (around 5-10%) where the lymphoblasts expressed ≥10% CD19. The B- and T- markers were assessed by flow cytometry immunophenotyping and immunohistochemistry, and an expression by 10-50% of lymphoblasts was scored as partial and ≥50% as substantial. B and T-cell clonality were assessed by PCR and or NGS (ClonoSeq); mutations were assessed by targeted NGS, and fusions by FISH or OGM.

Results

cCD3 was substantial in 17 and partial in 6. CD19 expression was positive in all (substantial in 11), CD79a in 16/21 (76%, 10 substantial), CD22 in 5/23 (22%, 3 substantial) and PAX5 in 12/21 (57%, half substantial). According to the current lineage assignment (CD19 substantial plus CD79a and/or CD22; if CD19 weak, CD22+CD79a+), 9 (39%) cases fulfilled the criteria for MPAL B/T-ALL.

Clonal *IGH* rearrangement was detected in 3/21(14%) cases, and clonal *TRG/TRB* in 15/23(65%). T-ALL characteristic genetic abnormalities were detected in 9 patients, including *NOTCH1* mutations (8/21, 38%), *JAK3* (4/21, 19%), *TLX::BCL11B*, *TRB::HOXA13* and *SPTAN1::NUP214* (one each). Combining immunophenotype with molecular genetics, only 4 cases were considered as true mixed B/T-ALL, including 2 bilineal MPAL, and remarkably all 4 were blast crisis of a myeloproliferative neoplasm (MPN) (3 CML and 1 primary fibrosis). The other 19 cases were ETP (n=17) and near ETP (n=2). In addition to CD19, other B-markers were also expressed, including CD79a (12/17) and Pax5 (9/17), but rarely CD22 (1/19). No cases had clonal *IGH*. 11/19 (57%) had clonal *TRG/TRB*, and 9 had T-ALL characteristic genetic abnormalities including 3 with no *TRG/TRB* clonality. All patients were treated with high dose chemotherapy; 12 also received transplant. CD19 was stably expressed in residual/relapse/refractory cases (n=16/17).

Conclusion

Our data show that true mixed B/T-ALL is extremely rare, occurring mostly in cases of lymphoblastic crisis of MPN. Instead, aberrant B cell markers, especially CD19, CD79a, PAX5 and rarely CD22, may be expressed in a subset of T-ALL, mostly in ETP ALL. A substantial proportion of these T-ALL cases do not carry *TCR* rearrangement, indicating a very primitive stem cell or common lymphoid progenitor origin.

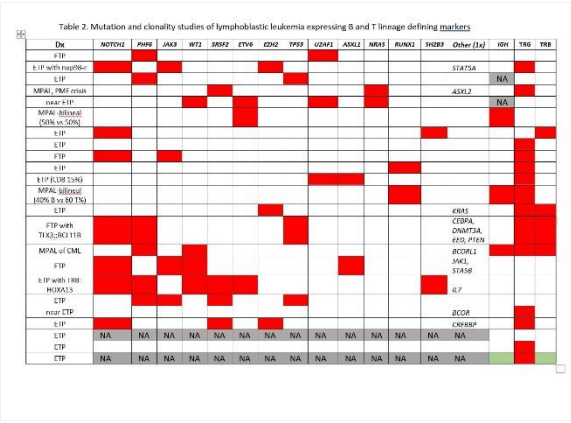

Figure 2

EA4HP24-ABS-597

BCR::ABL-1 positive Early T- cell precursor lymphoblastic leukemia/lymphoma (ETP-ALL): case report and awareness of a rare acute leukemia with unique genetic findings.

Dr. Sara Javidiparsijani[1], Dr. Theresa C. Brown[2], Dr. Joel F. Gradowski[1]

[1] Methodist University Hospital, Pathology/ Hematopathology, Memphis, USA; [2] Pathgroup, Molecular oncology/Cytogenetics, FISH and Arrays, Nashville, USA

Background

In the most recent WHO, BCR::ABL-1 rearrangement has been associated with multiple hematological malignancies includiing chronic myeloid leukemia (CML), acute myeloid leukemia, B lymphoblastic leukemia/lymphoma and mixed phenotype acute leukemias. We are reporting a case of early T cell precursor lymphoblastic leukemia/ lymphoma (ETP-ALL) with BCR::ABL-1 rearrangement.

Principles/Methodology

71 y/o male with multiple medical conditions including severe congestive heart failure presented with diffuse lymphadenopathy and hepatosplenomegaly. His peripheral smear shows mild leukocytosis, no anemia or thrombocytopenia and 64% blasts which prompted flow cytometry, lymph node and bone marrow biopsies.

Results

Flow cytometry results from peripheral blood, lymph node and marrow show large population of blasts with the following immunophenotype: CD34 (+), CD117 (-), CD13 (+), CD33 (+), HLA-DR (-), CD16 (-), CD11b (+), CD15 (subset +), CD64 (-), CD14 (-), CD10 (-), CD19 (-), CD2 (-), CD3 (-), CD4 (-), CD8 (-), CD7 (+), CD5 (+ in 57% of the cells), CD56 (-), CD1a (-), cytoplasmic CD3 (+), cytoplasmic CD79a (+), MPO (-), CD20 (-), CD22 (-), cytoplasmic CD22 (-), TDT (-). Tissue examination show extensive lymph node and bone marrow involvement by blasts with the same immunophenotype (CD34 positive, CD3 positive, MPO negative). Cytogenetics show: BCR::ABL-1 and a complex male karyotype including t(9;22). Molecular studies show p190 variant.

Conclusion

The immunophenotype show definite T cell lineage by cytoplasmic CD3 positivity by flow cytometry and lack of myeloid lineage (MPO and monocytic markers negativity) and B cell lineage (negative CD19, CD10, CD22) markers. The blasts express some myeloid lineage associated markers (CD33 and CD13) and show <75% CD5. Therefore, they are classified as Early T cell precursor acute lymphoblastic leukemia/lymphoma (ETP-ALL). Intrstingly, cytogenetics and molecular studies showed BCR::ABL-1 and the final diagnosis was ETP-ALL with BCR::ABL-1. This patient had no prior history of CML and his prior CBCs was not compatible with CML. Unfortunately, our patient could not tolerate the treatment regimen, predominantly due to the severe heart failure and marked tumor burden at the time of diagnosis. To our knowledge, Philadelphia chromosome association with ETP-ALL was not previously reported. Awareness of the BCR::ABL-1 rearrangement in these acute leukemias may open additional therapeutic options for the patients and change their clinical outcome.

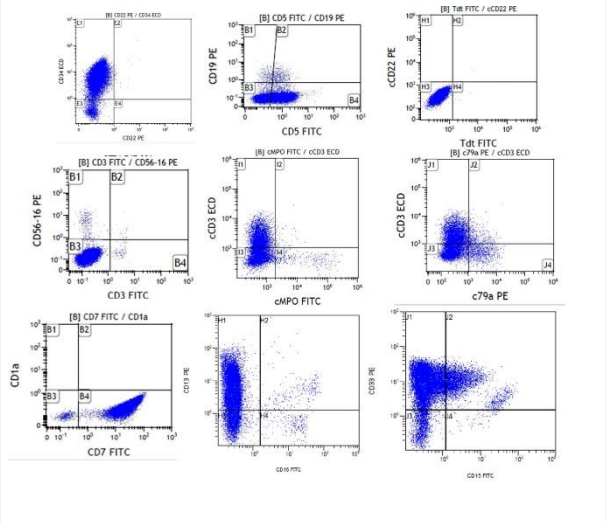

Peripheral blood flow cytometry, blast gate

The CD34 positive blasts show cytoplasmic CD3 positivity, CD7 positivity and are negative for MPO, CD22a and surface CD3.

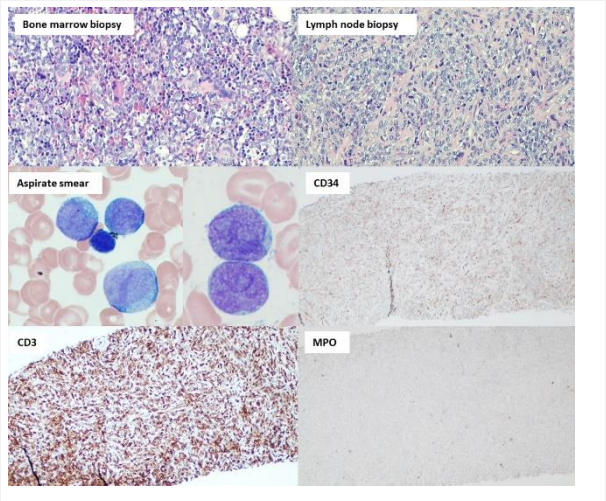

Histology and IHC of ETP-ALL

Bone marrow and lymph node biopsies with sheets of blasts (20 x maginfication), Apirate smears with large blasts and small to modetare amount of agranular cytoplasm (100x maginfication), Immunostains are performed on the lymph node and shows CD34/CD3 positive cells that are negative for MPO (10x maginfication)

EA4HP24-ABS-631

ERG/CD117 Double-Staining May Help Avoid Overcounting Myeloblasts in Specific Scenarios

Dr. Jackson A. Barbosa

Hospital Israelita Albert Einstein, Anatomia Patológica, São Paulo, Brazil

Background

Enumerating myeloblasts in bone marrow trephine biopsy can be crucial, especially when aspirate smear and/or flow cytometry are impaired due to dilution or fibrosis. CD34 and CD117 immunohistochemistry are routinely used for this purpose. Myeloblasts might be partially CD34 positive or even negative in some cases. CD117 improves the detection of myeloblasts, but it also stains erythroid precursors. Therefore, distinguishing actual myeloblast excess from an increase in erythroid precursors can be challenging, notably when there is left-shifted erythroid hyperplasia. "Subtracting" E-cadherin-positive cells from total CD117-positive cells helps enumerate myeloblasts, as the former is a specific erythroid marker.

Principles/Methodology

We investigated whether ERG/CD117 double-staining could serve as an additional diagnostic tool, given that the normal erythroid lineage is typically ERG-negative. In selected cases of left-shifted erythroid hyperplasia, where hematopoietic series proportions appeared equivalent in bone marrow smear, flow cytometry, and trephine biopsy samples, we employed ERG (clone EP111) and CD117 (Polyclonal) double-staining. Fast Red and DAB were used as chromogens for ERG and CD117, respectively.

Results

In selected cases from our routine, ERG/CD117 double-staining sharply sorted ERG-/CD117+ cells, mostly erythroid precursors, from ERG+/CD117+ cells, mostly mast cells and myeloblasts, and facilitated the estimation of the percentage of myeloblasts in trephine biopsy, in correlation with bone marrow smear and flow cytometry counts. Abnormal localization of immature precursors (ALIP) could also be easily distinguished from grouped erythroid precursors.

Considering what has been described in the literature about ERG expression in hematopoietic and lymphoid normal tissue and neoplastic lesions, potential confounders to be aware of when counting ERG+/CD117+ cells include mast cells, abnormal plasma cells, and left-shifted granulocytic lineage, for which morphology assessment and additional markers should be properly applied.

Conclusion

Despite potential limitations and pitfalls, ERG/CD117 double-staining may be an effective tool for the enumeration of myeloblasts in selected challenging cases. More detailed studies are needed to confirm its value.

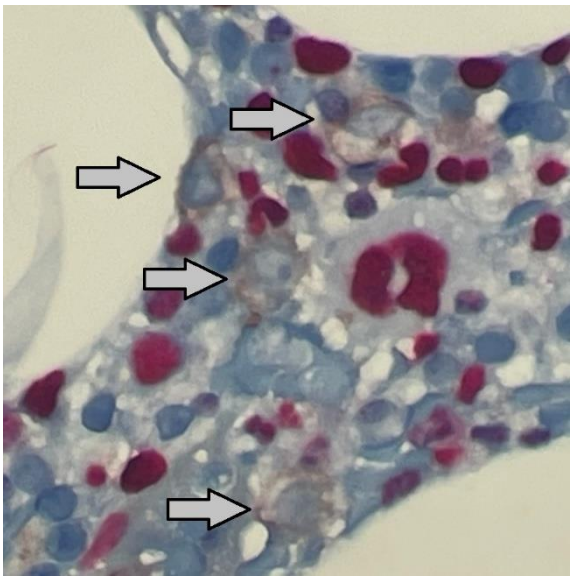

ERG/CD117 double-staining pattern in erythroid precursors
Erythroid precursors (arrows) can be identified as large cells, weakly positive for CD117 and negative for ERG. These cells might have been erroneously interpreted as CD34-/CD117+ myeloblasts.

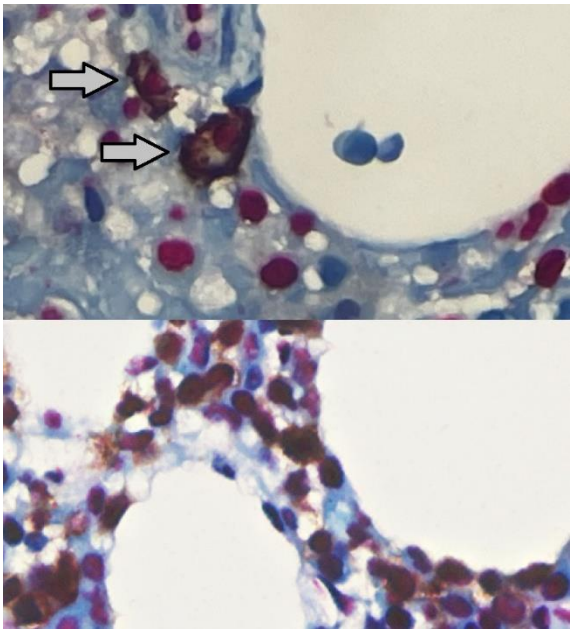

Mast cells and myeloblasts
In the upper half of the image, mast cells (arrows) display positive ERG staining and typical strong CD117 expression. The lower half features predominantly myeloblasts, which also exhibit CD117 and ERG positivity.

EA4HP24-ABS-668

The use of deep learning neural networks in analysis and differentiation of cells in bone marrow aspirate from patients with hematological diseases

PhD/MD Ingrid Brezaniova, M.Sc./M.A. Marie Salin

West Medica Produktions- und Handels- GmbH, Clinical Department, Wiener Neudorf, Austria

Background

In the continually growing field of hematopathology, the integration of artificial intelligence with digital microscopy has transformed diagnostic capabilities. In this study, we explore the application of deep learning neural networks within the Vision Bone Marrow Clinical Application Module to simplify the analysis and differentiation of cells in bone marrow aspirates obtained from patients diagnosed with various hematological diseases.

Principles/Methodology

The samples were scanned using the Vision Bone Marrow Clinical Application Module, employing both 10x (digital slide creation) and 100x objectives (pre-classification). The Regions of Interest (ROIs) were selected on digital slides by a hematology specialist. Using deep learning neural networks, the system autonomously conducted scanning, pre-classification, and cell counting of bone marrow elements. The study specifically targeted samples diagnosed with 5q minus syndrome (MDS), Refractory Anemia with Ringed Sideroblasts Associated with Marked Thrombocytosis (RARS-T), Chronic Myeloid Leukemia (CML), and Chronic Myelomonocytic Leukemia (CMML).

Results

In all samples, the sensitivity for granulocytes (eosinophils, basophils, neutrophils at various stages of maturation), lymphocytes, and monocytes was higher than 88%, and specificity was higher than 95%. The most significant differences were observed in the sensitivity for blasts: MDS - 65.2%, RARS-T - 81.3%, CML - 75.0%, CMML - 48.8%; the system demonstrated a specificity higher than 98% for all samples.

Conclusion

We should note that the quality of cell pre-classification using deep learning neural networks largely depends on the correct choice of ROIs and the quality of sample preparation (smear preparation and staining). Our study demonstrates high accuracy of cell pre-classification for the major cell groups and satisfactory results for blast cells in various hematological diseases including MDS, RARS-T, CML and CMML. The pre-classification of bone marrow elements by AI enhances efficiency and reduces the workload for laboratory specialists.

Lymphoma Abstracts Oral Presentations

EA4HP24-ABS-557	Single cell sequencing reveals shared clonal signatures of non-malignant B- and tumor cells in T-prolymphocytic leukemia
EA4HP24-ABS-661	Fusion gene landscape of peripheral T- cell lymphomas
EA4HP24-ABS-549	Genetically Divergent Routes to Lymphomagenesis associated with Epstein-Barr Virus (EBV)-positive Versus EBV-negative Classical Hodgkin Lymphoma (cHL)
EA4HP24-ABS-589	Semimethylation is a feature of Diffuse Large B-cell Lymphoma, and subgroups with poor prognosis are characterized by global hypomethylation and short telomere length
EA4HP24-ABS-578	Increased incidence of lymphomas in patients with Activated PI3k syndrome (APDS): a single center experience
EA4HP24-ABS-634	Unravelling the genetic basis of pediatric B-cell non-Hodgkin lymphoma pathogenesis in patients with underlying primary immunodeficiency
EA4HP24-ABS-500	SOX11: An Achilles' heel of mantle cell lymphoma enhancing sensitivity to DNA damaging agents by impairing DNA repair.
EA4HP24-ABS-503	Acquired MYC Rearrangement Contributes to Bruton Tyrosine Kinase Inhibitor Resistance in Mantle Cell Lymphoma
EA4HP24-ABS-536	Mutational and transcriptional landscape of pediatric B-cell precursor lymphoblastic lymphoma
EA4HP24-ABS-481	Genetic subtyping by Whole Exome Sequencing across Diffuse Large B Cell Lymphoma and Plasmablastic Lymphoma.
EA4HP24-ABS-482	Classic Hodgkin Lymphomas with Syncytial Morphology Exhibit a Primary Mediastinal Large B-Cell Lymphoma-Like Expression Signature by Lymph3Cx Analysis
EA4HP24-ABS-520	The genetic landscape of primary breast marginal zone lymphoma identifies a mutational-driven disease with similarities to ocular adnexal and nodal marginal zone lymphoma
EA4HP24-ABS-550	Aggressive B-cell lymphomas with MYC-R single hit show Burkitt-like mutations in a subset of cases
EA4HP24-ABS-559	Checkpoint inhibition enhances cell contacts between CD4+ T cells and Hodgkin-Reed-Sternberg cells of classic Hodgkin lymphoma
EA4HP24-ABS-562	Mutational profile of multifocal/recurrent extranodal marginal zone lymphoma of mucosa-associated lymphoid tissue; Insights into the clonal heterogeneity and disease progression
EA4HP24-ABS-567	Primary cutaneous follicle centre lymphoma- differential diagnostic and prognostic aspects.
EA4HP24-ABS-573	Identifying genomic abnormalities of aggressive B-cell lymphomas (BCLs) by optical genome mapping (OGM): A feasibility study with potential new discoveries
EA4HP24-ABS-586	Spatial transcriptomics reveal the prognostic values and macrophage heterogeneity in natural killer/ T cell lymphoma
EA4HP24-ABS-591	Molecular characterisation of Epstein–Barr virus in classical Hodgkin's lymphoma
EA4HP24-ABS-595	Cyclin D1 rearranged diffuse large B-cell lymphoma (DLBCL) – an evolving concept
EA4HP24-ABS-608	Dark zone Signature in diffuse large B-Cell Lymphoma of the German high-grade Lymphoma study group/German Lymphoma Alliance

EA4HP24-ABS-625	Deciphering the molecular mechanisms behind IRF4-rearranged large B-cell lymphomas
EA4HP24-ABS-633	Pediatric-type follicular lymphoma lacks n-glycosylation sites and positive antigen selection despite ongoing somatic hypermutation.
EA4HP24-ABS-656	CCND1-Rearranged Large B-Cell Lymphomas Have Different IG Breakpoints and Genomic Profile Than Mantle Cell Lymphoma
EA4HP24-ABS-662	LYMPHOMA WITH CONCURRENT MYC TRANSLOCATION AND 11q ABERRATION: BURKITT LYMPHOMA OR NOT?
EA4HP24-ABS-666	Association to both BCL2-positive and negative follicular lymphoma to Clasical Hodgkin Lymphoma and/or Gray Zone Lymphoma.
EA4HP24-ABS-671	Multimodal spatial profiling reveals unique immunobiological features of EBV+ Hodgkin-like lymphoproliferations

EA4HP24-ABS-557

Single cell sequencing reveals shared clonal signatures of non-malignant B- and tumor cells in T-prolymphocytic leukemia

Dr. Caroline Hesselager[1], PhD/MD Ingrid Thörn[1], PhD/MD Millaray Marincevic Zuniga[1], PhD/MD Claes Ladenvall[2], PhD/MD Jonas Almlöf[2], PhD/MD Sara Löfgren[2], PhD/MD Simone Weström[2], PhD/MD Lesley Ann Sutton[3], PhD/MD Lucia Cavelier[2,3], PhD/MD Panagiotis Baliakas[1,2], **Prof. Rose-Marie Amini**[1,2]

[1] Uppsala University and Uppsala University Hospital, Dept of Immunology, Genetics and Pathology, Uppsala, Sweden; [2] Uppsala University, Dept of Immunology, Genetics and Pathology, Science for Life Laboratory, Uppsala, Sweden; [3] Karolinska Institute, Dept of Molecular Medicine and Surgery, Stockholm, Sweden

Background

T-prolymphocytic leukemia (T-PLL) is one of the most common mature T-cell leukemias with poor survival. The aim of this study was to elucidate the clonal origin and evolution of T-PLL by using targeted sequencing of paired samples from diagnosis and relapse.

Principles/Methodology

DNA from both germline and malignant cells were extracted from magnetic bead cell-sorted cells from frozen peripheral blood (n=10) or bone marrow aspirates (n=6). Next generation sequencing (NGS) was performed on genomic DNA (gDNA) using a Haloplex Sequencing Panel (Agilent and Illumina, San Diego, California) comprising 19 genes frequently mutated in T-PLL (*ATM* and *JAK/STAT* pathway). Digital droplet polymerase chain reaction (ddPCR) was performed to confirm mutations with low variant allele frequencies (VAF) detected by NGS. Single-cell analysis of gDNA combined with cell surface protein markers was performed in two samples from two different patients using the Mission Bio Tapestri Platform.

Results

Sixteen patients were included in the study; relapse samples were available for 9/16 patients with a median of 12 months (range 2-36) from the time of diagnosis. The most commonly mutated gene was *ATM* (n=10) followed by *STAT5B* (n=7), *JAK3* (n=3), *EZH2* (n=3), *BCOR* (n=1) and *STAT6* (n=1). Varying clonal shifts were observed between diagnosis and relapse (increase: 5/9, decrease: 2/9, increase/decrease: 1/9, no change: 1/9). In particular, we were able to confirm the presence of pathogenic variants in *ATM, EZH2, STAT5B* and *JAK3* in both normal B-cells and sorted clonal T-cells with VAFs varying from 0.04-31% in the non-malignant compartment. Single cell analysis revealed shared mutations in both non-malignant B and clonal T-cells (Figure 1). Of note, a likely germline mutation in *ATM* was observed with a VAF of approximately 50% by NGS and ddPCR in all cell populations tested.

Conclusion

T-PLL exhibits variable patterns of clonal evolution between diagnosis and relapse. Single cells multiomics analysis reveals shared mutational signature in both non-malignant B-cells and clonal T-cells. Finally, the role of germline *ATM* mutations in the pathogenesis of T-PLL should be further investigated.

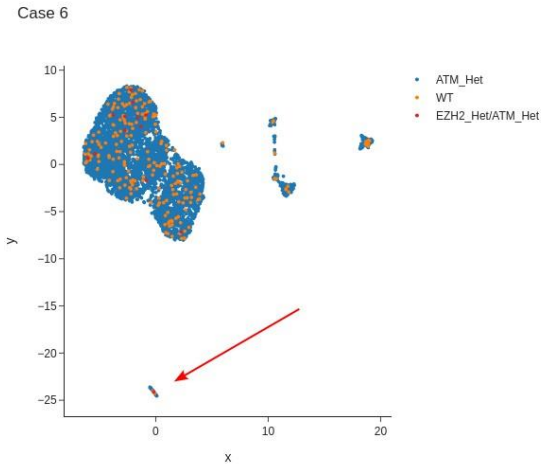

Figure 1.
DNA protein UMAP. Red arrow *EZH2* and *ATM* mutation in fraction of B-cell cluster.

EA4HP24-ABS-661

Fusion gene landscape of peripheral T- cell lymphomas

Dr. Baptiste Guey[1], Venkatesh Kancherla[1], Dr. David Vallois[1], Dr. Bettina Bisig[1], Dr. Anja Fischer[2], Dr. Karine Lefort[1], Vimel Rattina[1], Prof. Norbert Schmitz[3], Prof. Gerald Wulf[4], Prof. Olivier Tournilhac[5,6], Prof. Andreas Rosenwald[7], Prof. Philippe Gaulard[8], Prof. Reiner Siebert[2], Prof. Laurence de Leval*[1], **Priv.-Doz. Edoardo Missiaglia***[1,9]

[1] Lausanne University Hospital and Lausanne University, Institute of Pathology, Lausanne, Switzerland; [2] Ulm University and Ulm University Medical Center, Institute of Human Genetics, Ulm, Germany; [3] Muenster University Hospital, Division of Hematology and Oncology, Department of Medicine A, Muenster, Germany; [4] Georg August University Goettingen, Department of Hematology and Oncology, Goettingen, Germany; [5] Clermont-Ferrand University Hospital, Cellular Therapy and Clinical Haematology Department, Clermont-Ferrand, France; [6] Clermont Auvergne University, EA7453 (CHELTER), Clermont-Ferrand, France; [7] University of Wuerzburg, Institute of Pathology, Wuerzburg, Germany; [8] Hôpitaux Universitaires Henri Mondor, Assistance Publique des Hôpitaux de Paris, Département de Pathologie, Créteil, France; [9] SIB Swiss Institute of Bioinformatics, Molecular Modelling Group, Lausanne, Switzerland

Background

Fusion genes favor tumorigenesis through promoting gain-of-function of oncogenes or inactivation of tumor suppressor genes. In peripheral T-cell lymphomas (PTCLs), which comprise rare and usually aggressive neoplasms, various gene fusions involving signaling pathways or tyrosine kinase genes have been reported, which could be of diagnostic or therapeutical relevance. This study explores the detection of fusion transcripts in routinely processed PTCLs using RNA-seq.

Principles/Methodology

Strand-specific RNA-seq was performed on 91 routinely processed (FFPE) PTCL samples (49 follicular helper TCLs (TFHLs), 24 PTCLs not otherwise specified (NOS), 11 ALK-negative anaplastic large cell lymphomas (ALCLs), 7 others) from two European clinical trial cohorts, the ACT-2 and the AATT trials (TRANSCAN project). Gene fusions were called using both *STAR-Fusion* and *Arriba* tools starting from

hg19 human reference-aligned sequences. Fusion candidates were selected using *annoFuse* and internal filtering, including literature-based search. A custom fusion gene NGS panel based on the AMP technology (anchored multiplex PCR, Archer) and specific RT-PCR assays were used for further verification.

Results

Through in-silico steps and prioritization, we identified 32 putative driver fusions, including 30 unique ones, in 24/91 PTCL samples (26.4%). Two or more fusion genes were identified in 3 samples. Among those putative fusion genes, out of the 14 selected for further orthogonal validation, 7 were confirmed by NGS (custom Archer panel) and 4 by specific RT-PCR, while 3 were not confirmed. The prevalence of fusions was 22.4% in TFHLs (11/49 cases), 33.3% in PTCLs-NOS (8/24 cases) and 27.3% in ALK-negative ALCLs (3/11 cases). We identified recurrentrearrangements involving *IKZF2* and *VAV1* genes, both previously reported in PTCLs. Among others, *VAV1*::*THAP4, IKZF2*::*ERBB4, PCM1*::*JAK2, LINC-PINT*::*DUSP22* and *FYN*::*TRAF3IP2,* already known or resembling known oncogenic fusions, were identified in different samples. Additionally, we observed new potential driver fusions not yet described in PTCLs.

Conclusion

This RNA-seq study revealed 32 potential driver fusions across diverse PTCL entities. We highlighted recurrent fusions involving genes such as *IKZF2*, *PCM1* and *VAV1,* previously reported in PTCLs and other cancers, along with new candidate fusions. Our findings provide insights into fusion-mediated oncogenesis and potential therapeutic targets in PTCLs.

EA4HP24-ABS-549

Genetically Divergent Routes to Lymphomagenesis associated with Epstein-Barr Virus (EBV)-positive Versus EBV-negative Classical Hodgkin Lymphoma (cHL)

Karen Gomez*[1], Gianluca Schiavoni*[2], Yoonhee Nam[1], Jean B. Reynier[1], Cole Khamnei[1], Mick Aitken[1], Carel van Noesel[3], Brunangelo Falini[2], Laura Pasqualucci[1,2], Raul Rabadan^[1], **Prof. Enrico Tiacci^**[2]

[1] Columbia University, Program for Mathematical Genomics and Department of Systems Biology, New York, USA; [2] University and Hospital of Perugia, Institute of Hematology and Center for Hemato-Oncology Research, Department of Medicine and Surgery, Perugia, Italy; [3] University of Amsterdam, Amsterdam University Medical Centers, Department of Pathology, Amsterdam, Netherlands

Background

Latent EBV infection of the cHL clone is more frequent in the mixed-cellularity (MC) histological subtype, in early childhood and older adulthood, and in developing countries. Based on these and other epidemiologic features, EBV+ cHL was hypothesized to have distinct etiology and pathogenesis compared to EBV- cHL. However, the genomic landscape of EBV+ cHL is incompletely defined.

Principles/Methodology

We studied 57 cHL cases (10-83 year-old; 41 EBV-, 16 EBV+) by whole exome (WES) and/or whole genome (WGS) sequencing of tumor and normal cells purified from frozen samples, at identical median depths for EBV+ and EBV- cases (WGS 44X; WES 146X).

Results

Clonal nonsynonymous somatic mutations were much fewer in EBV+ than in EBV- cHL (median 4.5 vs 57; p=0.0013), and the same was for total mutations genome-wide (median 112 vs 6826; p<0.0001). Conversely, within EBV- cHL, MC (n=6) and non-MC (n=33) cases had similar mutation load (p=0.56), indicating a link with viral status rather than histology. AID-associated mutational signatures were stronger in EBV- than in EBV+ cHL, both genome-wide (SBS9, q=0.069; SBS85, q=0.023) and in the target region of 126 genes known to undergo AID-driven aberrant somatic hypermutation (median of 4 vs 0 mutations/Mb; p=0.045).

Compared to EBV- cHL, EBV+ cHL had fewer mutations or copy number alterations in genes of several pathways (Fig. A) that drive cHL pathogenesis and can be activated by EBV latent proteins (possibly surrogating cellular genetic lesions): i) JAK-STAT signaling genes STAT6, SOCS1, CSF2RB and JAK2 were altered in 85% EBV- vs 47% EBV+ cases (p=0.0057); ii) PI3K-AKT signaling genes GNA13 and ITPKB were mutated in 34% EBV- vs 7% EBV+ cases (p=0.047); and iii) NF-κB signaling genes TNFAIP3, NFKBIE and REL were altered in 85% EBV- vs 47% EBV+ cases (p=0.0057).EBV- cHL had also more frequent mutations of the MHC-I genes B2M and HLA-A/B/C (56%, vs 20% in EBV+ cHL, p=0.0032; Fig. A), possibly to prevent presentation of tumor neo-antigens generated by the much higher mutation burden. Conversely (Fig. B), EBV+ cases had germline homozygosity of ≥1 HLA-I genes more often than EBV- cases (53% vs 19%; p<0.05), particularly for HLA-C (33% vs 2%; p=0.0039), which may favor EBV+ cHL development through a reduced diversity of HLA-I alleles available for viral antigen presentation.

Conclusion

In the largest series characterized genome-wide so far, EBV+ and EBV- cHL genetically diverged in their germline and somatic routes to lymphoma development.

*Cofirst / ^Colast authors

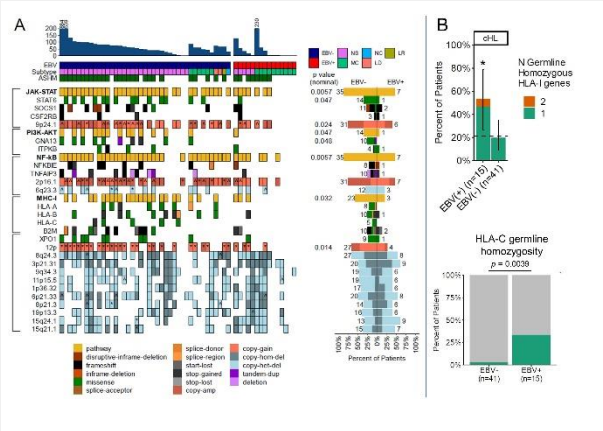

Figure

EA4HP24-ABS-589

Semimethylation is a feature of Diffuse Large B-cell Lymphoma, and subgroups with poor prognosis are characterized by global hypomethylation and short telomere length

PhD/MD student Olivia Carlund[1], PhD/MD student Elina Thörn[1,3], Pia Osterman[1], Dr. Maja Fors[1], Dr. Andy Dernstedt[2], Prof. Mattias Forsell[2], PhD/MD Martin Erlanson[3], Dr. Mattias Landfors[1], Prof. Sofie Degerman[1,2], **Prof. Magnus Hultdin**[1]

[1] Umeå University, Department of Medical Biosciences, Pathology, Umeå, Sweden; [2] Umeå University, Department of Clinical Microbiology, Umeå, Sweden; [3] Umeå University, Department of Diagnostics and Intervention, Oncology, Umeå, Sweden

Background

Large B-cell lymphoma (LBCL) is the most common lymphoma and is a biologically heterogeneous disease regarding genetic, phenotypic, and clinical features. Although the prognosis is good, one-third has a primary refractory or relapsing disease which underscores the importance of developing predictive biological markers capable of identifying high- and low-risk patients. DNA methylation (DNAm) and telomere maintenance alterations are hallmarks of cancer and aging. Both these alterations may contribute to the heterogeneity of the disease, and potentially influence the prognosis of LBCL.

Principles/Methodology

We studied the DNAm profiles (Infinium MethylationEPIC BeadChip) and relative telomere lengths (RTL) with qPCR of 93 LBCL cases: Diffuse large B-cell lymphoma NOS (DLBCL, n=66), High-grade B-cell lymphoma (n=7), Primary CNS lymphoma (n=8), and transformation of indolent B-cell lymphoma (n=12).

Results

There was a substantial methylation heterogeneity in DLBCL and other LBCL entities compared to normal cells and other B-cell neoplasms. LBCL cases had a particularly aberrant semimethylated pattern ($0.15 \leq \beta \leq 0.8$) with large intertumor variation and overall low hypermethylation ($\beta > 0.8$). DNAm patterns could not be used to distinguish between germinal center B-cell-like (GC) and non-GC DLBCL cases. In DLBCL cases treated with R-CHOP-like regimens, a high percentage of global hypomethylation ($\beta < 0.15$) was in multivariable analysis associated with worse disease-specific survival (DSS) (HR=6.920, 95% CI=1.499-31.943) and progression-free survival (PFS) (HR=4.923, 95% CI=1.286-18.849). These cases with a high percentage of global hypomethylation also had a higher degree of CpG island methylation, including islands in promoter-associated regions, than the cases with less hypomethylation. Short RTL was independently associated with worse DSS (HR=5.077, 95% CI=1.121-22.997) in DLBCL treated with R-CHOP-like regimens.

Conclusion

Our results showed that semimethylated, heterogeneous DNAm patterns were a feature of LBCL but not common in other B-cell neoplasms. Furthermore, DLBCL cases with a high percentage of hypomethylated CpGs and with short RTLwere associated with worse DSS in multivariable analysis. These hypomethylated cases also had a higher frequency of hypermethylated CpG islands and in this group of DLBCL patients, treatment with hypomethylating agents could potentially be beneficial but needs to be investigated in future studies.

EA4HP24-ABS-578

Increased incidence of lymphomas in patients with Activated PI3k syndrome (APDS): a single center experience

Dr. Stefania Pittaluga[1], Dr. Evsen Apaydin Arikan[1], Dr. Mark Raffeld[1], Dr. Dimana Dimitrova[1], Dr. Gulbu Uzel[2], Dr. Joao Alves De Castro[1]

[1] NIH/NCI, Laboratory of Pathology, Bethesda, USA; [2] NIH/NIAID, Laboratory of Clinical Immunology and Microbiology, Bethesda, USA; [3] NIH/NCI, Center for Immuno-Oncology, Bethesda, USA

Background

Patients with APDS due heterozygous mutations in *PI3KCD* (APDS1) or *PIK3R1* (APDS2) develop EBV and CMV viremia, hypogammaglobulinemia, autoimmunity and lymphoproliferation with increased incidence of B-cell lymphomas. Patients are often intermittently viremic with EBV.

Principles/Methodology

A single institution cohort of genetically proven 96 APDS patients from 68 families were retrospectively evaluated for the frequency of lymphomas. These included classic Hodgkin and non-Hodgkin lymphomas, incidence of EBV + cases in association with disease specific mutations and patients' demographics. Marginal zone hyperplasia, nodular lymphoid hyperplasia of respiratory/gastrointestinal tract were excluded. Review of pathology with immunophenotype was performed. Next Gen Sequencing using TSO500 panel was performed when possible.

Results

Twenty-one patients with diagnosis of lymphoma/lymphoproliferative disorder were identified, making the incidence 22% for the entire cohort, 27% for APDS1. There was no lymphoma diagnosis among 13 patients with APDS2. Incidence of lymphoma was highest among patients carrying *PIK3CD* E525K mutation (5/13: 38%) compared to all others (16/83: 19%). Median age was 22 (range: 13-64) among 11 females and 10 males at the time of diagnosis. Majority of patients (57%) developed lymphomas before 25 years of age, while older patients were identified retrospectively due to family history. In 2 out of the 3 cases NGS was performed (CHL, EBV-DLBCL, PBL), additional somatic mutations were identified.

	CHL			**DLBCL**		**PL**	**MZL**	**B-NHL NOS**	**EBV-LPD**	**NHL**
Cases	4			10		1	2	2	1	1
EBV Status	POS N2	NEG N1	UNK 1	POS N 8	NEG N2	NEG N1	NEG N2	POS N2	POS N1	UNK
Gender F/M	2F	1M	1F	5F 3M	1F1M	1M	1F1M	2M	1M	1M
Age at Dx	14,20	32	16	13,13,17,25,38,52,59,64	22,36	34	13,21	11,21	60	37

Conclusion

Our findings confirm a high incidence of B cell lymphoma, predominantly EBV positive diffuse large B cell lymphoma in APDS1 and an overall association with EBV for all lymphomas in this disease. Clinical awareness is important to monitor these patients aggressively for an early diagnosis and treatment.

EA4HP24-ABS-634

Unravelling the genetic basis of pediatric B-cell non-Hodgkin lymphoma pathogenesis in patients with underlying primary immunodeficiency

PhD/MD student Sara Mato[1], PhD/MD student Natalia Castrejón de Anta[2], PhD/MD student Ariadna Colmenero[1], PhD/MD Julia Salmerón-Villalobos[1], PhD/MD Angela Deya-Martinez[3], PhD/MD Eugenia Garcia-Fernandez[4], PhD/MD Gabriel Olmedilla[4], Prof. Wolfram Klapper[5], PhD/MD Konnie Hebeda[6], PhD/MD Ingrid Simonitsch-Klupp, PhD/MD Julia Richter[5], PhD/MD Jaime Verdu-Amoros[8], PhD/MD Mara Andrés[9], PhD/MD Pedro Jares[2], Noelia Garcia[1], PhD/MD Maria Jose Ortega[10], PhD/MD Pilar Guerra-Garcia[11], PhD/MD Berta Gonzalez[11], PhD/MD Margarita Llavador[12], PhD/MD Luis Ignacio Gonzalez[13], PhD/MD Eduardo Quiroga[14], PhD/MD Itziar Astigarraga[15,16], PhD/MD Idoia Martin-Guerrero[15,17], Prof. Elias Campo[2], PhD/MD Olga Balagué[2], **PhD/MD Itziar Salaverria**[1]

[1] Institut d'Investigacions Biomèdiques August Pi i Sunyer, Molecular Genetics of Pediatric Lymphomas, Barcelona, Spain; [2] Hospital Clínic de Barcelona, Pathology Department, Barcelona, Spain; [3] Hospital Sant Joan de Deu, Clinical Immunology and Primary Immunodeficiencies Unit, Barcelona, Spain; [4] Hospital La Paz, Pathology Department, Madrid, Spain; [5] UKSH, Pathology Department, Kiel, Germany; [6] Radboud UMC, Pathology, Nijmegen, Netherlands; [7] AKH, Pathology Department, Wien, Austria; [8] Hospital Clínico Universitario de Valencia., INCLIVA Biomedial Research Institute, Valencia, Spain; [9] Hospital La Fe, Pediatric Oncology Department, Valencia, Spain; [10] Hospital Virgen de las Nieves, Pediatric Oncology Department, Granada, Spain; [11] Hospital La Paz, Pediatric Oncology Department, Madrid, Spain; [12] Hospital La Fe, Pathology Department, Valencia, Spain; [13] Hospital 12 de Octubre, Immunodeficiencies Unit, Madrid, Spain; [14] Hospital Virgen del Rocío, Pediatric Oncology Department, Sevilla, Spain; [15] BioBizkaia Health Research Institute, Pediatric Oncology Group, Barakaldo, Spain; [16] Hospital Universitario Cruces, Pediatrics Department, Bilbao, Spain; [17] University of the Basque Country (UPV/EHU), Department of Genetics, Physical Anthropology & Animal Physiology, Science and Technology Faculty, Leioa, Spain

Background

Primary immunodeficiencies (PID) are rare genetic disorders characterized by impaired immune function, leading to frequent infections and immune dysregulation. Individuals with PID have an increased risk of developing lymphoproliferative disorders including lymphoma, being the clinical management challenging due to its poor prognosis and complex therapeutic approaches. This study aims to unravel the biological factors driving the development of B-cell lymphoma in the context of PID in pediatric population.

Principles/Methodology

Twenty-five children with PID and B-cell lymphoma were included (mean age 8.3 y, 2-17y; 16M/9F). Forty-eight percent had combined immunodeficiencies with syndromic features, mainly DNA repair defects. Diseases of immune dysregulation affected 8 patients. Three and 2 patients presented combined immunodeficiencies and antibody disorders, respectively (**Fig1A**). Two patients developed more than one independent lesion over time.

The lymphoma diagnosis was performed according to the revised 2017 WHO classification. *MYC*, *BCL6* and *BCL2* rearrangements and the 11q aberration were determined by fluorescence in situ hybridization. Gene expression profile (GEP) of these tumors was analyzed by NanoString Lymph2Cx and 770-gene PanCancer Immune Profiling panels. LBCL in immunocompetent (IC) patients were used as controls. Seventeen tumors were analyzed by Copy number (CN) arrays. Tumor analysis by

whole exome sequencing and clinical correlations are ongoing and will be included in the meeting communication.

Results

DLBCL was the main diagnosis (16/25) followed by BL and LBCL/HG-11q (3/25 each), all the last with Ataxia Telangiectasia. Two patients had a HGBCL, NOS and one B-cell lymphoma, NOS (**Fig1B**). *MYC* rearrangements were found in 3/15 cases, *BCL6* in 2/11, and no *BCL2* breaks were detected. Fifty-seven percent of tumors were classified as germinal center derived and 9/16 were EBV+. CN analysis revealed recurrent 11q23 and 13q31-q32 gains (**Fig2A**). Cases with syndromic DNA repair disorders showed a significant increase in total CN alterations compared with tumors from other PID subtypes (**Fig2B**). GEP revealed 5 up and 5 downregulated genes in PID-tumors compared to IC ones.

Conclusion

B-cell lymphomas in children in the context of PID include a heterogeneous subset of aggressive B-cell lymphomas with complex genetic profiles, particularly in cases with DNA repair syndromes, and certain deregulation of the immune response by GEP.

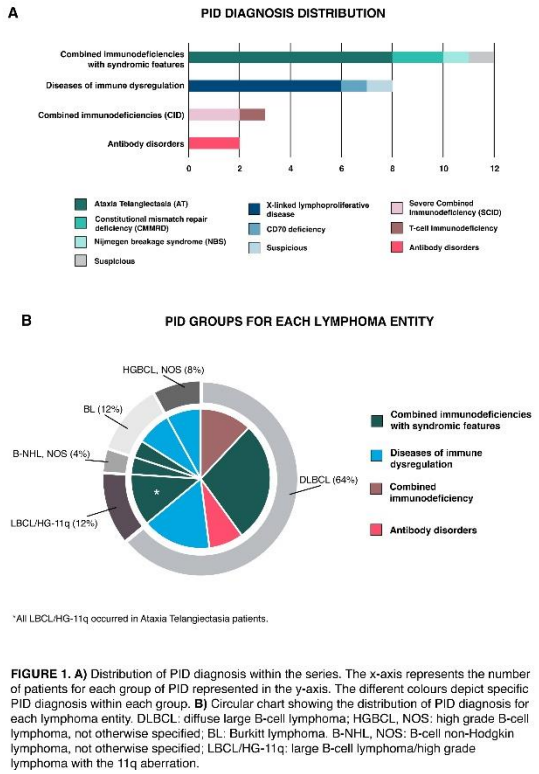

FIGURE 1. A) Distribution of PID diagnosis within the series. The x-axis represents the number of patients for each group of PID represented in the y-axis. The different colours depict specific PID diagnosis within each group. **B)** Circular chart showing the distribution of PID diagnosis for each lymphoma entity. DLBCL: diffuse large B-cell lymphoma; HGBCL, NOS: high grade B-cell lymphoma, not otherwise specified; BL: Burkitt lymphoma. B-NHL, NOS: B-cell non-Hodgkin lymphoma, not otherwise specified; LBCL/HG-11q: large B-cell lymphoma/high grade lymphoma with the 11q aberration.

Figure 1. Primary immunodeficiency and lymphoma diagnosis distribution within the series.
A) Distribution of PID diagnosis within the series. The x-axis represents the number of patients for each group of PID represented in the y-axis. The different colours depict specific PID diagnosis within each group. B) Circular chart showing the distribution of PID diagnosis foreach lymphoma entity. DLBCL: diffuse large B-cell lymphoma; HGBCL, NOS: high grade B-cell lymphoma, not otherwise specified; BL: Burkitt lymphoma. B-NHL, NOS: B-cell non-Hodgkin lymphoma, not otherwise specified; LBCL/HG-11q: large B-cell lymphoma/high grade lymphoma with the 11q aberration.

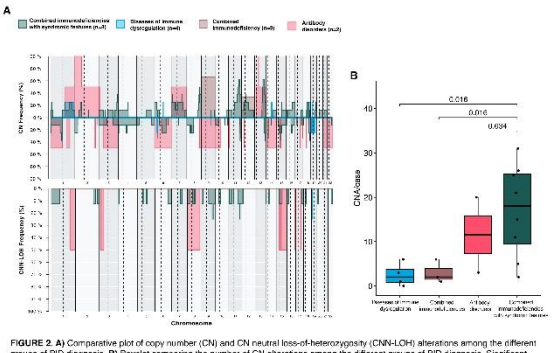

FIGURE 2. **A)** Comparative plot of copy number (CN) and CN neutral loss-of-heterozygosity (CNN-LOH) alterations among the different groups of PID diagnosis. **B)** Boxplot comparing the number of CN alterations among the different groups of PID diagnosis. Significant differences were observed when comparing combined immunodeficiencies with syndromic features with diseases of immune dysregulation and combined immunodeficiencies (adjusted P-val < 0.05).

FIGURE 2. Copy number profile in B-cell lymphoma patients with an underlying PID.
A) Comparative plot of copy number (CN) and CN neutral loss-of-heterozygosity (CNN-LOH) alterations among the different groups of PID diagnosis. B) Boxplot comparing the number of CN alterations among the different groups of PID diagnosis. Significant differences were observed when comparing combined immunodeficiencies with syndromic features with diseases of immune dysregulation and combined immunodeficiencies (adjusted P-val < 0.05).

EA4HP24-ABS-500

SOX11: An *Achilles'* heel of mantle cell lymphoma enhancing sensitivity to DNA damaging agents by impairing DNA repair.

Dr. Mohammad H.A. Morsy[1], Dr. Ingrid Lilienthal[2], Dr. Virginia Amador[3], Dr. Nikolaos Tsesmetzis[2], Prof. Elias Campo[3], Dr. Nikolas Herold[2], Prof. Birgitta Sander[1]

[1] Karolinska Institute, Laboratory medicine/Pathology, Stockholm, Sweden; [2] Karolinska Institute, Women's and Children's Health/3. Childhood Cancer Research Unit, Stockholm, Sweden; [3] Institut d'Investigacions Biomèdiques August Pi Sunyer (IDIBAPS), Barcelona, Spain

Background

Mantle cell lymphoma (MCL) is an aggressive malignancy with mature B-cell differentiation and a median overall survival of 5 years. A characteritic hallmark of MCL is the aberrant expression of the transcription factor sex determining region on Y chromosome (SRY)-related and high mobility group (HMG) domain containing protein 11 (SOX11) in approximately 90% of the cases. The role of SOX11 in MCL pathogenesis has been widely attributed to transcriptional dysregulation, ultimately driving malignant phenotype of MCL. However, little is known about the potential transcription factor-independent modes of action of SOX11. We recently identified SOX11 as a novel binding partner and endogenous inhibitor of SAMHD1. SAMHD1 has been shown involved in DNA repair by homologous recombination.

Principles/Methodology

Functional studies including confocal microscopy-based immunofluorescence imaging, immunoblotting, and cell viability assay were employed to study the role of SOX11, dependently or independently of its recently characterized partner SAMHD1 in MCL models in response to double stranded breaks induced by camptothecin treatment.

Results

Immunofluorescent imaging showed that SOX11 impairs homologous recombination in MCL, evidenced by reduced accumulation of RAD51 foci at chromatin and abrogated phosphorylation of DNA-break binding protein RPA32 (S4/8), in response to the topoisomerase1 inhibitor camptothecin (CPT) treatment in SOX11-positive conditions. Inducing SOX11 expression in JVM-2 resulted in increased accumulation of cytosolic single-stranded DNA upon CPT treatment which translated in an enhanced sensitivity to CPT. Moreover, this enhanced sensitivity was reflected in increased levels of cleaved PARP1, cleaved caspase 3 and persistent γ-H2A.X in SOX11-positive cells.

Depletion of SAMHD1 yielded a similar, yet attenuated, sensitizing phenotype to CPT compared to SOX11 induction in JVM-2. SAMHD1 depletion in addition to SOX11 induction showed no significant additional impact on the response to CPT in JVM-2 under the conditions tested.

Conclusion

Our findings suggest that SOX11 may impair homologous recombination, at least in part, through inhibiting SAMHD1. These results highlight SOX11 as an *Achilles' heel* that renders MCL vulnerable to DNA damaging and suggest that incorporating DNA damaging agents including topoisomerase inhibitors or anthracyclines into currently used treatment modalities for MCL might be clinically beneficial.

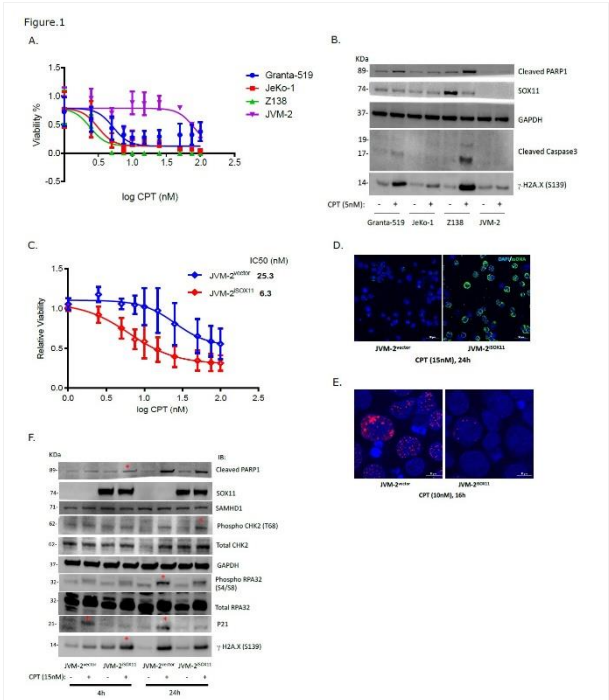

SOX11 enhances sensitivity of MCL cells to CPT

A. Dose response curve for CPT in different MCL cell lines with variable SOX11 expression levels.
B. Immunoblotting showing the abundance of the stated proteins.
C. Dose response curve for CPT in JVM-2 with empty vector versus SOX11 construct.
D. Immunofluorescence staining showing the intensity of single stranded DNA in the cytoplasm
in the indicated conditions.
E. Immunostaining showing RAD51 foci chromatin in response to CPT.

F. Immunoblot showing apoptosis and DNA damage markers in the indicated conditions and timepoints.

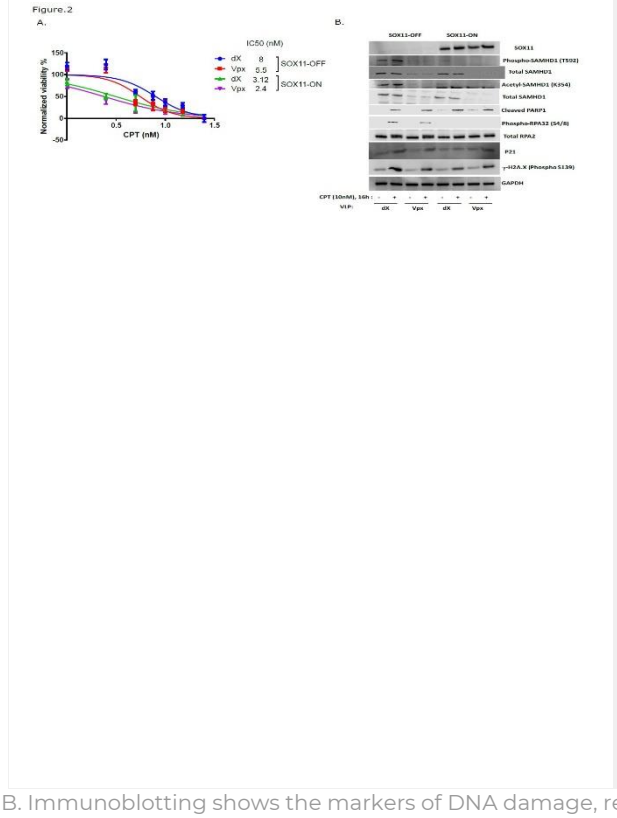

SOX11 impairs homologous recombination partially dependent of SAMHD1

A. Dose response curve for CPT in the four indicated conditions, wherein SOX11 induction and/or SAMHD1 depletion are generated in JVM-2 cells.

B. Immunoblotting shows the markers of DNA damage, repair and apoptosis in the indicated conditions. Related to A.

EA4HP24-ABS-503

Acquired *MYC* Rearrangement Contributes to Bruton Tyrosine Kinase Inhibitor Resistance in Mantle Cell Lymphoma

PhD/MD Chang-Tsu Yuan[1,2], Li-Yu Sun[2], PhD/MD Chieh-Lung Cheng[3], Dr. Bor-Sheng Ko[4], Dr. Ming Yao[3], PhD/MD Wei-Li Ma[5]

[1] National Taiwan University Cancer Center, Department of Pathology, Taipei, Taiwan; [2] National Taiwan University Hospital and National Taiwan University College of Medicine, Department of Pathology, Taipei, Taiwan; [3] National Taiwan University Hospital, Division of Hematology, Department of Internal Medicine, Taipei, Taiwan; [4] National Taiwan University Cancer Center, Department of Hematological Oncology, Taipei, Taiwan; [5] National Taiwan University Hospital, Department of Oncology, Taipei, Taiwan

Background

Mantle cell lymphoma (MCL) is a subtype of mature B-cell lymphoma associated with IGH::CCND1 rearrangement. Traditionally considered incurable, recent advancements in treatment, particularly with Bendamustine and Bruton tyrosine kinase inhibitors (BTKi), have significantly improved patient outcomes. However, some cases exhibit intrinsic or secondary resistance to BTKi, some of which are resulted from c-Myc overexpression.[1-3] In addition, *MYC* rearrangement is an uncommon (1.5%) event in primary MCL diagnosis, and it results in a dismal prognosis.[4] Whether and how often *MYC* rearrangement contributes to BTKi resistance in MCL remains unclear.

Principles/Methodology

We conducted a retrospective observational study of MCL patients who had ever received BTKi at the National Taiwan University Hospital and National Taiwan University Cancer Center. The tumor specimens were stratified into BTKi-responsive and BTKi-resistant groups by reviewing the follow-up images and clinical responses after BTKi therapy. Clinicopathological features, including *MYC*, *BCL2*, and *BCL6* rearrangement status, were compared between the resistant and responsive groups.

Results

Our findings reveal significantly higher c-Myc expression in the BTKi resistance group compared to the BTKi-responsive group (25% vs. 5%, p=0.019). Additionally, *MYC* rearrangement was only found in the BTKi-resistant group (33% vs. 0%, p=0.013) (Table 1). Among the tumor specimens within the treatment window of BTKi, *MYC* rearrangement was observed in 8% of specimens. All tumors with *MYC* rearrangement were not detected in initial diagnostic specimens. A case received multiple biopsies during the initiation of BTKi, and the tumor without *MYC* rearrangement was responsive to BTKi, whereas tumors with *MYC* rearrangement were resistant to BTKi (Figure 1). After cessation of BTKi, further sampling of progressive tumors revealed *MYC* rearrangement with higher split signals, indicating potential selection of *MYC*-rearranged tumor cells under BTKi treatment. *MYC*-rearranged tumors frequently displayed blastoid or pleomorphic cytomorphology, CD10 expression, high c-Myc expression, and a high Ki-67 proliferative index.

Conclusion

In conclusion, *MYC* rearrangement contributes to BTKi resistance in MCL. Although it is a rare event, subclones of *MYC*-rearranged tumor cells might have survival benefits under BTKi. Our findings suggest the importance of detecting *MYC* rearrangement in selected MCL cases to optimize treatment decisions.

Parameter	BTKi-resistant tumor, N=9	BTKi-responsive tumor, N=26	*P* Value
BTKi regimen			0.10
Ibrutinib, single agent	6 (67%)	23 (88%)	
Ibrutinib, combined[a]	1 (11%)	3 (12%)	
Acalabrutinib, single agent	2 (22%)	0 (0%)	
Morphology: blastoid or pleomorphic – no. (%)	4 (44%)	5 (19%)	0.19
CD5 – no. (%)[b]	7/7 (100%)	19/23 (83%)	0.55
Cyclin D1 – no. (%)	9 (100%)	26 (100%)	1.00
SOX11 – no. (%)[b]	3/4 (75%)	9/12 (75%)	1.00
CD10 – no. (%)	3 (33%)	5 (19%)	0.40
p53 – %			
Medium (IQR)	10 (18)	2.5 (1)	0.36
Range	0-70	0-60	
c-Myc – %			
Medium (IQR)	25 (25)	5 (6.5)	0.019 *
Range	3-100	1-60	
Ki67 – %			
Medium (IQR)	65 (50)	32.5 (43.75)	0.058
Range	25-90	1-90	
MYC rearrangement – no. (%)	3 (33%)	0 (0%)	0.013 *
BCL2 rearrangement – no. (%)[c]	1 (11%)	1/25 (4%)	0.47
BCL6 rearrangement – no. (%)[c]	1 (11%)	0/25 (0%)	0.26

Table 1. Comparison of Pathology between BTKi-resistant and BTKi-responsive tumros
a. Combined regimen include Rituximab + ibrutinib, Rituximab + Bortezomib + Ibrutinib , and Bendamustine + Rituximab + Bortezomib + Ibrutinib

b. Nominator is listed due to missing value.
c. Nominator is listed due to experiment failure of BCL2 fluorescence in situ hybridization in one case.
Significant: *: <0.05
Abbreviation: BTKi: Bruton tyrosine kinase inhibitor

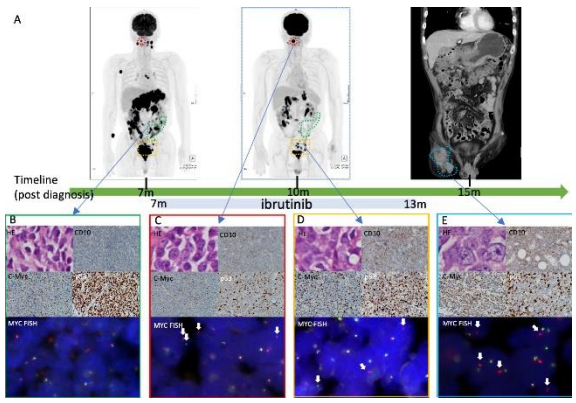

Figure 1. Pathological Features of Tumors with Different Responsiveness to Ibrutinib in A Patient
A) The patient was diagnosed with mantle cell lymphoma, stage IV, and started ibrutinib treatment. After 3 months, a PET scan showed metabolic response in the descending colon tumor, stable activity in the rectal tumor, and progression in the right tonsillar tumor. Treatment was switched due to progression. However, a CT scan revealed a new inguinal tumor.

B-E) Pathology features of the descending colon tumor, the tonsilar tumor, the rectal tumor, and the inguinal tumor.

EA4HP24-ABS-536

Mutational and transcriptional landscape of pediatric B-cell precursor lymphoblastic lymphoma

Ingram Iaccarino[1,2], Emma Kroeze[3], Michelle Kleisman[3], Mayukh Mondal[4,2], Thomas Beder[5,2], Mouhamad Khouja[5], Marijn Scheijde-Vermeulen[3], Lennart Kester[3], Monika Brüggemann[5,2], Claudia Baldus[5,2], Gunnar Cario[6,2], Reno Bladergroen[3], Nathalie Garnier[7], Andishe Attarbaschi[8], Jaime Verdu-Amoros[9,10], Elizabeth Macintyre[11,12], Kenneth Scholten[13], Laura A. Padilla[13], Birgit Burkhardt[13], Auke Beishuizen[3], Monique den Boer[3,14], Roland Kuiper[3,15], Jan Loeffen[3], Judith Boer[3], **Wolfram Klapper**[1,2]

[1] University of Kiel, Department of Pathology, Hematopathology Section and Lymph Node Registry, Kiel, Germany; [2] University of Kiel, Clinical Research Unit CATCH-ALL (KFO 5010/1), Kiel, Germany; [3] Princess Máxima Center for Pediatric Oncology, Utrecht, Netherlands; [4] University of Kiel, Institute of Clinical Molecular Biology, Kiel, Germany; [5] University of Kiel, Medical Department II, Hematology and Oncology, Kiel, Germany; [6] University of Kiel, Department of Pediatrics, Berlin-Frankfurt-Münster ALL Study Group Germany, Kiel, Germany; [7] Hospices Civils de LyonInstitut d'Hematologie et d'Oncologie Pediatrique, Lyon, Germany; [8] Medical University of Vienna, Department of Pediatric Hematology and Oncology, Vienna, Germany; [9] University of Valencia, Department of Pediatric Hematology and Oncology, Valencia, Spain; [10] INCLIVA, Biomedical Research Institute, Valencia, Spain; [11] Université Paris Cité, Institut Necker Enfants Malades, Paris, France; [12] Necker Children's Hospital, Laboratory of Onco-Hematology, Paris, France; [13] University Hospital Münster, Paediatric Haematology and Oncology, Münster, Germany; [14] Sophia Children's Hospital, Erasmus Medical Center, Rotterdam, Netherlands; [15] Utrecht University Medical Center, Department of Genetics, Utrecht, Netherlands

Background

Pediatric B-cell precursor (BCP) lymphoblastic malignancies are neoplasms with manifestation either in bone marrow/blood (BCP acute lymphoblastic leukemia, BCP-ALL) or less common in extramedullary tissue (BCP lymphoblastic lymphoma, BCP-LBL). Although both presentations are similar in morphology and immunophenotype the paucity of studies aimed at defining molecular characteristics of BCP-LBL makes it difficult to compare the two manifestations at the molecular level. Furthermore, treatment strategies for BCP-ALL have evolved with the finding that molecular genetic subtypes can be associated with patient outcome. Given that molecular studies defining disease subtypes in BCP-LBL are currently missing, it is unknown if BCP-LBL patients may also benefit from subtype-specific BCP-ALL treatment strategies.

Principles/Methodology

We collected material for what we consider the largest pediatric BCP-LBL cohort described to date (n=97). On this material we performed whole exome sequencing (n=80), whole RNA sequencing (n=80) and analysis of Immunoglobins (IG) and T cell receptors (TR) rearrangements (n=52). The data were analyzed to identify recurrent single nucleotide variants, copy number alterations, IG and TR rearrangements and gene fusions. Data were compared to similar data of pediatric BCP-ALL.

Results

We found that BCP-LBL has a mutational spectrum similar to BCP-ALL. However, epigenetic modifiers were more frequently mutated in BCP-LBL, whereas BCP-ALL was more frequently affected by mutation in B-cell development genes. IG and TR rearrangement analysis confirmed the precursor cell origin of the lymphomas. Integrating copy number alterations, somatic mutations and RNA-sequencing data we found that virtually all molecular subtypes defined in BCP-ALL are present in BCP-

LBL. Similar to BCP-ALL, the most frequent subtypes of BCP-LBL were high hyperdiploidy and *ETV6::RUNX1*.

Conclusion

In the analysis of the genomic and transcriptomic landscape of pediatric BCP-LBL we found more similarities than differences compared to BCP-ALL, reinforcing the concept of two manifestations of the same entity. These striking biological similarities challenge the concept of classification as leukemia or lymphoma based on the extent of bone marrow infiltration. Our work presents the basis for further studies aimed at defining new, genetics-based treatment protocols, in which many BCP-LBL patients may also benefit from current BCP-ALL treatment strategies.

EA4HP24-ABS-481

Genetic subtyping by Whole Exome Sequencing across Diffuse Large B Cell Lymphoma and Plasmablastic Lymphoma.

Prof. Santiago Montes Moreno[1], PhD/MD student Aitana Avendaño Pomares[1], PhD/MD Laura Rodriguez Merino[1], PhD/MD Sonia Gonzalez de Villambrosia[2], PhD/MD Jordi Morata[3], PhD/MD Raul Tonda[3], PhD/MD Estrella Carrillo[5], PhD/MD Antonio Gutierrez[11], PhD/MD Angel Ramirez Payer[7], PhD/MD Josep Maria Roncero[9], PhD/MD Carlos Grande[6], PhD/MD Jaime Perez de Oteyza[4], PhD/MD Concepcion Nicolas[7], PhD/MD Pau Abrisqueta[10], PhD/MD Alejandro Martin Garcia Sancho[8], PhD/MD Eva Gonzalez Barca[12], On behalf of GELTAMO group.

[1] Hospital Universitario Marques de Valdecilla/IDIVAL, Anatomic Pathology/Translational Hematopathology, Santander, Spain; [2] Hospital Universitario Marques de Valdecilla/IDIVAL, Hematology, Santander, Spain; [3] Centre Nacional d'Anàlisi Genòmica, Barcelona, Spain; [4] CIOCC, Madrid, Spain; [5] Hospital Virgen del Rocío, Sevilla, Spain; [6] Hospital12 de octubre, Madrid, Spain; [7] Hospital Central de Asturias, Oviedo, Spain; [8] Hospital de Salamanca, IBSAL, Salamanca, Spain; [9] ICO Girona, Girona, Spain; [10] Hospital Vall d'Hebron, Barcelona, Spain; [11] Hospital Son Espases, Palma de Mallorca, Spain; [12] Insititut Català d'Oncologia Hospitalet, Universitat de Barcelona, Barcelona, Spain

Background

Recently genomic based algorithms have been proposed for DLBCL classification. Specific large B cell lymphoma entities such as plasmablastic lymphoma remain poorly characterized.

Principles/Methodology

We retrieved samples from 108 large B cell lymphoma cases and performed whole exome sequencing. We used somatic variants, predicted CNAs and available fusion data to classify the cases according to Lymphgen tool 2.0. *TP53*, *MYC* and MAPK/ERK pathways mutation enrichment were also analyzed.

Results

Genetic subtype was assigned in ~55% of cases. Cases with a specific genetic subtype showed a significantly higher TMB than cases molecularly unclassified (median TMB 31.5 vs 7.29 respectively, p<0.0001). Prevalence of subtypes varies according to cell of origin phenotypes (Figure 1). All three cases of HGBCL/DLBCL DH (MYC&BCL2) were classified as EZB-MYC. MYC pathway mutations were significantly enriched in cases with EZB and ST2 genetic features, including composite cases and absent in the MCD subtype. *TP53* mutations were found in 11%of the cases. Plasmablastic lymphomas showed ST2 genetic features (6/22, 27%), including pure ST2 (4 cases) and composite ST2/EZB in two additional cases. Genes overrepresented in the ST2 cluster include *TET2, STAT3, PRRC2C, DOCK8* and

CLTC. The rest of plasmablastic lymphoma cases were considered molecular NOS/Other (68%) and one isolated case was classified as MCD. An enrichment in MAPK/ERK pathway mutated genes in the plasmablastic lymphoma cohort was found, in contrast to DLBCL NOS. Recurrent mutations in *NF1, BRAF, KRAS, NRAS, MAPK3* as well as JAK/STAT pathway, including mutations in *JAK2* were found. Unexpectedly, recurrent mutations in other Tyrosine kinase genes were found, including *EGFR, ERBB2, ERBB4, ALK, NTRK2/3* and *ROS1* among others. TP53 pathway genes such as *ATM, MDM2* and *CHEK2* were found mutated in five out of six ST2(/EZB) plasmablastic cases and three out of fifteen molecular NOS/Other plasmablastic cases.

Conclusion

DLBCL molecular subtyping using WES and FISH supplies exact molecular classification in ~55% of our cohort. Clear associations between phenotypes and genetic subtype were confirmed. Application of the LymphGen molecular classifier to plasmablastic lymphomas shows intraspecific genetic diversity with a significant fraction of ST2 tumors. Widespread somatic mutations point toward dysregulation of JAK/STAT, MAPK/ERK and Tyrosine Kinase signaling as potential markers for targeted therapy in this uncommon aggressive lymphoma entity.

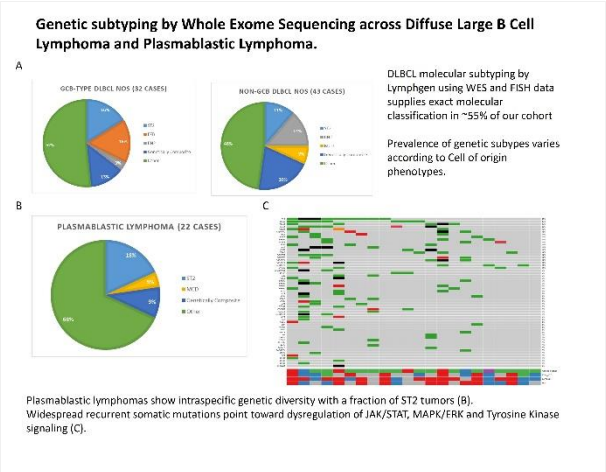

Figure 1

EA4HP24-ABS-482

Classic Hodgkin Lymphomas with Syncytial Morphology Exhibit a Primary Mediastinal Large B-Cell Lymphoma-Like Expression Signature by Lymph3Cx Analysis

PhD/MD Ryan S. Robetorye[1,3], Jon Ocal[3], Laura Budvytyte[2], PhD/MD Sarah E. Gibson[1], PhD/MD Lisa M. Rimsza[1,3]

[1] Mayo Clinic in Arizona, Department of Laboratory Medicine and Pathology, Phoenix, USA; [2] Mayo Clinic Aix School of Medicine, Scottsdale, USA; [3] Molecular Diagnostics - Arizona Laboratory, Department of Laboratory Medicine and Pathology, Scottsdale, USA

Background

Hodgkin lymphomas (HL) are comprised of 2 major types: nodular lymphocyte predominant and and classic HL (CHL). CHL accounts for 90% of all Hodgkin lymphomas and includes 4 subtypes, including nodular sclerosis (NSCHL), mixed cellularity (MCCHL), lymphocyte rich (LRCHL), and

lymphocyte depleted (LDCHL). When the neoplastic Hodgkin cells in NSCHL form prominent aggregates, this phenomenon is referred to as the “syncytial variant” of NSCHL (SVNSCHL). Although the Lymph3Cx gene expression profiling assay is intended to be used to distinguish between primary mediastinal large B-cell lymphoma (PMBL) and diffuse large B-cell lymphoma (DLBCL), we were interested to determine the results of this testing in CHL cases since CHL has been reported to be closely related to PMBL.

Principles/Methodology

26 total cases of CHL were subjected to Lymph3Cx analysis, including 10 cases of NSCHL, 4 cases of MCCHL, 2 cases of LRCHL, 1 case of LDCHL, and 9 cases of SVNSCHL. Case demographics, immunohistochemical findings, and Lymph3Cx results are summarized in Table 1. For Lymph3Cx analysis, tumor content is assessed using H&E-stained slides, and then additional unstained slides are used to isolate total RNA from the specimen. The RNA is hybridized overnight on a thermal cycler to the probes in the 58-gene Lymph3Cx assay panel. Probe/RNA complexes are quantitated on a NanoString nCounter® Digital Analyzer and subsequently subjected to an algorithmic analysis for further classification and subtyping. The assay produces a calculated score on a scale of 0.00 to 1.00 to classify each sample based on the probability that the sample is PMBL. Samples with a ≥90% probability of being PMBL (a score of 0.90–1.00) are classified as PMBL, with probability scores of 0.00–0.10 classified as DLBCL, and samples with scores >0.10 and <0.90 categorized as UNCLEAR.

Results

The characteristics of the 26 CHL cases included in the study, including Lymph3Cx analysis results, are summarized in Table 1.

Conclusion

26 cases of CHL were subjected to Lymph3Cx analysis, including all 4 subtypes of CHL as well as 9 cases of the syncytial variant of NSCHL. Interestingly, all 9 cases of SVNSCHL exhibited a PMBL-like gene expression signature (only 2 mediastinal cases), but none of the other CHL subtypes exhibited this signature. These findings suggest that SVNSCHL may actually represent a variant of PMBL rather than CHL. However, additional clinical correlation will be necessary to determine the true biological relationship between these 2 entities.

Table 1: CHL Case Characteristics and Lymph3Cx Analysis Results

Table 1: CHL Case Characteristics and Lymph3Cx Analysis Results

Case #	Age	Sex	Anatomic Location of Biopsy	Immunohistochemistry Profile of Hodgkin Cells	Diagnosis	Lymph3Cx Assignment with Probability Score
1	27	M	Cervical LN	CD15+, CD30+, CD45-	NSCHL	UNCLEAR (0.43)
2	39	M	Axillary LN	CD15+, CD30+, CD45-	NSCHL	UNCLEAR (0.88)
3	12	M	Cervical LN	CD15+, CD30+, CD45-	MCCHL	UNCLEAR (0.66)
4	45	F	Cervical LN	CD15+, CD30+, CD20-, CD79a-, CD45-	SVNSCHL	PMBL (0.93)
5	60	M	Iliac LN	CD15+, CD30+, CD45-	MCCHL	UNCLEAR (0.33)
6	51	F	Cervical LN	CD15+, CD30+, CD45-	LDCHL	UNCLEAR (0.25)
7	32	F	Mediastinum	CD15+, CD30+, CD20-, CD45-	SVNSCHL	PMBL (0.99)
8	30	M	Cervical LN	CD15+, CD30+, CD20+ (p/w), PAX5+ (w), CD45-	NSCHL	UNCLEAR (0.47)
9	27	M	Axillary LN	CD15+, CD30+, PAX5+ (w), CD20-, CD45-	SVNSCHL	PMBL (0.99)
10	25	M	Cervical LN	CD15+, CD30+, CD20+ (p), PAX5+ (w), CD45-, CD79a-	SVNSCHL	PMBL (1.00)
11	22	F	Cervical LN	CD15+, CD30+, CD20+ (v), CD79a+ (v), PAX5+ (w), CD45-	SVNSCHL	PMBL (1.00)
12	64	M	Supraclavicular LN	CD15+, CD30+, CD20+ (r), PAX5+ (w), CD45-	NSCHL	UNCLEAR (0.70)
13	52	M	Cervical LN	CD15+, CD30+, CD20+ (r), PAX5+ (w), CD45-	SVNSCHL	PMBL (0.99)
14	58	M	Axillary LN	CD30+, PAX5+ (w), CD15-, CD20-, CD45-	SVNSCHL	PMBL (0.99)
15	20	F	Mediastinum	CD15+, CD30+, PAX5+ (w), CD20-, CD45-	SVNSCHL	PMBL (1.00)
16	46	F	Axillary LN	CD15+, CD30+, CD20+ (v), PAX5+ (w), CD45-	SVNSCHL	PMBL (1.00)
17	22	F	Axillary LN	CD15+, CD30+, PAX5+ (w), CD20-, CD45-	NSCHL	UNCLEAR (0.25)
18	24	F	Cervical LN	CD30+, CD15-, PAX5+ (w), CD20-, CD45-	NSCHL	UNCLEAR (0.45)
19	20	F	Cervical LN	CD15+, CD30+, PAX5+ (w), CD20-, CD45-	NSCHL	DLBCL (0.07)
20	67	F	Mediastinum	CD15+, CD30+, PAX5+ (w), CD20-, CD45-	MCCHL	DLBCL (0.07)
21	63	M	Mediastinum	CD15+ (w), CD30+, CD20+ (subset), PAX5+, CD45-	LRCHL	DLBCL (0.01)
22	72	M	Supraclavicular LN	CD15+, CD30+, PAX5+ (w), CD20-, CD45-	LRCHL	DLBCL (0.02)
23	24	M	Cervical LN	CD15+ (w), CD30+, CD20 + (v), PAX5 + (w), CD45-	MCCHL	UNCLEAR (0.13)
24	65	M	Peritoneal LN	CD15+ (w), CD30+, PAX5+ (w), CD20-, CD45-	NSCHL	UNCLEAR (0.87)
25	63	M	Cervical LN	CD15+, CD30+, PAX5+ (w), CD20-, CD45-	NSCHL	UNCLEAR (0.60)
26	35	M	Mediastinum	CD15+ (w), CD30+, CD20+ (w, subset), PAX5+ (w), CD45-	NSCHL	UNCLEAR (0.73)

Abbreviations: LN = lymph node; p = partial expression; w = weak expression; v = variable expression; r = rare positive cells; NSCHL = nodular sclerosis classic Hodkin lymphoma; MCCHL = mixed cellularity classic Hodgkin lymphoma; SVNSCHL = syncytial variant nodular sclerosis classic Hodgkin lymphoma; LDCHL = lymphocyte depleted classic Hodgkin lymphoma; PMBL = primary mediastinal large B-cell lymphoma; DLBCL = diffuse large B-cell lymphoma

EA4HP24-ABS-520

The genetic landscape of primary breast marginal zone lymphoma identifies a mutational-driven disease with similarities to ocular adnexal and nodal marginal zone lymphoma

Vanesa-Sindi Ivanova*[1], Thomas Menter*[1], Joel Zaino[1], Kirsten D. Mertz[2], Baptiste Hamelin[2], Stefan Dirnhofer[1], Veronika Kloboves-Prevodnik[3,5], Alexandar Tzankov*[1], Gorana Gašljević*[4,5], *Equal contribution

[1] University Hospital Basel, University of Basel, Pathology, Institute of Medical Genetics and Pathology, Basel, Switzerland; [2] Cantonal Hospital Baselland, Institute of Pathology, Liestal, Switzerland; [3] Institute of Oncology Ljubljana, Department of Cytopathology, Ljubljana, Slovenia; [4] Institute of Oncology Ljubljana, Department of Pathology, Ljubljana, Slovenia; [5] University of Maribor, Faculty of Medicine, Maribor, Slovenia

Background

Extranodal marginal zone lymphomas (eMZL) manifest in diverse organs and sites throughout the body. Recent studies have shown that they differ from organ to organ in terms of their mutational profile. This study focuses on primary breast marginal zone lymphomas (PBMZL) to elucidate their morphological and molecular characteristics.

Principles/Methodology

Fifteen cases (14 female, 1 male) underwent comprehensive analysis, including immunohistochemistry, fluorescence *in situ* hybridization (FISH), and high throughput sequencing (HTS) with a lymphoma panel comprising 172 genes. Additionally, PCR for *Borrelia spp.* specific detection and metagenomics whole genome sequencing for microbial profiling were performed.

Results

Most cases showed follicular colonization, with rather subtle lymphoepithelial lesions observed in several instances. All cases were positive for BCL2 and pan B-cell markers and negative for CD5, CD11c, CD21. *BCL2, BCL10, IRF4, MALT1,* and *MYC* translocations were absent, with only one case presenting a *BCL6* rearrangement. Notably, *TNFAIP3* (n=4), *KMT2D* (n=2), and *SPEN* (n=2) were the most frequently mutated genes identified by HTS. No *Borrelia spp.* or other pathogens were detected, in spite of the fact that one patient had a clinical history of erythema chronicum migrans affecting the same breast.

Conclusion

PBMZL appears to be primarily driven by gene mutations rather than gene fusions, with alterations observed in genes associated with the NF-κB pathway, chromatin modification and the NOTCH pathway. Its mutational profile shares similarities with ocular adnexal and nodal MZL.

EA4HP24-ABS-550

Aggressive B-cell lymphomas with *MYC*-R single hit show Burkitt-like mutations in a subset of cases

Dr. Dominik Nann[1], Franziska Otto[1], Vannessa Borgmann[1], Barbara Mankel[1], Priv.-Doz. Irina Bonzheim[1], Prof. Laurence de Leval[2], Prof. Falko Fend[1], Prof. Leticia Quintanilla-Martinez[1]

[1] University Hospital Tübingen, Institute of Pathology and Neuropathology, Tübingen, Germany; [2] Lausanne University Hospital and Lausanne University, Institute of Pathology, Department of Laboratory Medicine and Pathology, Lausanne, Switzerland

Background

Aggressive B-cell lymphomas with *MYC*-R single hit (*MYC*-SH) other than Burkitt lymphoma (BL) show either a diffuse large B-cell lymphoma (DLBCL) morphology, features intermediate between DLBCL and BL (BCLU) or blastoid morphology. These cases often express BCL2 and/or lack CD10 and the Ki67 fraction is usually < 100%. The aim of the study was to genetically characterize a group of aggressive B-cell lymphomas other than BL with *MYC*-SH.

Principles/Methodology

33 aggressive B-cell lymphomas with *MYC*-SH were analyzed by FISH for *MYC*, *BCL2*, *BCL6*, IGH, IGK, and IGL translocations. A custom NGS panel (ThermoFisher), the FUSIONPlex lymphoma panel (Archer), and the Euroclonality NDC assay (Univ8 Genomics) were used for the detection of clonality, mutations and gene fusions.

Results

Median age was 70.5 years (range 19 - 94 years). The majority of cases had a centroblastic cytology (64%), followed by BCLU (21%), blastoid (9%), and immunoblastic (6%) morphology. By Hans algorithm and/or GEP, 25 cases (76%) were of GCB-type and 8 cases (24%) of non-GCB/ABC-type. BCL2 was expressed in 70% of cases, median proliferation was 90% (range 50-100%), and median MYC expression was 90% of the tumor cells (range 20-100%). By FISH, *MYC* was translocated in 25/33 cases (76%) to IG loci; in 22 cases the partner was IGH, demonstrated by fusion (13 cases) and/or by break apart probe (21), in 2 cases IGK and in 1 cases IGL. In 8 cases the partner remained unknown. In 13/18 cases (72%), Archer fusion analysis confirmed the *MYC*::*IGH* translocation, whereas 5 cases remained negative[MOU1] . All cases were monoclonal. The most frequent mutations (>10% of cases) identified were *MYC* (48%), *TP53* (30%), *MYD88* (21%), *PIM1*, *CCND3*, *CD79B*, *KMT2D* (each 18%), *ID3*, and *EZH2* (each 12%). The NDC assay showed

concordant results for most variants. However, it showed superior performance for alterations in homopolymeric or hypermutated regions and also a higher sensitivity than Archer assay for the detection of *MYC*-R. Interestingly, 6 cases showed a mutational and phenotypic profile characteristic of BL (*ID3*, *TCF3*, *SMARCA4*) (Figure 1). Three cases each had a centroblastic or BCLU morphology, and all a proliferation rate of ≥90%.

Conclusion

1) A subgroup of *MYC*-SH cases with DLBCL or BCLU morphology exhibit typical BL mutations, suggesting that the cytological spectrum of BL is broader than previously thought. 2) The NDC assay is a robust tool to analyze mutations, gene fusions and clonality in parallel.

sample ID	22	34	6	23	1	32
age	19	73	76	68	62	94
sex	m	m	m	m	w	m
morphology						
COO	GCB	GCB	GCB	GCB	GCB	GCB
IHC: BCL2	-	-	+	-	-	-
IHC: CD10	+	+	+	+	+	+
IHC: MIB [%]	100	90	95	100	95	>95
IHC: MYC [%]	90	70	90	100	20§	40
MYC						
ID3						
CCND3						
SMARCA4						
DDX3X						
TCF3						
NOTCH2						
MYC BAP-FISH	+	+	+	+	+	+
IGH BAP-FISH	+	+	+	+	10% +§	-
TriColor FISH (IGH::*MYC*)	n.d.	+	q.f.	n.d.	10% +§	-
11q-FISH	n.d.	-	-	-	-	-
Archer heme	-	-	q.f.	MYC-IGH	q.f.	-

centroblastic
BCLU
1 mutation
≥2 mutations

n.d. not done
q.f. quality failure
§ bad fixation

Results of 6 cases with Burkitt-like mutations
The figure shows the morphological and molecular characteristics of the 6 cases of aggressive B-cell lymphoma with Burkitt-like mutations. The NGS custom panel used included the 80 most frequent genes mutated in B-cell lymphomas. Genes with a wild type result are not mentioned.

EA4HP24-ABS-559

Checkpoint inhibition enhances cell contacts between CD4⁺ T cells and Hodgkin-Reed-Sternberg cells of classic Hodgkin lymphoma

PhD/MD student Kübra Yadigaroglu[1], M.Sc./M.A. Sonja Scharf[1], Dr. Steffen Gretser[1], Dr. Hendrik Schäfer[1], Dr. Aresu Sadeghi Shoreh Deli[2], Dr. Andreas G. Loth[2], M.Sc./M.A. Hasmik Yegoryan[3], Prof. Roland Schmitz[3], Prof. Emmanuel Donnadieu[4], Prof. Martin-Leo Hansmann[5], **Prof. Sylvia Hartmann**[1]

[1] Goethe Universität- Uniklinik, Pathology, Frankfurt, Germany; [2] Goethe Universität- Uniklinik, ENT, Frankfurt, Germany; [3] Gießen University, Pathology, Gießen, Germany; [4] Institut Cochin, Paris, France; [5] Goethe Universität- Uniklinik, Pharmacology, Frankfurt, Germany

Background

Although checkpoint molecules like CTLA-4 and PD1 have been described several years ago, checkpoint inhibitors such as Nivolumab (an anti-PD-1 antibody) have only recently been used to treat classic Hodgkin lymphoma (cHL). Several studies have shown convincing therapeutic effects of Nivolumab in cHL. However, the mechanism of action of Nivolumab in cHL is not fully understood.

Principles/Methodology

The aim of this study was to monitor changes in cell motility and cell contacts after administration of Nivolumab to an *in vitro* model of cHL as well as to native hyperplastic lymphoid tissue and native human tissue from cHL. Time-lapse 4D imaging was used to assess cell movement and the duration of cell-cell contacts.

Results

In both tissue and *in vitro*, $CD4^+$, $CD8^+$, $CD30^+$ and $CD20^+$ cell velocities were unchanged after Nivolumab incubation. In contrast, in primary cHL tissue, the duration of cell contacts between $CD4^+$ T cells and HRS cells was significantly increased after 5 h Nivolumab treatment, and the number of contacts with HRS cells was also slightly increased for $CD4^+$ T cells (not significant), suggesting that $CD4^+$ T cells in particular contribute to the cytotoxicity observed as a result of Nivolumab therapy. There was no change in the duration of cell contacts in the hyperplastic lymphoid tissue after Nivolumab incubation.

Conclusion

In conclusion, we show here for the first time by imaging of native lymphoma tissue an enhanced interaction of $CD4^+$ T cells and HRS cells in cHL 5 hours after Nivolumab administration.

EA4HP24-ABS-562

Mutational profile of multifocal/recurrent extranodal marginal zone lymphoma of mucosa-associated lymphoid tissue; Insights into the clonal heterogeneity and disease progression

Dr. Hee Kyung Kim[1], Dr. Uiju Cho[2], Dr. Yoon Kyung Jeon[3], Dr. Hyun-Jung Kim[4], Dr. Hee Jeong Cha[5], **Dr. Ji Eun Kim**[6]

[1] Soonchunhyang University Hospital, Department of Pathology, Bucheon, South Korea; [2] St. Vincent's Hospital, College of Medicine, The Catholic University of Korea, Department of Pathology, Seoul, South Korea; [3] Seoul National University Hospital, Seoul National University College of Medicine, Department of Pathology, Seoul, South Korea; [4] Inje University Sanggye Paik Hospital, Department of Pathology, Seoul, South Korea; [5] Ulsan University Hospital, Department of Pathology, Ulsan, South Korea; [6] Seoul National University Boramae Hospital, Department of Pathology, Seoul, South Korea

Background

Extranodal marginal zone lymphoma of mucosa-associated lymphoid tissue (ENZL) is generally perceived as an indolent lymphoma that tends to remain localized within a single organ for an extended period. However, multifocal and multiorgan involvement at presentation or late metastasis/recurrence without high-grade transformation occurs in patients with ENZL. Despite advancements in understanding the mutational landscape of ENZL, a genetic comparison between multifocal and recurrent cases remains lacking.

Principles/Methodology

We collected paired samples from eight patients with multiorgan or recurrent ENZL consisting of two gastric and 14 non-gastric tissues. Two patients exhibited multifocal ENZL in more than two different organs at the time of diagnosis, four patients experienced recurrent ENZL in different organ sites, and one initially had multifocal ENZL and later developed recurrence in other organ sites. We employed targeted, massively parallel DNA sequencing to analyze 50 genes recurrently mutated in lymphoma. Single nucleotide variants (SNVs) and small insertions/deletions (Indels) were analyzed, while copy-number variation was excluded. We evaluated the shared genetic characteristics of paired samples from individual patients.

Results

One or more mutations of the following 14 genes were detected across samples. The most frequently recurring mutations included KMT2D (23.2%), ARID1A (15.2%), TNFAIP2 (14.3%), MYC (13.4%), NOTCH1 (13.4%), and CARD11 (7.1%). Other genes were found in less than 3% of the samples. Among the three multifocal ENZL pairs, identical variants of ARID1A, KMT2D, MYC, NOTCH1, and TNFAIP3 were commonly shared in one of the pairs (Fig 1). In patients with recurrent ENZL, three experienced late recurrences, occurring more than five years after the initial diagnosis. The initial and recurrent MALT lymphoma cases shared identical variants of ARID1A, BCL10, CARD11, KMT2D, MYC, NOTCH1, and TNFAIP3 (Fig 2). Additionally, PLCG2 and STAT3 were uniquely present in the recurrent ENZL tissues among the mutated genes.

Conclusion

Our analysis provides insights into the mutational landscape of multifocal and recurrent ENZL. Recurrent mutations in ARID1A, KMT2D, MYC, NOTCH1, and TNFAIP2 were identified in multifocal, multi-organ ENZL cases. These findings suggest that these genes may contribute to the pathogenesis and progression of advanced or refractory ENZL.

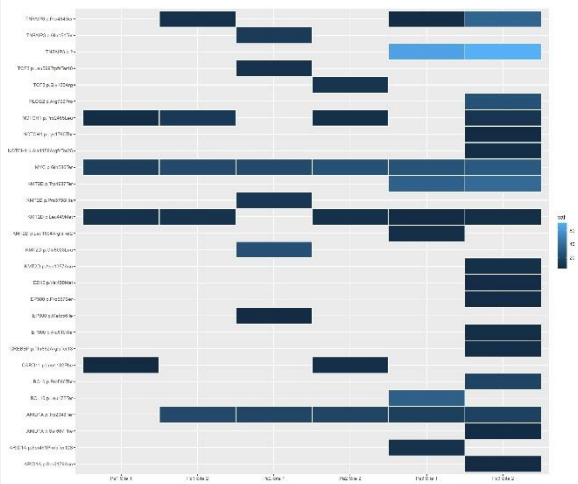

Figure 1
Mutational landscape of multifocal, multiorgan extranodal marginal zone lymphoma of mucosa-associated lymphoid tissue.

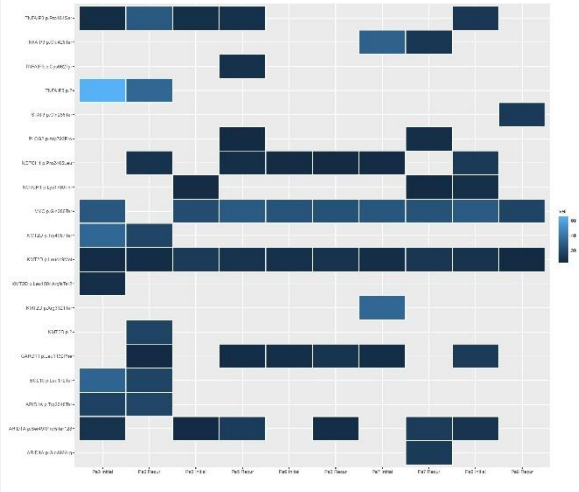

Figure 2
Mutational landscape of recurrent extranodal marginal zone lymphoma of mucosa-associated lymphoid tissue.

EA4HP24-ABS-567

Primary cutaneous follicle centre lymphoma- differential diagnostic and prognostic aspects.

PhD/MD Agota Szepesi[1], PhD/MD Bence Bátai[2,5], Dr. Jozsef Szakonyi[3], Dr. Tamas Schneider[4], Prof. Csaba Bodor[1,5]

[1] Semmelweis University, Department of Pathology and Experimental Cancer Research, Budapest, Hungary; [2] Semmelweis University, Department of Internal Medicine and Hematooncology, Budapest, Hungary; [3] Semmelweis University, Department of Dermatology, Venereology and Dermatooncology, Budapest, Hungary; [4] National Institute of Oncology, Budapest, Hungary; [5] Semmelweis University, Molecular Oncohematology Research Group Institute of Pathology and Experimental Cancer Research, Budapest, Hungary

Background

Primary cutaneous follicle center lymphoma (PCFCL) is an indolent, localized disease of the neoplastic follicular centre B-cells. Local relapses are common, however, distant cutaneous spread and systemic progression are rare and these cases are difficult to differentiate from secondary cutaneous manifestation of nodal follicular lymphoma (nFL). Unlike the systemic disease, the genetic background of PCFCL is remains unexplored.

Principles/Methodology

Thirty-nine cutaneous specimens from 30 patients with PCFCL diagnosed and followed up at Semmelweis University were studied. Collection of clinical data, histopathological revision, cytogenetic studies by fluorescent in situ hybridization and shallow (low-coverage) whole genome sequencing (lcWGS) was performed and was compared to 64 cases of nFL samples.

Results

Ninety-seven % of the PCFCL patients (21 female, 9 male) are alive, 70% are in complete remission after 52 months median follow up time. Progression was detected in 11 patients: distant cutaneous spread was found in 7 with systemic involvement documented in 4 cases. Sixty % of the lesions occurred at the head and neck area and these cases more often remained localized (p=0.023). Although the copy number profile of PCFCL was similar to that of nFL, PCFCL lacked amplifications of 18q (p=0.018). Development of distant cutaneous spread was significantly associated with higher genomic instability, as well as the enrichment of 2p22.2-p15 amplification involving *REL* and *XPO1 (*p=0.005), 3q23-q24 amplification (p=0.004), 6q16.1-q23.3 deletion (p=0.018) and 9p21.3 deletion covering *CDKN2A* and *CDKN2B* loci (p=0.014) in PCFCL. Analysis of sequential tumour samples in a case developing distant cutaneous spread, and a case showing nodal progression pointed to the acquisition of 2p amplification in the earliest common progenitor underlining its pivotal role in malignant transformation.

Conclusion

Based on our results, the copy number profile of PCFCL is only slightly different from that of nFL, with the notable exception of the scarcity of 18q amplifications including 18q21.33 covering the *BCL2* locus. This further highlights its potential utility in differential diagnosis of PCFCL and secondary cutaneous infiltration of nFL. Our results point to higher genomic instability in patients developing distant disease spread. We further deciphered the role of 2p amplifications in the disease course of PCFCL, which could be an early prognostic marker in the future for the prediction of distant disease spread.

EA4HP24-ABS-573

Identifying genomic abnormalities of aggressive B-cell lymphomas (BCLs) by optical genome mapping (OGM): A feasibility study with potential new discoveries

George Deeb[1], Tatiana Tvrdik[1], Shiyong Li[1], Saja Asakrah[1], Kristie Blum[2], Kristin Deeb[1]

[1] Emory University School of Medicine, Department of Pathology and Laboratory Medicine, Atlanta, USA; [2] Emory University School of Medicine, Department of Hematology and Medical Oncology, Atlanta, USA

Background

The identification of genomic structural and/or copy number variations (S/CNVs) is essential for diagnosis, classification, and prognostication of aggressive BCLs such as diffuse large B-cell lymphoma (DLBCL)/high-grade BCL (HGBCL) with *MYC* and *BCL2* rearrangements, HGBCL with 11q aberrations, large B-cell lymphoma (LBL) with *IRF4* rearrangement, and Burkitt lymphoma (BL). In the absence of defining S/CNVs, LBLs are classified as DLBCL-not otherwise specified (NOS). OGM, a nanochannel array for high-throughput imaging of long single DNA molecules (0.15-2.5 Mb) has been used to identify S/CNVs (such as deletions, insertions, inversions, translocations) in various hematologic neoplasms but has not been broadly utilized in tissue-based lymphomas. In this feasibility study we utilized OGM as a potential robust approach to investigate S/CNVs in tissue samples of aggressive BCLs.

Principles/Methodology

Sequential frozen tissue samples carrying the diagnosis of aggressive BCLs including biopsies of lymph nodes (5), tonsil (1), and bone (proximal tibia) (1) were analyzed by OGM (Saphyr instrument and Access software, Bionano Genomics, Inc.). One case ran in duplicate had concordant results. The results of morphology, immunophenotyping, fluorescence in-situ hybridization (FISH) studies for *BCL2*, *BCL6*, and *MYC* rearrangements, and OGM were reported.

Results

The analyzed cases included 5 DLBCL-NOS, 1 BL, and 1 follicular lymphoma with DLBCL. S/CNVs were detected in all cases by OGM (table 1). The results of OGM were concordant with those of FISH analyses. Interestingly, OGM confirmed DLBCL-NOS classification by excluding specific genetic classifiers, detected amplification of 9p24 in Case 3 (LBL with increased reactive CD8+ T-cells) and t(6;7)(p21.1;q21.3) in Case 5 (tibial bone LBL, figure 1), depicted deletion 17p in FL-transformed DLBCL, and affirmed the presence of *IGH::MYC* in BL, among others.

Conclusion

We demonstrated in this limited proof-of-concept study the ability of OGM to detect S/CNVs in tissue samples of aggressive BCLs. This high-resolution cytogenomic technology has the potential to detect S/CNVs required for definite classification as well as to elucidate other genetic aberrations that may further contribute to the discovery of novel subtypes or biomarkers. OGM has a promising potential of playing a critical role in the routine diagnostic work-up of tissue-based lymphomas including aggressive BCLs.

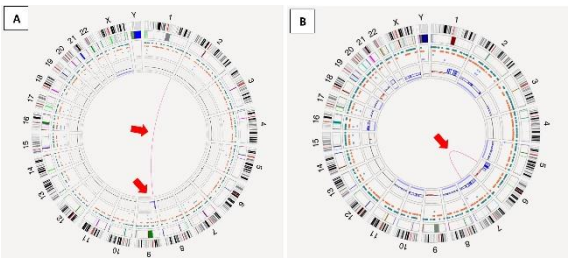

Figure 1. Circos plots of Cases 3 (A) and 5 (B). Circos plots highlighting the detection of genetic structural/copy number variants including amplification of 9p24.3p24.1 and t(1;9)(q44;p24.1) with no reported putative gene fusion in Case 3 (arrows), and t(6;7)(p21.1;q21.3) with putative gene fusion of *USP49-DYNC1I1* in Case 5 (arrow) .

Case	Sample	WHO 5th; (COO)	FISH	OGM [GRCh38]
1	LN	DLBCL, NOS (GCB)	**Positive for t(14;18)/*IGH::BCL2*** Negative for *BCL6* (3q27) rearrangement Negative for *MYC* (8q24) rearrangement	12q24.11(109967286-110793044)x1, 13q12.3q21.1(30098119-77156874)x1, **t(14;18)(q32.33;q21.33)**, 16p12.3p12.1(18905987-28308519)x3
2	LN	DLBCL, NOS (nGCB)	Negative for t(14;18)/*IGH:BCL2* **Positive for gain of one copy of 18q *BCL2*** Negative for *BCL6* (3q27) rearrangement **Positive for gain of one copy of 3q27** Negative for *MYC* (8q24) rearrangement **Positive for gain of one copy of 8q24**	t(3;13)(q24;q32.2), **3q24q29(146021846-198144878)x3**, **8q24.12q24.3(121413811-141099662)x3**, 12q24.31(121018491-123557452)x1, 13q32.2q34 (98022630-114352102)x1, 17p13.2p13.1(5105735-8133744)x1, **(18)x3**, **18q12.1q23(32140868-80256375)x4**
3	LN	DLBCL, NOS (nGCB)**	Negative for t(14;18)/*IGH:BCL2* Negative for *BCL6* (3q27) rearrangement Negative for *MYC* (8q24) rearrangement	t(**1;9**)(**q44;p24.1**), **9p24.3p24.1(638145-6721515)amp**, **9p24.1q11(6724125-43279152)x2~3**.
4	Tonsil	DLBCL, NOS (UD)	Negative for t(14;18)/*IGH:BCL2* **Positive for gain of one copy of 18q *BCL2* (gain of all or a portion of chromosome 18)** **Positive for *BCL6* (3q27) rearrangement** Negative for *MYC* (8q24) rearrangement	**t(3;17)(q27.3;q22)**, and multiple copy number changes including gain 3, and **18**
5	Bone***	DLBCL, NOS (UD)	ND	t(6;7)(p21.1;q21.3), 19p13.3p13.2(5985680-10575528)x1, and multiple copy number changes
6	LN	Follicular lymphoma, and DLBCL (GCB)	**Positive for t(14;18)/*IGH:BCL2*** Negative for *BCL6* (3q27) rearrangement Negative for *MYC* (8q24) rearrangement	**t(14;18)(q32.33;q21.33)** and multiple copy number changes including loss of 13 and 17p
7	LN	Burkitt lymphoma (NA)	Negative for t(14;18)/*IGH:BCL2* Negative for *BCL6* (3q27) rearrangement **Positive for t(8;14)/*IGH::MYC***	**t(8;14)(q24.21;q32.33)**

* – FISH analyses were performed on formalin-fixed paraffin-embedded tissue sections for t(14;18) rearrangements of BCL6 and MYC, and in one case t(8;14).
** – A reactive background significant for T-cells with CD4:CD8 ratio of 1:12 is detected by flow cytometry analysis. *** – DLBCL, NOS involving proximal tibial bone. WHO 5th – World Health Organization Classification of Haematolymphoid Tumours (5th edition). COO – Cell of origin is determined based on Hans algorithm utilising CD10, BCL6, and MUM1 immunostains. GRCh38 – Genome Reference Consortium human build 38. GCB – Germinal center B cell COO. nGCB – Non GCB. Amp – Amplification. UD – Undetermined. LN – Lymph node. DLBCL, NOS – diffuse large BCL, not otherwise specified. ND – Not done due to insufficient tissue material for analysis. NA – Not applicable.

Table 1. FISH and selected OGM results. Fluorescence in-situ hybridization (FISH)* and selected optical genome mapping (OGM) results of analyzing tissue samples of aggressive B-cell lymphomas (BCLs).

EA4HP24-ABS-586

Spatial transcriptomics reveal the prognostic values and macrophage heterogeneity in natural killer/ T cell lymphoma

PhD/MD student Min Liu[1,2], PhD/MD Reagan E. Linton[3], PhD/MD Giorgio Bertolazzi[4], PhD/MD student Shruti Sridhar[1], PhD/MD student Nicholas Syn[5], PhD/MD student Fan Shuangyi[3], Dr. Sai M. Leong[3], Dr. Anand D. Jeyasekharan[1], Prof. Claudio Tripodo[4], Prof. Siok-Bian Ng[1,3]

[1] National University of Singapore, Cancer Science Institute, Singapore, Singapore; [2] Chongqing University Cancer Hospital, Department of Radiation Oncology, Chongqing, China; [3] National University of Singapore, Department of Pathology, Singapore, Singapore; [4] University of Palermo, Tumour Immunology Unit, Palermo, Italy; [5] National University of Singapore, Department of Biomedical Informatics, Singapore, Singapore

Background

Natural killer/T cell lymphoma (NKTL) is a rare aggressive lymphoma with limited therapeutic options and poor outcome. Patients with relapsed and refractory NKTL respond to immune checkpoint therapy. Characterizing components of the tumour immune microenvironment (TME), specifically macrophages, in NKTL would enable a deeper understanding of the key determinants of tumour heterogeneity and associated clinical behaviour.

Principles/Methodology

The CD3+ tumour and CD68+ macrophage segments in NKTL FFPE tissues were profiled using Digital Spatial Profiling (DSP) protein (n = 62) and whole transcriptome atlas (WTA, n = 40), comprising 37 Immune-Oncology protein markers and an unbiased map of >18000 RNA targets, respectively.

Results

We first evaluated the expression of 37 Immune-Oncology protein markers in CD3+ tumour and CD68+ macrophage segments. As expected, CD3 and Ki67 were highly enriched in the tumour segment, while CD68 and CD163 were highly expressed in macrophage segment. Interestingly, most of the remaining immune-associated markers were upregulated within the macrophage compared to the tumour segments and overexpression of B7H3, CD127, CD163, and CD68 in the macrophage segment positively correlated with the Prognostic Index for NKTL (PINK) score. Furthermore, Kaplan-Meier survival analyses revealed that high expressions of B7-H3, CD163, CD66b, and OX40L in the macrophage segment are associated with poor overall survival (OS), whereas PD-1 overexpression was correlated with improved OS. To further explore the role of macrophages in NKTL, unsupervised clustering analysis of the macrophage segments in DSP WTA data was performed and revealed two distinct clusters of macrophages. Gene set enrichment analysis showed enrichment of signalling pathways, such as Interferon response and MYC target pathways in Cluster 2 compared to Cluster 1.

Conclusion

Spatial transcriptomic profiling of macrophages in NKTL unveils a previously unrecognized complexity of TME immune composition in this lymphoma. The expression of immunoregulatory receptor (i.e. CD163, CD127) and immune checkpoint (i.e. B7-H3) markers associated with worse prognosis in NKTL-associated macrophages hints at a role of myeloid immunosuppression. The identification of two distinct macrophage subclusters with unique signalling pathways underscores the need for a comprehensive characterization of macrophage subsets with different biological functions, highlighting their emerging roles in NKTL oncogenesis.

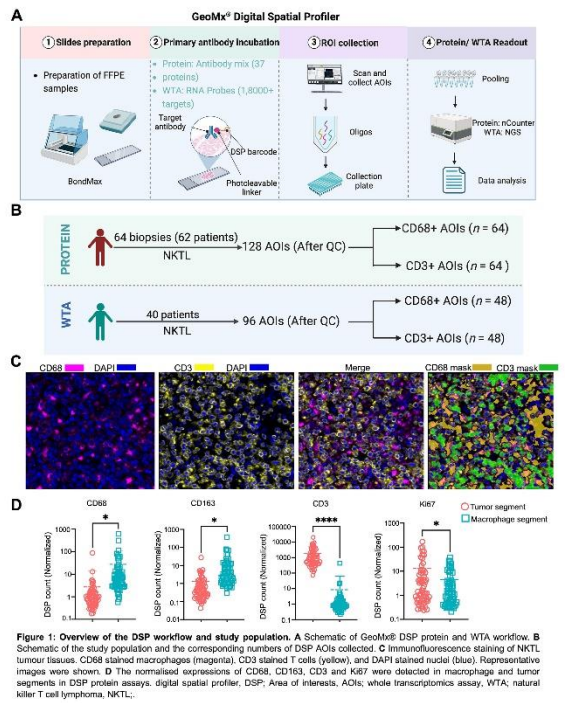

Figure 1: Overview of the DSP workflow and study population. A Schematic of GeoMx® DSP protein and WTA workflow. **B** Schematic of the study population and the corresponding numbers of DSP AOIs collected. **C** Immunofluorescence staining of NKTL tumour tissues. CD68 stained macrophages (magenta), CD3 stained T cells (yellow), and DAPI stained nuclei (blue). Representative images were shown. **D** The normalised expressions of CD68, CD163, CD3 and Ki67 were detected in macrophage and tumor segments in DSP protein assays. digital spatial profiler, DSP; Area of interests, AOIs; whole transcriptomics assay, WTA; natural killer T cell lymphoma, NKTL;.

Overview of the DSP workflow and study population

The figure outlines the GeoMx® DSP protein and WTA workflow, illustrating the study population and the quantity of DSP AOIs (Area of Interests) collected, thereby providing insights into sample size and distribution. The immunofluorescence images of NKTL (natural killer/T cell lymphoma) tumour tissues offer visual representations of cellular components within the tumour microenvironment. As a platform QC, the dot plot graphs showed the protein markers are detected within expected segment, such as CD68 and CD163 in the macrophage segment, and CD3 and Ki67 in the tumour segment.

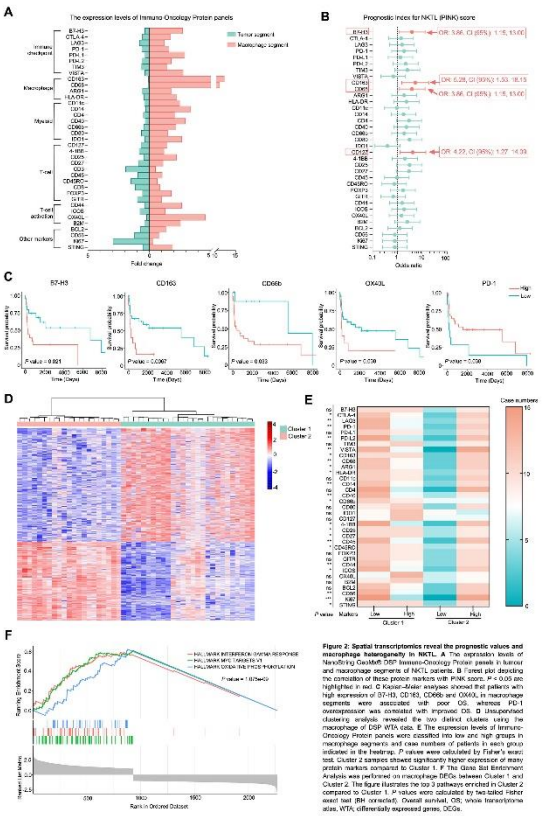

Spatial transcriptomics reveal the prognostic values and macrophage heterogeneity in NKTL
The figure presents findings from a spatial transcriptomics study on NKTL, revealing prognostically significant proteins and macrophage heterogeneity. Protein expressions are higher in the macrophage segment and positively correlated with the PINK score and poor survival. Cluster analysis identifies two distinct macrophage groups. Gene enrichment analysis reveals pathways enriched in one macrophage group compared to the other. These results shed light on the complex interplay between proteins and macrophages in NKTL, with potential implications for prognosis and treatment strategies.

EA4HP24-ABS-591

Molecular characterisation of Epstein–Barr virus in classical Hodgkin's lymphoma

M.Sc./M.A. Valerija Begić[2,1], Prof. Slavko Gašparov[3,4], M.Sc./M.A. Suzana Hančić[3], M.Sc./M.A. Marija Rozman[5], M.Sc./M.A. Petra Šimičić[5], M.Sc./M.A. Kristian Bodulić[5], M.Sc./M.A. student Roberto Galov[1], Dr. Snježana Židovec Lepej[5], **Prof. Petra Korać**[1]

[1] Faculty of Science, University of Zagreb, Department of Biology, Zagreb, Croatia; [2] Primary School "Sesvetski Kraljevec", Zagreb, Croatia; [3] Institute of Clinical Pathology and Cytology, Merkur University Hospital, Zagreb, Croatia; [4] Department of Pathology, Medical School Zagreb, University of Zagreb, Zagreb, Croatia; [5] Department of Immunological and Molecular Diagnostics, University Hospital for Infectious Diseases, Zagreb, Croatia

Background

Epstein-Barr virus (EBV) or human herpesvirus 4 is a ubiquitous virus belonging to the Herpesviridae family, which is considered to be an important etiological co-factor in the development of classical Hodgkin's lymphoma (cHL). Existing data about the molecular diversity of EBV and the connection between the genetic variability of the virus and the pathogenesis of classical Hodgkin's lymphoma are very scarce. Moreover, there are no specific antiviral drugs or available vaccines against EBV. The aim of this study was to analyse the distribution of genotypes, subtypes and gene variants of EBV subtypes in classical Hodgkin's lymphoma.

Principles/Methodology

The study was performed on formalin-fixed, paraffin-embedded samples from 90 patients with EBV-positive classical HL selected from a cohort of 289 histologically verified cases collected over a 9-year period. After the PCR amplification of selected genes, targeted population-based sequencing was performed.

Results

Our results showed the exclusive presence of EBV EBNA3 genotype 1 in all cHL samples, a predominance of the LMP1 wild-type strain B95-8, and the Mediterranean subtype with 30-bp deletion, as well as the predominance of EBNA1 prototype P-Thr. Based on EBER sequence analysis, we proposed a new algorithm for genotype determination with two main EBER subtypes.

Conclusion

Our findings define the molecular variety of EBV in the Croatian cHL cohort. We believe that such results can contribute to the understanding of EBV's roles in cHL pathogenesis and be helpful in the development of therapeutic vaccines.

EA4HP24-ABS-595

Cyclin D1 rearranged diffuse large B-cell lymphoma (DLBCL) – an evolving concept

Dr. Katrin S. Kurz[1], Prof. Alberto Zamo[2], Dr. Ewelina Madej[3], Prof. Camille Laurent[4], Dr. Barbara Burroni[5], Dr. Marie Donzel[6], Prof. Luc Xerri[7], Dr. Lenaïg Mescam[7], Prof. Lukas Plank[8], Prof. Lise Mette R. Gjerdrum[9,10], Dr. Julia Geyer[11], Dr. Julia Richter[12], Prof. Ilske Oschlies[12], Prof. Wolfram Klapper[12], Dr. Susanne Gramlich[2], Dr. Julia Doll[2], Sabine Roth[2], Dr. Heike Horn[1,13], Dr. Katja Maurus[2], Dr. Annette M. Staiger[1,13], Prof. Ming-Qin Du[3], Prof. Andreas Rosenwald[2], Prof. German Ott[1]

[1] Robert Bosch Hospital, Department of Clinical Pathology, Stuttgart, Germany; [2] Julius-Maximilians-Universität Würzburg, Institute of Pathology, Würzburg, Germany; [3] University of Cambridge, Department of Pathology, Cambridge, UK; [4] Centre Hospitalier Universitaire (CHU) Toulouse, Institut Universitaire du Cancer-Oncopole de Toulouse, Toulouse, France; [5] Cochin University Hospital, AP-HP, Pathology Department, Paris, France; [6] Centre Hospitalier Lyon Sud, Hospices Civils de Lyon, Service de Pathologie Multi-Site, Site Sud, Pierre-Bénite, France; [7] CRCM and Aix-Marseille University, Institut Paoli-Calmettes, Marseille, France; [8] Jessenius Medical Faculty of Comenius University and University Hospital, Department of Pathological Anatomy, Martin, Slovakia; [9] University of Kopenhagen, Department of Clinical Medicine, Kopenhagen, Denmark; [10] Zealand University Hospital, Department of Pathology, Roskilde, Denmark; [11] Weill Cornell Medicine, Department of Pathology and Laboratory Medicine, New York, USA; [12] University Hospital Schleswig-Holstein, University of Kiel, Department of Pathology, Hematopathology Section and Lymph Node Registry, Kiel, Germany; [13] Bosch Health Campus, Dr. Margarete Fischer-Bosch-Institute of Clinical Pharmacology, Stuttgart, Germany

Background

The Cyclin D1 (*CCND1*) translocation is strongly associated with mantle cell lymphoma (MCL) and plasma cell myeloma. However, tumors with DLBCL or high grade B-cell lymphoma morphology have been described carrying a *CCND1* rearrangement (*CCND1*R), most of them also with rearrangements of *BCL2, BCL6* and/or *MYC* posing the question if these are *bona fide* DLBCL or pleomorphic/large cell MCL. We have extensively characterized the immunophenotypic and genetic profiles of 15 DLBCL with *CCND1*R (DLBCL-*CCND1*R).

Principles/Methodology

15 DLBCL-*CCND1*R were characterized for CD10, BCL6, BCL2, CD5, Sox11, Cyclin D1, and MUM1 expression. FISH analyses for *MYC, BCL2, BCL6*, and *CCND1* translocations were done. IGVH mutational status and intraclonal variations were assessed by pooled library sequencing on an Illumina MiSeq. Exome sequencing was done and focussed on selected genes from the exome panel (~500 genes).

Results

14/15 cases with *CCND1*R had the typical morphology of DLBCL. 12 cases had centroblastic morphology (Fig.1 A,B), one tumor each was immunoblastic and immunoblastic/plasmacytoid. One case could not be properly assigned to a defined morphology, but did not have MCL morphological features (Fig.1 C,D). CD5 was positive in 3/15 (20%) cases. Cell lineage according to the Hans classifier was GCB in 3 cases (20%) and non-GCB in 12 cases (80%). CyclinD1 was positive and SOX11 was negative in all 15 DLBCL. FISH disclosed a *CCND1*Rin all cases with varying numbers of nuclei harboring split signals (50-85%). Additional translocations were detected in 8 cases (53%) involving *MYC, BCL2* and *BCL6*. 8/12 cases (67%) showed significantly mutated IGHV genes revealing <97% identity to germline. 8/12 cases showed evidence of intraclonal variations in their rearranged IGHV genes. In 14 evaluable DLBCL-*CCND1*R *TP53* and *CCND1* were the most frequently altered genes with pathogenic or likely pathogenic mutations each found in 5/14 (36%) cases. Table 1 illustrates the recurring alterations in the cases. Of note, *ATM, BIRC3* and *MEF2B* mutations typically encountered in MCL were recognized in only one case each. No mutations were observed in *NOTCH2, NSD2*, *KMT2A*, or *S1PR1*.

Conclusion

We conclude that DLBCL-*CCND1*R do exist and that *CCND1*R in these cases can occur as sole rearrangement *without* demonstration of additional breakage in *MYC, BCL2* or *BCL6*. These DLBCL-*CCND1*R are usually of non-GCB-type and carry mutated IGVH genes (<97% germline) in 67%, in contrast to MCL. The mutational spectrum of DLBCL-*CCND1*R is different from that of MCL.

Figure 1

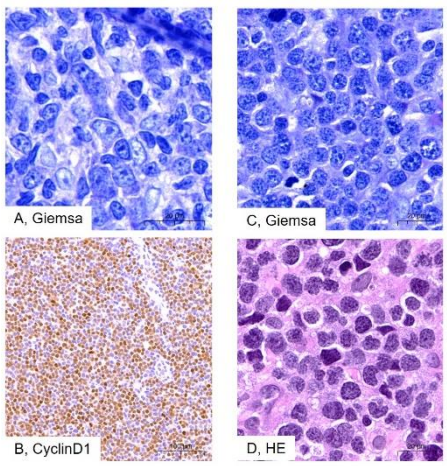

Figure 1

Table 1

ID	Mutations/Variants
4	TP53, TNFAIP3, NOTCH1, KLF2, ARID1A, FAS
5	CARD11, MYD88, PIM1, SOCS1, FBXO11
6	TP53, PIM1, PCLO, DDX3X, CCND1, POT1, FAT4
8	CREBBP, MYD88, CD79B, PIM1
10	TP53, BIRC3, PTBRD
11	CREBBP, NOTCH1, B2M, KMT2D, IRF4, PCLO, CCND1
12	poor quality
13	CXCR4, KMT2D, SPEN
15	NFKBIE, BCOR
16	KMT2D, MEF2B, BCL2, DTX3
17	EZH2, CREBBP, TNFRSF14, ATM, KMT2D, SOCS1, FOXO1, MYC, NOTCH1, ATM, CARD11
18	TP53, MYD88, KMT2C, CARD11, PIM1, TCF3, KMT2C
20	MYC, IRF8, CXCR4, PCLO, BTG1
21	CD79B, BCL2, PTBRD, SPEN
22	TP53, KMT2D, PIM1, H1-4

Table 1

EA4HP24-ABS-608

Dark zone Signature in diffuse large B-Cell Lymphoma of the German high-grade Lymphoma study group/German Lymphoma Alliance

Dr. Annette M. Staiger[1,2], Priv.-Doz. Ellen Leich[3], Dr. Robin Kosch[4], Prof. David W. Scott[5], Dr. Heike Horn[2,1], Dr. Marita Ziepert[6], Prof. Michael Altenbuchinger[4], Prof. Andreas Rosenwald[3], Prof. German Ott[1]

[1] Robert-Bosch-Krankenhaus, Institut für Klinische Pathologie, Stuttgart, Germany; [2] Dr. Margarete Fischer-Bosch - Institut für Klinische Pharmakologie, University of Tuebingen, Stuttgart, Germany; [3] University of Wuerzburg, Institute of Pathology, Wuerzburg, Germany; [4] University of Goettingen, Department of Medical Bioinformatics, Goettingen, Germany; [5] University of British Columbia, Department of Lymphoid Cancer Research, Vancouver, Canada; [6] University of Leipzig, IMISE, Leipzig, Germany

Background

Diffuse large B-cell lymphoma (DLBCL) is a heterogeneous disease category with various factors identifying clinical risk such as the cell of origin (COO), concomitant *MYC*- and *BCL2*-rearrangements ("double hit") and dual expression of MYC and BCL2 protein (DE). Since about 30-40% of patients with DLBCL relapse under R-CHOP treatment, their identification is of pivotal impact. With the DLBCL90 assay indicating COO and the newly defined Dark zone (DZ) signature (Ennishi et al., 2019; Alduaij et al., 2023), a robust tool for risk stratification in the diagnostic setting. The aim of the present study was to determine the frequency of DZsig^{pos} tumors and the prognostic impact of the signature in clinical trial cohorts of the DSHNHL/GLA.

Principles/Methodology

Digital gene expression profiling was performed using the DLBCL90 assay on the nCounter platform (nanoString Technologies, Seattle, WA) to assign COO and DZsig status. 848 tumors with DLBCL morphology, enrolled in DSHNHL/GLA clinical trials, were analyzed. All patients were treated with a R-CHO(E)P-regimen and clinical data were available. Data of fluorescence in situ hybridization (FISH) for *MYC*, *BCL2* and *BCL6* rearrangements and immunohistochemistry (IHC) for MYC and BCL2 protein were available from 490/848 tumor samples (Horn et al., 2013 and 2015, Staiger et al., 2020).

Results

815/848 tumor samples were evaluable. COO classification revealed 248/815 (30%) were ABC and 456/815 (56%) were GCB molecular type, while 111/815 (14%) were unclassified. DZsig was expressed in 56/815 (7%) of tumors. The great majority of tumors with DZsig^{pos} had a GCB-COO (54/56; 96%), 2/56 (4%)

were classified as ABC-COO. FISH and IHC data were available for 27/56 DZsig^{pos} tumors. 10/27 of DZsig^{pos} tumors (37%) were DLBCL-DH-*MYC/BCL2*, 1/27 (4%) DLBCL-DH-*MYC/BCL6*, 6/27 (22%) had sole *MYC* rearrangement. 18/27 (67%) were DE (MYC^{pos}/BCL2^{pos}).

Conclusion

In 815 tumor samples with DLBCL morphology of the DSHNHL the distribution of COO subtypes was comparable to previously published cohorts. The frequency of DZsig^{pos} expressing tumors (7%) and DZsig^{pos} tumors within GCB COO (12%) is lower than previously reported in a population-based Western cohort (Alduaij et al., 2023: 12% and 21%, respectively). Clinical correlations are ongoing and will be available during the meeting.

EA4HP24-ABS-625

Deciphering the molecular mechanisms behind *IRF4*-rearranged large B-cell lymphomas

PhD/MD student Ariadna Colmenero[1], PhD/MD student Sara Mato[1], Dr. Leonie Frauenfeld[2], PhD/MD Ferran Nadeu[1,3], PhD/MD Julia Salmerón-Villalobos[1], PhD/MD Joan Enric Ramis-Zaldivar[1], PhD/MD Anna Montaner[1], PhD/MD student Natalia Castrejón-de-Anta[4], Noelia Garcia[1], PhD/MD Mara Andrés[5], PhD/MD Jaime Verdú-Amorós[6], PhD/MD Maitane Andión[7], PhD/MD Daniel Azorín[8], Prof. Elaine S Jaffe[9], Prof. Leticia Quintanilla-Martinez[2], Prof. Elias Campo[1,3], PhD/MD Olga Balagué[1,3], **PhD/MD Itziar Salaverria**[1]

[1] Institut d'Investigacions Biomèdiques August Pi i Sunyer (IDIBAPS), Barcelona, Spain; [2] University Hospital and Comprehensive Cancer Center Tübingen, Institute of Pathology and Neuropathology, Tübingen, Germany; [3] Centro de Investigación Biomédica en Red de Cáncer (CIBERONC), Madrid, Spain; [4] Hospital Clínic de Barcelona, Hematopathology Section, Laboratory of Pathology, Barcelona, Spain; [5] Hospital La Fe, Pediatric Oncology Department, Valencia, Spain; [6] Hospital Clínico Universitario de Valencia, Department of Pediatric Oncology and Hematology, Valencia, Spain; [7] Hospital Niño Jesús, Pediatric Oncology Department, Madrid, Spain; [8] Hospital Niño Jesús, Anatomic Pathology Department, Madrid, Spain; [9] National Institutes of Health, National Cancer Institute, Bethesda, USA

Background

Large B-cell lymphoma with *IRF4* rearrangement (LBCL-*IRF4*) is a recently identified entity predominantly presenting in children and young adults (CAYA) as a localized disease (stage I/II) with excellent prognosis after systemic treatment. The tumor cells express germinal center markers, along with IRF4/MUM1. *IGH*::*IRF4* rearrangements are detected in most cases, though cryptic translocations have been suggested in some cases. Recent next-generation sequencing (NGS) studies have identified a distinct molecular profile in CAYA LBCL-*IRF4*, with recurrent *IRF4* and NF-kB-related mutations. LBCLs with *IRF4*-rearrangement (R) have also been observed in adults, but if they correspond to the same entity as tumors in CAYA is not well known. This study aims to characterize the structure of the *IRF4* translocation and mutational profile of *IRF4*-Rtumors and to assess if both age groups of tumors correspond to the same biological entity.

Principles/Methodology

Twenty-one CAYA LBCL-*IRF4* (mean age, 11.5y; range, 5-21) and 5 *IRF4*-R adult DLBCL (mean age, 56.4y) were studied by whole exome sequencing, and structural variant custom NGS. Two CAYA LBCL-*IRF4*

were *IRF4* non-R but carried IGH breaks. The diagnosis was established according to the revised 2017 WHO classification.

Results

6p25rearrangements were detected by NGS in 12/15 CAYA LBCL-*IRF4* andall *5* adult DLBCL. The breakpoints in 83% (10/12) of the CAYA tumors occurred in the 3‘ region of *IRF4,* 8 of them within introns 22-25 and exon 28 of *EXOC2*.IGH was the most common translocation partner with most breakpoints spread along class switch regions, suggesting an AID-mediated recombination. Only one case had an *IGK*::*DUSP22* rearrangement andone tumor exhibited a complex *IGH*::*IRF4*::*CD74* translocation (**Fig 1A-C**).

Breakpoints in the 5 adult LBCL-R occurred in the 5’ region of *IRF4*, generating an *IG*::*DUSP22* translocation in two of them. One tumor had a non-IG translocated partner *BATF*::*IRF4*, while another tumor showed a complex rearrangement involving *IRF4*, *BCL2* and IGH (**Fig 1B**-**C**).

CAYA LBCL-*IRF4* cases exhibited driver mutations in *IRF4* (15/18), *CCND3* (4/18), and *CARD11* (4/18). Adult cases shared the presence of *IRF4* mutations (4/5) and carried mutations in *KMT2D* (2/4)and non-L265P *MYD88* (2/4), which is virtually absent in CAYA.

Conclusion

This study reveals that *IRF4* translocation architecture and mutational profile in CAYA and adult DLBCL are different suggesting that not all large B-cell lymphomas with *IRF4* translocation may correspond to the LBCL-*IRF4* entity.

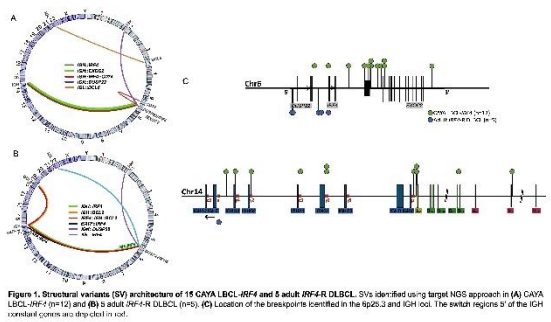

Figure 1. Structural variants (SV) architecture of 15 CAYA LBCL-IRF4 and 5 adult IRF4-R DLBCL.
SVs identified using target NGS approach in (A) CAYA LBCL-IRF4 (n=12) and (B) 5 adult IRF4-R DLBCL (n=5). (C) Location of the breakpoints identified in the 6p25.3 and IGH loci. The switch regions 5' of the IGH constant genes are depicted in red.

EA4HP24-ABS-633

Pediatric-type follicular lymphoma lacks n-glycosylation sites and positive antigen selection despite ongoing somatic hypermutation.

Dr. Leonie Frauenfeld[1,2], Dr. Julia Steinhilber[1], Dr. Nika Abdollahi[3], Dr. Véronique Giudicelli[3], Dr. Itziar Salaverria[2], Dr. Praveen Baskaran[4], Dr. Sven Nahnsen[4], Prof. Falko Fend[1], Prof. Elias Campo[2,5], Prof. Elaine Jaffe[6], Priv.-Doz. Irina Bonzheim[1], Prof. Leticia Quintanilla-Martinez[1]

[1] University Tuebingen, Institute for Pathology and Neuropathology, Tuebingen, Germany; [2] August Pi i Sunyer Biomedical Research Institute (IDIBAPS), Barcelona, Spain; [3] University Montpellier, IMGT, The International ImMunoGeneTics Information System, National Center for Scientific Research (CNRS), Institute of Human Genetics (IGH), Montpellier, France; [4] University Tuebingen, QBiC (Zentrum für Quantitative Biologie), Tuebingen, Germany; [5] Hospital Clinic, Laboratory of Pathology, Hematopathology section, Barcelona, Spain; [6] National Cancer Institute, NIH, Hematopathology Section, Laboratory of Pathology, Bethesda, USA

Background

Pediatric-type follicular lymphomas (PTFL) occur mainly in children and young adults and shows a very indolent course. PTFL exhibits a distinct molecular profile compared to conventional follicular lymphoma (cFL) characterized by lack of t(14;18) translocations and recurrent mutations in *TNFRSF14*, *KMT2D*, *MAP2K1* and *IRF8*. Given the important role of the rearranged immunoglobulin for cFL lymphomagenesis, we aimed to investigate the pathogenesis of PTFL further by characterizing the immunogenetic features of this entity.

Principles/Methodology

We investigated 31 PTFL with known mutational status. As controls, 5 cFL, 2 cases of chronic lymphocytic leukemia (CLL-U) and 3 reactive lymph nodes were included. NGS-based sequencing of the immunoglobulin (IG) genes with the LymphoTrack assay was performed. All sequenced cases were then analyzedby IMGT/HighV-QUEST.

Results

A clonally rearranged IGH gene was amplified in 28/31 cases, and a rearranged IGK in 3/31. Most cases (18/31; 58%) used the VH3 gene family, comparable to the normal circulating B cells. 3/28 cases used the gene rearrangement VH3-07*01, and 3/3 cases VK3-15*01, all other rearrangements occurred exclusively in one case of the cohort. Among the mutated cases, the distribution of the VH gene family usage was not skewed (Fig.1). Somatic hypermutations (SHM) were found in most of the PTFL (26/31 mutated), similar to cFL. Ongoing SHM were found in all 7 investigated PTFL (Fig.2), in contrast, SHM was absent in CLL cases used as control. Antigen driven lymphomagenesis was investigated by calculating the R/S mutation rate. No clear evidence of antigen driven proliferation was demonstrated. N-glycosylation sites, that are known to stimulate BCR signaling, were identified in only 3/31 PTFL cases, in contrast to 4/5 cases of cFL (9.6% vs 80%, p=0.0027). The results from the LymphoTrack software and the additional IMGT/HighV-QUEST analyses were concordant in 32 of 36 cases, being differences most probably related to biostatistical pipelines.

Conclusion

PTFL is characterized by a distinct mutational profile with lack of t(14;18) translocation. In this study, we demonstrated that PTFL shows ongoing SHM but lacks N-glycosylation sites typical of cFL. Furthermore, PTFL does not have skewed usage of VH genes making an antigen driven mechanism to

explain lymphomagenesis unlikely. Further studies are warranted to elucidate the mechanism(s) that trigger the development of the disease.

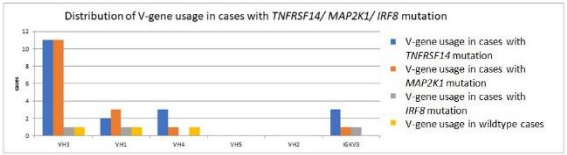

Distribution of V-gene usage according to mutations

Fig.1 PTFL cases with mutations in *TNFRSF14*, *MAP2K1* and/or *IRF8* according to their V-gene usage. Some cases have multiple mutations.

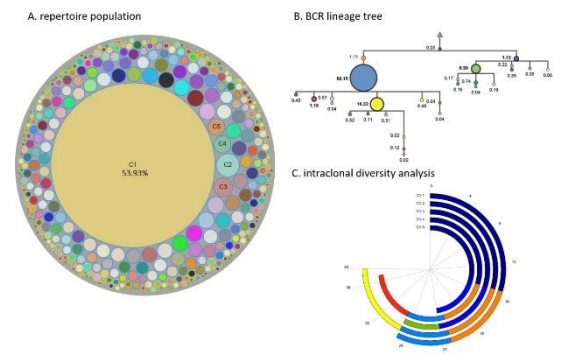

Phylogenetic tree of PTFL- case 14

Fig. 2 Case 14. A. shows the repertoire population with the 5 most abundant clonal lineages (C1-C5, clone C1: 52.93%) within the complete repertoire. B. depicts the BCR lineage tree as a phylogenetic tree of C1 clonotype. The branch lengths represent the number of SHM among connected clonotypes. C. circular bar chart represents the number of SHM of the ancestral (dark blue, hypothetical naïve sequence) in comparison to the selected clonotypes' sequence C1.

EA4HP24-ABS-656

CCND1-Rearranged Large B-Cell Lymphomas Have Different IG Breakpoints and Genomic Profile Than Mantle Cell Lymphoma

Dr. Ece Ozogul[1,2], Dr. Melina Pol[1], Anna Montaner[1], Dr. Gerard Frigola[1,3], Prof. Olga Balagué[1,3], Dr. Charlotte Syrykh[4,5], Pablo Bousquets-Muñoz[6,7], Dr. Juliette Fontaine[8], PhD/MD Alexandra Traverse-Glehen[8], Dr. Marco M. Bühler[9], Dr. Luca Giudici[9], Dr. Marco Roncador[9], Prof. Thorsten Zenz[9], PhD/MD Sylvain Carras[10], Dr. Severine Valmary-Degano[10], Prof. Laurence de Leval[11], Julia Salmeron-Villalobos[1], Silvia Ruiz[1], Dr. Dolors Costa[1,3], Dr. Silvia Bea[1,3], Dr. Itziar Salaverria[1], Prof. Leticia Quintanilla-Martinez[12], Dr. Pierre Brousset[4,5], Dr. Mark Raffeld[13], Prof. Elaine S Jaffe[13], Xose S Puente[6,7], Cristina Lopez[1,3], Ferran Nadeu[1,3], Prof. Elias Campo[1,3]

[1] Institut d'Investigacions Biomèdiques August Pi i Sunyer (IDIBAPS), Barcelona, Spain; [2] Hacettepe University Faculty of Medicine, Pathology Department, Ankara, Turkey; [3] Hospital Clínic de Barcelona, Barcelona, Spain; [4] Toulouse University Hospital Center, Cancer Institute University of Toulouse-Oncopole, Toulouse, France; [5] University of Toulouse III Paul-Sabatier, INSERM UMR1037 Cancer Research Center of Toulouse (CRCT), ERL 5294 National Center for Scientific Research (CNRS), Toulouse, France; [6] Centro de Investigación Biomédica en Red de Cáncer (CIBERONC), Madrid, Spain; [7] Universidad de Oviedo, Instituto Universitario de Oncología (IUOPA), Oviedo, Spain; [8] Hopital Lyon Sud, Pierre-Bénite, France; [9] University Hospital Zurich, Zurich, Switzerland; [10] CHU Grenoble Alpes and INSERN UMR 1209/CNRS 5309, Institute for Advanced Biosciences, Grenoble, France; [11] Lausanne University Hospital and Lausanne University, Lausenne, France; [12] University Hospital Tübingen, Eberhard Karls University of Tübingen and Comprehensive Cancer Center, Tübingen, Germany; [13] National Cancer Institute, National Institutes of Health, Bethesda, MD, USA, Bethesda, USA

Background

Mantle cell lymphoma (MCL) is genetically characterized by the *IG*::*CCND1* translocation mainly mediated by an aberrant V(D)J rearrangement. *CCND1* translocations and cyclin D1 overexpression have been identified in occasional aggressive B cell lymphomas with unusual features for MCL. The mechanism generating *CCND1* rearrangement in these tumors and their genomic profile are not known. The aims of this study were to characterize the *IG*::*CCND1* translocation in these aggressive B-cell lymphomas, define their mutational profile, and determine the diagnostic value of these alterations.

Principles/Methodology

Twelve cases of SOX11-negative aggressive B-cell lymphomas expressing cyclin D1 and carrying *CCND1* rearrangement were selected. All samples had been fixed in formalin and embedded in paraffin (FFPE). Frozen tumor and non-involved peripheral blood were also available in 3 and 4 patients, respectively. FISH studies using fusion and/or break-apart probes for *CCND1*, *BCL2*, *BCL6,* and *MYC* were performed in all cases and for *IRF4* in 3. Whole-genome sequencing (WGS) and whole-exome sequencing (WES) were performed in 3 and 4 cases, respectively. Target next-generation sequencing panels interrogating a wide spectrum of genes involved in B-cell lymphomas were used for mutational analysis in 11 patients. We also designed a custom NGS panel covering all IG loci and the relevant MCL driver genes.

Results

CCND1 was rearranged with IG genes in all tumors. Three cases had RAG-mediated breaks during V(D)J recombination, while the remaining 9 involved AID through aberrant class-switch recombination (CSR) (8 cases) or somatic hypermutation (SHM) mechanism (1 case) regions. The tumors with a VDJ-mediated translocation were two blastoid MCL and one high-grade B-cell lymphoma carrying a *MYC* rearrangement. These 3 tumors had *TP53* mutations but none of them had a mutational profile suggestive of DLBCL. Two tumors with CSR/SHM mediated *IGH*::*CCND1* were large B-cell lymphomas transformed from marginal zone lymphomas carrying mutations in *KLF2*, *TNFAIP3* and *KMT2D*. The seven remaining tumors had mutated genes commonly seen in DLBCL. *BCL6* was rearranged in 5 of these tumors and *IRF4* in one.

Conclusion

These findings expand the spectrum of lymphomas carrying *CCND1* rearrangement that may occur as a secondary event in DLBCL mediated by aberrant CSR/SHM and associated with a mutational profile different from that of MCL. These findings provided insight for distinguishing MCL and cyclin D1+ DLBCL, improving diagnostic accuracy.

EA4HP24-ABS-662

LYMPHOMA WITH CONCURRENT MYC TRANSLOCATION AND 11q ABERRATION: BURKITT LYMPHOMA OR NOT?

PhD/MD Margherita Vannucchi[1], Dr. Anja Fischer[17], Dr. Pierre Isnard[3], Dr. Maria Chiara Siciliano[1], Dr. Domenico Ferrara[1], Dr. Massimo Granai[1], Dr. Raffaella Guazzo[1], Prof. Elena Sabattini[8], Prof. Claudio Agostinelli[9], Prof. Alexandra Traversae–Glehen[10], Dr. Susanne Bens[11], Prof. Leticia Quintanilla-Martinez[12], Prof. Cristiana Bellan[1], Prof. Thierry Molina[14], Prof. Stefano Lazzi[1], Prof. Lorenzo Leoncini[1], Prof. Reiner Siebert[17]

[1] University of Siena, Department of Medical Biotechnology, Siena, Italy; [2] Ulm University Medical Center, 89081, Ulm, Germany., Institute of Human Genetics, Ulm University, ulm, Germany; [3] AP-HP_Centre, Necker University Hospital, Paris University, Paris, Department of Pathology, Paris, France; [4] University of Siena, Department of Medical Biotechnology, Siena, Italy; [5] University of Siena, Department of Medical Biotechnology, siena, Italy; [6] University of Siena, Department of Medical Biotechnology, siena, Italy; [7] University of Siena, Department of Medical Biotechnology, Siena, Italy; [8] University of Bologna, Bologna, Italy, Haematopathology Unit, Department of Experimental Diagnostic and Specialty Medicine (DIMES), Bologna, Italy; [9] University of Bologna, Bologna, Italy, Haematopathology Unit, Department of Experimental Diagnostic and Specialty Medicine (DIMES), Bologna, Italy; [10] Hospices Civils de Lyon/Department of Pathology/ Université Lyon 1/ Centre International de Recherche en Infectiologie (CIRI), Lyon, France., Hospices Civils de Lyon/Department of Pathology, Lyon, France; [11] Ulm University Medical Center, 89081, Ulm, Germany., Institute of Human Genetics, Ulm University, Ulm, Germany; [12] University Hospital Tübingen, Tübingen, Germany, Institute of Pathology and Neuropathology, Tubingen, Germany; [13] University of Siena, Department of Medical Biotechnology, Siena, Italy; [14] AP-HP_Centre, Necker University Hospital, Paris University, Paris, Department of Pathology, Paris, France; [15] University of Siena, Department of Medical Biotechnology, siena, Italy; [16] University of Siena, Department of Medical Biotechnology, Siena, Italy; [17] Ulm University Medical Center, 89081, Ulm, Germany., Institute of Human Genetics, Ulm University, Ulm, Germany

Background

High-grade B-cell lymphoma with 11q aberrations (HGBCL-11q) is an aggressive mature B-cell lymphoma harboring a characteristic chromosome 11q gain/loss pattern in the absence of a *MYC* rearrangement (*MYC*-R).Currently, it is unclear how to deal with rare cases of HGBCL that have both, 11q aberrations and a *MYC*-R. Here, we report 5 cases of lymphomas with concurrent 11q aberrations and *MYC* -R with the aim to better define their morphological, immunophenotypic and molecular characteristic for a correct diagnosis.

Principles/Methodology

We performed histological and immunohistochemical characterization (n = 5), FISH (n = 5), targeted NGS analysis (72 genes panel, Sophia Genetics) (n = 4), copy number analysis with OncoScan (n = 5) and DNA methylation analysis (n = 2).

Results

Except case 1 (7-year old girl), all patients were male (median age 63 years). 3 cases were diagnosed as BL, 1 as HGBCL-11q and o1 as HGBCL, NOS. The cases were characterized by mixed features either favoring BL (starry sky, narrow basophilic cytoplasm, moderately dense chromatin) or against BL (cell polymorphism, irregular nuclear shape). All cases showed positivity for CD10, CD20, BCL6, a Ki67 > 95% and were negative for EBV. However, immunophenotypic features non-characteristic of BL were detected, with BCL2 and MUM1 positivity in one case and two cases positive for LMO2. Interestingly, sequencing analysis did not reveal mutations in genes typically altered in BL, except for one case (case

n.3), which revealed alterations in *ID3*, *TP53*, *ARID1A* and *FOXO1*. Mutations in *DDX3X* common in both BL and HGBCL-11q were detected in 2/4 cases, in addition to genetic alteration typical of DLBCL (*TNFAIP3*, *STAT6* and *NOTCH2). TP53* mutations were also present in 2/4 cases analyzed. Copy number analysis also showed mixed features of BL (gain 13 and gain 1q) in 3/5 as well as gain 7 and trisomy 12, which can be found in both types in 3/5 cases. DNA methylation analysis showed inconclusive clustering of two cases.

Conclusion

HGBCLs with 11q aberration and concurrent *MYC*-R appear to be genetically distinct from both classic BL and HGBCL/LBCL with 11q aberration demonstrating an intermediate morphological and mutational landscape.The number of such cases may be underestimated as screening for 11q aberrations is recommended only for *MYC*-R negative B-cell lymphomas that are morphologically similar to BL. It is important to identify these cases that seems to have a worst prognosis, at least in adults, and should be classified as HGBCL, NOS.

EA4HP24-ABS-666

Association to both BCL2-positive and negative follicular lymphoma to Clasical Hodgkin Lymphoma and/or Gray Zone Lymphoma.

Francisco Javier Diaz de la Pinta[1], Rebeca Manso[1], Isabel Betancor-Fernandez[3], Daniel M. Gilles[2], Manuela Mollejo[4], Socorro Maria Rodriguez Pinilla[1]

[1] FJD, Pathology, Madrid, Spain; [2] FJD, Haematology, Madrid, Spain; [3] Complejo Hospitalario Universitario de Canarias, Pathology, Tenerife, Spain; [4] Hospital Universitario Virgen de la Salud de Toledo, Pathology, Toledo, Spain; [5] Fundacion Jimenez Diaz, Pathology, Madrid, Spain

Background

Histological transformation (HT) of Follicular (FL) is considered a common event in the natural history of the disease with an estimated risk of 3% per year. FL evolving into classical Hodgkin lymphoma has been previously reported. Nevertheless, its biological background is not fully known yet.

Principles/Methodology

We studied FL and CHL components using HE, IHQ, FISH for BCL2/BCL6 gene rearrangements, PCR for IgH and targeted next genaration sequencing

Results

We present a series of 9 follicular lymphomas that progressed/transformed into classical Hodgkin lymphoma (CHL). Three cases of CHL showed a syncytial pattern (SCHL) making the differential diagnosis to Gray zone lymphoma (GZL) challenging. None of these three cases presented in the mediastinum. Based in all molecular data analyzed (BCL2/BCL6 FISH studies, IgH PCR and TNGS with a customized gene panel) we did find clonal relationship between the BCL2-positive FL cases and their CHL components in all cases. The three SCHL/GZL cases showed an activated phenotype according to Hans algorithm, presented the t(14;18)(q32;q21), two out of three showed B cell markers and all expressed CD30 and p53. Interestingly, we identified three BCL2-negative FL cases with a further diagnosis of CHL expanding the spectrum of these association. In one of these three cases a different mutational profile was found in both the FL and the CHL components.

Conclusion

All this data together suggests that CHL associated to BCL2-positive FL could be originated in a common progenitor cell (CPC) that give rise to both FL and CHL, acquiring this last component further genetic events in a linear fashion. On the other hand, no clonal relationship between CHL and BCL2-negative FL could be found, suggesting a fortuity association. Nevertheless, ample series of cases studied with more sensitive techniques are needed to confirm our hypothesis.

EA4HP24-ABS-671

Multimodal spatial profiling reveals unique immunobiological features of EBV+ Hodgkin-like lymphoproliferations

Dr. Matthew R. Pugh[1], Dr. Eanna Fennell[2], M.Sc./M.A. student Jacob Skidmore[1], Dr. Gareth Leopold[3], Dr. Graham Taylor[1], Prof. Paul Murray[2], Prof. Stefan Dojcinov[3]

[1] University of Birmingham, Institute of Immunology and Immunotherapy, Birmingham, UK; [2] University of Limerick, Bernal Institute, Limerick, Ireland; [3] Swansea Bay Health Board, Cellular Pathology, Swansea, UK

Background

Epstein-Barr virus-positive lymphoproliferative disorders can exhibit overlapping Hodgkin-like morphological features but show a wide spectrum of clinical behaviours. This study aimed to identify the immuno-biological basis of this divergent clinical behaviour using multimodal spatial profiling of the immune microenvironment and tumour cells.

Principles/Methodology

Multiplex immunofluorescence (mIF) and Nanostring GeoMX spatial profiling (GeoMX-DSP) were performed on formalin-fixed paraffin-embedded (FFPE) sections, comparing indolent EBV+ mucocutaneous ulcer (EBVMCU) to malignant EBV+ classical Hodgkin lymphoma (EBVCHL) and EBV+ diffuse large B-cell lymphoma (EBVDLBCL). Chromosome 9 ploidy and PDL1 amplification status were assessed by DNA fluorescent *in situ* hybridisation (FISH).

Results

MIF demonstrated a significant increase in CD4+ T-regulatory and PDL1+IDO1+M1 macrophages in EBVMCU ($p<0.05$), whilst EBVDLBCL showed a significant increase in immunosuppressive IDO1+M2 macrophages ($p<0.05$). Macrophages were enriched in the immediate vicinity of HRS/-like cells. Analysis of GeoMX-DSP by gene set enrichment analysis revealed that EBVMCU was characterised by marked antiviral responses, showing upregulation of pathways involved in T-regulatory chemotaxis in HRS cells (odds ratio (OR) 120; $p <0.0001$), interferon-alpha; (OR 50; $p <0.0005$) and interferon-beta (OR 40; $0 < 0.0004$) responses in macrophages. Similarly, EBVMCU HRS-like cells, in comparison to EBVDLBCL HRS-like cells, showed upregulation of type 1 interferon responses (OR 20; $p< 0.00025$). Differential gene expression analysis shows increased expression of tumour suppressor CRIP1 (FDR>0.001), chemotactic CXCL10 and pro-inflammasome IL1RN (FDR>0.001) in EBVMCU, and upregulation of anti-inflammasome IL1R2 (FDR>0.001) in EBVCHL and EBVDLBCL. CXCL10 expression was validated by RNAscope showing expression in 100% of EBVMCU, and 0% of ulcerating EBVDLBCL or EBVCHL. EBVMCU showed no chromosome 9 aneuploidy above 3n by DNA FISH compared to 50% in EBVDLBCL and 33% EBVCHL. Amplification of PDL1/PDL2 (>2n+1) was not present in EBVMCU or EBVDLBCL, but characterised 66% of cHL.

Conclusion

EBVMCU showed evidence of active inflammation, T-regulatory cell chemotaxis and anti-viral response, whereas EBV+cHL and EBVDLBCL showed evidence of immune permissive, and immune suppressive microenvironments, with loss of inflammasome related signalling and decreased tumour suppressor mechanisms. CXCL10 and FISH for PDL1 are potential diagnostic discriminatory markers.

Lymphoma Abstracts with Mini Presentations

EA4HP24-ABS-522	Bone marrow pathology in patients with cold agglutinin disease: Preliminary results of the Re-CAD study.
EA4HP24-ABS-532	High ADAM8, ADAM9 and ADAM15 expression is associated with proliferation signaling and progressive disease in multiple myeloma
EA4HP24-ABS-538	SOX11 expression is restricted to EBV-negative Burkitt lymphoma and associates with molecular genetic features
EA4HP24-ABS-561	An ultrasensitive dual in situ hybridization (ISH) mRNA assay is equivalent in performance to flow cytometry in determination of kappa/lambda (K/L) restriction status in B cell lymphomas and plasma cell malignancies
EA4HP24-ABS-563	Cytoplasmic Lipid Droplets Predict Worse Prognosis in Diffuse Large B-cell Lymphoma: Next Generation Sequencing Deciphering Lipogenic Genes
EA4HP24-ABS-564	NPM-ALK Oncoprotein Suppresses STAT3-Mediated Anti-Tumor Immune Responses Partially Through cGAS-STING Pathway in ALK+ Anaplastic Large Cell Lymphoma.
EA4HP24-ABS-566	Genome-wide copy-number profiling identifies novel therapeutic targets in follicular lymphoma
EA4HP24-ABS-577	Clonal hematopoiesis of indeterminate potential is associated with inferior outcome in patients with lymphoma
EA4HP24-ABS-584	Homologous recombination deficiency in follicular dendritic cell sarcoma.
EA4HP24-ABS-596	Genomic Characterization of Peripheral T-cell Lymphomas with Co-expression of CD30/CD15 Suggests a Close Relationship to Anaplastic Large-Cell Lymphoma, ALK-negative
EA4HP24-ABS-619	Unravelling TOX2 expression in B and T Cell Lymphomas
EA4HP24-ABS-626	Insights into T-Follicular Helper Cell Lymphomas and Peripheral T-Cell Lymphomas, Not Otherwise Specified, in Slovenian Patients: Mutational Landscape, Clinicopathological Characteristics, and Outcomes
EA4HP24-ABS-648	HGBCL-11q: the darkest Lymphoma Microenvironment?
EA4HP24-ABS-654	Genetic alterations and CCDN1 rearrangement mechanisms in mantle cell lymphomas with plasmacytic differentiation
EA4HP24-ABS-657	RHOA G17V Potentiates CD28-Induced NFAT Transcriptional Activity by Modulating p300 Activity: A Step Further in the Understanding of Follicular Helper T-cell Lymphoma
EA4HP24-ABS-667	Lymphoproprolipherative disorders with with Castleman and Castleman-like morphology: challenges in the diagnostic workup.

EA4HP24-ABS-522

Bone marrow pathology in patients with cold agglutinin disease: Preliminary results of the Re-CAD study.

PhD/MD Anne-Marie L. Becking[1], Dr. Sophie J. Bernelot Moens[1], Prof. Marie José Kersten[1,3], Prof. Steven T. Pals[2,3], Dr. Josephine M.I. Vos[1,3], Dr. Lianne Koens[2]

[1] Amsterdam University Medical Centers, Department of Hematology, University of Amsterdam, Cancer Center Amsterdam, Amsterdam, Netherlands; [2] Amsterdam University Medical Centers, Department of Pathology, University of Amsterdam, Cancer Center Amsterdam, Amsterdam, Netherlands; [3] Lymphoma and Myeloma Center Amsterdam (LYMMCARE), Amsterdam, Netherlands

Background

Cold agglutinin disease (CAD) is a newly defined entity in the 5th WHO Classification of Haematolymphoid Tumours (WHO-HAEM5). The criteria include a clonal B-cell lymphoproliferation in the bone marrow (BM) distinct from other B-cell lymphomas, called CAD-associated lymphoproliferative disorder (CAD-LPD; **Figure 1**). Aim of this study was to reassess the pathologic characteristics of a large cohort of patients with cold agglutinins (CA) using the WHO-HAEM5 criteria.

Principles/Methodology

All patients with chronic hemolysis and a direct antiglobulin test strongly positive for C3d were included, if ≥1 archival BM trephine biopsies were available. Patients with cold agglutinin syndrome (CAS) secondary to overt infection, autoimmune disease or extramedullary lymphoma were excluded. The CA titer criterium was disregarded since it is not routinely used. Archival BM biopsies were reviewed by 2 haematopathologists, clinical data were collected retrospectively.

Results

A total of 81 patients were identified, of whom 34 were evaluated thus far. Per patient, 1-6 BM biopsies were revised. In 32 patients, there was evidence of a clonal B-cell disorder in electrophoresis, flow cytometry, and/or histopathology. Pathology revision revealed B-cell malignancies other than CAD-LPD in 6 patients (19%), classifying them as CAS(**Figure 2**). In the remaining 26, infiltration with mature B-cells was found in 20 (77%), with a median infiltration of 4% at first biopsy (range 1 to 10%). Plasma cell infiltration was present in 24 (92%), with monotypia in 10 patients. CAD-LPD was confirmed in only 3 patients (12%). All three had IgM kappa monoclonal gammopathy and 2/2 tested lacked the MYD88 exon 5 L265P mutation. CAD-LPD criteria were not met in 23/26 (88%) due to polytypic plasma cells (n=9), absence of B-cells (n=8), paratrabecular growth (n=4), B-cell immunophenotype (n=4), lack of nodular aggregates (n=3) or plasma cells (n=2), location of plasma cells (n=2), lymphoplasmacytic maturation (n=2), increased mast cells (n=1), and/or fibrosis (n=1). Of these 23, 21 (91%) had a monoclonal gammopathy, and 15/15 tested were MYD88 wild-type.

Conclusion

The majority of CAD patients do not meet the histological criteria of CAD-LPD as described in WHO-HAEM5, nor are they classifiable as other B-cell lymphomas. They display a highly heterogeneous BM infiltration pattern, accompanied by a monoclonal gammopathy in the absence of a MYD88 mutation. These results indicate that the WHO-HAEM5 criteria do not capture the majority of CAD cases.

Features	Cold agglutinin disease-associated lymphoproliferative disorder (CAD-LPD)
Histology	Nodular non-paratrabecular lymphoid infiltration, surrounded by mature plasma cells.
Morphology	Small lymphoid cells with round to oval nuclei, dense uniform chromatin pattern, limited clear cytoplasm.
Immunophenotype	B-cells: CD19+, CD20+, PAX5+, CD79a+, CD22+, CD79b+, monotypic light chain (usually kappa), IgM. CD5+ in 40%. BCL6-, MUM1-, CD23-, cyclin D1-. Plasma cells: IgM and monotypic light chain (usually kappa)
Absent	*Paratrabecular growth, lymphoplasmacytic morphology, mast cell infiltration, fibrosis and MYD88 p.L265P.*

Figure 1. Bone marrow histopathology characteristics of CAD-LPD according to WHO-HAEM5 (1)
1. Rossi D, Chen X, Berentsen S, et al. Cold agglutinin disease. In: WHO Classification of Tumours Editorial Board. Haematolymphoid tumours [Internet]. Lyon (France): International Agency for Research on Cancer; 2024 [cited 2024 May 16]. (WHO classification of tumours series, 5th ed.; vol. 11). Available from: https://tumourclassification.iarc.who.int/chapters/63.

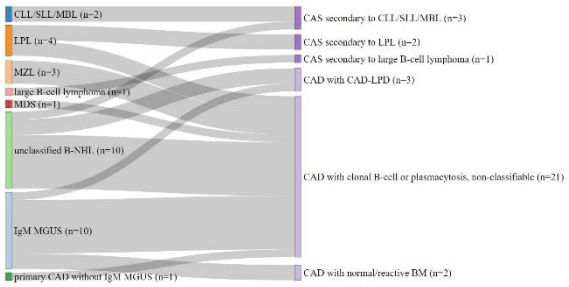

Figure 2. Reclassification of underlying disease after bone marrow pathology revision
Sankey diagram depicting flow from original diagnosis (left) to new classification after revision conform WHO-HAEM5 classification criteria (right), of 32 patients meeting CAD criteria for chronic hemolysis, strongly positive direct antiglobulin test for C3d and evidence of a clonal B-cell disorder.

EA4HP24-ABS-532

High *ADAM8*, *ADAM9* and *ADAM15* expression is associated with proliferation signaling and progressive disease in multiple myeloma

Marietheres Evers[1], Dr. Martin Schreder[2], Dr. Thorsten Stühmer[3], Dr. Torsten Steinbrunn[4], Prof. Martina Rudelius[6], Prof. Franziska Jundt[5], Prof. Regina Ebert[7], Prof. Tanja N. Hartmann[8], Prof. Ralf C. Bargou[3], Prof. Andreas Rosenwald[1], Priv.-Doz. Ellen Leich[1]

[1] University of Würzburg, Institute of Pathology, Würzburg, Germany; [2] Klinik Ottakring, First Department of Medicine, Vienna, Austria; [3] University Hospital of Würzburg, Comprehensive Cancer Center Mainfranken, Würzburg, Germany; [4] Harvard Medical School, Department of Medical Oncology, Dana-Farber Cancer Institute, Boston, USA; [5] University Hospital of Würzburg, Department of Internal Medicine II, Würzburg, Germany; [6] Ludwig Maximilians University Munich, Institute of Pathology, Munich, Germany; [7] University of Würzburg, Department of Musculoskeletal Tissue Regeneration, Würzburg, Germany; [8] University of Freiburg, Department of Medicine I, Medical Center-University of Freiburg, Freiburg, Germany

Background
Multiple myeloma (MM) is a hematological malignancy that remains incurable due to therapy resistance and recurrent patient relapse, underlining the need to find novel therapeutic targets and biomarkers associated with disease progression. Our previous data propose ADAM (A Disintegrin And Metalloproteinase) family members as potential adverse prognostic markers. This study focused on the thus far understudied clinical and functional role of these ADAMs in MM.
Principles/Methodology
RNA-sequencing (RNA-Seq) data was available from the MM research foundation (MMRF CoMMpass study) and RNA-Seq was performed for 73 primary MM samples (validation cohort) and seven human MM cell lines (HMCL) before and after siRNA-mediated *ADAM8/9/15* knockdowns (kd). Differentially

expressed genes between *ADAM8/9/15*$^{high/low}$ patient samples and before/after kd were analyzed using DESeq2 and gene set enrichment analysis. Downstream signaling was assessed by immunoblotting after *ADAM8/9/15* kd. MYC and Ki67 expression was determined by immunohistochemistry in the validation cohort. *ADAM8/9/15* gene expression (GE) was compared between paired baseline and progressive disease samples (MMRF dataset, Wilcoxon test) as well as between patients with/without extramedullary disease (EMD) and between untreated and relapsed/refractory MM (RRMM) (validation cohort, Mann-Whitney U test). MYC and Ki67 expression was compared between *ADAM8/9/15*$^{high/low}$ samples (Mann-Whitney U test). Cox regressions were used to determine the effect of Ki67 (≥30% in CD138+ cells), MYC (≥40% in CD138+ cells) and *ADAM8/9/15* expression (>mean GE) in the validation cohort.

Results

Increasing *ADAM8/15* expression was associated with disease progression in RRMM compared to untreated samples and *ADAM8/9/15* were upregulated in patients with EMD. Several proliferation-associated gene sets were upregulated in *ADAM8/9/15*^{high} MM in both patient cohorts and downregulated by *ADAM8/9/15* kd in HMCL. Additionally, *ADAM8* kd downregulated (p)IGF1R and pAKT and *ADAM9* kd reduced pmTOR in HMCL. Virtually all proliferation markers were upregulated in *ADAM8/9/15*^{high} MM in both patient cohorts on RNA level and high *ADAM8/9/15* GE was associated with high MYC and/or Ki67 protein expression in the validation cohort. Moreover, Cox regressions confirmed high *ADAM8* and *ADAM15* GE as independent prognostic markers.

Conclusion

These data suggest an involvement of *ADAM8/9/15* in MM progression and proliferation signaling, underlining their potential to serve as novel therapeutic targets in MM.

EA4HP24-ABS-538

SOX11 expression is restricted to EBV-negative Burkitt lymphoma and associates with molecular genetic features

Ingram Iaccarino[1], Marta Sureda-Gómez[2], Anna De Bolòs[2], Mieke Meyer[1], Patricia Balsas[2], Julia Richter[1], Marta L. Rodríguez[2], Cristina López[2,4], Maria Carreras[2], Selina Glaser[4], Ferran Nadeu[2,3], Pedro Jares[2,7], Maria C. Siciliano[5], Cristiana Bellan[5], Salvatore Tornambè[5], Roberto Boccacci[5], Guillem Clot[2,3], Lorenzo Leoncini[5], Elias Campo[2,7], Reiner Siebert[4], Virginia Amador[2,3], **Wolfram Klapper**[1]

[1] University of Kiel, Department of Pathology, Hematopathology Section and Lymph Node Registry, Kiel, Germany; [2] Institut d'Investigacions Biomèdiques August Pi i Sunyer, Barcelona, Spain; [3] Centro de Investigación Biomédica en Red de Cáncer, Madrid, Spain; [4] Ulm University and Ulm University Medical Center, Institute of Human Genetics, Ulm, Germany; [5] University of Siena, Department of Medical Biotechnologies, Section of Pathological Anatomy, Siena, Italy; [6] University of Barcelona, Barcelona, Spain; [7] University of Barcelona, Department of Hematology Hospital Clinic of Barcelona, Barcelona, Spain

Background

Burkitt lymphoma (BL) is a highly proliferative B-cell neoplasm that originates from germinal centre B-cells. It is the most common B-cell lymphoma in children and adolescents. At the molecular and genetic level BL is a relatively homogeneous disease, characterized by a chromosomal translocation that juxtaposes the *MYC* gene to one of the immunoglobulins (*IG*) loci. Recent studies have started to

reveal genetic and molecular differences in BLs that are associated with patients' positivity for Epstein Bar virus (EBV) infection. At the transcriptional level a gene that shows a nonuniform expression in BL is the SRY-related HMG-box gene 11 (*SOX11*) transcription factor. Because SOX11 is known to have an oncogenic role in the pathogenesis of mantle cell lymphoma (MCL), we investigated the significance of SOX11 expression in BL.

Principles/Methodology

We analysed the expression of SOX11 in several cohorts of pediatric BL patients. Expression levels of SOX11 were compared with genetic features of the patients, including EBV status, mechanism of *IG::MYC* translocation and mutational signatures. SOX11 was ectopically expressed in SOX11-negative BL cell lines and knocked-out in a SOX11-positive BL cell line. A SOX11-specific BL gene expression signature was derived and compared to a similar signature previously identified in MCL and a SOX11 signature from BL patient samples.

Results

We found that positivity for EBV and SOX11 expression were mutually exclusive in BL. Furthermore, SOX11 expression in EBV-negative BLs was associated with an *IG::MYC* translocation generated by aberrant class switch recombination, while in EBV/SOX11 double negative tumors the *IG::MYC* translocation was mediated by mistaken somatic hypermutations. EBV-negative SOX11 expressing BLs showed higher frequency of *SMARCA4* and *ID3* mutations compared to EBV/SOX11 double negative cases. By RNA-sequencing we identified a SOX11-associated gene expression signature, with functional annotations showing a partial overlap with the SOX11 transcriptional program of MCL. Contrary to MCL, no differences on cell migration or BCR signalling were found between SOX11- and SOX11+ BL cells.

Conclusion

In conclusion, SOX11 expression and EBV infection occur in alternative subsets of BL with different profile of somatic mutations and different mechanism generating *MYC* translocations. The predominance of IGH class switch mediated *MYC* translocation in SOX11-positive BL suggests an earlier development than in SOX11-negative tumors.

EA4HP24-ABS-561

An ultrasensitive dual in situ hybridization (ISH) mRNA assay is equivalent in performance to flow cytometry in determination of kappa/lambda (K/L) restriction status in B cell lymphomas and plasma cell malignancies

Sarah Gladden[3], Andy Babic[3], Amanda Baker[3], Aamir Ehsan[2], Philip Ferguson[4], Bridget Herschap[2], Brian Mosteller[3], Bowdoin Su[1], Jing Su[3], Andrew Evans[5]

[1] Roche Diagnostics Solutions, Santa Clara, USA; [2] CorePath Laboratories, San Antonio, USA; [3] Roche Tissue Diagnostics, Tucson, USA; [4] Northwest Arkansas Pathology Associates, Fayetteville, USA; [5] University of Rochester Medical Center, Rochester, USA

Background

Light chain restriction with flow cytometry is an established method for determining clonality in suspected B cell malignancies, albeit with limitations such as the need for fresh tissue. Ultrasensitive dual ISH mRNA is an emerging technology that has the potential to detect a broader range of B cell non-Hodgkin lymphomas than established, less sensitive options like immunohistochemistry. The aim

of this study was to establish the clinical validity of the dual ISH assay in the qualitative detection of light chain mRNA in FFPE tissues as an aid in the identification of B-cell lymphomas and plasma cell neoplasms, via a method comparison study to flow cytometry.

Principles/Methodology

Three U.S.-based laboratories identified bone marrow and lymphoid tissue specimens with historical light chain restriction results using flow cytometry that met inclusion and exclusion criteria. 742 cases were enrolled across the three study sites, with roughly similar numbers of kappa (K) restricted, lambda (L) restricted and non-restricted cases. Of the 742 cases, 658 cases were analyzed as part of the primary analysis. Evaluable cases stained with the VENTANA K/L Dual ISH assay were independently interpreted for restriction status by four study pathologists across the three study sites, and the pathologists' assessments for each case were compared to the historical flow derived K/L restriction status and final pathology diagnosis associated with the same patient to assess the assay performance.

Results

93.5% of cases were deemed to have acceptable overall staining [Figure 1]. Background staining and morphology was deemed acceptable in 99.8% and 100% of cases evaluated, respectively. The overall percent agreement (OPA) was 92.7%. Kappa restricted percent agreement (KRPA) was 90.0%, lambda restricted percent agreement (LRPA) was 93.3%, and non-restricted percent agreement (NRPA) was 95.2% [Figure 2].

Conclusion

In this study, we compared the VENTANA K/L Dual ISH assay for clonality with flow cytometry in bone marrow and lymphoid tissue with a variety of B cell lymphoma and plasma cell malignancies. Overall staining performance was judged acceptable by the readers. The high rates of agreement between these two methods suggest that this ultrasensitive dual ISH assay is equivalent to flow cytometry for determining the light chain restriction status for the evaluation of suspected B cell lymphoma and plasma cell neoplasms.

VENTANA is a trademark of Roche.

Staining Acceptability Rates for the VENTANA K/L Dual ISH Assay

Parameter	Final Acceptability Rate	
	% (n/N)	95% CI*
Overall Staining	93.5 (758/811)	(91.6, 95.0)
Background Staining	99.8 (802/804)	(99.1, 99.9)
Morphology	100.0 (742/742)	(99.5, 100.0)

* Two-sided 95% CIs were calculated using the Wilson score method.

Staining Acceptability Rates
Subjective acceptability rates and 95% confidence intervals.

Pooled Agreement of K/L Restriction Status Between the VENTANA K/L Dual ISH Assay and Flow Cytometry (All Evaluable Cases)

Endpoint Type	Rate	Agreement	
		% (n/N)	95% CI*
Co-Primary	Kappa-Restricted Percent Agreement (KRPA)	90.0 (824/916)	(86.7, 93.2)
	Lambda-Restricted Percent Agreement (LRPA)	93.3 (742/795)	(90.1, 96.2)
	Non-Restricted Percent Agreement (NRPA)	95.2 (810/851)	(93.3, 96.8)
Additional	Overall Percent Agreement (OPA)	92.7 (2376/2562)	(91.1, 94.2)

* Two-sided 95% CIs were calculated using the percentile bootstrap method with 2000 replicates with stratification by the 6 applicable tissue-type/flow status enrollment bins used during case screening for the All Evaluable Cases population.

Pooled agreement rates of light chain restriction status
Agreement rates and 95% confidence intervals.

EA4HP24-ABS-563

Cytoplasmic Lipid Droplets Predict Worse Prognosis in Diffuse Large B-cell Lymphoma: Next Generation Sequencing Deciphering Lipogenic Genes

Prof. Kung-Chao Chang

National Cheng Kung University Hospital, Department of Pathology, Tainan, Taiwan

Background

Burkitt lymphoma is characterized by high cell turnover and numerous cytoplasmic vacuoles that are demonstrated to be lipid droplets (LDs) decorated by adipophilin. By contrast, cytoplasmic vacuoles are variably observed in diffuse large B-cell lymphoma (DLBCL) and less well characterized. We, thus, aimed to test the role of lipid biogenesis in clinicopathologic features of DLBCL patients.

Principles/Methodology

The study cohorts were composed of the following three groups: 1) DLBCL patients with lymphomatous effusional cytology smears available (n=52); 2) DLBCL cases with solid lymphoma tissues for adipophilin immunostaining (n=85); and 3) B-cell lymphoma cell lines (n=4) for validation of next-generation sequencing (NGS) findings. NGS with whole exomes and transcriptomics was performed to decipher relevant lipogenic genes by comparing DLBCL effusional samples with versus without LDs. Real-time PCR and Western blotting were used to validate the NGS findings.

Results

We first validated cytoplasmic vacuoles to be LDs. Then, we found that DLBCL patients (n=52) with LDs in effusional lymphoma cells carried a worse prognosis (p=0.029, log-rank test) and had a higher IPI score (94% vs. 66%, p=0.026) than those without LDs in effusional lymphoma cells. Moreover, using adipophilin as a surrogate marker for the presence of LDs, we found that in another cohort of DLBCL (n=85), expression of adipophilin in solid tumor cells predicted a poorer prognosis than those without adipophilin expression (p=0.007, log-rank test), and correlated with a higher IPI score (63% vs. 30%, p=0.005). In addition, whole exome sequencing showed LD-positive DLBCL (n=10) shared genetic features with the MCD subtype. Whole transcriptome analysis identified top five up-regulated genes *EHHADH, SLC1A1, CD96, INPP4B*, and *RNF183* relevant for lymphoma lipogenesis in LD-positive samples (n=5) when compared to LD-negative samples (n=2). Gene set enrichment analysis (GSEA) revealed up-regulation of pathways, including epithelial-mesenchymal transition and KRAS signaling pathways in the LD-positive samples compared to LD-negative samples. We also confirmed the higher expression of *EHHADH* and *CD96* in LD-rich cell lines than LD-poor cell lines along with the known lipogenic gene, *FASN* (fatty acid synthase).

Conclusion

Our findings, therefore, highlight the roles of LDs and adipophilin expression in prognostic prediction in DLBCL patients and the genes underlying enhanced lipogenic pathways as potential therapeutic targets.

EA4HP24-ABS-564

NPM-ALK Oncoprotein Suppresses STAT3-Mediated Anti-Tumor Immune Responses Partially Through cGAS-STING Pathway in ALK+ Anaplastic Large Cell Lymphoma.

Dr. Ioanna Xagoraris[1], M.Sc./M.A. Dora Trogrlic[1], Dr. Ying Yang[1], PhD/MD student Christina Plastira[1], M.Sc./M.A. Konstantina Stathopoulou[1], Prof. Andreas Lundqvist[1], Dr. Vasiliki Leventaki[2], Prof. George Rassidakis[1,2]

[1] Karolinska Institute, Department of Oncology-Pathology, Stockholm, Sweden; [2] The University of Texas MD Anderson Cancer Center, Department of Hematopathology, Houston, USA

Background

Anaplastic lymphoma kinase-positive anaplastic large cell lymphoma (ALK+ ALCL) is a distinct type of aggressive T-cell non-Hodgkin lymphoma with high frequency in childhood and young adults. ALK+ ALCL is characterized by overexpresion and activation of ALK due to chromosomal translocations with the most frequent being the t(2;5)(p23;q35) resulting in the chimeric NPM-ALK oncoprotein. The latter activates multiple oncogenic pathways; however the potential role of NPM-ALK in anti-tumor immune responses is largely unknown to date.

Principles/Methodology

The *in vitro* system included 3 ALK+ (Karpas 299, DEL, SUPM2) and 2 ALK- (Mac1, Mac2a) ALCL cell lines as well as murine BaF3 cells stably transfected with NPM-ALK plasmid. Quantitative RT-PCR and Western blot analysis were used for the assessment of mRNA and protein levels, respectively. Silencing of various genes was performed using transient transfections with Nucleofector system (Lonza). Ceritinib was used as a next generation ALK inhibitor. Cytokine arrays and functional NK cell killing assays were utilized to assess the cytokine profile and anti-tumor responses, respectively.

Results

Stable transfection of BaF3 cells with a NPM-ALK plasmid resulted in STAT3 activation associated with downregulation of CXCL10 gene expression. These effects were linked to substantial changes in cytokine profile *in vitro*. Treatment with Ceritinib led to a dramatic increase of IFN-β (>100-fold) and CXCL10 (>30-fold) mRNA levels along with altered cytokine profile in ALK+ ALCL and murine BaF3/NPM-ALK cells. Silencing of ALK gene also resulted in upregulation of IFN-β and CXCL10 gene expression in ALK+ ALCL and BaF3/NPM-ALK cells. Similarly, silencing of STAT3, an important downstream target of NPM-ALK, also led to a significant increase in the IFN-β (>120-fold) and CXCL10 mRNA levels in ALK+ ALCL cells associated with activation of the cGAS-STING pathway as shown by increased phosphorylation of TBK1 and IRF3. Similar results were obtained after STAT3 gene silencing. Stimulation of the cGAS-STING pathway by a STING agonist resulted in upregulation of type I IFN gene expression and increased NK cell killing suggesting that cGAS-STING pathway is functional in ALK+ and ALK- ALCL cells *in vitro*.

Conclusion

NPM-ALK oncogenic kinase suppresses cGAS-STING-associated anti-tumor immune responses through STAT3 activation in ALK+ ALCL. Modulation of cGAS-STING activity, in addition to ALK inhibition, might represent a novel therapeutic target in ALK+ ALCL.

EA4HP24-ABS-566

Genome-wide copy-number profiling identifies novel therapeutic targets in follicular lymphoma

Dr. Heike Horn[1,2], Dr. Sabrina Kalmbach[1], Emma Attwood[1], Sophia Steinlein[1], Dr. Annette M. Staiger[1,2], Dr. Katrin S. Kurz[2], Dr. Claudia Kalla[1], Prof. German Ott[2]

[1] Bosch Health Campus, Dr. Margarete Fischer-Bosch-Institute of Clinical Pharmacology, Stuttgart, Germany; [2] Bosch Health Campus, Department of Clinical Pathology, Robert Bosch Hospital, Stuttgart, Germany

Background

Follicular lymphomas (FL) are among the most common indolent B cell neoplasms and are incurable with conventional chemotherapy. Therapeutic strategies depend mainly on the clinical stage of the disease as well as the patients' condition including co-morbidities. A main problem constitutes the high number of relapses and a potential transformation into aggressive lymphoma. The highly variable clinical course of patients suffering from FL requires improved knowledge of the genetic heterogity of FL. Thus, it is of pivotal impact to identify FL subtypes to understand their molecular pathogenesis and to improve targeted treatment options, especially for high-risk patients.

Principles/Methodology

Based on the results of genome-wide profiling of FL reported by Kalmbach et al. 2023, regions harboring significant and frequent copy-number gains were evaluated for candidate genes. Downstream effects were assessed by analyzing gene and protein expression of target genes by RT-PCR, immunohistochemistry and immunoblotting in representative B cell lymphoma cell lines. Moreover, response to targeted specific treatments were assessed by cell viability assays.

Results

Novel frequently and significantly affected regions were detected in FL including gains in 7p12, 11q24 and 18q21 containing *IKZF1*, *ETS-1* and *MALT1,* respectively. Transcript and protein expression of IKZF1, ETS-*1* and MALT1 was enhanced in cell lines and tumor samples harboring gains in the respective locus. Treatment with specific inhibitors targeting IKZF1 (Lenalidomide) and MALT1 (MI-2) efficiently impaired the survival and growth of B cell lymphoma cell lines. The efficacy of both therapeutic agents correlated with the copy number of the respective target gene. However, presence of gains of the specific target genes failed to predict response to treatment using the respective inhibitor.

Conclusion

Detecting novel frequent aberrations in FL is a suitable means to identify putative targets for the efficient therapy of B cell malignancies. Pharmacological inhibition of IKZF1 and MALT1 are promising treatment options that warrant further investigation.

EA4HP24-ABS-577

Clonal hematopoiesis of indeterminate potential is associated with inferior outcome in patients with lymphoma

Caroline Hesselager[1], Peter Hollander[1], Gunilla Enblad[1], Simone Weström[2], Daniel Eriksson[2], Arielle R. Munters[2], Daniel Molin[1], Panagiotis Baliakas[2], Rose-Marie Amini[1]

[1] Uppsala University and Uppsala University Hospital, Dept of Immunology, Genetics and Pathology, Uppsala, Sweden; [2] Uppsala University, Dept of Immunology, Genetics and Pathology, Science for Life Laboratory, Uppsala, Sweden

Background

Clonal hematopoiesis of indeterminate potential (CHIP) in lymphoma patients treated with autologous stem cell transplantation has been reported in up to 30% and correlates with inferior outcome. Almost half of refractory lymphoma patients treated with chimeric antigen receptor (CAR) T-cells have CHIP which however seems to lack any clinical importance within this group of patients. The prevalence of CHIP in untreated lymphoma is less investigated. The aim of this study was to examine the prevalence and clinical impact of CHIP in a cohort of patients with different types of lymphomas at the time of diagnosis.

Principles/Methodology

A total of 270 patients diagnosed with high grade B-cell lymphoma (HGBCL) (n=179), Hodgkin lymphoma (HL) (n=64) and NK/T-cell lymphoma (n=27) were included. Next generation sequencing (NGS) on DNA extracted from blood samples, with a targeted gene panel covering either full coding region or hotspot region of 33 genes with a sensitivity of a variant allele frequency (VAF) down to 2%, was performed.

Results

In 102 patients a total of 157 variants were detected; 63 were classified as pathogenic or likely pathogenic (P/LP) and 94 as variants of uncertain significance (VUS). The mutational landscape varied, with the three most commonly mutated genes in the P/LP categories being *DNMT3A* (n=20), *TET2* (n=19) and *TP53* (n=6), and in the VUS category, *HRAS* (n=14), *CEBPA* (n=12) and *RUNX1* (n=9). Patients with CHIP (P/LP and VUS considered as one group) were generally older (p=0.016) and had a significantly inferior overall survival (OS) compared to patients without variants ($p < 0.001$), figure 1. In a subanalysis, this association was even more pronounced for HGBCL and NK/T cell lymphomas, whereas no difference was observed in HL patients with VUS. The 5-year OS rate was 25% in the NK/T-cell lymphoma group and 58% for HGBCL patients, compared to 66% and 75%, respectively, for patients without detected variants. When adjusted for age and stage using Cox regression analysis, the presence of CHIP still significantly affected both OS and progression free survival (p=0.002 and p=0.015 respectively).

Conclusion

CHIP seems to be an independent unfavorable prognostic marker for patients with lymphoma treated according to the standard praxis. Even VUS seem to be equally important, except in HL. Our results argue in favor of further investigating the clinical impact of CHIP and suggests that the presence of CHIP could serve as a biomarker for identifying candidates for alternative treatments.

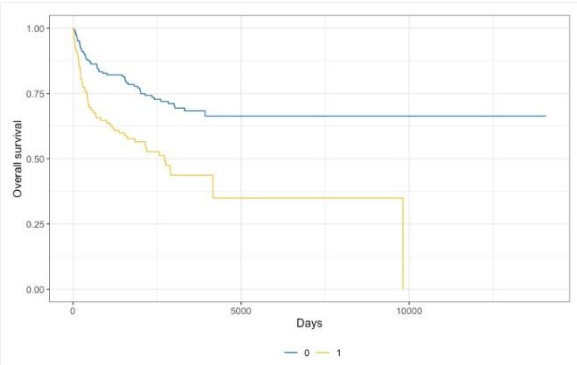

Figure 1. Overall survival in all lymphoma patients (n=270)

0 = No detected variants **1** = CHIP including VUS

EA4HP24-ABS-584

Homologous recombination deficiency in follicular dendritic cell sarcoma.

Dr. Luisa Lorenzi[1], Prof. Torsten Haferlach[2], Dr. Luigi Mori[1], Dr. Matteo Simbeni[1], Dr. Wencke Walter[2], Dr. Piera Balzarini[1], Dr. Silvia Lonardi[1], Dr. Manja Meggendorfer[2], Dr. Claudia Döring[3], Dr. Mattia Bugatti[1], Claudio Agostinelli[4], Dr. Jay Mehta[5], Prof. Anita Borges[6], Prof. Abbas Agaimy[7], Prof. Ingrid Simonitsch-Klupp[8], Prof. José Cabeçadas[9], Prof. Elias Campo[10], Prof. Stefano Pileri[11], Prof. Fabio Facchetti[1], Prof. Martin-Leo Hansmann[12], **Prof. Sylvia Hartmann**[3]

[1] University of Brescia - ASST Spedali Civili di Brescia, Pathology, Brescia, Italy; [2] MLL Munich Leukemia Laboratory, Munich, Germany; [3] Goethe University Frankfurt, Frankfurt, Germany; [4] Department of Medical and Surgical Sciences, University of Bologna, Bologna, Italy; [5] Neuberg Oncopath, Mumbai, India; [6] Histopathology, SRL Diagnostics, Mumbai, India; [7] Institute of Pathology, University Hospital, Erlangen, Germany; [8] Institute of Pathology, Medical University of Vienna, Vienna, Austria; [9] Department of Pathology, Portuguese Institute of Oncology, Lisbon, Portugal; [10] Hematopathology Section, Hospital Clinic, IDIBAPS, University of Barcelona, Barcelona, Spain; [11] Division of Haematopathology, European Institute of Oncology (IEO) IRCCS), Milan, Italy; [12] Institute for General Pharmacology and Toxicology, Goethe University, Frankfurt, Germany

Background

Complete tumor resection is the treatment of choice for Follicular dendritic cell sarcoma (FDCS) with localized disease; standardized treatment options are lacking for patients with unresectable or multifocal disease and mortality is as high as 20%.

Dendritic and histiocytic derived tumors of haematopoietic derivation share activation of the MAPK/ERK pathway with good clinical responses after targeted therapies in some cases; accumulating evidence indicates that the molecular mechanisms driving FDCS are different.

Principles/Methodology

Thirteen cases of FDCS were selected by tissue availability, tumor cell content and DNA quality to undergo massive parallel sequencing. One case underwent whole genome sequencing (WGS), 12 cases whole exome sequencing (WES). They were included in Tissue Micro Arrays (TMA) together with 22 additional cases (validation cohort). Diagnosis was classical FDCS in all cases but one (#3), which was

diagnosed as Epstein-Barr virus–positive inflammatory follicular dendritic cell sarcoma/tumor (EBV-IFDCS/T).

Results

Massive parallel sequencing showed high frequency of mutations on oncosuppressor genes, particularly in *RB1*, *CARS* and *BRCA2* and unveiled alterations on homologous recombination DNA damage repair related genes in 70% (9/13) of cases. This indicates that patients with high stage FDCS may be eligible for poly ADP ribose polymerase inhibition protocols. FDCS were associated with low tumor mutational burden, confirming previous studies. This argues against the efficacy of immune checkpoint inhibitors, despite common PDL1 expression in FDCS, previously reported and confirmed in this study. *CDKN2A* deletion, detected by WGS was confirmed by FISH in 41% of cases (9/22) indicating impairment of cell cycle regulation as a mechanism of FDCS pathogenesis. Absence of mutations in the RAS/RAF/MAPK pathway was confirmed in FDCS by MPS.

Conclusion

WGS and WES in FDCS provides additional information on the molecular landscape of this rare tumor, proposing novel candidate genes for innovative therapeutical approaches to improve survival of patients with multifocal disease.

EA4HP24-ABS-596

Genomic Characterization of Peripheral T-cell Lymphomas with Co-expression of CD30/CD15 Suggests a Close Relationship to Anaplastic Large-Cell Lymphoma, ALK-negative

Dr. Joao V. Alves de Castro, PhD/MD Jung Kim, PhD/MD Manoj Tyagi, PhD/MD Liqiang Xi, PhD/MD Stefania Pittaluga, Dr. Mark Raffeld, Dr. Elaine S. Jaffe

NCI/NIH, Laboratory of Pathology, Bethesda, USA

Background

The proper categorization of mature T-cell neoplasms with expression of both CD30 and CD15 is unresolved. Prior studies suggested overlap with ALK-negative anaplastic large cell lymphoma (ALCL), but the morphologic spectrum is broad. We sought to carry out a comprehensive analysis evaluating morphologic, immunophenotypic, and molecular features.

Principles/Methodology

23 Peripheral T-cell lymphomas expressing CD30 and CD15 were identified from the pathology archives. 8 ALK/CD15-negative ALCL cases were used as controls. Clinical information was retrieved from the submitting physician. Immunohistochemical analysis and TRG and IG gene rearrangement by fragment analysis were performed. Next-generation sequencing analysis included a targeted DNA panel in all cases, and an RNA fusion panel in a subset of cases. Cases were classified as conforming to three histological variants: ALCL-like, Hodgkin-like, and PTCL-NOS-like.

Results

Median age was 66 years (range: 33-87). Male : Female ratio was 2.8:1. 18 cases presented with lymphadenopathy (18/23, 78.3%), mainly inguinal (11/18, 61.1%). 7 cases had skin involvement (7/23, 30.4%), including 2 with a primary cutaneous presentation (2/23, 8.7%). Based on histological review, cases were designated as ALCL-like (8 cases), Hodgkin-like (10 cases), and PTCL-NOS-like (3 cases). There was

frequent loss of many T-cell markers, with expression of CD3 in 7/23 cases (30.4%), CD2 in 14/21 (66.7%), and expression of at least one cytotoxic marker in 11/18 (61.1%). EBER was negative in all cases tested (0/13, 0.0%). The JAK-STAT pathway was most frequently altered; mutated genes were *JAK1* (5/23, 21.7%) and *STAT3* (5/23, 21.7%). Most *JAK1* mutations occurred at the p.Gly1097 hotspot (4/5, 80%). *PIK3R1* mutations occurred in 4 cases, all in the ALCL-like subgroup (4/8, 50.0%). *JAK2* fusions were identified in 2 cases (2/23, 8.7%), 1 Hodgkin-like and 1 primary cutaneous T-cell lymphoma.

Conclusion

In summary, most PTCLs with CD30 and CD15 co-expression share clinical, morphologic, immunophenotypic, and molecular features with ALK-negative ALCL, including mutations in *JAK1, STAT3, PIK3R1*, and rearrangements in *JAK2*. These findings suggest that they might be best categorized as ALK-negative ALCL. However, the genomic profile is varied.

Marker	ALCL-like (n=8)	Hodgkin-like (n=10)	PTCL-NOS like (n=3)	pc-CD30-LPD (n=2)	Total (n=23)	Control (n=8)	p-value*
CD30	100.0%	100.0%	100.0%	100.0%	23/23 (100.0%)	8/8 (100.0%)	>0.9999
CD15	100.0%	100.0%	100.0%	100.0%	23/23 (100.0%)	0/8 (0.0%)	**<0.0001**
CD20	0.0%	10.0%	0.0%	0.0%	1/23 (4.35%)	0/8 (0.0%)	>0.9999
PAX5	0.0%	20.0%	0.0%	50.0%	3/23 (13.0%)	0/8 (0.0%)	>0.9999
CD79a	0.0%	0.0%	0.0%	0.0%	0/10 (0.0%)	0/3 (0.0%)	>0.9999
CD3	37.5%	11.1%	33.3%	50.0%	7/23 (30.4%)	2/8 (25.0%)	0.6378
CD2	62.5%	50.0%	100.0%	100.0%	14/21 (66.7%)	6/7 (85.7%)	0.2826
CD5	25.0%	22.2%	100.0%	100.0%	7/17 (41.2%)	3/8 (37.5%)	0.6687
CD7	0.0%	0.0%	0.0%	0.0%	0/11 (0.0%)	1/5 (20.0%)	0.3125
CD4	62.5%	44.4%	100.0%	100.0%	14/22 (63.7%)	7/8 (87.5%)	0.3816
CD8	12.5%	0.0%	0.0%	0.0%	1/22 (4.5%)	1/8 (12.5%)	0.4310
TIA1	60.0%	66.7%	33.3%	0.0%	10/18 (55.5%)	0/5 (0.0%)	0.2911
Granzyme B	50.0%	75.0%	33.3%	0.0%	11/18 (61.1%)	4/6 (66.7%)	>0.9999
Perforin	60.0%	80.0%	33.3%	NP	9/12 (75.0%)	4/4 (100.0%)	>0.9999
BF1	0.0%	0.0%	NP	NP	0/3 (0.0%)	0/2 (0.0%)	>0.9999
TCR gamma	0.0%	NP	NP	NP	0/1 (0.0%)	1/1 (100.0%)	>0.9999
TCR delta	NP	0.0%	NP	NP	0/2 (0.0%)	1/2 (50.0%)	>0.9999
EMA	50.0%	25.0%	0.0%	0.0%	3/10 (30%)	1/6 (16.7%)	>0.9999
CD25	100.0%	66.7%	NP	NP	3/4 (75.0%)	NP	NP
EBER	0.0%	0.0%	0.0%	0.0%	0/13 (0.0%)	0/7 (0.0%)	>0.9999

Immunophenotypic characteristics of the cohort
Description of markers used and percentages according to morphological subgroups, overall cohort, and comparison with Anaplastic large-cell lymphoma, ALK-negative, used as controls. Note: *p-values calculated with Fisher's exact test between the "total" cohort and the "control" group. NP: not performed. ALCL: anaplastic large cell lymphoma. PTCL-NOS: peripheral T-cell lymphoma, not otherwise specified.

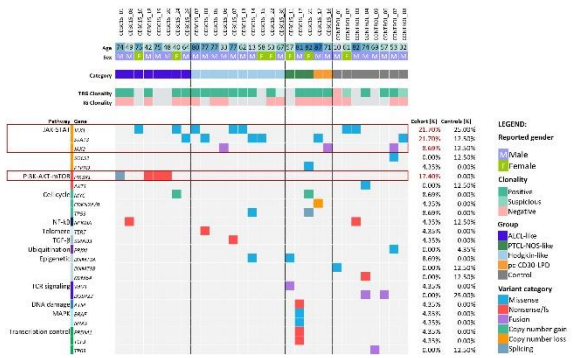

Genomic features of CD30+/CD15+ peripheral T-cell lymphomas.
Note: ALCL: Anaplastic large-cell lymphoma; fs: frameshift; PTCL-NOS: Peripheral T-cell lymphoma, not otherwise specified; pc-CD30-LPD: primary cutaneous CD30-positive lymphoproliferative disorder.

EA4HP24-ABS-619

Unravelling TOX2 expression in B and T Cell Lymphomas

PhD/MD Maria Rodriguez-Pinilla[1], PhD/MD Juan F. Garcia[2], PhD/MD Joaquim Carreras[3], Scherezade Jimenez[4], Carmen San Juan[4], Dr. Lorena Maestre[4], **Dr. Giovanna Roncador**[4]

[1] Department of Pathology, Fundación Jiménez Díaz, Autónoma University, Madrid, Spain; [2] Department of Pathology, MD Anderson Cancer Center, Madrid, Spain; [3] Department of Pathology, School of Medicine, Tokai University, Tokai, Japan; [4] Monoclonal Antibodies Unit, Biotechnology Program, Spanish National Cancer Research Centre (CNIO), Madrid, Spain

Background

TOX2, a member of the thymocyte selection-related HMG box protein family, shares structural similarities with TOX, TOX3, and TOX4. While TOX is linked to T cell exhaustion, TOX2 exhibits diverse functions, playing a critical role in human natural killer (NK) cell maturation by positively regulating TBX21 expression. Additionally, TOX2 modulates T follicular helper cells (Tfh) cell differentiation by directly regulating a set of Tfh-associated genes by activating their chromatin accessibility.

Principles/Methodology

Despite the importance of TOX2 in immune regulation, its distribution in reactive and neoplastic lymphoid tissues remains largely unexplored.

To address this gap, we have investigated TOX2 expression in normal and neoplastic lymphoid tissue using a novel rat monoclonal antibody (TOM924D) that recognizes its target molecule in paraffin-embedded tissue sections. A comprehensive study was conducted on a large number of normal tissues and B and T-cell lymphomas (comprising more than 300 cases), utilizing both whole tissue sections and tissue microarrays.

Results

We identified a restricted expression pattern of TOX2 within lymphocytes. Furthermore, in T lymphomas, TOX2 was expressed in NK/T Cell, angioimmunoblastic T cell and peripheral T cell lymphomas. In B cell lymphomas, TOX2 was found exclusively in diffuse large B cell lymphoma. In the other types of lymphomas, its expression was confined to the tumour microenvironment, especially in follicular and Hodgkin's lymphomas, indicating its potential role in tumour response.

Conclusion

By unravelling its expression patterns, this study not only expands our knowledge of TOX2 roles in health and disease, but also lays the foundations for potential diagnostic and therapeutic applications, especially in the context of lymphomas originating from NK and Tfh cells.

EA4HP24-ABS-626

Insights into T-Follicular Helper Cell Lymphomas and Peripheral T-Cell Lymphomas, Not Otherwise Specified, in Slovenian Patients: Mutational Landscape, Clinicopathological Characteristics, and Outcomes

PhD/MD student Eva Erzar[1,2], PhD/MD student Vanesa S. Ivanova[3], PhD/MD Stefan Dirnhofer[3], PhD/MD Lučka Boltežar[4,2], PhD/MD Veronika Kloboves-Prevodnik[1,5], PhD/MD Alexandar Tzankov[3], PhD/MD Gorana Gašljević[6,5]

[1] Institute of Oncology Ljubljana, Department of Cytopathology, Ljubljana, Slovenia; [2] University of Ljubljana, Faculty of Medicine, Ljubljana, Slovenia; [3] University Hospital Basel, University of Basel, Institute of Medical Genetics and Pathology, Pathology, Basel, Switzerland; [4] Institute of Oncology Ljubljana, Department of Medical Oncology, Ljubljana, Slovenia; [5] University of Maribor, Faculty of Medicine, Maribor, Slovenia; [6] Institute of Oncology Ljubljana, Department of Pathology, Ljubljana, Slovenia

Background

T-follicular helper cell lymphomas (T-FHL) are one of the most frequently occurring subtypes of mature nodal T-cell lymphomas (nTCL). They have distinct clinical and morphological features, an aggressive course, and a poor clinical outcome. However, a comprehensive understanding of their tumour microenvironment, mutational landscape and clinicopathological characteristics remains limited. Herein, we aimed to better depict nTCLs' features within a Slovenian cohort.

Principles/Methodology

We evaluated 108 patients diagnosed with nTCL by performing immunohistochemistry, clonality testing and high-throughput sequencing with a lymphoma panel comprising 172 genes. We performed survival and correlation analyses with clinicopathological and mutational characteristics.

Results

Out of 108 patients (50 females, 58 males), 91 had T-FHL, 9 peripheral T-cell lymphomas, not otherwise specified (PTCL-NOS), and 8 composite lymphomas (T-FHL combined with diffuse large B-cell lymphoma or marginal zone lymphoma). The median follow-up time was 23 months, with most patients receiving COP/modified COP treatment regimens. Mutational analysis (n=99) revealed *TET2* (43%), *RHOA* (26%), *IDH2* (9%), *PLCG1* (8%), *DNMT3A* (6%), and *VPS13B* (4%) as the most commonly mutated genes, being present in T-FHL only. Correlation analysis of the clinicopathological and mutational characteristics demonstrated that the M2/M1 ratio correlated with T-bet and PD1 expression, as well as initial peripheral blood leukocytosis. The number of RORγt+ lymphocytes negatively correlated with the International Prognostic Index (IPI). Cases with *TET2* mutations more commonly expressedCD10 and CXCL13, and displayed higher density of follicular dendritic cells. Moreover, patients with high IPI, poor response to first-line treatment, ≥2 mutations, M2/M1 ratio >0.77, and low Treg count had shorter overall survival (OS).

Conclusion

Our study is one of the largest nTCL series to date. It reinforces existing findings indicating that T-FHL outnumber PTCL-NOS (92% vs. 8%). We are also the first to reveal that ≥2 mutations and a low Treg count have a significant negative impact on the OS of patients with nTCL. Our research marks the first instance of reproducing the correlation between the M2/M1 ratio and nTCL OS within a European demographic. These findings hold the potential to refine prognostic accuracy, lay groundwork for

personalised treatment approaches, and aid in developing novel therapeutic strategies targeting tumour-infiltrating immune cells.

EA4HP24-ABS-648

HGBCL-11q: the darkest Lymphoma Microenvironment?

Dr. Maria Chiara Siciliano[1], Dr. Saveria Mazzara[2], Dr. Giorgio Bertolazzi[3,4], Dr. Massimo Granai[1], Dr. Margherita Vannucchi[1], Dr. Roberto Boccacci[1], Dr. Raffaella Guazzo[1], Dr. Domenico Ferrara[1], Prof. Stefano Pileri[5], Dr. Anja Fisher[6], Dr. Heike Horn[7], Prof. Reiner Siebert[6], Prof. German Ott[7], Prof. Claudio Tripodo[3], Prof. Stefano Lazzi[1], Prof. Lorenzo Leoncini[1]

[1] University of Siena, Department of Medical Biotechnologies, Siena, Italy; [2] Bocconi University, Department of Computing Science and Bocconi Institute for Data Scienc and Analytics (BIDSA), Milan, Italy; [3] University of Palermo, Department of Health Sciences, Tumor Immunology Unit, Palermo, Italy; [4] University of Palermo, Department of Economics, Business, and Statistics, Palermo, Italy; [5] Istituto Europeo di Oncologia (IEO), IEO, Milan, Italy; [6] Ulm University, Institute of Human Genetics, Ulm, Germany; [7] InstitutfürKlinischePharmakologie, AbteilungfürKlinischePathologie, Robert-Bosch- Krankenhaus and Dr. Margarete Fischer- Bosch, Stuttgart, Germany

Background

High grade B-cell lymphoma with 11q aberration (HGBCL-11q) is a mature B-cell lymphoma with morphology and gene expression profile (GEP) similar to Burkitt Lymphoma (BL). These cases usually show a diffuse lymphomatous infiltrate sometimes with a starry sky pattern characterized by the presence of macrophages with enhanced number of phagocytized apoptotic bodies. Although there have been numerous studies investigating Lymphoma Microenvironment (LME) in B-cell lymphomas, there has been a limited amount of research conducted in iHGBL-11q and BL where the functional status of macrophages may impact on tumour immune response. Here we aim to compare the LME in 8 HGBCL- 11q, 8 BL EBV-negative, 5 HGBCL-BCL2r/MYCr and 10 Diffuse Large B Cell Lymphomas (DLBCL) EBV-negative (5 ABC, 5 GCB)

Principles/Methodology

GEP of 730 immune-related genes in Formalin Fixed Paraffin Embedded (FFPE) samples was performed using the NanoString Immune Profiling Panel and validated by multiplex immunohistochemistry

Results

A principal component analysis (PCA) showed that HGBCL-11q, BL-EBV neg and HGBL-DH grouped together as compared to DLBCL EBV-negative (ABC, GCB), based on ANOVA analysis on 365 Differentially Expressed Genes (DEGs) ($p<0.05$). Since BL, HGBCL-11q and HGBCL-BCL2r/MYCr all show a GEP of Dark Zone (DZ) B-cells, to better reveal differences among them, we applied a newly identified DZ\LZ spatial signature (201-LZ and 169-DZ genes). Unsupervised clustering analysis of the differentially expressed genes revealed two gene clusters: cluster 1 enriched in DZ-genes and cluster 2 enriched in LZ-genes. DZ-enriched genes (cluster 1) were up-regulated in BL EBV-negative, and to a lesser extent in HGBL-11q. Finally, to further characterize differences between BL EBV-negative and HGBL-11q, we applied 3 spatially- derived macrophage signatures (MacroSig) which revealed significant differences for the Germinal Center (GC) sign and DZ\LZ sign between BL EBV-negative and HGBL-11q.

Conclusion

Based on LZ\DZ-spatial signature, HGBCL-11q and BL EBV-negative showed similarities but also differences. In particular,HGBCL-11q was characterized by a lower expression of DZ genes related to LME and macrophage signatures. These results are in accordance with recent evidence that HGBCL-11q may originate from a more intermediate step in the dynamic process of Germinal Center Reaction. Ongoing analyses aim at assigning further the detected GEP differences to the tumor microenvironment as compared to the lymphoma cells.

EA4HP24-ABS-654

Genetic alterations and *CCDN1* rearrangement mechanisms in mantle cell lymphomas with plasmacytic differentiation

Núria Vidal-Robau[1], Cristina López[1,2], Ferran Nadeu[2,3], Anna Enjuantes[2], Irene Blázquez[4], Evsen Apaydin Arikan[5], Gerard Frigola[1], Olga Balagué[1,2], Inmaculada Ribera-Cortada[1,2], Patrícia López[6], Sílvia Beà[1,2], Andrew Wotherspoon[7], Fina Climent[4], Mark Raffeld[5], Elaine S Jaffe[5], Elias Campo[1,2]

[1] Hospital Clínic Barcelona, Hematopathology Section, Department of Pathology, Barcelona, Spain; [2] Institut d'Investigacions Biomèdiques August Pi i Sunyer (IDIBAPS), Barcelona, Spain; [3] Centro de Investigación Biomédica en Red de Cáncer (CIBERONC), Madrid, Spain; [4] Hospital Universitari de Bellvitge-IDIBELL, Department of Pathology, L'Hospitalet de Llobregat, Barcelona, Spain; [5] Center for Cancer Research, National Cancer Institute, Bethesda, Hematopathology Section, Laboratory of Pathology, MD, Spain; [6] Institut Català d'Oncologia-IDIBELL, Hematopathology Department, L'Hospitalet de Llobregat, Barcelona, Spain; [7] The Royal Marsden Hospital, Histopathology Department, London, UK

Background

Mantle cell lymphoma (MCL) is an aggressive mature B-cell neoplasm expressing CD5 and SOX11. Some MCL are SOX11- and frequently present with an indolent leukemic non-nodal disease. Both subtypes are characterized by constitutive cyclin D1 overexpression and *CCND1* rearrangement *(CCND1*-R*)* to IGH genes acquired in immature B-cells via aberrant V(D)J rearrangement mediated by RAG1/2. *CCND1*-R may also occur in multiple myeloma mediated by AID during an aberrant IGH class switch recombination (CSR) or somatic hypermutations (SHM). A subset of MCL have a striking plasma cell differentiation that seem to occur exclusively in SOX11- MCL and some of them may carry *MYD88* mutations. The proper classification of these cases may be controversial.

Principles/Methodology

In this study we have investigated the mechanism of *CCND1*-R and mutational profile of 8 SOX11- MCL with plasmacytic differentiation using an NGS panel designed to capture all IG loci and 17 relevant driver genes in MCL. *CCND1-R* was demonstrated in all cases by FISH and/or cytogenic studies and cyclin D1 overexpression by immunohistochemistry. *MYD88* mutations were independently studied by L265P allelic specific mutation PCR and exon 5 sequencing.

Results

Clinicopathological features of 6 patients were previously published (PMID26360498). Five cases presented a leukemic phase. Three patients had a monoclonal IgM-k component in serum. The samples corresponded to 4 lymph nodes, 2 spleens, 1 orbit and 1 intraocular tumor. Dutcher bodies were seen in 4 tumors and cytoplasmic IG inclusions in tumor cells and histiocytes in 1. Neoplastic cells

showed kappa (7) or lambda (1) restriction; and expressed IgM (2), IgD (2), IgM-IgD (1) or IgA (1) (non-contributory/non-available in two). MUM1 was positive in the plasma cells in all cases and CD5 in 6/8. The *CCND1*-R was mediated by RAG in 7 cases and by AID (CSR) in 1. Interestingly, the later carried the L265P *MYD88* mutation and was CD5-negative without additional gene mutations. The *CCND1*-R in a second tumor carrying a non-canonical *MYD88* mutation (S219C) was mediated by RAG. All cases had mutated IGHV (92.63-97.92% identity). Mutational study showed alterations in *TP53*(2/8), *NOTCH1*(1/8), *BIRC3*(1/8), *CARD11*(1/8) and in *CCND1* due to SHM (3/8).

Conclusion

In conclusion, most *CCND1*-R lymphomas with plasmacytic differentiation seem to correspond genetically and molecularly to MCL. However, the taxonomy of occasional tumors with *CCND1*-R mediated by CSR and canonical *MYD88* mutation might be debatable.

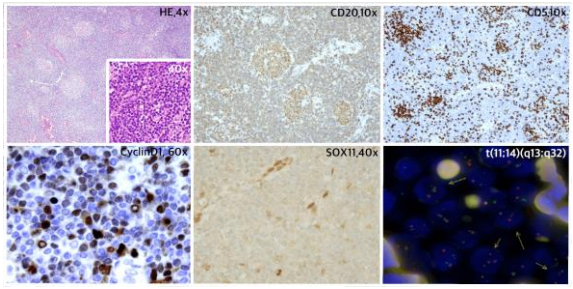

SOX11- MCL with plasmacytic differentiation (case with CCND1-R mediated by AID (CSR))
Lymph node with partially preserved architecture with an atypical lymphoid proliferation. Tumor cells appear polymorphic with a population of small lymphocytes with irregular nuclei, larger lymphoid cells and cells with plasmacytic differentiation that in many of them contain Dutcher bodies. The immunostaining shows that the tumor cells are B-cells with expression of CD20, are negative for CD5, express cyclin D1 and are SOX11 negative. The tumor have the t(11;14) translocation demonstrated by FISH.

EA4HP24-ABS-657

RHOA G17V Potentiates CD28-Induced NFAT Transcriptional Activity by Modulating p300 Activity: A Step Further in the Understanding of Follicular Helper T-cell Lymphoma

Dr. David Vallois[1], Dr. Mélanie Juilland[2], Dr. Kalliopi Ioannidou[1], PhD/MD François Lemonnier[3], Dr. Edoardo Missiaglia[1], PhD/MD Bettina Bisig[1], Prof. Margot Thome[2], Prof. Laurence de Leval[1]

[1] Lausanne University Hospital and University of Lausanne, Department of Laboratories and Medicine, Institute of Pathology, Lausanne, Switzerland; [2] University of Lausanne, Department of Immunobiology, Lausanne, Switzerland; [3] Hôpitaux Universitaires Henri Mondor, Assistance Publique des Hôpitaux de Paris, Unité Hémopathies Lymphoïdes, Créteil, France

Background

Follicular helper T-cell (TFH) lymphoma of the angioimmunoblastic type (AITL) carries a highly recurrent RHOA G17V mutation (60-70% cases) and frequent mutations in other T-cell receptor (TCR) signaling-related genes (50% cases), including CD28 mutations, which often co-occur with RHOA G17V.

Principles/Methodology

We sought to elucidate the potential cooperation of RHOA and CD28 variants in sustaining T-cell activation. We generated stable Jurkat T-cell lines expressing the wild type (wt) or G17V mutant form

of RHOA in combination with either the wt or T195P variant form of CD28 and analyzed their responses to TCR and CD28 co-stimulation.

Results

Concomitant expression of RHOA G17V and CD28 T195P variants induced significantly higher levels of interleukin 2 (IL2) transcription and secretion than either variant alone upon cell stimulation with agonistic anti-CD3 and anti-CD28 antibodies. The combination of both variants also induced significantly higher levels of NFAT transcriptional activity than either variant alone. We further dissected the signaling events underlying this effect and found that CD28 T195P, but not RHOA G17V, enhanced the phosphorylation of key TCR signaling molecules, suggesting that RHOA G17V modulates NFAT transcriptional activity through a distinct mechanism. Co-immunoprecipitation experiments identified the histone acetyltransferase (HAT) p300 as a major interacting partner of RHOA G17V. This interaction was confirmed in human primary T-cells transduced with plasmids expressing wt or RHOA G17V. p300 inhibition abolished the increased IL-2 secretion induced by CD3/CD28 stimulation in cells expressing RHOA G17V and/or CD28 T195P. Chromatin immunoprecipitations revealed an increase of p300-specific H3K18ac and H3K27ac marks at the *IL2* promoter, and immunofluorescence staining revealed an increase of these marks at the whole genome level in cells harboring the RHOA G17V mutant. Finally, multiplex immunofluorescence staining of tumor samples from four AITL patients harboring RHOA G17V showed that neoplastic TFH cells had increased H3K18ac and H3K27ac levels compared to non-neoplastic T cells.

Conclusion

Collectively, these findings reveal an unexpected role for RHOA G17V in potentiating CD28 T195P-induced NFAT transcriptional activity through the modulation of p300 HAT activity and expand the notion that epigenetic deregulation contributes to the pathogenesis of TFH lymphomas. Our results suggest that targeting p300 HAT activity may open new avenues for TFH lymphoma therapies.

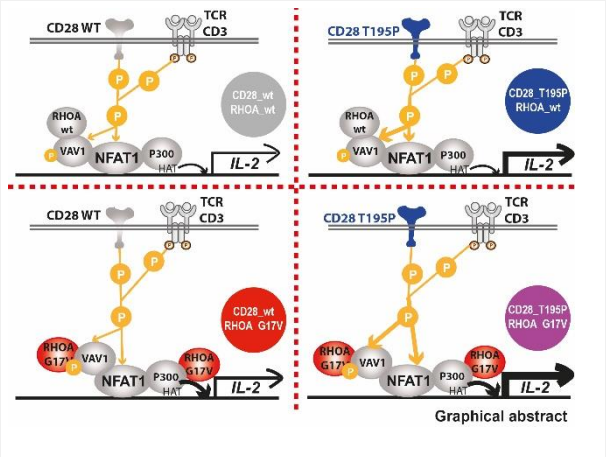

Graphical abstract

RHOA G17V levels up TCR activation by modulating p300 histone acetyltransferase activity

Upper left and right panels. Compared to CD28 wt,CD28 T195P variant enhances the phosphorylation cascade leading to NFAT activation upon CD3/CD28 co-stimulation and therefore increases *IL-2* transcription. **Lower left panel.** RHOA G17V binds to P300 and increases its histone-acetyltransferase activity leading to increased *IL-2* promoter acetylation and increased *IL-2* transcription. **Lower right panel.** When both CD28 and RHOA variants are present, we observe an increased IL-2 transcription and secretion as compared to variants alone.

EA4HP24-ABS-667

Lymphoproprolipherative disorders with with Castleman and Castleman-like morphology: challenges in the diagnostic workup.

PhD/MD Massimo Granai[1], PhD/MD Margherita Vannucchi[1], M.Sc./M.A. Maria Chiara Siciliano[1], Dr. Domenico Ferrara[1], Dr. Ledi Bardhi[1], Dr. Libero Antonio De Nicola[1], Dr. Fredrik Okiny[2], Dr. Timothy Oniuma[2], Prof. Cristiana Bellan[1], Prof. Lorenzo Leoncini[1], Prof. Stefano Lazzi[1]

[1] University of Siena, Institute of Pathology, Siena, Italy; [2] University of Nairobi, Institute of Pathology, Nairobi, Kenya

Background

Human herpesvirus type 8 (KSHV/HHV8), also known as Kaposi's sarcoma-associated herpesvirus, is a human γ herpesvirus that underlies the pathogenesis of a subset of lymphoproliferative disorders with a wide spectrum of overlapping but distinctive clinical and morphological features both in immunocompetent and immunocompromised patients. The diagnosis of such cases can be highly challenging for the pathologist peculiarly in cases with confection by other herpesviruses like Epstein-Barr virus (EBV).

Principles/Methodology

The aim of this study was to assess the presence of KSHV/HHV8 and EBV among 37 cases of Castleman's disease and lymphomas with Castleman-like features comprising 4 extracavitary PEL, 6 DLBCL and 2 cHL. Our cohort of 49 cases were analyzed through droplet digital PCR for EBV latency and HHV8 and EBV viral load and then validated with immunohistochemistry.

Results

The investigation highlighted five cases with unusual viral immunophenotypical patterns. Case 1 represented HHV8/EBV-positive extracavitary nodal PEL followed by pleural PEL. The striking characteristic of this case was the almost focal and intrasinusoidal localisation of the neoplastic cells and the association with Castleman's disease (CD) features. In case 2, we found the entire spectrum of HHV8-related disorders, i.e. KSHV/HHV8-MCD, GLPD, and PEL, coexisting in the same lymph node, underlining the variability, possible overlap and evolution among these entities. Case 3 involves a EBV+ DLBCL with intrasinusoidal pattern and concomitant KSHV/HHV8 negative iMCD. In case 4 we describe a KSHV/HHV8-MCD with EBV reactivation. Case 5 comprises an otherwise typical HHV8-MCD but with scattered small and large EBV positive cells in perifollicular and intrasinusoidal areas of the lymph node.

Conclusion

These cases raise the question of whether EBV and may play a role in the evolution of such entities and how the interplay between HHV8 and EBV may impact on the progression. Our findings expand the current knowledge of EBV and HHV8 traditionally associated lymphoproliferative disorders and hightlight potential diagnostic pitfalls for the pathologist.

Lymphoma Abstracts Poster

EA4HP24-ABS-483	Detection of Hepatitis C Virus Infection and CD30 Expression by Immunohistochemistry in Diffuse Large B Cell Lymphoma
EA4HP24-ABS-485	Patients with Classic Hodgkin Lymphoma and Follicular Lymphoma Compared to Single Malignancy Controls
EA4HP24-ABS-490	Prognostic factors in shock patients
EA4HP24-ABS-491	Effects of medicines on the nerve cells in hypoxia
EA4HP24-ABS-496	Abnormal reactive patterns in lymphoid tissues from patients with inborn errors of immunity
EA4HP24-ABS-497	Comparative Clinicopathological Analysis of Primary Effusion Lymphoma and Fluid-Overload Large B-cell Lymphoma
EA4HP24-ABS-499	T-lymphoblastic lymphoma with co-expression of epithelial markers – a diagnostic pitfall
EA4HP24-ABS-501	Genetic features of primary bone marrow diffuse large B-cell lymphoma
EA4HP24-ABS-504	Gp350-targeted CAR-T therapy in EBV-positive burkitt lymphoma: pre-clinical development of gp350CAR-T
EA4HP24-ABS-513	Outcome of Atypical Lymphoid Proliferations
EA4HP24-ABS-518	Lumping versus Splitting in Hematologic Malignancies. A Case for Splitting Based on a Specific Clinical Scenario: Micronodular T-cell/Histiocyte-rich Large B-cell Lymphoma.
EA4HP24-ABS-525	PD-L1, CTLA-4 and STAT proteins expression in Hodgkin lymphoma with clinicopathological features correlation
EA4HP24-ABS-540	Idiopathic Multicentric Castleman Disease and IgG4-Related Disease: A Diagnostic Conundrum
EA4HP24-ABS-541	Hodgkin lymphoma: The role of EBV plasma DNA viral load testing in an HIV endemic setting.
EA4HP24-ABS-543	Characterization of lymphoproliferative disorders arising in patients with common variable immunodeficiency (CVID): Potential correlation between aggressive subtypes and clinical parameters
EA4HP24-ABS-551	The Impact of SNP rs2228001 of Xeroderma Pigmentosum Complementation Group C (XPC) on The Risk and Prognosis of Hodgkin's Lymphoma: A case-control study
EA4HP24-ABS-555	Overview of CLL patients in Croatian population based on SHM IGHV status and subset identity
EA4HP24-ABS-569	The incidence of Castleman disease in The Netherlands: a retrospective study based on Dutch pathology reports.
EA4HP24-ABS-571	Extramedullary plasmacytoma in children
EA4HP24-ABS-575	Aberrant CD45 expression on metastatic renal cell carcinoma: a potential diagnostic pitfall in daily practice.
EA4HP24-ABS-579	Celiac-like/CVID-like pattern in duodenal biopsy in a patient treated with CAR-T cell
EA4HP24-ABS-580	The Expression of Targeted Therapy-Associated Receptors in Patients with Aggressive Post-Transplant Lymphoproliferative Disorders
EA4HP24-ABS-588	Clinical and molecular features of primary spinal epidural lymphomas
EA4HP24-ABS-590	Role of microsatellite instability in the oncogenesis of primary intestinal T-cell lymphomas

EA4HP24-ABS-592	CD200 is a useful marker to distinguish Nodular Lymphocytic Predominant B-cell lymphoma from TFH lymphoma and classical Hodgkin lymphoma
EA4HP24-ABS-598	Prognostic significance of LEF1 expression in Angioimmunoblastic T-cell Lymphoma and Peripheral T-cell lymphoma with TFH-phenotype in the Spanish Population
EA4HP24-ABS-603	Small B-cell lymphomas with unclear morpho-phenotypic features: What adds the mutational landscape to further classification?
EA4HP24-ABS-606	Mediastinal grey zone lymphoma, challenging diagnosis
EA4HP24-ABS-607	An ultrasensitive dual in situ hybridization (ISH) mRNA assay in determination of kappa/lambda (K/L) restriction status shows strong concordance with historical light chain restriction in B cell lymphomas and plasma cell malignancies
EA4HP24-ABS-609	Follicular lymphoma with MNDA expression
EA4HP24-ABS-610	CPT1 inhibition sensitizes diffuse large B-cell lymphoma to vincristine and doxorubicin treatment
EA4HP24-ABS-615	Paediatric plasma cell variant of unicentric Castleman disease of the mesenteric lymph node: a case report
EA4HP24-ABS-616	Intussusception as a manifestation of Activated PI3K delta syndrome 1 (APDS1)
EA4HP24-ABS-620	Targeted panel sequencing for refining B cell lymphoma diagnosis: A real-life, reference center experience
EA4HP24-ABS-621	Challenging cases of primary CNS lymphoma and mimics
EA4HP24-ABS-623	Clonal T-cell lymphoproliferative disorder with leukemic presentation and non-Sézary phenotype: A new entity?
EA4HP24-ABS-627	Enhancing Molecular Subclassification of B-Cell Lymphomas: Targeted Next Generation Sequencing and Immunohistochemistry versus Fluorescence in Situ Hybridization
EA4HP24-ABS-630	Sellar solitary plasmacytoma with anaplastic features: rare presentation
EA4HP24-ABS-635	Protein Expression of the Novel Tumor Suppressor SAMHD1 is an Independent Prognostic Marker in ALK- Anaplastic Large Cell Lymphoma But Not in Other Peripheral T-Cell Lymphomas
EA4HP24-ABS-639	Dissecting CD47 expression in lymphoid neoplasms: implications for precise diagnosis and targeted immunotherapy
EA4HP24-ABS-641	Expression of TRBC1 and TRBC2 proteins in T- cell lymphomas: a new tool for detection of T cell clonality in routine diagnostics
EA4HP24-ABS-642	Lymphadenopathy inActivated PI3-Kinase Delta Syndrome (APDS).
EA4HP24-ABS-643	High-Grade B cell Lymphoma with MYC and BCL2 and/or BCL6 rearrangements : a genomic approach by targeted Next Generation Sequencing (NGS)
EA4HP24-ABS-647	DNA methylation-based determination of tumor cell content in haematolymphoid neoplasms: fact or fiction?
EA4HP24-ABS-649	Molecular Insights of Lymphoma-Like Lesions of the Lower Genital Tract Support a Reactive Process.
EA4HP24-ABS-650	Composite and sequential Hodgkin and other lymphomas: B cell plasticity and immune dysregulation?
EA4HP24-ABS-651	Primary cutaneous epidermotropic, cytotoxic, ALK+ T-cell lymphoma: appraisal of a novel pattern of disease.
EA4HP24-ABS-655	Burkitt-like lymphoma with 11q aberrations: systematic review
EA4HP24-ABS-659	Different molecular landscape among EBV/HHV8 negative effusion-based lymphomas and EBV or HHV8 positive ones?

EA4HP24-ABS-660	Clinicopathological and Genetic Features of Nodal Marginal Zone Lymphoma and Lymphoplasmacytic Lymphoma: A Korean Multicenter Study Focusing on Differential Diagnosis
EA4HP24-ABS-663	B-cell receptor immunogenetics in thyroid lymphomas
EA4HP24-ABS-664	Primary thyroid B-cell lymphoma: molecular insights of its clonal evolution and relapse

EA4HP24-ABS-483

Detection of Hepatitis C Virus Infection and CD30 Expression by Immunohistochemistry in Diffuse Large B Cell Lymphoma

PhD/MD Nungki Anggorowati[1,3], **Dr. Lili A. Saputra**[1], PhD/MD Mardiah S. Hardianti[2], Dr. Rizki A. Juwita[1], Dr. Indrawati Indrawati[1]

[1] Universitas Gadjah Mada, Anatomical Pathology, Faculty of Medicine/Dr. Sardjito Hospital, Yogyakarta, Indonesia; [2] Universitas Gadjah Mada, Division of Hematology and Medical Oncology, Department of Internal Medicine/Dr. Sardjito Hospital, Yogyakarta, Indonesia; [3] Universitas Gadjah Mada, UGM Academic Hospital, Yogyakarta, Indonesia

Background

Recent studies have shown persistent hepatitis virus infection, especially hepatitis C virus, is important pathogenic factors for high grade and low-grade B cell Non-Hodgkin Lymphoma (NHL). In defining the treatment and prognosis of NHL and Hodgkin Lymphoma, a recent study showed that CD30 immunohistochemical staining plays an important role. Literature states that high levels of CD30 are found in patients with EBV infection. However, the correlation between HCV infection and CD30 in DLBCL has not yet been recognized. This study aimed to determine the prevalence of CD30 and HCV expression and its correlation with clinicopathological characteristics of DLBCL patients.

Principles/Methodology

A total of 86 FFPE of DLBCL cases were collected over the course of two years from the Anatomical Pathology Department at Sardjito Hospital in the Special Region of Yogyakarta, Indonesia. Immunohistochemistry was performed to detect the two markers (CD30 and HCV NS3). Chi-square tests were used to examine the associations between CD30 expression and clinicopathological features in DLBCL patients.

Results

The positivity rate of CD30 expression in 86 DLBCL samples was 25.6% (22/86) when using a 0% cut-off, and 7.0% (6/86) when using a 20% cut-off. The positivity rate of HCV expression in 86 DLBCL samples was 34.9% (30/86). Positive CD30 expression, HCV NS3 expression and clinicopathological features (age, sex, Ann Arbor stage, extranodal involvement, and morphological variations) did not have statistically significant relationships ($p>0.05$).

Conclusion

There was no statistically significant association between CD30 immunoreactivity (cut-off >0% or >20%) and HCV NS3 expression and clinicopathological features (age, sex, Ann Arbor stage, extranodal involvement, LDH, ECOG status and morphological variants) in DLBCL.

EA4HP24-ABS-485

Patients with Classic Hodgkin Lymphoma and Follicular Lymphoma Compared to Single Malignancy Controls

Dr. Claudiu V. Cotta, Dr. Shweta Bhavsar, Dr. Scott Robertson, Dr. James R. Cook

Cleveland Clinic, Laboratory Medicine/Diagnostics Institute, Cleveland, USA

Background

Classic Hodgkin lymphoma (CHL) can arise in patients with low grade B-cell lymphoma. The features of CHL arising in follicular lymphoma (FL) and its outcome are still unclear, mainly due to the very few cases reported.

Principles/Methodology

After IRB approval we identified 8 cases of CHL with concurrent FL, 9 of CHL arising in patients with a history of FL, 26 of FL and 60 of CHL in patients over 40 years of age. In each case data was collected on patient's age at the diagnosis, the therapy received and the outcome. The diagnostic slides and the pathology reports were reviewed.

Results

We identified 8 cases with simultaneous CHL and FL and 9 with FL first and CHL second (Table 1). The age at diagnosis was similar for all: 61 years for the one with simultaneous FL and CHL, 61 years for the CHL controls, 59 for the FL controls, 60 for FL first and CHL second and CHL was diagnosed at an average age of 65 years (Table 1).

The Reed-Sternberg (RS) cells and their background significantly altered the architecture of the tissue. The RS cells were negative for CD20, BOB1, OCT2 and positive for CD30, CD15, Pax5 (dim). RS cells and variants were EBV positive in 38% of cases with FL and CHL, in 22% of cases with FL first CHL second and in 46% of the cases in the CHL only control group.

BCL2 rearrangements were detected in RS cells in every case of simultaneous FL and CHL in which FL carried the translocation (3 of the 4 cases tested). The translocation was identified in FL in 1 of 3 cases in which the diagnosis of FL was made first. (Table 1). EBV was detected in 2 cases with *BCL2* rearrangements (of 9 CHL cases tested 4 were *BCL2* positive).

The median survival of patients with FL alone was 156 months and 89 months for CHL alone patients. The median survival of the FL and CHL group could not be determined; however, at least for an initial period of time the survival was similar to that of patients with FL alone (Figure 1).

Conclusion

In conclusion, patients with FL that develop CHL tend to be male and a higher proportion of them have high grade FL, compared to the control group. CHL can be present at the diagnosis of FL, or develop later, tends not to be associated with EBV reactivation and is probably clonally related to FL. Treatment of patients with FL and CHL or with CHL after FL with regimens designed for CHL has initially an outcome resembling that of FL than that of CHL in a similar age group.

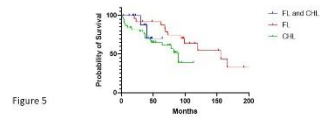

Figure 5

Survival

	FL and CHL	FL first CHL second	FL Controls	CHL Controls
N	8	9	26	60
Age (years, mean)	61	60 (FL); 65 (CHL)	59	61
M:F (%)	5:3 (62.5%)	6:3 (67%)	14:12 (54%)	34:26 (57%)
Grade 1-2/Total (%)	6/8 cases (75%)	6/9 cases (67%)	24/26 cases (92%)	N/A
BCL2 FISH Cases Positive/Total Cases Tested (%)	FL: 3/4 (75%) CHL: 3/4 (75%)	FL: 1/3 (33%) CHL: 1/5 (20%)	N/A	N/A
EBER positive	3/8 (38%)	2/9 (22%)	N/A	17/37 (46%)
Time to CHL (years)	0	5	N/A	N/A

Table

EA4HP24-ABS-490

Prognostic factors in shock patients

PhD/MD student Sung Hyuk Choi[1], PhD/MD Jae Kwan Lee[2], PhD/MD Kyung Whan Kim[3]

[1] Korea university Guro hospital, Emergency medicine, Seoul, South Korea; [2] Korea university Guro hospital, Gynecologic medicine, Seoul, South Korea; [3] Reginal Emergency control center, Seoul, South Korea

Background

Early predictable factors and preventive drugs are important, as secondary sepsis, multiple organ failure, despite appropriate treatment during shock, leads to poor prognosis. Recently, macrophage migration inhibitory factor (MIF), toll receptor 4 (TLR_4) and T cell viability, factor of infection and immunity, have been known for their usefulness in nonclinical experiments. Our study aims to explore the significance of TLR, MIF and T cell viability as predictors of sepsis in shock patients.

Principles/Methodology

In hemorrhagic shock patients who visited a single emergency centers between 2018 and 2020, MIF in serum, TLR_4 in polymorphonuclear neutrophils, and T cell viability and interleukin 2 in T lymphocytes were measured. The associations were identified by comparing the measured factors with patients mortality and the incidence of sepsis.

Results

1. Relationship between MIF, TLR_4, T cell viability and sepsis in shock patients

In 180 shock patients, MIF (2633±710pg/mL) was higher than MIF (588±485pg/mL) in normal people and higher than MIF (1460±680pg/mL) in non-occurrence groups. In addition, TLR_4 (16.27±2.05 (FACs), 5.05±1.94 (TLR_4/Actin) in the sepsis group were higher than TLR_4 (7.78±0.59 (FACs), 0.63±0.11 (TLR_4/Actin) in the non-occurrence group. In the MTT for the measurement of T cell viability, the sepsis group

(0.52±0.25) was lower than that of the non-occurrence group (0.78±0.45), and the IL-2 measured in FACs was significantly higher in the sepsis group (4.68±3.36) than in the non-occurrence group (2.41±2.58).
2. Relationship between MIF, TLR_4, T cell viability and mortality in shock patients
In shock patients, MIF in the death group were over 3000 pg/mL, and TLR_4 measured in FACs was 12.67 in the death group, higher than 9.74 in the survival group, but had no statistical significance. In the MTT for the measurement of T cell viability, the death group (0.66±0.46) was lower than the survival group (0.80±0.43). The IL-2 measured in FACs showed no difference between the survival group (2.84±3.15) and the death group (2.62±2.04).

Conclusion

The lower T cell viability, higher MIF and TLR_4 values were shown in the death group in shock patients, but only T cell viability had statistical significance. However, in the development of sepsis, higher MIF, TLR_4 and lower MTT values are shown which may be useful for the initial diagnosis of sepsis development.

EA4HP24-ABS-491

Effects of medicines on the nerve cells in hypoxia

PhD/MD student Sung Hyuk Choi

Korea University Guro hospital, Emergency medicine, Seoul, South Korea

Background

Hypoxia occurs in shock due to respiratory failure, bleeding, and severe trauma in patients visiting the emergency center, resulting in severe brain damage. Therefore, we would like to investigate the effects of pentoxifylline, steroid, and hypertonic saline on hypoxia and the effects of injection time of medicine in SH-SY5Y cells.

Principles/Methodology

After exposure to hypoxic state (1% O2) for two hours using SH-SY5Y cells, incubation at normoxic state (20% O2) for 24 hours, cell viability, apoptosis, and hydrogen peroxide were measured and compared to normal groups. In addition, various combinations of pentoxifylline, steroid, and hypertonic saline were injected simultaneously with hypoxia and after hypoxia to compare each condition.

Results

1. Cell viability, apoptosis, hydrogen peroxide in hypoxic condition
Cell viability decreased in hypoxia at 2 hours and apoptosis, hydrogen peroxide increased compared to the control group.
2. Cell viability, apoptosis, hydrogen peroxide according to various combinations of medicines and injection time of medicines
Most medicines had no effect on cell viability, a little reduced apoptosis without statistical significance, but had a significant effect on injection at the same time as hypoxia. Although overall the generation of hydrogen peroxide in injections of medicines was reduced compared to the control group, it had statistical significance when HTS, combination of HTS and PTX were injected simultaneously with hypoxia.

Conclusion

PTX, HTS were able to have a preventive effect on cell damage when applied at the earliest time of hypoxia in SH-SY5Y cells

EA4HP24-ABS-496

Abnormal reactive patterns in lymphoid tissues from patients with inborn errors of immunity

Dr. Shachar Naor[1], **Dita Gratzinger**[2]

[1] Sheba Medical Center, Pathology, Ramat Gan, Israel; [2] Stanford University School of Medicine, Pathology, Stanford, Germany

Background

Patients with inborn error of immunity (IEI) who undergo lymph node biopsy for lymphadenopathy often show abnormal lymphoid tissue architecture and disturbed activated immune reactions. In this work we attempt to characterize the morphologic and immunoarchitectural patterns in lymph node specimens from patients with various types of inborn errors of immunity.

Principles/Methodology

Tissue microarrays were constructed using two 2 mm cores. Immunohistochemical stains for immunoarchitectural characterization were performed (CD20, CD3, CD21, BCL6, CD10, BCL2, IgD, IgM, IgG, PD1) and number and distribution of IgM and IgG+ plasmablasts and plasma cells were recorded.

Results

Three abnormal patterns of germinal center reaction were observed (see **Figure 1**)

- Insufficiency pattern showing small underdeveloped germinal centers with paucity of plasmablasts and plasma cells showing predominance of IgM over IgG.
- Dissociative pattern showing large and irregular germinal centers with the production of only IgM positive plasmablasts/plasma cells and decreased IgG positive plasmablasts/plasma cells.
- Hyperreactive pattern showing larger and irregular germinal centers with increased number of interfollicular IgG plasmablasts/plasma cells.

Table 1: Distribution of cases (in parenthesis: number of patients)

Insufficiency pattern	Dissociative pattern	Hyperreactive pattern
CVID (2)	CVID(1)	CVID, CTLA4 HI (1) – intrafollicular distribution predominant
CGD (1)	CVID, TNFAIP3 (1)	WAS (1) – interfollicular distribution predominant
	Kabuki syndrome (2)	
	APDS1 (1)	

APDS1, activated PI3 kinase delta syndrome 1; CGD, Chronic granulomatous disease;CTLA4 HI, Cytotoxic T lymphocyte-associated antigen-4 haploinsufficiency; CVID, Common variable immunodeficiency; TNFAIP3, Tumor necrosis factor-α-induced protein 3; WAS, Wiskott-Aldrich syndrome

Conclusion

Patients with IEI show distinct abnormal morphological patterns of germinal center reaction, closely related to the type of mutation where known. Knowledge of these expected patterns may help the pathologist to avoid pitfalls in the diagnosis of these type of biopsies. In addition, recognition of these abnormal patterns of“germinal center maturation” may alert the pathologist to consider the possibility of an IEI even when such a diagnosis has not yet been made.

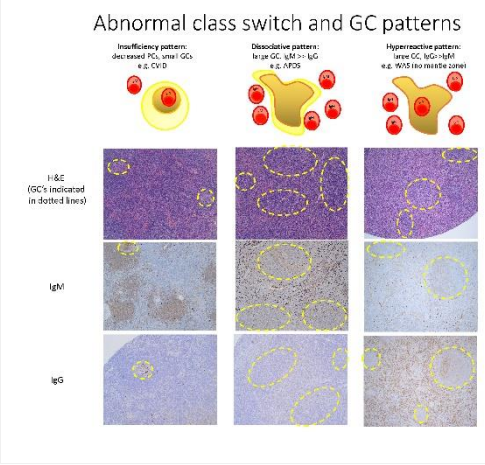

Abnormal class switch and germinal center patterns in inborn errors of immunity
Figure 1: Three abnormal reactive germinal center reaction patterns with illustrative cases for each. APDS1: Activated PI3K delta syndrome type 1, CVID: Common Variable Immunodeficiency unspecified, GC: germinal center, PC: plasmablasts/plasma cells, WAS: Wiskott-Aldrich syndrome

EA4HP24-ABS-497

Comparative Clinicopathological Analysis of Primary Effusion Lymphoma and Fluid-Overload Large B-cell Lymphoma

Dr. Taesung Jeon[2], PhD/MD Young-Hyeh Ko[3], PhD/MD You-Na Sung[1], PhD/MD Hyunsung Kim[4], PhD/MD Ka-Won Kang[5], PhD/MD Jongmin Sim[1], **PhD/MD Yeseul Kim**[1]

[1] Korea Anam Hospital, Department of Pathology, SEOUL, South Korea; [2] Korea Guro Hospital, Department of Pathology, SEOUL, South Korea; [3] Cheju Halla General hospital, Department of Pathology, SEOUL, South Korea; [4] Hanyang University College of Medicine, Department of Pathology, SEOUL, South Korea; [5] Korea University College of Medicine, Division of Hematology-Oncology, Department of Internal Medicine, SEOUL, South Korea

Background
Primary effusion lymphoma (PEL) and fluid overload-associated large B-cell lymphoma (FO-LBCL) represent distinct entities of B-cell neoplasms characterized by serous effusions without detectable tumor masses. Despite the crucial role of HHV-8 positivity in differentiating these entities, significant disparities exist in their immunophenotype and clinical outcomes. We conduct a comparative analysis of their clinicopathologic features to elucidate these differences further.
Principles/Methodology
This study enrolled 3 cases of PEL and 6 cases of FO-LBCL from two large hospitals. For all the cases, immunohistochemical staining, EBER (Epstein-Barr encoding region) in-situ hybridization, and gene rearrangement analyses were carried out.
Results
The median age of PEL patients was 72 years and FO-LBCL patients was 84 years. All PEL cases were CD20 negative, in contrast to FO-LBCL cases which were CD20 positive. All PEL and FO-LBCL cases showed positive Mum-1 expression, and CD138 was negative in all cases. In PEL, 2 out of 3 cases showed aberrant T antigen expression, with one case exhibiting dual rearrangement of the Immunoglobulin heavy chain (IgH) gene and T-cell receptor (TR) genes, and the other case showing clonal rearrangement of IgH and low intensity clonal peak for TCR-β. In both PEL and FO-LBCL, the Ki-67 labeling index was observed to be approximately 50-90%. All PEL patients succumbed to their

condition, while four out of six FO-LBCL patients exhibited a self-limited course, confirming a prognostic difference.

Conclusion

Although both PEL and FO-LBCL exhibit terminal B-cell features, PEL is distinguished from FO-LBCL by its frequent aberrant T cell antigen expression, loss of B cell antigens, and the genotypic complexity as well as presence of HHV-8. From a clinical perspective, FO-LBCL exhibited a better prognosis compared to PEL, and the older age of the patient cohort suggests a potential association with immune senescence in FO-LBCL.

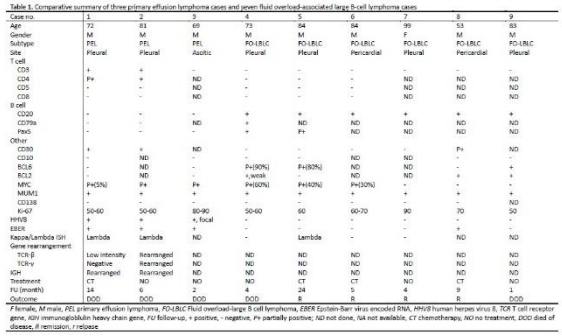

Table 1. Comparative summary of three primary effusion lymphoma cases and seven fluid overload-assoc

EA4HP24-ABS-499

T-lymphoblastic lymphoma with co-expression of epithelial markers – a diagnostic pitfall

PhD/MD student Ziva Ledinek[1,2], PhD/MD Aleš Rode[3], Prof. Alenka Repše Fokter[4], PhD/MD Maja Česen Mazić[5], PhD/MD Maja Jerše[6], PhD/MD Biljana Grčar Kuzmanov[7], PhD/MD Gorana Gašljević[7], Prof. Veronika Kloboves-Prevodnik[2,3]

[1] Universtiy Medical Center Maribor, Department for Pathology, Maribor, Slovenia; [2] Faculty of Medicine, University of Maribor, Department of Pathology, Maribor, Slovenia; [3] Institute of Oncology Ljubljana, Department of Cytopathology, Ljubljana, Slovenia; [4] General Hospital Celje, Department of Pathology and Cytopathology, Celje, Slovenia; [5] University Children's Hospital Ljubljana, Department of Haematology and Oncology, Ljubljana, Slovenia; [6] Faculty of Medicine, University of Ljubljana, Institute of Pathology, Ljubljana, Slovenia; [7] Institute of Oncology Ljubljana, Department of Pathology, Ljubljana, Slovenia

Background

The diagnosis of T-lymphoblastic lymphoma (T-LBL) from effusions can be challenging, especially if morphology and immunophenotype of lymphoma cells are not typical. In these cases, extensive flow cytometry (FC) must be performed. Immunocytochemistry (ICC) by itself could be insufficient and may result in inconclusive/erroneous diagnosis. We present a case of a child with pericardial effusion in whom T-LBL was missed in first two pericardial fluid specimens due to the misleading ICC results and lack of material for FC.

Principles/Methodology

Eleven-year-old boy presented with a few days lasting dyspnea and chest pain. Massive pericardial effusion was found and urgent pericardiocentesis at the community hospital (CH) was performed.

Pericardial fluid was sent for cytologic and microbiologic evaluation. He was then transferred to pediatric intensive care unit at the tertiary center (TC) where additional open tissue biopsy was performed.

Results

At the CH, initial cytology based on cell morphology was in favor of lymphoma. However, ICC analysis showed CKAE1/AE3+, CD45-, MOC31+, EMA+, NSE+ and Vimentin+. Therefore, differential diagnosis of small round cell malignant tumor of other etiology was preferred. At TC, 2nd effusion sample was sent for FC. It contained only 0.1 x10^6/ml cells; thus, only limited FC analysis was performed showing atypical lymphoid cells (CD45 dim+, CD7-, CD3-, CD5+, C99 bright+, CD4+, CD8+/-). Since the clinical diagnosis of T-LBL could not have been confirmed, revision of initial cytology and open tissue biopsy were performed. The revision of cytology suggested erroneous diagnosis of Ewing sarcoma due to the unusual cell morphology (vacuolization of cytoplasm, chromatin shrinkage, cell molding), epithelial markers, NSE and CD99 positivity and lack of FC data. Afterward histology reveled T-LBL with focal dot-like co-expression of cytokeratin and EMA. Extensive FC of 3rd effusion performed at the time of open biopsy was consistent with the diagnosis of T-LBL, cortical type (CD45 dim+, CD7-/+, CD3-, cytoplasmic CD5+, C99 bright+, CD4+, CD8+/-, TdT+/, CD1a+). Molecular testing showing rearrangements in TCRB and TCRG genes.

Conclusion

Unusual cell morphology and co-expression of epithelial markers in effusion samples may represent a diagnostic pitfall and preclude definitive diagnosis of T-LBL. In patients with clinical suspicion for lymphoma in effusions, extensive FC is mandatory.

EA4HP24-ABS-501

Genetic features of primary bone marrow diffuse large B-cell lymphoma

Dr. Ching-Fen Yang[1], Dr. Kung-Chao Chang[2], Dr. Chih-Yi Hsu[1], Dr. Yi-Chen Yeh[1]

[1] Taipei Veterans General Hospital, Department of Pathology and Laboratory Medicine, Taipei, Taiwan; [2] National Cheng Kung University Hospital, College of Medicine, National Cheng Kung University, Department of Pathology, Tainan, Taiwan

Background

Primary bone marrow diffuse large B-cell lymphoma (PBMDLBCL) is a clinically aggressive disease, and patients may be complicated by hemophagocytic
lymphohistiocytosis (HLH), resulting in high morbidity and mortality risk. The disease is rare and few previous studies for the genetic characteristics have been reported.

Principles/Methodology

A total of 20 cases of PBMDLBCL, labelled as G1, were analyzed, comprising 12 cell pellet samples and 8 paraffin sections. Additionally, 9 cases of conventional diffuse large B-cell lymphoma with bone marrow involvement, labelled as G2, were examined, and all of which were cell pellet samples. Whole exome sequencing procedures had been conducted on all specimens.

We employed the Agilent SureSelect XT Reagent kit protocol for constructing Illumina Hiseq paired-end sequencing libraries (catalog#G9611A). Utilizing the SureSelect XT Clinical Research Exome Version 2 probe set (67.3Mbp). All samples were sequenced on an Illumina Sequencer using the

150PE protocol. For variant analysis, qualified read data underwent genomic alignment against the Ensembl database using Burrows-Wheeler Aligner (BWA) to obtain basic sequence information. Further variant analysis, including variant calling and annotations, was performed using Genome Analysis Toolkit (GATK) and Variant Effect Predictor (VEP). Variants with a Global Minor Allele Frequency of <1% were categorized as rare variants. Fisher exact test was used to compare the distribution of categorical variables. The statistical difference was considered significant when the P value was <0.05.

Results

There are 30 genes with significant differences (P<0.05) between the PBMDLBCL and conventional diffuse large B-cell lymphoma with bone marrow involved cases. When analyzing the genes had been previously reported in DLBCL (lymphplex 35 genes), KMT2D and BTG1 were significant different (p<0.05).

Conclusion

Genes associated with poor prognosis were common in PBMDLBCL, and the resutls further confirmed PBMDLBCL to be an aggressive disease.

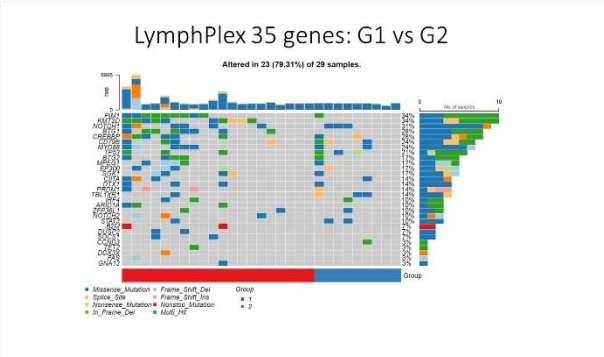

Lymphplex 35 genes of G1, primary bone marrow diffuse large B-cell lymphoma, vs G2, control

EA4HP24-ABS-504

Gp350-targeted CAR-T therapy in EBV-positive burkitt lymphoma: pre-clinical development of gp350CAR-T

Prof. Yan-Li Li[1], Dr. Jia-Jia Wang[2], Dr. Hui-Ping Wang[2], Dr. Zhi-Mai Gao[2], Prof. Reinhard Zeidler[3], Prof. Zhi-Min Zhai[2]

[1] Anhui Medical University, Pathology, Hefei,Anhui, China; [2] The Second Affiliated Hospital of Anhui Medical University, Hematologic Department/Hematologic Diseases Research Center, Hefei,Anhui, China; [3] University Hospital, Ludwig-Maximilians University Munich/Research Unit Gene Vectors, Helmholtz Zentrum München, German Research Center for Environmental Health, Otorhinolaryngology, Munich, Germany

Background

Epstein-Barr virus (EBV) is a type of human γ-herpesvirus, and its reactivation plays an important role in the development of EBV-positive Burkitt lymphoma (BL). Despite intensive chemotherapy, the prognosis of relapsed/refractory BL patients remains unfavorable, and a definitive method to completely eliminate latent EBV infection is lacking. Developing chimeric antigen receptor (CAR)-T

cells therapy targeting EBV specific protein in the context of this EBV-positive aggressive lymphoma will provide a novel therapeutic strategy for patients with limited treatment options.

Principles/Methodology

We developed EBV specific CAR-T cells targeting gp350 (a major glycoprotein on the surface of EBV during its lytic phase). Gp350 expression were analyzed by immunohistochemistry in paraffin sections from EBV-positive BL patients. Gp350 expression were analyzed in human BL cell lines (Raji, NAMALWA) and DLBCL cell line (SUDHL-4) by flow cytometry (FC), Western blot (WB) and Immunofluorescence confocal microscopy. Co-culture of gp350 CAR-T cells or vector-T cells with EBV-positive BL cell line or EBV-negative DLBCL cell line, the ratio of T cells (CD3) to target cells (gp350) in the co-culture system is detected by FC. The proportion of gp350+ cells represents the residual proportion of target cells. Co-culture supernatant was detected secreted IFN-γ, TNF-α and IL-2 by ELISA. The engraftment, tumor growth, dissemination and survival time were observed in BALB/c nude mice and NOD-SCID mice using gp350 CAR-T cell therapy.

Results

Gp350 were firstly expressed in paraffin sections from EBV-positive BL patients and in human BL cell lines (Raji, NAMALWA), but not expressed in DLBCL cell line (SUDHL-4). Gp350 CAR-T cells respond to gp350+ BL cell lines has specific killing effects. In the supernatant from the gp350 CAR-T cells co-cultured with gp350+ BL cell lines, the levels of IFN-γ, TNF-α and IL-2 were significantly increased compared to the vector-T cells group, and these were almost undetectable in the supernatant of gp350 CAR-T cells co-cultured with gp350- DLBCL cell line. Gp350 CAR-T cell therapy decreased tumor growth and dissemination of gp350+ BL cells, and increased survival time in the xenograft model.

Conclusion

In pre-clinical development, we designed, constructed, and screened gp350 CAR-T cells to demonstrate its efficacy in vitro and in vivo against and kill gp350+ BL cells and prevent formation and development BL in xenograft mice model.

EA4HP24-ABS-513

Outcome of Atypical Lymphoid Proliferations

Dr. Xiaohong Zhang

Geisinger Health System, Pathology, Wilkes-Barre, USA

Background

Atypical Lymphoid Proliferations (ALP) are conditions in which it is not possible to differentiate between the benign and the malignant nature of a given lymphoid infiltrate. The descriptive term ALP may be used as an interim label when morphologic and immunophenotypic features are not sufficient to render a positive diagnosis of lymphoma. This study aims to investigate the distribution and characters of benign and malignant outcome among ALP cases from different specimens in our institute.

Principles/Methodology

Total of sixty-nine cases of atypical lymphoid proliferation were retrieved from Geisinger Health System from 2022 to 2023. These cases include thirty-two cases from tissue, lymph nodes and fluid specimens and thirty-seven cases from skin biopsies. Morphological evaluation and immunohistochemical stains are performed followed by molecular studies.

Results

Out of sixty-nine cases, reactive lymphoid proliferation appears in 39.1 % of cases. 52.1% of cases are lymphoma including B-cell lymphoma of 24.6% of cases and T-cell lymphoma of 27.5% of cases. There are a few of cases, 8.7%, remains indeterminate as ALP. Among the cases from tissue/lymph nodes/fluid specimens, more than half of them are reactive (59.4%), some cases are B-cell lymphoma (28.1%) and a few of them remain ALP including EBV-related lymphoid proliferative disorder, lymphomatoid granulomatosis (12.5%) (Table 1). The cases from skin are different. Approximate half of ALP cases are T-cell lymphoma (45.9%), followed by reactive lymphoproliferation (32.4%), and B-cell lymphoma (16.2%); there are a few cases remains ALP (5.4%) even after thorough studies (Table 2).

Conclusion

Lymphocytic infiltrates in tissue are common. Various histologic features may suggest either a malignant or reactive process. Immunohistochemical studies are usually used to support or refute the initial histologic diagnosis. However, it is not uncommon in our routine practice that some cases with ALP cannot be easily diagnosed to be benign or malignant process by only morphological evaluation and immunophenotypic studies. In these situations, molecular techniques play a key role in the diagnosis of lymphoid neoplasms. In this study, more than half of ALP are reactive from tissue/lymph node/fluid specimens; only approximately one-third of cases is reactive from skin biopsies. Of note, there are still a small proportion of the cases remain in ALP. Clinical correlation and follow-up are particularly important in these situations.

EA4HP24-ABS-518

Lumping versus Splitting in Hematologic Malignancies. A Case for Splitting Based on a Specific Clinical Scenario: Micronodular T-cell/Histiocyte-rich Large B-cell Lymphoma.

Dr. Jackson A. Barbosa[1], Dr. Daniel S. Nogueira[2], Dr. Denise D.C. Pasqualin[1], Dr. Nydia S. Bacal[3], Dr. Elizabeth X. Souto[3], Dr. Aline Ueda[1], Dr. Ana Carolina D.B. Lyra[1]

[1] Hospital Israelita Albert Einstein, Anatomia Patológica, São Paulo, Brazil; [2] Hospital Alemão Oswaldo Cruz, Hematologia e Hemoterapia, São Paulo, Brazil; [3] Hospital Israelita Albert Einstein, Patologia Clínica, São Paulo, Brazil

Background

In the classification of both hematologic and non-hematologic neoplasms, two main schools of thought exist: "Splitters," who divide diseases into multiple subcategories or entities, and "Lumpers," who group diseases into fewer broad categories. This poster presents the case of a 64-year-old male patient who initially presented with neutropenia and frequent hospitalizations to treat infections, progressing to pancytopenia with lymphopenia. PET scan revealed isolated splenomegaly without significant lymph node enlargement. Bone marrow and peripheral blood flow cytometry detected a small population of clonal T-cells based on TRBC1 clonality. Bone marrow biopsy showed lymphoid aggregates, predominantly composed of small T and B lymphocytes, as well as large atypical lymphocytes with heterogeneous expression of CD20, PAX5, CD30, MUM1, bcl-6, OCT-2 and negative for CD10 and EBV. No significant intravascular lymphocytosis was detected. Overall findings favored micronodular T-cell/histiocyte-rich large B-cell lymphoma with an abnormal T cell background population, likely reactive.

Principles/Methodology

This case illustrates a challenging clinico-pathologic scenario nearly misdiagnosed as a T cell neoplasm. The clinical presentation and biopsy findings did not fit any specific T-cell neoplasm, prompting review of the literature, extensive work-up and additional immunohistochemistry. Recognition of the so-called "micronodular T-cell/histiocyte-rich large B-cell lymphoma" was key to a successful outcome, as this proposed subtype of TCHRBCL presents with peculiar clinical profile (splenic and bone marrow involvement, without lymph node enlargement). Not only is this a challenging case due to its rarity, the abnormal T-cell population posed a confounding factor. Detection of PCR-based clonal T-cell populations in contexts other than T-cell neoplasms is well-documented and it likely supports that, in the future, similar rationale will apply to TRBC1.

Results

After initial two cycles of R-CHOP, the patient's CBC normalized, and splenomegaly was significantly reduced.

Conclusion

In summary, recognizing subcategories, subtypes, or even separate entities for hematologic malignancies with unusual, confounding, and specific clinical features is crucial for achieving more precise diagnoses. Establishing formal designation of subgroups or subcategories within the broader classification systems may facilitate diagnostic processes and potentially reduce the risk of misdiagnosis, improving patient outcomes.

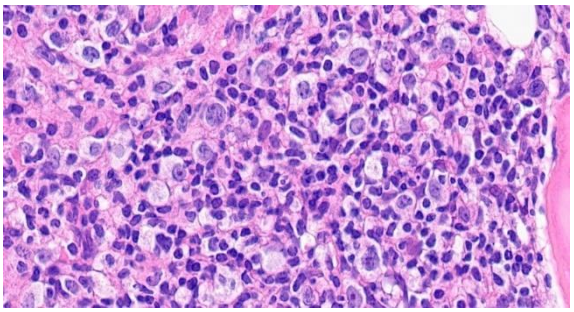

Atypical large lymphocytes in bone marrow aggregate
The small lymphocytes are predominantely T-cells with admixed B-cells. The large atypical lymphocytes are B-cells.

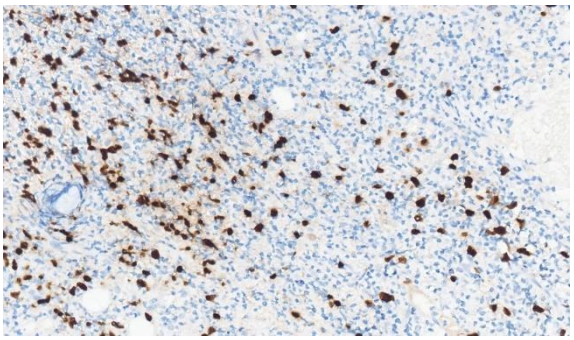

PAX-5 highlights large B-cells
PAX-5 shows some small B-cells and also highlights atypical large lymphocytes. T-cell neoplasms and reactive conditions with large B-cell immunoblasts can show similar features. However, the other immunophenotypic findings rule out these differentials.

EA4HP24-ABS-525

PD-L1, CTLA-4 and STAT proteins expression in Hodgkin lymphoma with clinicopathological features correlation

Prof. Janusz Dzieciol[2], Prof. Joanna Reszeć- Giełażyn[1], PhD/MD Zofia Dzieciol-Anikiej[3], Dr. Krzysztof Kobus[1]

[1] Medical University of Bialystok, of Medical Pathology, Białystok, Poland; [2] Medical UNiversity of Bialystok, of Human Anatomy, Białystok, Poland; [3] Medical Univeristy of Bialystok, of Rehabilitation, Białystok, Poland

Background

The aim of the study was to evaluate PD-L1, CTLA-4 and STAT 6 in cHL with clinicopathological features correlation.

Principles/Methodology

120 cases of cHL specimens were included in to the study. 70 cases were diagnised as nodular sclerosis type, 50 as mixed cellularity type.

Cut slides were procesed in PT Link and stained in the DAKO OMINS with PD-L1 (clone 22C3). The slides were also staine with CTLA-4 (ab237712) and STAT6 (ab32108) antibodies in DAKO autosteiner PLUS.

Results

The age raged form 11 to 17 years. 56 female and 64 male patients was in the examined group. 85% of caes was in I and II stage (80 and 22 respecively) , 10% in III stage (12 cases) and 5% in IV stage (6 cases). Splenomagaly was observed in 10% of cases in 5% hepatosplenomegaly was present. B symptomes was observed mainly in III and IV stage and in 10% of II stage cases. 5-year survival was observed in 98% of cases, while in 2% of cases patients dided within 3-5 years after the diagnosis. PD-L1 expression was observed both in HRS cells and T cells in the enviroment. In all cases in I and II stage, in 5 cases in III stage and in 1 case in IV stage. In I stage the expression was stong and diffuse in more than 80% of HRS cells (CPS more tahn 50%), in II strong and linear expression was observed in 12 cases)CPS more tah 50%), in 10 cases the expression was weak but linear (CPS 1%-49%). In III and IV stage PD-L1 positive cases the expression was weak but linear (CPS 1-49%).

Cytotoxic T lymphocyte-associated antigen 4 (CTLA-4) can inhibit antitumor immunity and promote cancer progression, but its role and mechanism in lymphoma are still unclear. In our study CTLA-4 was observed in 10 cases in I stage, in 13 cases in II stage, in 10 cases in III stage and in 6 cases in IV stage. The positive correlation was observed between CTLA-4 expression and total amount of T cells (esspecially T reg $CD4^{+}Foxp3^{-}$) p=0,003.

Nuclear STAT6 expression was observed in 68 cases in I stage, in 20 cases in II stage and in all cases in III and IV stage. The ragnge of the expression was as: 50-80% of HRS cells in I stage, 60-80% in II stage, 70-100% of HRS cells in III and IV stage. The result was statistically significant (p=0,005).

Conclusion

PD-L1 expression is an important event in early CHL stages, which may be used in the futher immunoterapy

CTLA-4 expression inhibits the activation of immune system and may be associated with disease progresion

STAT 6 is an ealry event in HRS cells and may be associated with disease progression

EA4HP24-ABS-540

Idiopathic Multicentric Castleman Disease and IgG4-Related Disease: A Diagnostic Conundrum

PhD/MD Philip Berardi[1], Prof. Luke Chen[2]

[1] The Ottawa Hospital/University of Ottawa, Pathology and Laboratory Medicine, Ottawa, Canada; [2] Dalhousie University, Department of Medicine, Halifax, Canada

Background

Idiopathic Multicentric Castleman Disease (iMCD) and IgG4-Related Disease (IgG4-RD) are immune-mediated conditions characterized by lymphadenopathy, polyclonal hypergammaglobulinemia and multi-organ involvement. Differentiating these diseases is challenging due to overlapping clinical, radiological and laboratory features. iMCD, a subtype of Castleman Disease, manifests as heterogeneous lymphoproliferative disorders with cytokine dysregulation, notably interleukin-6 (IL-6), contributing to systemic inflammation. Histologically, iMCD is typified by atypical lymphoid follicles and vasculopathy. Conversely, IgG4-RD, a fibro-inflammatory condition, shows lymphoplasmacytic infiltrates enriched in IgG4-positive plasma cells.

Principles/Methodology

This study is limited to rare cases encountered in Eastern Ontario between Jan 2018 and Dec 2023. Retrospective chart review shows common clinical presentations include fever, fatigue, weight loss and organ dysfunction. Diagnostic imaging often shows diffuse LAD and organomegaly. Laboratory findings, including elevated acute-phase reactants and **polyclonal hypergammaglobulinemia (PHGG)**, are nonspecific and commonly observed in both diseases. These criteria lack specificity and we aimed to implement a more integrated approach combining clinical, radiological and laboratory assessment to ensure an accurate diagnosis.

Results

Imaging modalities such as positron emission tomography-computed tomography and magnetic resonance imaging can aid in evaluating disease and guiding biopsy site selection. Histopathological examination remains the cornerstone for definitive diagnosis, necessitating careful assessment of lymph node architecture, immunohistochemistry and IgG4 immunostaining. Treatment strategies for iMCD and IgG4-RD involve immunomodulatory agents to suppress inflammation and cytokine-directed therapies to target IL-6 and other cytokines implicated in disease pathogenesis.

Conclusion

Distinguishing between iMCD and IgG4-RD presents a diagnostic dilemma due to shared clinical and histological features. Evaluation of cases using clinical, radiological, and histopathological findings is crucial, however robust clinico-pathological correlation is needed for accurate diagnosis. Despite overlapping therapeutic approaches, response to treatment varies between individuals, emphasizing the need for personalized management strategies. Research elucidating the distinct pathophysiological mechanisms and biomarkers is needed to enable early diagnosis and tailored treatment.

EA4HP24-ABS-541

Hodgkin lymphoma: The role of EBV plasma DNA viral load testing in an HIV endemic setting.

Prof. Jessica J. Opie[1], Prof. Estelle R. Verburgh[2], Prof. Zainab Mohamed[3], Dr. Dharshnee Chetty[1], M.Sc./M.A. Jenna Oosthuizen[2], Prof. Diana Hardie[1]

[1] University of Cape Town, Department of Pathology, Cape Town, South Africa; [2] University of Cape Town, Department of Medicine, Cape Town, South Africa; [3] Groote Schuur Hospital, Department of Radiation Medicine, Cape Town, South Africa

Background

South Africa (SA) has a high burden of HIV. Hodgkin lymphoma (HL) has a 7-fold increased risk in HIV, even with antiretroviral therapy (ART). HIV-associated HL is clinically aggressive, often with advanced disease and bone marrow infiltration and has poor outcomes. SA has poor access to functional imaging (PET/CT scanning), the standard of care for staging and monitoring HL, and thus a non-invasive biomarker of disease would have great clinical application. Hodgkin tumour cells are typically EBV infected in HIV positive (+) HL and EBV is detected using stains on diagnostic tissue. Peripheral blood EBV DNA testing is a potential biomarker in HL. In EBV tumour +ve HL, the plasma contains cell free (cf) EBV, derived from apoptotic HL tumour cells. Aims: To establish sensitivity and specificity of plasma EBV DNA viral load testing in HL. To correlate EBV plasma viral loads with EBV-tumour status, HIV status, stage of disease and overall survival.

Principles/Methodology

Prospective study of newly diagnosed HL patients presenting for treatment 2019 – 2023. EBV DNA plasma viral load was measured using RT PCR on the Abbott 2000 Real Time instrument. Data was extracted from medical and laboratory records including histological subtype, EBV tumour status, HIV status (CD4 count and viral load), clinical stage, therapy, and survival. Statistical analysis included receiver operative curve (ROC) analysis and Fisher's exact test.

Results

67 patients were included, 34 (51%) female and 21 (32%) HIV +ve. 95% of HIV +ve cases were EBV tumour +ve, and 30% of HIV-ve. ROC analysis found a plasma EBV DNA cut off >762 IU/ml provided an optimal threshold to predict EBV+ tumour status (sensitivity 89.3% and specificity 96.8%). Plasma EBV viral loads were significantly higher in EBV +ve versus EBV -ve HL (p = 0.002). On univariate analysis, age > 45 years, HIV +ve status and EBV plasma viral load > 10 000 IU/ml predicted poorer survival outcomes. On multivariate analysis, EBV tumour +ve status did not significantly predict poorer survival.

Conclusion

In this cohort, one third of newly diagnosed HL patients were HIV +ve, the majority of these EBV tumour +ve. Plasma EBV viral load testing holds promise as a non-invasive marker for EBV+ HL, due to circulating EBV derived from apoptotic HOdgkin tumour cells. Detectable plasma EBV by RT PCR has high sensitivity for predicting EBV +ve tumour status with high plasma EBV levels > 10 000 IU predicting poorer survival outcomes.

EA4HP24-ABS-543

Characterization of lymphoproliferative disorders arising in patients with common variable immunodeficiency (CVID): Potential correlation between aggressive subtypes and clinical parameters

Dr. Genevieve M. Crane, Dr. Claudiu V. Cotta

Cleveland Clinic, Diagnostics Institute, Cleveland Heights, USA

Background

CVID is a heterogeneous disorder affecting ~1/25,000 people, characterized by low levels of serum IgG, IgA and/or IgM which may present with primarily infectious/immunodeficiency vs. inflammatory/autoimmune complications. Underlying genetic causes vary geographically with at least 68 mutations described, but the causative mutation is unidentified in the majority of cases. CVID patients have increased risk of lymphoproliferative disorders (LPD). We further characterize those diagnosed at a large medical center.

Principles/Methodology

Following IRB approval, the pathology archives were searched to identify patients with a history of CVID diagnosed with LPD over a 20-year period (2004-2024). Clinical, laboratory and histopathologic data were collected. LPD were recategorized according to 5th edition WHO and ICC criteria.

Results

14 CVID patients (aged 23 to 71, male 10, female 4)were diagnosed with 16 LPD, including aggressive B-cell(3), plasmablastic lymphoma(1), nodular lymphocyte predominant Hodgkin/B-cell lymphoma(2), low grade B-cell/marginal zone(5), T-cell(2), non-destructive/follicular hyperplasia (FH, 2) and EBV+ polymorphic LPD(2). Three developed status post liver transplant (1 DLBCL and 2 FH). All 4 female patients were diagnosed with low grade LPD (marginal zone or MALT lymphoma). The male patients had aggressive B, T or post-transplant LPD. A male patient with initial diagnosis of low grade LPD had EBV+ transformation. EBV(-) DLBCL were CD10+ and presented in nodal or extranodal sites. Interstitial lung disease, cirrhosis (2 patients status post liver transplant), splenomegaly and pancytopenia were common in patients with LPD.

Two patients presented with syndromic features, one with suspicion of short telomere syndrome (not further characterized) and one with Kabuki syndrome and a *KMTD* (*MLL2)* mutation (c.16294C>T).

Conclusion

Even with a limited number of cases, our findings suggest LPD in the setting of CVID may show distinct features. While most mutations associated with CVID in US patients are autosomal dominant and not X-linked (PMID: 31942606), aggressive LPD in this series strongly associated with male sex. Interrogation of the underlying genetic defects in these cases may be of interest to better understand potential mechanisms predisposing to LPD and inform LPD risk and prognosis in patients with CVID. In addition, identification of hit and run cases suggests EBV may a play a role in tumor initiation in these patients with loss during progression.

Table. Aggressive lymphoproliferative disorders in CVID patients tend to correlate with male sex and are frequently seen in the setting of inflammatory complications including interstitial lung disease (ILD) and cirrhosis.

	# of cases	M:F	Age (mean)	PTLD	EBV+	Other	History of inflammatory/autoimmune complications
DLBCL	3	3:0	45	1	0	All CD10+, germinal center type	ILD (1) Cirrhosis (2)
EBV+ Plasmablastic	1	1:0	61	0	1	Synchronous tumors phenotypic variation	ILD Cirrhosis
EBV+ polymorphic	2	2:0	48	0	2	2/2 with subsequent EBV(-) progression compatible with hit and run	Colitis, vasculitis (1)
NLP Hodgkin/B-cell lymphoma	2	2:0	33	0	0	1 may represent EBV hit and run	Cirrhosis (1)
FH	2	2:0	38	2	1	1 subsequent DLBCL	Cirrhosis and liver transplant (2)
T-cell	2	2:0	42	0	0	Both gamma/delta subtype, aggressive	ILD (1) Granulomatous inflammation (2)
MZL/MALT	5	1:5	58	0	0/2	Sole male patient with transformation to EBV+ LPD	ILD (2) Rheumatoid arthritis (1)

Table1. LPD types arising in patients with CVID

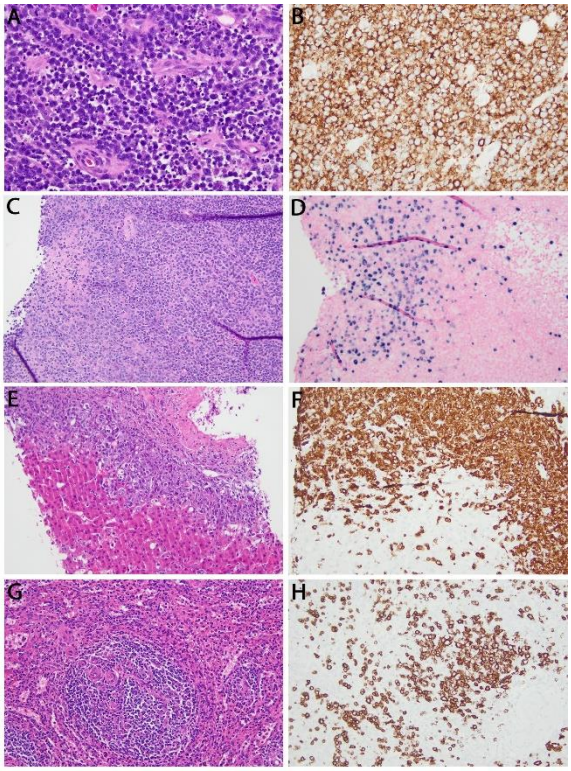

Figure 1. Lymphoproliferative disorders arising in the setting of common variable immunodeficiency
A, B. Diffuse large B-cell lymphoma, germinal center type (Hans criteria) in a male patient with Kabuki syndrome and *KMT2A* mutation (40x, H&E, CD20). C, D. EBV+ follicular hyperplasia in male patient following orthotopic liver transplant (20x, H&E, EBER). E, F. T-cell lymphoma, gamma/delta subtype involving the liver in a 50 year old male (20x, H&E, CD3). G, H. Splenic marginal zone lymphoma in a 71-year-old female (20X, H&E, CD20).

EA4HP24-ABS-551

The Impact of SNP rs2228001 of Xeroderma Pigmentosum Complementation Group C (XPC) on The Risk and Prognosis of Hodgkin's Lymphoma: A case-control study

Dr. Sohaib M. Al-Khatib, Dr. Samir Al-Bashir, Dr. Mohammed Al-Orjani

JORDAN UNIVERSITY OF SCIENCE AND TECHNOLOGY, Pathology and Laboratory Medicine, Irbid, Jordan

Background

Mature B-cell neoplasms are typically divided into Hodgkin and Non-Hodgkin Lymphomas. Many studies link between polymorphism in nucleotide excision repair (NER) pathway and solid organ cancer occurrence. Studies evidently trace the pathogenesis back to the genomic instability from altered DNA repair processes. Additionally, treatment efficacy by chemotherapy drugs and radiation largely depends on induction of DNA damage, polymorphisms in NER pathway would, by default, affect response to treatment. Xeroderma pigmentosum complementation group C (XPC) is a DNA damage recognition protein necessary for launching of global-genomic nucleotide excision repair (GG-NER).

In this study, we analyzed the relationship between a selected SNP in (XPC- G>C/G>T; rs2228001) and the risk and overall survival of HL patients. A total of 374 subjects; 136 cases of Hodgkin lymphoma and 238 matched healthy controls were incorporated in this study. The results show a statistically significant better overall survival in the codominant (p-value = 0.033), overdominant (p-value = 0.016), and recessive (p-value = 0.041) models. None of the models showed any statistically significant difference in risk of cancer development.

Principles/Methodology

DNeasy Blood & Tissue Kit (Qiagen Ltd., West Sussex, UK) was used to DNA extraction for the HL patients from formalin-fixed paraffin-embedded tissue. The SNP was genotyped using the the Sequenom MassARRAY® system (iPLEX GOLD). Genotyping was performed according to the manufacturer's recommendations (Sequenom, San Diego, CA, USA). Genotype distributions were compared between patients and controls. Unconditional logistic regression analysis was used to estimate the association between the genotype frequency and the risk of developing HL.

Results

The results show no statistically significant difference in distribution of the rs2228001 (XPC- G>C/G>T) alleles among the case/control population. These results support an almost two-fold increase in risk of developing HL associated with the rs2228001 (XPC- G>C/G>T) SNP. However; findings show a statistically significant better overall survival in the codominant (p-value = 0.033), overdominant (p-value = 0.016), and recessive (p-value = 0.041) models among the case group (Figure 1).

Conclusion

In this study, we demonstrated and for the first time in our sample a significant association between rs2228001 (XPC- G>C/G>T) SNP and the overall survival of HL patients.

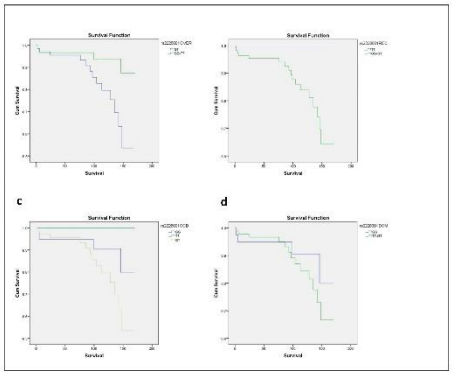

Figure 1: Kaplan Meier plots demonstrating the probability of overall survival

EA4HP24-ABS-555

Overview of CLL patients in Croatian population based on SHM IGHV status and subset identity

Monika Kolundžić[1], Margareta Radić Antolic[1], PhD/MD Ivana Lapić[1,2], Prof. Dunja Rogić[1,2]

[1] University Hospital Centre Zagreb, Department of Laboratory Diagnostics, Zagreb, Croatia; [2] University of Zagreb, Faculty of pharmacy and biochemistry, Zagreb, Croatia

Background

According to the latest recommendations of the European Research Initiative on CLL(ERIC),the somatic hypermutation (SHM) status of the clonotypic immunoglobulin heavy variable (IGHV) gene has definitive predictive value in CLL patients who developed active disease therefore require therapy. Development of bioinformatics revealed stereotyped B cell receptor immunoglobulin gene (BcR Ig) which shares specific IGHV-IGHJ-IGHD gene rearrangement in VH CDR3 region. Patients in certain stereotyped subsets display the same biological characteristics and clinical presentation irrespective of SHM IGHV status and therefore subset defining contributes to more precise risk stratification.

Principles/Methodology

To get an overview of BcR Ig gene mutational status, prevalence of stereotyped cases and their classification into subsets among CLL patients in Croatian population, analysis of data collected from 2020 to 2023 in the Department of Laboratory Diagnostics, University Hospital Centre Zagreb was performed. SHM IgHV gene status in comparison with a germline reference gene panel was

determined using the IMGT/V-QUEST tool. For identification of stereotyped IGHV-IGHJ-IGHD gene rearrangement ARResT/AssignSubsets tool was used.

Results

All patients had a single productive IGHV-IGHD-IGHJ gene rearrangement. The incidence of stereotyped BcR Ig was higher in the group of unmutated CLLs. Among U-CLL 14.9% of patients were assigned to a distinct stereotyped subset, while among M-CLL there were 7.4% stereotyped cases. The most prevalent IGHV-IGHJ-IGHD gene rearrangements among stereotyped cases were IGHV1-69 and IGHV3-21. IGHV4-34 gene was present in 6/11 mutated stereotyped patients. A total of 15 subsets were identified. Subset #2 was the largest (13 cases, 2.9% of U-CLL and 2.0% of M-CLL), followed by subsets #1 (3.2% U-CLL) and #3 (2.0% U-CLL). The most prevalent subset among M-CLL was #4 (3.4%) with no occurrence in U-CLL group. There were 3 cases, all among U-CLL patients, of subset #8 encoded by the IGHV4-39, which is characterized by the highest risk for Richter's transformation.

Conclusion

Although subset identity report is currently recommended only for subsets #2 and #8, as they have the best-established clinical value, growing number of studies and meta-analysis collects evidence for novel candidates. Overall, a low percentage of CLL patients express BcR Ig stereotype, but a membership to a certain subset can change the complete course of patient treatment.

subset	SHM IgHV status (N= 496)	
	unmutated N=347 (70%)	mutated (including borderline cases) N=149 (30%)
#1	11 (3.2%)	0
#2	10 (2.9%)	3 (2.0%)
#3	7 (2.0%)	0
#4	0	5 (3.4%)
#5	4 (1.2%)	0
#6	6 (1.7%)	0
#7H	2 (0.6%)	0
#8	3 (0.9%)	0
#14	0	2 (1.3%)
#16	0	1 (0.7%)
#28A	1 (0.3%)	0
#31	2 (0.6%)	0
#64B	2 (0.6%)	0
#99	2 (0.6%)	0
#202	2 (0.6%)	0
no subset	295	138

Table 1. SHM IgHV status and BcR Ig subset in Croatian CLL patients

EA4HP24-ABS-569

The incidence of Castleman disease in The Netherlands: a retrospective study based on Dutch pathology reports.

Kim Landsbergen, Dr. Arjan Diepstra, On behalf of Recordati-Collaboration

University Medical Centre Groningen, Pathology, Groningen, Netherlands

Background

Castleman disease (CD) constitutes a group of lymphoproliferative disorders involving one lymph node (unicentric) or multiple lymph nodes (multicentric). Diagnosis is challenging due to its rarity and nonspecific clinical and histologic characteristics. It is especially important to recognize idiopathic multicentric CD (iMCD) because patients often develop life-threatening multi-organ failure. Limited

data about the incidence of CD exist: in the US it's estimated at 16 per million person-years (PYs) for unicentric CD and 5 per million PYs for multicentric CD [1]. The incidence of CD and iMCD in the Netherlands is currently unknown.

Principles/Methodology

We took advantage of the pathology database PALGA, a unique nationwide registry that encompasses every pathology report generated in The Netherlands since 1971. We requested all reports mentioning CD or related terms from 2000 to 2022 and included reports on additional lymph node biopsies for each index case. Based on text in the fields "microscopy" and "conclusion", reports were categorized into definitive or highly probable CD, and unlikely or definitely not CD.

Results

Our search identified 810 patients (1318 reports in total) with mentions of CD or related terms. This included cases where the disorder was either excluded or considered unlikely to be present. We concluded that 445 patients had definitive or highly probable CD, comprising 52% males and 48% females, with a mean age of 44.8 years (SD 18.4 years). 43% of the reports mentioned hyaline vascular subtype, 33% plasmacytic, 4% mixed type, and 20% unspecified. Although a diagnosis of iMCD cannot be based on histology alone, we tried to estimate how many cases could potentially fit. From the 445 patients we excluded cases with HIV, a concurrent lymphoma, positive HHV8 or a clear designation as being unicentric. This resulted in a maximum of 203 patients potentially having iMCD. We are currently pruning these numbers by adding information from the report field "clinical data".

Conclusion

Our results indicate that the incidence of CD in the Netherlands is 1 per million PYs, which is approximately 20 times lower than the incidence rates reported in the US. Variances in study methodologies (pathology vs. ICD-coding), surgical approaches (needle biopsy vs. excision), clinical and diagnostic practice may contribute to some extent, but we consider it likely that a true difference in CD incidence exists.

1. Simpson, D. *Epidemiology of Castleman Disease*. Hematol Oncol Clin North Am. 32, 1-10 (2018)

EA4HP24-ABS-571

Extramedullary plasmacytoma in children

Ilske Oschlies[1], Julia Richter[1], Amelie Alfert[2], Stephanie Mueller[2], Fernando Chahud[3], Willhelm Woessmann[4], Birgit Burkhardt[2], Wolfram Klapper[1]

[1] Christian Albrecht University, University-Hospitals Schleswig Holstein, Kiel, Department of Pathology, Hematopathology Section, Kiel, Germany; [2] NHL-BFM study center, University Hospital Muenster, Department of Paediatric Hematology and Oncology, Muenster, Germany; [3] Ribeirão Preto Medical School, University of São Paulo, Department of Pathology, São Paulo, Brazil; [4] NHL-BFM study center, University Medical Center Hamburg-Eppendorf, Department of Paediatric Hematology and Oncology, Hamburg, Germany

Background

Extramedullary plasmacytomas (EMP) are extremely rare in children with < 10 published cases. The clinical behaviour, treatment options and molecular features of this disease are unknown.

Principles/Methodology

Ten cases of EMP in patients (≤ 18 years) were identified. Clinical and histopathological features were reviewed. Molecular features were investigated by Next generation sequencing (NGS) and Fluorescence in situ hybridization (FISH).

Results

The series included 4 females and 6 males with a mean age of 6.6 years (range 3-18). EMP presented at localized stage (IAE,10/10) without evidence of systemic disease including investigation of the bone marrow. Involved sites were the Waldeyer´s ring (n=7), the larynx/vocal cord (n=2) and the eye lid/conjunctiva (n=1). In two patients with EMP in the tonsils an IgM titre for Epstein-Barr virus (EBV) was positive. Lesions were treated by resection only (n=9), combined with local irradiation in one case. Two patients experienced a local relapse and were excised again. All 10 patients are currently in complete remission (mean follow-up of 37 months, range 8-102m).

Histologically, lesions consisted of interfollicular or diffuse sheets of mature to slightly pleomorphic CD20-negative plasma cells with light chain restriction kappa (n=5) or lambda (n=5) and heavy chain IgA (n=8), IgG (n=1) and IgG- and IGA-positive areas in one case. EBV/EBER was negative in all cases tested (8/8). One of two EMP with positive EBV-IgM displayed peritumoral EBV-positive cells. EMP were negative for CD56 (6/6) and Cyclin D1 (7/7). Ki67 was low. Amyloidosis was seen in 1 case (vocal cord). A clonal B-cell receptor-generearrangement was confirmed in all cases (10/10). FISH (n=7) revealed absence of abnormalities associated with plasma cell neoplasia (e.g. *MAF, FGFR3, IGH, RB1, TP53*). NGS with a panel covering 83 genes or mutation hot-spots commonly involved in lymphomas (including *MAP2K*1, *TNFRSF14*, *IRF8, TP53)* was performed in 7 samples. In total, only 4 potential protein changing variants were identified (*ATM, CDNK2A, CDNK2B, TENT5C* in 3/7 patients). A productive rearrangement of the *IGH/IGL* was detected in 7/7 specimen without biased *IGH*-gene usage.

Conclusion

EMP in paediatric and adolescent patients is a localized clonal, light-chain restricted B-cell neoplasia of the head/neck lacking molecular alterations known from plasma cell neoplasia of adult patients. An infectious trigger might be envisioned. This rare disorder may be sufficiently managed by resection only.

EA4HP24-ABS-575

Aberrant CD45 expression on metastatic renal cell carcinoma: a potential diagnostic pitfall in daily practice.

Prof. Howayda S. ABD EL All[1,2]

[1] *Suez Canal University, Pathology, Ismailia, Egypt;* [2] *Nasser Institute, IHC Lab, Oncolog Center, Cairo, Egypt*

Background

CD45 and cytokeratins (CK) expression are almost mutually exclusive in diagnosis. CD45 is present on all white blood cells except erythrocytes and their preccursors, megakaryocytes and platelets (1) while epithelial markers may be expressed on hematologic malignanies (2, 3).

Principles/Methodology

We report a case of metastatic renal cell carcinoma (mRCC) positive for both CK clone AE1/AE3 and CD45 clone 2B11 PD7/26. A male patient 57 years old presented with metabolically active FDG avid supra and infra diaphragmatic lymphadenopathy on PET/CT. Cervical lymph node excision revealed diffuse infiltration by sheets of large neoplastic cells, histiocyte like and clear cells having eosinophilic cytoplasm and nucleolated nuclei. Based on radiologic and histologic data, the differential diagnosis was between anaplastic large cell lymphoma and to a lesser extent metastatic carcinoma.

Results

The initial panel showed positivity of 10% of neoplastic cells for CD45 (fig 1) while CK is expressed on all (fig 2). The second panel including hematopoeitic markers CD79a, CD20, PAX5, CD3, CD68 and CD30 and epithelial markers CKs 7 and 20, revealed negativity for all. A third panel included, hepatocyte marker hepar-1, CA19.9, prostein, alfa inhibin, p63 and PAX8. Of these markers only PAX8 was positive (fig 2), making the diagnosis of metastatic renal cell carcinoma, clear cell variant.

Conclusion

CD45 expression in RCC, not previously reported, is a surprising finding and could be attribuated to adhesion between CD45, a protein tyrosine phostatase receptor type C (1), to it's ligand SKPA1 present on normal renal distal tubules (4) and still expressed on malignant tubules. This case, if diagnosed on small core biopsy using a limited panel of markers, could be misinterpreted as lymphoma, pointing out to crucial role of whole node excision.

References

1. Kaplan et al 1990
2. Adams et al 2008
3. Dadfarnia Ameri et al 2015
4. The human Protein Atlas

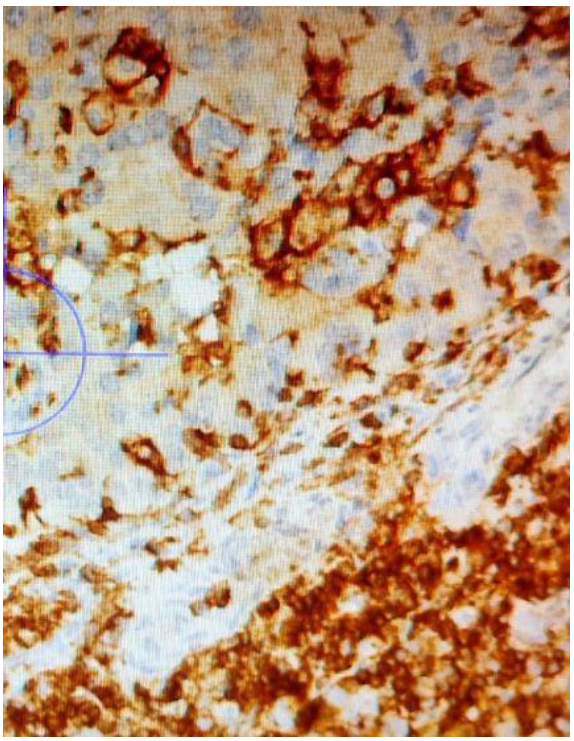

Fig 1
CD45 clone 2B11 PD7/26 expression on malignant epithelial cells (upper and middle) and reactive lymphocytes (lower right); DAB X 20

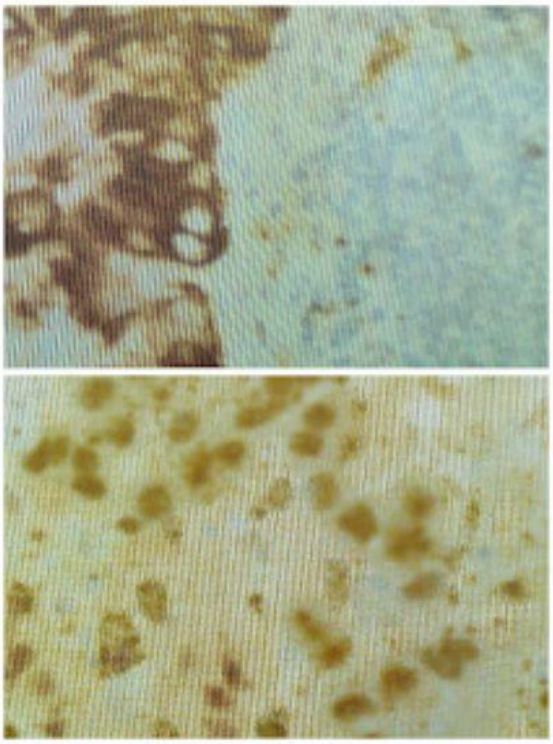

Fig 2
Upper: CK clone AE1/AE3 expression on malignant epithelial cells, DAB x 20; lower: PAX8 clone MRQ-50 expression on RCC; DAB X 40

EA4HP24-ABS-579

Celiac-like/CVID-like pattern in duodenal biopsy in a patient treated with CAR-T cell

Dr. Jackson A. Barbosa, Dr. Denise D.C. Pasqualin, Dr. Aline Ueda, Dr. Ana Carolina D.B. Lyra

Hospital Israelita Albert Einstein, Anatomia Patológica, São Paulo, Brazil

Background
Intraepithelial lymphocytosis with villous atrophy in the duodenum is the hallmark of celiac disease. This pattern, however, is not totally specific for this entity, as it can also have different etiologies such as *H. pylori* gastritis, viral infection, medications, inflammatory bowel disease and common variable immunodeficiency. In the latter, a consistent additional feature is the scarcity or absence of plasma cells in the lamina propria which is thought to represent the key event in the pathogenesis, leading to inadequate immune response followed by intraepithelial lymphocytosis and villous atrophy. Here, we report a case with such findings in a post CAR-T cell therapy setting.
Principles/Methodology
CAR-T therapy targeting CD19 results in the depletion of normal B cells, leading to hypogammaglobulinemia, which is associated with an increased risk of infections. There is a significant lack of evidence-based guidelines for the use of immunoglobulin replacement therapy in CAR-T cell therapy recipients. Current recommendations are often extrapolated from data on primary immune deficiencies.

Results

We present a case of a 58-year-old female patient that underwent CD19-directed CAR-T cell to treat relapsed diffuse large B-cell lymphoma. Two months post-therapy, the patient complained of abdominal discomfort, bloating and nausea. Upper endoscopy found no changes in duodenal mucosa. On histology, the duodenum had marked villous blunting with intraepithelial lymphocytosis. The diagnosis of celiac disease was suggested. After additional work-up, Anti-Endomysium, Anti-Gliadin and Anti-Transglutaminase were negative as was genotyping for HLA DQ2/DQ8, which argued against celiac disease. Norovirus infection was detected by fecal PCR test. The patient received intravenous immunoglobulin and Nitazoxanide.

Conclusion

To the best of our knowledge, this is the first case report of such histopathologic finding in an intestinal biopsy of a patient undergoing CAR-T cell. We cannot attribute it entirely to this immunotherapy, as prior chemotherapy must have also played an important role in the depletion of plasma cells. However, it is plausible that targeting CD19 would have such repercussion. We believe this case introduces an important new differential diagnosis to this histopathologic pattern and underscores the interplay of different components in orchestrating the immune environment of the gastrointestinal tract.

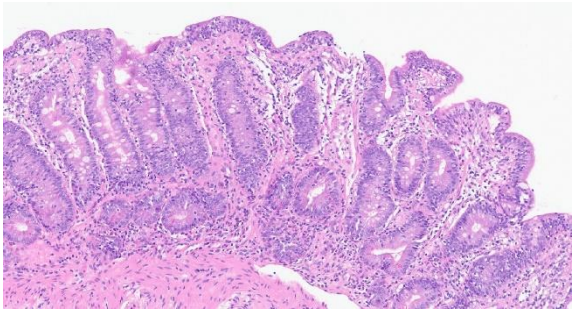

Villous atrophy and intraepithelial lymphocytosis
This duodenal biopsy shows marked villous atrophy with intraepithelial lymphocytosis. Upon further inspection, lack of plasma cells is also noticeable.

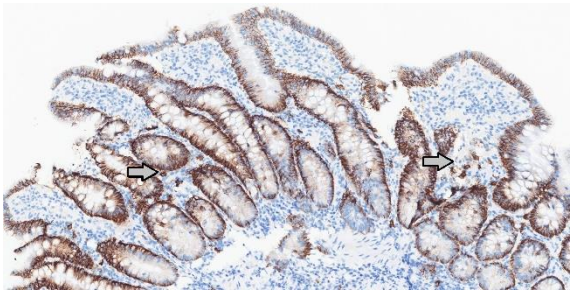

CD138 shows only few plasma cells in the lamina propria
On higher magnification, only scarce plasma cells (arrows) are found in the lamina propria. In a patient without history of CAR-T cell therapy, this finding would be highly suggestive of Common Variable Immunodeficiency and prompt additional work-up.

EA4HP24-ABS-580

The Expression of Targeted Therapy-Associated Receptors in Patients with Aggressive Post-Transplant Lymphoproliferative Disorders

Chandler Sy, Ivo Sahbandar, Nadine Demko, Maneeza Bilal, Ethel Cesarman, Amy Chadburn

Weill Cornell Medicine / NewYork Presbyterian Hospital, Pathology and Laboratory Medicine, New York, USA

Background

Post-transplant patients are at increased risk of developing post-transplant lymphoproliferative disorders (PTLD). Post-transplant lymphomas (NHL-PT) and some polymorphic (poly-PT) cases require more therapy than a reduction in immunosuppression for disease resolution. However, reduction in immunosuppression and treatment with chemotherapy can result in an increased risk of infection and organ loss. A variety of novel targeted agents, which may be less toxic for these patients, are now available. These agents target proteins or pathways containing proteins that can be identified with commercially available antibodies. Here, we evaluated 58 cases of PTLDs for expression of 6 of these potential targets.

Principles/Methodology

TMAs of FFPE/B5 fixed PTLDs were evaluated by immunohistochemistry (IHC) for CD79b, PD-L1, CD30, CD38, phospho-S6 ribosomal protein (p-S6), and B-cell maturation antigen (BCMA; CD269), which are targeted by polatuzumab vedotin, check point inhibitors (i.e., avelumab), brentuximab vedotin, daratumumab, MTOR pathway inhibitors (i.e., sirolimus), and CAR-T (i.e., idecabtagene vicleucel), respectively. Cases were sorted based on the percentage of tumor cells positive for a “target protein”. The NHL-PTs were further classified as germinal center (GCB) or non-GCB based on CD10, BCL6, and MUM1 IHC (Hans algorithm).

Results

The 58 PTLDs were classified as NHL-PT GCB (13), NHL-PT non-GCB (6), or poly-PT (39).

Conclusion

This study suggests that patients with the more aggressive PTLDs may benefit from newer targeted agents as an alternative to immunosuppression reduction and chemotherapy. However, the expression level of the “target proteins” is variable based on lesion type, indicating that the different PTLD subtypes may need to be differentially targeted. Specifically, the NHL-PT GCB lesions show relatively high expression (at least 50%) of CD38 and CD79b, suggesting that daratumumab and polatuzumab vedotin, respectively, may be effective, while at least half of the poly-PTs show relatively increased expression (at least 20%) of CD30 and CD38, targets of brentuximab vedotin and daratumumab, implying these agents may be helpful in poly-PT disease resolution. Thus, this study supplies rationale for the potential development of clinical trials to evaluate these agents in the post-transplant setting for efficacy and to determine if they are associated with less complications such as infection and graft loss.

	CD79b n (%)	CD30 n (%)	PD-L1 n (%)	CD38 n (%)	p-S6 n (%)	BCMA n (%)
NHL-PT GCB						
<5%	2 (17%)	12 (92%)	13 (100%)	3 (23%)	6 (46%)	7 (54%)
5-19%	1 (8%)	0 (0%)	0 (0%)	1 (8%)	4 (31%)	0 (0%)
20-49%	2 (17%)	1 (8%)	0 (0%)	1 (8%)	3 (23%)	1 (8%)
50-100%	7 (58%)	0 (0%)	0 (0%)	8 (62%)	0 (0%)	5 (38%)
NHL-PT non-GCB						
<5%	4 (67%)	5 (83%)	5 (83%)	3 (50%)	3 (50%)	5 (83%)
5-19%	1 (17%)	0 (0%)	0 (0%)	0 (0%)	2 (33%)	1 (17%)
20-49%	0 (0%)	0 (0%)	0 (0%)	0 (0%)	1 (17%)	0 (0%)
50-100%	1 (17%)	1 (17%)	1 (17%)	3 (50%)	0 (0%)	0 (0%)
Poly-PT						
<5%	25 (64%)	7 (18%)	36 (92%)	10 (26%)	23 (61%)	19 (49%)
5-19%	9 (23%)	12 (32%)	0 (0%)	7 (18%)	6 (16%)	11 (28%)
20-49%	2 (5%)	15 (39%)	2 (5%)	11 (28%)	8 (21%)	7 (18%)
50-100%	3 (8%)	4 (11%)	1 (3%)	11 (28%)	1 (3%)	2 (5%)

Target Protein Expression in NHL and Polymorphic PTLDs

EA4HP24-ABS-588

Clinical and molecular features of primary spinal epidural lymphomas

Prof. Martina Rudelius[1], Dr. Louisa Adolph[2], Dr. Veit Bücklein[2], Dr. Sophia Stöcklein[4], Prof. Oliver Weigert[2]

[1] Ludwig Maximilians University, Pathology, Munich, Germany; [2] Ludwig Maximilians University, III. Medical Clinic, Munich, Germany; [3] Ludwig Maximilians University, III. Medical Clinic, Munich, Germany; [4] Ludwig Maximilians University, Radiology, Munich, Germany; [5] Ludwig Maximilians University, III. Medical Clinic, Munich, Germany

Background

Lymphomas which are confined to the spinal epidural space at initial diagnosis are rare and referred to as primary spinal epidural lymphoma (PSEL). Thourough analysis of PSEL is limited, therefore we analysed 13 PSEL cases including molecular and transcriptome analysis.

Principles/Methodology

13 PSEL cases were classified according to the WHO HAEM-5 and ICC 2022 and consisted of follicular lymphoma (PSEL-FL, N=4), marginal zone lymphoma (PSEL-MZL, N=3), diffuse large B-cell lymphoma (PSEL-DLBCL, N=5), and Burkitt lymphoma (PSEL-BL, N=1). Clinical data and MRI imaging were available for all patients. For diagnosis standard immunohistochemistry and FISH analysis were performed. In addition, targeted molecular subtyping and gene expression analysis (770 genes related to immune-oncology pathways) with nCounter IO360 panel was completed.

Results

Lymphoma manifestations were most often located in the thoracic spine. All patients exhibited an epidural mass with homogenous contrast enhancement on T1-weighted images. Despite localized initial presentation, PSEL with aggressive histologies demonstrated unfavorable outcomes, contrasting with the highly indolent clinical course observed in indolent PSEL. In contrast to published results, indolent NHL were as prevalent as aggressive NHL in our series (7/13, 53%), including 4 cases of follicular lymphoma. The targeted mutational profiles of all evaluable PSEL largely reflected the mutational landscape of their nodal counterparts.

Recognizing that cFL relies heavily on the interactions with the TME of lymphoid tissues, we sought to identify distinct TME-related gene expression patterns that allow PSEL-FL to thrive in the epidural space. Differential gene expression analysis of PSEL-FL and its nodal counterpart cFL-LS identified significantly up-regulated (N=20) and down-regulated (N=32) genes; including lower expression of the

T cell chemotactic cytokine CCL21, and higher expression of genes involved in the organization of extracellular matrix and angiogenesis, including SFRP4, COMP, MMP7, and VCAN.

Conclusion

Molecular analysis showed similarities of PSELs to nodal counterparts and a clear separation by entity. Comparison of PSEL-FL and classical FL revealed activated tumor microenvironment-associated pathways, potentially supporting lymphoma growth in this rare extranodal site.

EA4HP24-ABS-590

Role of microsatellite instability in the oncogenesis of primary intestinal T-cell lymphomas

PhD/MD Luis Veloza[1], PhD/MD student Anja Fischer[2], PhD/MD David Vallois[1], M.Sc./M.A. Vimel Rattina[1], M.Sc./M.A. Karine Lefort[1], PhD/MD Bettina Bisig[1], Dr. Doriane Cavalieri[3], Prof. Olivier Tournilhac[4], Prof. Philippe Gaulard[5], Prof. Reiner Siebert[2], Prof. Laurence de Leval[1], **PhD/MD Edoardo Missiaglia**[1]

[1] Institute of Pathology, Lausanne University Hospital and Lausanne University, Lausanne, Switzerland; [2] Institute of Human Genetics, Ulm University and Ulm University Medical Center, Ulm, Germany; [3] Department of Hematology, Lille University Hospital, Lille, France; [4] Adult Clinical Hematology, CHU Clermont-Ferrand, INSERM CIC501, EA 7453, Clermont Auvergne University, Clermont-Ferrand, France; [5] Paris-Est Créteil University, Faculty of Medicine and Health, Campus Henri Mondor; Department of Pathology, Henri Mondor University Hospital, Créteil, France

Background

Primary intestinal T-cell lymphomas (ITCLs) are a group of rare and aggressive T-cell lymphomas with poor outcome. Microsatellite instability (MSI) status has not been thoughtfully explored in these lymphomas. Our aim was to assess the prevalence of MSI in ITCLs and to identify its underlying molecular mechanisms and possible clinical implications.

Principles/Methodology

Whole Exome Sequencing (WES) was performed on 63 ITCL samples (37 Monomorphic epitheliotropic intestinal T-cell lymphomas (MEITLs) and 26 Enteropathy-associated T-cell lymphomas (EATLs). MSI/Mismatch repair deficiency (MMRd) status was assessed by PCR and fragment analysis using 5 well-established mononucleotide repeat markers in 46 cases (31 MEITLs, 15 EATLs), and by MLH1, MSH2, MSH6 and PMS2 immunohistochemistry (IHC) in 79 cases (57 MEITLs, 22 EATLs).

Results

Based on mutational profile, 3/37 MEITLs (8%) and 0/26 EATLs (0%) showed MSI-associated signatures and higher tumor mutational burden (TMB) (8-14 mutations/Mb) compared to a median TMB of 1.6 and 2.1, in all MEITLs and EATLs, respectively. No germline or somatic mutations of *MLH1, PMS2, MSH2* or *MSH6* were found in any of the 63 patients with WES data. The MSI status of the 3 cases was confirmed by PCR, while the other MEITLs and all EATLs tested (43/46) were microsatellite stable. Besides, MSI cases showed complete loss of PMS2 (1/3) or MLH1&PMS2 (2/3) expression, in association with a biallelic deletion of the *PMS2* or *MLH1* locus, respectively. Further 2 MEITLs showed heterogeneous (partially lost or weak) expression of MLH1 or MLH1&PMS2, associated with the loss of one copy of the *MLH1* locus, in the absence of MSI phenotype. Of note, *MLH1* locus is relatively close to *SETD2* (~10Mb), a tumor suppressor gene and well-known driver in MEITL tumorigenesis. The presence of frequent codeletionsof *MLH1* and *SETD2* genes may suggest that MSI occurs as a secondary genetic event in

MEITLs. The three MEITL patients with MSI had an overall survival (OS) of 5, 17 and 71 months, while the median OS of 29 MEITL patients was 8 months.

Conclusion

We identified MSI/MMRd in a small subset of MEITLs (8%), due to biallelic deletions of the *MLH1* or *PMS2* locus. This may have prognostic and therapeutic implications in ITCL patients.

EA4HP24-ABS-592

CD200 is a useful marker to distinguish Nodular Lymphocytic Predominant B-cell lymphoma from TFH lymphoma and classical Hodgkin lymphoma

Carmen Lome-Maldonado[1], Andrea Molina-Alvarez[1], Natalia Papaleo[2], Hristo Iliev Iliev[3], Begoña Fuertes[3], David Lopez[1], Ivonne Vazquez[1], Luis Colomo[1]

[1] Hospital del Mar, Department of Pathology, Barcelona, Spain; [2] Hospital Parc Tauli, Department of Pathology, Barcelona, Spain; [3] Hospital Universitario Doctor Josep Trueta, Department of Pathology, Barcelona, Spain

Background

CD200 is a membrane glycoprotein that is expressed in B-cells, some T-cells, dendritic follicular cells (FDC) and endothelial cells. Few studies have been published regarding CD200 expression in T-cell neoplasms, with controversial results.

Nodal T Follicular helper cell lymphoma (TFH-L) is now classified as TFH-L angioimmunoblastic type (AITL), TFH-L follicular type and TFH-L NOS type. It's characterized by an array of morphological patterns, a TFH cell phenotype, and mutations including TET2, DNMT3A, IDH2 and RHOA.

Differential diagnoses include reactive lymphoid hyperplasia, other PTCL subtypes, Classic Hodgkin Lymphoma (CHL) and B-cell lymphomas such as nodular lymphocyte-predominant B-cell lymphoma (NLPBL) or T-cell/histiocyte-rich large B-cell lymphoma (TCHRBCL). Our objective is to assess the diagnostic utility of CD200 in distinguishing TFH-L from other lymphoma subtypes.

Principles/Methodology

A total of 96 lymphoid neoplasms were studied: 46 cases of TFH-L (41 AITL type, 3 Follicular type and 2 TFH-L NOS type), 20 cases of NLPBL, 20 cases of CHL and 10 cases of diffuse large B-cell lymphoma (DLBCL).

All cases were studied with a common panel of B and T-cell markers. Formalin-fixed, paraffin-embedded tissue sections were stained for CD200 employing a monoclonal antibody (clone E5I9V, dilution 1:100, Cell Signalling).

Stained tissue sections were evaluated by two pathologists. Discordant cases were resolved through consensus review. CD200 expression was semi-quantitatively assessed based on staining intensity and distribution within the tumor microenvironment.

Results

We observed variability in CD200 expression among different subtypes of lymphoid neoplasms. Most cases of TFH-L displayed a complete absence of CD200 staining in atypical lymphoid cells (35/46 cases) with focal CD200 expression in FDC, and some scattered lymphoid neoplastic cells (≤5%) in 12/46 TFH-L cases. Notably, in all 20 NLPBL cases positive staining was observed in accompanying T reactive-cells (CD3+, CD4+, PD1+), forming a distinct rosette-like pattern around the negative tumor B cells. In CHL-

EBV+, CD200 positive staining was mainly localized in Reed-Sternberg cells (RSC). DLBCL cases were mostly negative for CD200.

Conclusion

Our findings reveal a persistent rosetoid-like CD200 expression pattern in T-cell helper cells surrounding neoplastic B cells in all NLPBL cases. This unique staining pattern represents a distinctive feature that could facilitate the differential diagnosis between NLPBL, AITL, TCRBCL and CHL.

EA4HP24-ABS-598

Prognostic significance of LEF1 expression in Angioimmunoblastic T-cell Lymphoma and Peripheral T-cell lymphoma with TFH-phenotype in the Spanish Population

Dr. Socorro Maria Rodriguez-Pinilla[1], Dr. Raul Cordoba[2], Dr. Alejandro Martin Garcia-Sancho[4], Marta Grande[3], Lourdes Baeza Montañez[3]

[1] FJD, Pathology, Madrid, Spain; [2] FJD, Haematology, Madrid, Spain; [3] Takeda Company, Haematology, Madrid, Spain; [4] Hospital Universitario, Haematology, Salamanca, Spain

Background

Complete-response to coventional treatment implies prognosis in AITL patients. Nevertheless, there are no biomarkers who identify these patients.

Principles/Methodology

Patients diagnosed with AITL and TFH for which biopsies were available were identified from the clinical records of 13 Spanish centers. In addition to demographic data, we recorded the treatment administered, response rate, progression-free survival (PFS) and overall survival (OS), the international prognostic index (IPI), and the prognostic index for PTCL (PIT). From the biopsies, among other markers, we assessed the expression of LEF1, Ki67, and CD30 as well as the percentage of Epstein-Barr virus-encoded RNA/EBER cells.

Results

A total of 78 patients with AITL and TFH were identified. Median age was 71.7 years, 61.5% were male, 15.4% had Ann Arbor stage I-II, and 80.8% had stage III-IV. In the first-line, 75.6% received CHOP (or CHOP-like) treatment and 19.2% non-CHOP treatment, and in the second-line 23.1% received ESHAP-DHAP, 33.3% received other schemes, and 33.3 received no treatment. The median expression for each of the biomarkers was: LEF1 70%, Ki67 30%, CD30 10%, and EBER 1%. Categorizing the patients according to the median expression of LEF1 (<70%, ≥70%), it was observed that the higher the expression of LEF1 (≥70%), the lower the percentage of positive EBER cells (p=0.048). In addition, in both first- and second-line treatment, the higher the expression of LEF1(≥70%), the higher the rate of relapse or progression to treatment (Table 1). On the other hand, the higher the percentage of positive EBER cells (≥1%), the higher the expression of CD30 (p=0.003). After a univariate analysis, of all the biomarkers evaluated, a low expression of CD30 was associated with a better response to the first-line treatment, with a complete response rate of 56.4% for patients expressing less than 15% compared to 31.0% for those expressing more than 15% (p=0.040). On the other hand, a cut-off point greater than 5% CD30 was predictive of better PFS (p=0.036).

Conclusion

An expression of LEF1 above 70% seems to correlate with a higher rate of relapse or progression to treatment, both in first- and second-line. In addition, a CD30 expression below 15% is associated with a higher rate of complete responses, and an expression below 5%, with better PFS.

EA4HP24-ABS-603

Small B-cell lymphomas with unclear morpho-phenotypic features: What adds the mutational landscape to further classification?

Gioia Di Stefano[1,2], Margherita Vannucchi[2], Maria Chiara Siciliano[2], Cosima Drewes[3], Raffaella Santi[4], Arianna Di Napoli[5], Stefano Lazzi[2], Reiner Siebert[3], Cristiana Bellan[2], Lorenzo Leoncini[2]

[1] Careggi Teaching Hospital, Section of Pathology, Florence, Italy; [2] University of Siena, Section of Pathology, Department of Medical Biotechnologies, Siena, Italy; [3] Ulm University and Ulm University Medical Center, Institute of Human Genetics, Ulm, Germany; [4] University of Florence, Pathology Section, Department of Health Sciences, Florence, Italy; [5] Sapienza University, School of Medicine and Psychology, Sant' Andrea Hospital, Department of Clinical and Molecular Medicine, Rome, Italy

Background

Small B-cell lymphomas (SBCL) comprehend a heterogeneous group of B-cell malignancies that in some instances can be difficult to diagnose due to their unclear morpho-phenotypic features. Previous studies using Next-Generation Sequencing (NGS) have identified genes recurrently affected by mutations in SBCL, leading to the development of mutational spectra for each subtype. A few research groups have also proposed that the assessment of genomic alterations in challenging cases could help the diagnostic process. Therefore, in the present study, we investigated the added value of genomic studies to SBCL, NOS diagnosis.

Principles/Methodology

We gathered 21 cases with unusual morpho-phenotypic characteristics including chronic lymphocytic leukemia (CLL), mantle cell lymphoma (MCL), marginal zone lymphoma (MZL), and follicular lymphoma (FL). A broad immunohistochemical panel was applied on all samples followed by NGS analyzing 54 genes that are commonly mutated in B-cell lymphomas as well as, in selected cases, FISH and copy number variant (CNV) analysis using the Onco Scan CNV Assay.

Results

A preliminary histopathological reassessment enabled a differential diagnosis between two entities, dividing the study cohort into three groups. There were 15 cases classified as borderline between CLL/MZL, 4 as CLL/MCL, and 2 cases that did not have a clear diagnosis between MZL and FL. Based on the genomic landscape, a diagnosis supported by genomic aberrations was reached in over half of the cases (76%), mainly within the MZL/FL and CLL/MCL groups. In contrast, despite molecular data integration, it was not possible to label quite a few CLL/MZL cases.

Conclusion

Molecular analysis by NGS, FISH and CNV determination successfully differentiated FL from MZL and CLL from MCL. However, genomic studies hardly discriminated against CLL and MZL due not only to their morphological, immunophenotypic and cell origin overlap but also to their similar molecular profiles. More studies are needed to confirm the benefit of NGS studies in SBCL diagnosis and aid the molecular distinction between CLL and MZL.

EA4HP24-ABS-606

Mediastinal grey zone lymphoma, challenging diagnosis

Dr. Khalida M. Itatahine, Dr. Thourya Bendimerad, Dr. Farida Acherar, Prof. Assia Slimani

Ben Youcef Ben Khedda university, Pathology, Algiers, Algeria

Background

Mediastinal grey zone lymphoma (MGZL) is a B-cell lymphoma with overlapping features between primary mediastinal B-cell lymphoma (PMBL) and nodular sclerosis classic Hodgkin lymphoma (NSCHL). It is a rare lymphoma that generally involves the mediastinum of young, male subjects and is associated with a more aggressive clinical course than CHL or PMLB.

Principles/Methodology

We report two cases.

- A 16-year-old adolescent presented with cervical lymph node, a cough, dyspnoea and mediastinal mass.
- A 25-year-old woman presented with left cervical lymphadenopathies, B symptoms and mediastinal mass.

Based on PET scanning, the two cases were classified as stage II bulky.

Formalin-fixed paraffin embedded tissues obtained from cervical nodal biopsy of these cases were examined with histology and immunohistochemistry (IHC)

Results

Microscopically, the two biopsies revealed the same aspect represented by an obliterated architecture by a sheet-like growth pleomorphic lymphoid cells.

Some cells are binucleated with prominent nucleoli and abundant pale cytoplasm in a background containing a paucity of inflammatory cells with seldom eosinophils and foci of necrosis.

IHC stains show that the neoplastic cells are positive for CD20 and PAX5. Numerous cells are CD15 positive and also CD30 positive. ALK and LMP1 are negative. The diagnosis of mediastinal grey-zone lymphoma was retained.

The cases were treated with six cycles of R-CHOP ((rituximab, cyclophosphamide, doxorubicin, vincristine and prednisone) chemotherapy and radiotherapy and achieved complete response (CR) both clinically and radiographically with a follow-up of 36 months, for first case and 18 months for the second.

According to some authors, MGZL are subdivided into three groups based on morphology and phenotype, with CHL like morphology (group 0), cases with PMBL-like morphology (group 2) and cases with truly intermediate features (group 1). Our two cases would belong to this last group since tumoral cells maintained B cell program (CD20+, PAX5+) with expression of CD30 and CD15 in numerous cells showing true morphological and phenotypical hybrid features.

The CR with a follow-up of 36 and 18 months of our two cases, strongly suggests that DLBCL-based regimens are effective in the treatment of MGZL.

Conclusion

Given the rarity of MGZL, these cases illustrate the immense challenges in making the diagnosis and discuss the current treatment options.

EA4HP24-ABS-607

An ultrasensitive dual in situ hybridization (ISH) mRNA assay in determination of kappa/lambda (K/L) restriction status shows strong concordance with historical light chain restriction in B cell lymphomas and plasma cell malignancies

Bowdoin Su[1], Mohammad Vasef[2], Jordan Redemann[2], Rebecca Kunak[3], Sarah Gladden[4], Brian Mosteller[4], Jing Su[4], Ivonne Vazquez[5], Luis Colomo[5]

[1] Roche Diagnostics Solutions, Santa Clara, USA; [2] TriCore Reference Laboratories, Albuquerque, USA; [3] Michigan Pathology Specialists, Grand Rapids, USA; [4] Roche Tissue Diagnostics, Tucson, USA; [5] Hospital Del Mar, Barcelona, Spain

Background

Determination of immunoglobulin light chain restriction status is crucial in determining clonality in suspected B cell malignancies. Conventional immunohistochemistry and ISH assays are useful for determining clonality in plasma cell tumors but fail to detect surface immunoglobulins expression status in most B cell neoplasms. Ultrasensitive dual ISH mRNA is an emerging technology that detects a broader spectrum of B cell non-Hodgkin lymphomas including cases without plasmacytic differentiation. In this study, we determined the clinical utility of an ultrasensitive dual ISH assay in the qualitative detection of light chain mRNA status in FFPE tissues from a spectrum of B cell lymphomas and plasma cell neoplasms.

Principles/Methodology

100 bone marrow and lymphoid tissue specimens with known historical light chain restriction results that met inclusion and exclusion criteria were identified at a study site. 80 cases were either B cell lymphomas or plasma cell malignancies, while 20 cases were reactive mimics. Evaluable cases stained with the VENTANA K/L Dual ISH assay were independently interpreted for restriction status by four study pathologists across two study sites using glass slides or digital images and the pathologists' assessments for each case were compared to the available historical flow derived K/L restriction status and final pathology diagnosis associated with the same patient to assess the assay performance.

Results

First pass rate was 97% [Figure 1]. Background staining and morphology was deemed acceptable in 100% and 100% of cases evaluated, respectively. The overall percent agreement (OPA) was 92.4% [Figure 2]. Kappa restricted percent agreement (KRPA) was 91.3%, lambda restricted percent agreement (LRPA) was 88.0%, and non-restricted percent agreement (NRPA) was 100%.

Conclusion

In this study, we assessed the clinical utility of an ultrasensitive dual ISH mRNA light chain restriction assay for clonality in bone marrow and lymphoid tissue with a variety of B cell malignancies and reactive mimics. A high first pass rate and excellent overall staining performance was noted by the readers. Strong concordance between the VENTANA K/L Dual ISH assay and flow cytometry suggest that this ultrasensitive assay is a viable alternative to flow cytometry for determining light chain restriction status in the evaluation of the full range of suspected B cell lymphoma and plasma cell neoplasms.

Slide Type	Site	Reader	First Pass Rate	Background Acceptability Rate	Morphology Acceptability Rate
Glass	TriCore Ref Lab	Reader 1	92.0% (92/100)	100.0% (92/92)	100.0% (92/92)
		Reader 2	96.0% (96/100)	100.0% (96/96)	100.0% (96/96)
		Combined	94.0% (188/200)	100.0% (188/188)	100.0% (188/188)
Digital	Hospital Del Mar	Reader 1	100.0% (100/100)	100.0% (100/100)	100.0% (100/100)
		Reader 2	100.0% (100/100)	100.0% (100/100)	100.0% (100/100)
		Combined	100.0% (200/200)	100.0% (200/200)	100.0% (200/200)
Overall			97.0% (388/400)	100.0% (388/388)	100.0% (388/388)

Staining acceptability rates
Subgroup analysis by reader and site

Slide Type	Site	Reader	Comparison to Historical Flow K/L Restriction Status KRPA	LRPA	NRPA	OPA
Glass	TriCore Ref Lab	Reader 1	94.3% (33/35)	92.0% (23/25)	100.0% (20/20)	95.0% (76/80)
		Reader 2	88.9% (32/36)	81.5% (22/27)	100.0% (19/19)	89.0% (73/82)
		Combined	91.5% (65/71)	86.5% (45/52)	100.0% (39/39)	92.0% (149/162)
Digital	Hospital Del Mar	Reader 1	89.7% (35/39)	88.0% (22/25)	100.0% (20/20)	91.7% (77/84)
		Reader 2	92.5% (37/40)	91.3% (21/23)	100.0% (19/19)	93.9% (77/82)
		Combined	91.1% (72/79)	89.6% (43/48)	100.0% (39/39)	92.8% (154/166)
Overall			91.3% (137/150)	88.0% (88/100)	100.0% (78/78)	92.4% (303/328)

Agreement rates of light chain restriction status
Subgroup analysis by reader and site

EA4HP24-ABS-609

Follicular lymphoma with MNDA expression

Dr. Francisco Javier Diaz de la Pinta, PhD/MD student Marcos Rebollo Gonzalez, PhD/MD Rebeca Manso, PhD/MD Sandra Perez Buira, Dr. Socorro Maria Rodriguez-Pinilla

FUNDACION JIMENEZ DIAZ UNIVERSITY HOSPITAL, PATHOLOGY, MADRID, Spain

Background

Myeloid cell nuclear differentiation antigen (MNDA) is a protein involved in cell proliferation, and is positive in 78% of marginal zone lymphomas (MZL), being very useful in the differential between nodal MZL and follicular lymhpomas (FLs). However, 5% of FL are MNDA+, although histomorphological and molecular features still have to be elucidated

Principles/Methodology

We have collected and analyzed histological and immunohistochemical features of 18 MNDA+ FL cases since 2020 to date.

FISH BA for *BCL2*, *BCL6*, *MYC* genes were perfomed as well as NGS with a customized panel of 73 genes (Agilent SureSelect)

Results

8 males and 10 females. 11 cases were cathegorized as low grade FL and 7 as high-grade FL. Marginal differentiation was observed in 4 cases and plasmacytic differentiation in 2 cases.

3 of the 7 cases with samples at different time points (42%) were initially MNDA-, adquiring its expression after progression/recurrence.

10 of 18 cases carried *BCL2* rearrangement (R), including 2 high-grade cases, with only 1 lacking CD10 expression. 3 cases carried *BCL6*-R, and 1 of these *MYC*-R.

8 out of 18 cases lacked *BCL2*-R and included 5 out of 7 (71 %) high-grade cases. 4 of them lost CD10 expression, preserving follicular pattern and LMO2 and/or OCT2 expression. 4 of them carried *BCL6*-R. Marginal and plasmacytic differentiation were identified across both groups (*BCL2*-R and NR).
Pathogenic variants in 23 genes were identified, being *KMT2D* the most frequently mutated (57%), followed by *ARID1A* and *CREBBP*. 2 cases carried *TP53* mutations and 2 in *SPEN* or *MEF2B*, which are more typical of MZL. Both were grade 3A, lacked *BCL2*-R and CD10 expression, but preserved follicular pattern and LMO2 and OCT2 expresison.
5 cases (28%) presented unusual clinical features for FL: 2 infiltrated the skin, 1 the base of tongue, 1 the conjunctiva and 1 colorectal tissue

Conclusion

MNDA+ FL comprises a heterogeneus group including low and high grade cases, harboring *BCL2* – R and *BCL2* – NR. The latter shows more high-grade cases with loss of CD10 expression. This, together with MNDA+ and lack of *BCL2* – R constitute a diagnostic challenge, but all preserved follicular pattern and other germinal center-derived markers, so were considered FLs.

MNDA may be acquired over time, so the fact that a FL is MNDA- at baseline does not exclude it from this group. Its biological significance needs further investigation.
Most cases show a typical FL mutational profile.
MNDA+ FL appear to have a greater tendency to involve extranodal territories.

N°	Grade	CD20	CD10	BCL2	BCL6	CD23	OCT2	LMO2	BCL6	MYC	IGH	
1	3A	+	-	-	+	-	+	+	T	NT	T	
2	3A	Focal	Weak	Focal	+	-			NV	NT	NT	
6	3A	+	+	Focal	+	-			T	NT	NT	
7	3A	+	-	Weak	+	-		+	T	NT		
8	Low	+	Weak	+	+	+		+	NT	NT	NT	
14	3A	+	-	+	+	-		+	T	NT	T	
16	Low	-	-	-	+	+		+	NT	NT	NV	
17	Low	-	+	-	+	+	+	+	NT	NT	NT	
	Low	+	+	-	+							

N°	Grade	CD20	CD10	BCL2	BCL6	CD23	OCT2	LMO2	BCL2	BCL6	MYC	
3	Low with high Ki67	-	+	+	+	-			T+G	T	NT	Infiltrated secondarily skin
	Low with high Ki67	+	+	+	+							
		-	+	+	+							
4	Low with high Ki67	+	+	Focal	+	-			T	NT	NT	
5	3B	+	Focal	+	Focal	-			T	NT	NT	
9	Skin	+	+	+	+	-			T	NT	NT	Infiltrated secondarily skin
	Low with high Ki67	+	+	+	+	-			T	NT	NT	
10	Low	+	+	+	+	+			T	NV	NV	Infiltrated secondarily conjuntiva
	Low											
11	Low	-	+	+	+	-			T	T	T	
12	Low	+	+	+	+	+			T	NT	NV	
	Low	+	+	+	+	+			T	T	NT	
		+	+	-	+	-			T	NT	NT	
13	Low	+	+	Weak	+	-			T	NT	NT	
15	Low	+	+	+	+	+			T	NT	NV	Affecting colorectal tissue
	Low	+	+	+	+				T	NT	NT	Affecting colorectal tissue
18	3A	+	-	+	+	-	+		T	T	NT	Affected base of tongue at same time

Table of cases
Cases classified between *BCL2*-R and *BCL2*-NR, with all morphological and immunohistochemical data.
Refered unusual clinical evolutions are highlighted

Caso	Gen	Locus	Cambio de aa	Cambio en DNA	VAF (%)	Tipo de mutación	Significado
1	KMT2D		p.Q1213*	c.3637C>T	26	Nonsense	PP
			p.E1241*	c.3721G>T	31	Nonsense	PP
	TP53		p.H193D	c.577C>G	38.6	Missense	PP
	SPEN		p.N2072Kfs*51	c.6215dup	22	Frameshift	PP
2	ARID1A		p.G285*	c.853G>T	13.1	Nonsense	PP
	CD58		p.V45Ffs*2	c.133_137delinsTTTTAA	13.4	Frameshift	PP
	EP300		p.Q2213R	c.6638A>G	13	Missense	VUS
	EZH2		p.Y641N	c.1921T>A	9	Missense	PP
	FBXW7		p.Y401C	c.1202A>G	13.4	Missense	VUS
	KMT2D		p.S42Lfs*88	c.123_125delinsAT	13.2	Frameshift	PP
			p.L5219Sfs*24	c.15655del	15.1	Frameshift	PP
	NOTCH2		p.R2400*	c.7198G>T	13.8	Nonsense	PP
	TNFAIP3		p.Q110Vfs*29	c.327_328del	15.6	Frameshift	PP
3	BCL2		p.A4V	c.11C>T	34.6	Missense	VUS
	CREBBP		p.W1464C	c.4392G>C	36.6	Missense	VUS
	KMT2D		p.Q3788*	c.11362C>T	33.7	Nonsense	PP
	TP53		p.R248Q	c.743G>A	25.8	Missense	PP
4							
5	PIM1		p.R164_D167del	c.490_501del	3	Frameshift	PP
	TP53		p.T284Efs*65	c.848_849insGGAGACCGGCG	5	Frameshift	PP
6	B2M		p.A8P	c.22G>C	9	Missense	VUS
	NFKBIE		p.I159Hfs*2	c.473dup	7	Frameshift	PP
	SOCS1		p.T68A	c.202A>G	7	Missense	VUS
			p.S106C	c.316A>T	9	Missense	VUS
	TNFAIP3		p.C627Ffs*4	c.1880_1881del	8	Frameshift	PP
7	R3HDM1		p.V905Tfs*15	c.2713_2714del	10	Frameshift	PP
	TNFRSF13B		p.R9*	c.25C>T	43	Nonsense	PP
8	ARID1A		p.P1048Lfs*11	c.3143del	11	Frameshift	PP
	KMT2D		p.A221Cfs*12	c.660_661del	7	Frameshift	PP
	TNFRSF14		p.W12*	c.35G>A	24	Nonsense	PP
9	ARID1A		p.Y422Tfs*11	c.1264del	34	Frameshift	PP
	CREBBP		p.Y1125Ifs*5	c.3373del	34	Frameshift	PP
	KMT2D		p.V3089Gfs*9	c.9265dup	32	Frameshift	PP
	SOCS1		p.A184V	c.9265dup	39	Missense	VUS
	KLF2		p.E318K	c.952G>A	29	Missense	VUS
10	KMT2D		p.T4568Rfs*5	c.13095_13102dup	15	Frameshift	PP
	TNFRSF8		p. K39Gfs*25	c.115_116del	18	Frameshift	PP
11	KMT2D		p. Q3602Nfs*56	c.10804del	40	Frameshift	PP
	CREBBP		p. R1446C	c.4336C>T	27	Missense	PP
	NFKBIE		p. A80V	c.239C>T	46	Missense	VUYS
	BCL2		p. N143T	c.428A>C	24	Missense	VUS
			p. P53S	c.157C>T	22	Missense	VUS
12							
13	ARID1A		p. Q269*		30	Nonsense	PP
14	MEF2B	chr19:18260045	p.D83G	c.248A>G	31	Missense	PP
15	KMT2D		p.W141Lfs*79		15.6	Frameshift	PP
	PLCG2		p. Leu835Ile		15.5	Missense	PP
16	EP300		p. Pro1041Arg		49.8	Missense	VUS
	CREBBP		p. E1758Dfs*16		3.5	Frameshift	PP
17	SPEN	chr1:16262243	p. R3211Lfs*7	c.9515_9630dup	3	Frameshift	PP
	NOTCH1	chr9:139395051	p.T1963Pfs*6	c.5808_5886dup	3	Frameshift	PP
		chr9:139400128	p.S1407Pfs*38	c.4219del	4	Frameshift	PP
	KMT2D	chr12:49426107	p.S4129Rfs*8	c.12290_12380dup	3	Frameshift	PP
	TCF3	chr19:1627368	p.A107_G118del	c.320_355del	3	Missense	PP
	CCND1	chr11:69462809	p.V208M	c.622G>A	3	Missense	VUS
	BIRC3	chr11:102196031	p.N264I	c.791A>T	16	Missense	VUS
	TCF3	chr19:1619130	p.R477Q	c.1430G>A	6	Missense	VUS
		chr19:1621956	p.H279L	c.836A>T	3	Missense	VUS

NGS results
Table with NGS findings of each case.

In the abstract submitted we only emphasized on pathogenic variants

EA4HP24-ABS-610

CPT1 inhibition sensitizes diffuse large B-cell lymphoma to vincristine and doxorubicin treatment

PhD/MD student Sophia Steinlein[1,2], M.Sc./M.A. Emma Attwood[1,2], Dr. Heike Horn[1,2], Dr. Annette M. Staiger[1,2], Dr. Katrin S. Kurz[1], Prof. German Ott[1], Dr. Claudia Kalla[1,2]

[1] Robert-Bosch-Krankenhaus, Department of Clinical Pathology, Stuttgart, Germany; [2] Dr. Margarete Fischer-Bosch Institute of Clinical Pharmacology, Stuttgart, Germany

Background

In up to 40% of patients with diffuse large B-cell lymphoma (DLBCL), first-line immunochemotherapy fails to achieve a durable response. Therapy resistance is mediated, in part, by the ineffective elimination of B-cells protected by the stromal microenvironment. Carnitine palmitoyltransferase 1A (CPT1A), a component of the prognostic DLBCL-LAMI signature (Staiger et al. 2020), plays a major role in transporting fatty acids – partly provided by stromal cells – into mitochondria to support B-cell metabolism. We investigated the CPT1A inhibitors ST1326 and perhexiline for their ability to eliminate lymphoma cells and sensitize them to chemotherapeutic agents in the presence of stromal cells.

Principles/Methodology

CPT1A protein expression in DLBCL patient samples was evaluated by immunohistochemistry. Therapeutic efficacy of CPT1A inhibitors was tested in 15 DLBCL cell lines using MTT cytotoxicity assay. Effects on lipid metabolism and induction of apoptosis were investigated by oil red O staining, NAO

staining, and annexin V/PI flow cytometry. Co-culture models of DLBCL cell lines and either the stromal cell line HS-5 or primary DLBCL-cancer associated fibroblasts were established to evaluate the induction of B-cell death in a stromal environment.

Results

CPT1A protein was expressed in 77% (67/87) of primary DLBCL. Both CPT1A inhibitors impaired the viability of lymphoma cells: perhexiline was cytotoxic in 5/5 cell lines (IC50 = 5.5-7.5μM), ST1326 in 10/15 cell lines (IC50 = 5-18μM). Viability of normal cells, fibroblasts, was not affected by either drug. Perhexiline lost its cytotoxic effect against lymphoma cells when these were co-cultured with stromal cells. In contrast, ST1326 remained effective in killing DLBCL cells also in stromal environment. Suppression of fatty acid transport into mitochondria by ST1326 resulted in cytoplasmic lipid accumulation, depletion of cardiolipin and induction of apoptosis. The combination of ST1326 with vincristine or doxorubicin (components of R-CHOP) increased their cytotoxic efficacy. Three DLBCL cell lines resistant to vincristine and doxorubicin when co-cultured with stromal cells were sensitized by ST1326 to both chemotherapeutics, an effect that persisted in the presence of stromal cells.

Conclusion

Targeting the fatty acid metabolism using ST1326 effectively eliminates lymphoma cells in the presence of stromal cells and increases significantly the efficacy of standard chemotherapeutic agents, thus providing a new candidate approach in the treatment of DLBCL.

EA4HP24-ABS-615

Paediatric plasma cell variant of unicentric Castleman disease of the mesenteric lymph node: a case report

Prof. Tatjana Terzic[1], Dr. Relja Kovacevic[2], PhD/MD Marija Dencic Fekete[1], PhD/MD student Jelena Stanojevic[1], Dr. Zivana Stevancevic[3], Prof. Jelena Lazic[4]

[1] Faculty of Medicine University of Belgrade, Institute of Pathology, Belgrade, Serbia; [2] General Hospital, Department of Pathology, Valjevo, Serbia; [3] University Children's Hospital, Department of Radiology, Belgrade, Serbia; [4] University Children's Hospital, Faculty of Medicine University of Belgrade, Department of Hematology and Oncology, Belgrade, Serbia

Background

Castleman disease (CD) is a non-neoplastic lymphoproliferative disorder that is uncommon in the paediatric population, especially plasma cell (PC) variant.

Principles/Methodology

Clinical history of patient and morphological and phenotypic features of mesenteric lymph node biopsy are presented. Routine immunohistochemistry, in situ hybridization and fluorescence in situ hybridization (FISH) were performed.

Results

An 8-year-old boy was admitted to pediatric surgery at General Hospital due to fever and a one-week history of pain in the ileocecal region, no diarrhea or vomiting. Laboratory test showed leukocytosis (17.4x10^9/l) and increased CRP (11.14 mg/L). There was no peripheral lymphadenopathy or organomegaly. An appendectomy was performed and a large amount of transudate was evacuated. Numerous mesenteric enlarged lymph nodes were found (less than 15mm in diameter). The appendix and one lymph node were removed for PH analysis.

Pathohistologically, appendicitis was not observed. Basic lymph node architecture was preserved, with dilated and prominent sinuses. Subcapsular, interfollicular (Fig. 1), paracortical, as well as peri- and intrasinusoidal confluent aggregates of polyclonal cells of immunoblastic/ plasmablastic morphology, B-phenotype were revealed (LCA+, Oct2+, Bob.1+, PAX5+, CD20-/+, MUM-1+, CD30+/-, EMA+, CD138+, CD38+, kappa+, lambda+ (Fig. 2)), with numerous regular mitoses and high proliferative activity (Ki-67+). Those cells were negative for: Cytokeratin, S-100, CD34, TdT, CD3, IgG4, CD56, cyclinD1, CD123, ALK. Human herpes virus 8 (HHV8), cytomegalovirus (CMV) and EBER were negative. To exclude the possibility of neoplastic changes, FISH analysis was performed: no rearrangement of BCL-2, BCL-6, C-MYC or IRF4 genes was detected. A plasma cell variant of CD was diagnosed based on morphology and immunohistochemistry. Serology for CMV, HHV8, EBV and human immunodeficiency virus was negative. Clinical finding of normal serum IL-6 (3.58 pg/ml), no associated autoimmune disease, and an isolated mass involving multiple lymph nodes in the same region was consistent with diagnosis of unicentric CD. The patient has been followed up for three years after the diagnosis. He is without any treatment and free of disease.

Conclusion

Paediatric unicentric PC-CD is extremely rare and pose a particular diagnostic challenge. In this case, morphologic and immunophenotypic features may simulate ALK-positive large B-cell lymphoma, plasmablastic lymphoma and primary (extracavity) effusion lymphoma.

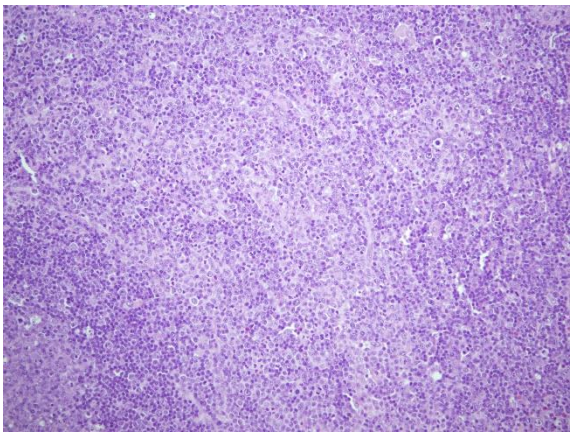

Figure 1. Interfollicular confluent aggregates of plasmablastic cells. (H&E, x200)

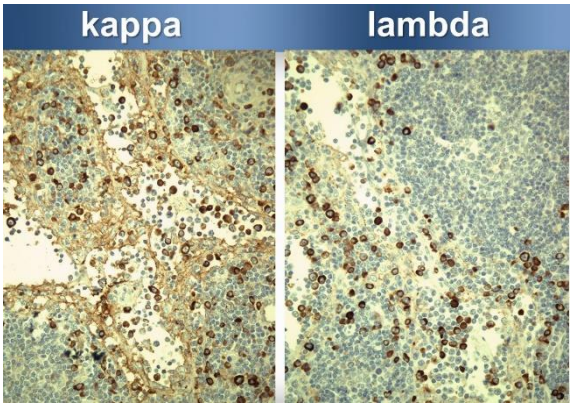

Figure 2. Intrasinusoidal and perisinusoidal aggregates of polyclonal plasmablastic cells

EA4HP24-ABS-616

Intussusception as a manifestation of Activated PI3K delta syndrome 1 (APDS1)

Dr. Joao V. Alves de Castro[1], Dr. Mark Raffeld[1], PhD/MD Gulbu Uzel[2], PhD/MD Stefania Pittaluga[1]

[1] NIH/NCI, Laboratory of Pathology, Hematopathology Section, Bethesda, USA; [2] NIH/NIAID, Laboratory of Clinical Immunology and Microbiology, Bethesda, USA

Background

Primary immune deficiencies (PID) caused by gain-of-function mutations in *PIK3CD* are termed Activated phosphoinositide 3-kinase (PI3K) delta syndrome 1 (APDS1) and may cause lymphoid proliferations in childhood. Among these proliferations, nodular lymphoid hyperplasia in the gastrointestinal tract leading to intussusception can be seen. We aimed to describe the clinicopathologic and molecular features of a subset of *PIK3CD* patients presenting with intussusception.

Principles/Methodology

A single institution cohort of APDS patients (n=78) was searched for cases of intestinal intussusception. Complementary clinical information was retrieved from the database of the clinician. Clonality by IG gene rearrangement fragment analysis was performed in a subset of patients (n=3). Whole exome sequencing or Whole genome sequencing was performed as previously described to confirm the presence of a *PIK3CD* mutation in all patients.

Results

Twelve cases of intussusception were identified (12/78, 15%). Median age at presentation was 1 year old (range: 0.5-5 years old). Median age at intussusception was 13 years old (range: 6-23 years old) The time interval from presentation to intussusception ranged from 1 to 22 years (median=12 years). Based on this time difference, 2 groups were identified: cases in which intussusception presented early (n=1, case CD4), and cases in which intussusception was a late complication (n=6); of note, in 5 cases the age at intussusception could not be retrieved. Most of the cases were diagnosed as reactive (5/7, 71.4%), and 2 were diagnosed as “atypical lymphoid infiltrate” (2/7, 28.6%). Nine cases showed mucosal nodular hyperplasia (9/12, 75.0%). There was a marked increase in PD1-positive T-cells in 2 out of 2 cases. EBV-in situ hybridization and CMV immunohistochemistry were negative in cases tested (2/2, 100.0%; 1/1, 100.0%, respectively). All cases tested were polyclonal for IGH and IGk (n=3). The main *PIK3CD* mutation noted was p.Glu1021Lys (E1021K) in 10/12 cases (83.3%). Clinical and molecular characteristics are summarized in Figure 1.

Conclusion

APDS1 may present with intussusception in childhood. Some can be dismissed as nonspecific reactive lymphoid hyperplasia. Awareness of this condition should prompt genetic screening for PID and may lead to early diagnosis and prevention of further complications. In cases with late intussusception, it is key to avoid misdiagnosing the mucosal nodular hyperplasia as lymphoma.

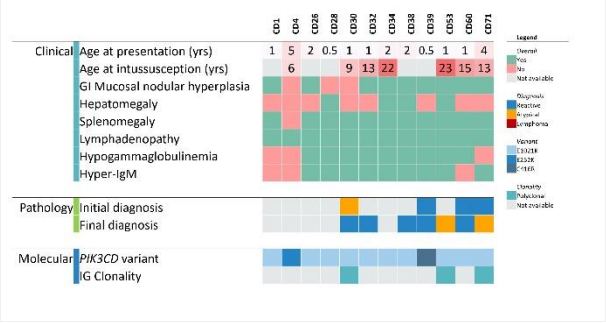

Clinical and molecular characteristics of APCD1 cases associated with intussusception
Legend: GI: gastrointestinal; IG: immunoglobulin genes; *PIK3CD*: phosphatidylinositol-4,5-bisphosphate 3-kinase catalytic subunit delta; yrs: years.

EA4HP24-ABS-620

Targeted panel sequencing for refining B cell lymphoma diagnosis: A real-life, reference center experience

Dr. Julia Böck[1,2], Priv.-Doz. Katja Maurus[1,2], Dr. Julia Doll[1,2], Priv.-Doz. Stephanie Brändlein[1,2], Dr. Katrin Kurz[3], Prof. German Ott[3], Prof. Ioannis Anagnostopoulos[1,2], Prof. Andreas Rosenwald[1,2], Prof. Alberto Zamo[1,2], Priv.-Doz. Elena Gerhard-Hartmann[1,2]

[1] University of Würzburg, Institute of Pathology, Würzburg, Germany; [2] Comprehensive Cancer Center Mainfranken, Würzburg, Germany; [3] Robert-Bosch-Hospital, Department of Clinical Pathology, Stuttgart, Germany

Background
The diagnosis of one of the many types of B-cell lymphoma (BCL) currently requires an integrated approach comprising morphological expertise, inclusion of clinical data and immunophenotyping, but may also incorporate cytogenetics, flow cytometry and clonality analysis. In recent years, several studies have defined the mutational landscape of BCLs, which may also serve as a complementary diagnostic tool. We have developed a custom NGS panel for the routine diagnostics of BCL based on available literature and our own diagnostic questions. The panel was designed to i) provide high informative value relative to cost, ii) include mutations with diagnostic or prognostic value, iii) enable the analysis of individual samples, and iv) ensure rapid turnaround time. We have applied this panel to challenging cases in our routine work in order to obtain further diagnostic support.

Principles/Methodology
The panel contains 40 genes selected based on specific criteria, such as entity-specific mutation frequencies, minimization of co-mutated genes, inclusion of recurrent hotspots, and functional domains. Library preparation was performed using the Ion AmpliSeq Library Kit Plus chemistry and sequencing was performed on the Ion GeneStudio S5 Plus System. Data were analyzed using the Torrent Suite and the Ion Reporter Software (Thermo Fisher). A total of 157 cases were analyzed, including 139 cases of BCL and 18 cases in which a differential diagnosis between a reactive condition and a BCL was considered.

Results
Evaluable results were obtained in all but one of the sequenced cases, although 3 cases exhibited fixation artifacts. Diagnostically informative molecular genetic profiles were identified in 73%. Focusing on 20 challenging cases with the differential diagnosis of Burkitt lymphoma (BL) and diffuse large B-

cell lymphoma (DLBCL), we detected at least one mutation in all cases. In 18/20 cases with this differential diagnosis, panel sequencing provided significant decision guidance.

Conclusion

We have successfully applied a custom NGS-panel to 157 cases of BCL and samples with this differential diagnosis. Although morphology and immunohistochemistry remain the backbone of diagnosis, panel sequencing provided substantial diagnostic assistance in many cases. It was particularly useful in resolving the clinically important differential diagnosis between BL and DLBCL in challenging cases.

EA4HP24-ABS-621

Challenging cases of primary CNS lymphoma and mimics

PhD/MD Evelyn O. Ilori, Prof. Kimmo J. Hatanpaa, Prof. Mingyi Chen

University of Texas Southwestern Medical Center, Pathology, Dallas, USA

Background

CNS lymphomas are rare malignancies arising from the brain, spinal cord, cerebrospinal fluid, leptomeninges, and retinal (primary CNS lymphoma) or hematogenous seeding from non-CNS sites (secondary CNS lymphomas). These non-Hodgkin lymphomas can result in severe comorbidity and increased mortality, therefore timely, accurate, and efficient diagnosis is crucial. The diagnosis of CNS lymphomas can be challenging based on solely histological examination due to the plethora of mimickers featuring lymphocytes and other background inflammatory cells.

Principles/Methodology

A retrospective review of institutional records of a large teaching hospital between 2006 and 2023 was performed to identify diagnostically challenging cases of CNS lymphomas and histologic mimics. Pathologic features, immunophenotypic findings, imaging, cytogenetic and molecular studies, clinical diagnoses, along with therapy and outcomes for the cases were analyzed.

Results

The twenty-four cases revealed the average age of 55 years with 62.5% female. Lesions in the cases were found in the frontal lobe bilaterally, occipital lobe, temporal lobe, thalamus, suprasellar, dura, cerebellum, and basal ganglia. Primary CNS lymphoma consist of 70.8% of cases, vasculitis comprised 12.5% of cases, granulomatous inflammatory disorders 12.5% of cases, and IgG4-related disease comprised 4.2%. The majority of lymphomas (93.8%) were high grade lymphomas. Atypical cytologic features including cellular pleomorphism, irregular nuclear contours, nuclear hyperchromatism, and high nuclear-to-cytoplasmic ratio, mitotic figures were helpful in the diagnosis of lymphomas. Tissue architecture, immunohistochemical studies, and flow cytometry aided in classifying the lymphomas.

Conclusion

Diagnosis of CNS lymphoma could be challenging because of the number of histological mimickers. However, an understanding of inflammatory entities such as lymphocytic vasculitis and autoimmune disorders, along with careful clinicopathologic correlation and judicious use of immunohistochemistry, molecular studies, and flow cytometry analysis can ensure an accurate diagnosis and classification of lymphomas.

EA4HP24-ABS-623

Clonal T-cell lymphoproliferative disorder with leukemic presentation and non-Sézary phenotype: A new entity?

Dr. Magdalena M. Brune[1,2], Dr. Ioanna Xagoraris[1], Dr. Claes Karlsson[3], Dr. Elin Ljung[1], Prof. Anders Österborg[3], Prof. Alexandar Tzankov[2], PhD/MD Leonie Saft[1], PhD/MD Anna Kwiecinska[1], Prof. Georgios Rassidakis[1]

[1] Karolinska Institutet and Karolinska University Hospital, Department of Oncology-Pathology, Stockholm, Sweden; [2] University Hospital Basel, Institute of Medical Genetics and Pathology, Basel, Switzerland; [3] Karolinska University Hospital Solna, Department of Hematology, Stockholm, Sweden

Background

T-cell lymphoid proliferations and lymphomas comprise a broad spectrum of entities ranging from indolent diseases to highly aggressive lymphomas and their classification merits further investigation, particularly since peripheral T-cell lymphomas, not otherwise specified (PTCL, NOS) still comprise a substantial subset of mature T-cell lymphomas, but do probably not represent a homogenous disease category. Here, we describe 5 cases of clonal, leukemic T-cell lymphoproliferations, which are difficult to classify according to the current classification schemes, likely lying between indolent T-cell lymphoid proliferations and leukemic presentation of PTCL, NOS.

Principles/Methodology

All patients were diagnosed and followed at the Karolinska University Hospital Solna, Stockholm, Sweden. Morphology was assessed in peripheral blood (PB) smears and paraffin-embedded histological specimens of bone marrow (BM), skin and lymph nodes (LN), as appropriate. Immunophenotyping was performed by flow cytometry of fresh PB samples, BM aspirates and cell suspensions of LN tissue as well as by immunohistochemistry on tissue samples of BM, skin and LN. *In situ* hybridization was used to assess the EBER1/2 transcripts of EBV. T-cell clonality was studied by polymerase chain reaction (PCR). FISH was applied to investigate various chromosomal alterations. NGS analysis using a broad lymphoma panel (200 genes) was performed in 3/5 cases.

Results

We identified 5 patients with clonal T-cell lymphoproliferation and primarily leukemic presentation. Four patients showed BM, 2 skin and 2 LN involvement. In all cases, T-cell clonality was indicated by flow cytometry (monotypic TCRCb1 expression) and confirmed by PCR, showing clonal TCRβ/γ rearrangements. The details of immunophenotype, genetics, treatment and outcome are shown in Table 1. In one patient (case #5) reactivation of EBV was observed. The median follow-up was 30 months, and all patients are still alive. NGS revealed (likely) pathogenic mutations in 2 cases, including mutation of *STAT3* (case #2), a gene which is commonly mutated among various T-cell lymphomas.

Conclusion

Clonal T-cell lymphoproliferative disorders with non-Sézary phenotype may represent either a new entity of mature T-cell lymphomas or an early presentation of a leukemic PTCL, NOS. Larger series should be studied to draw definite conclusions regarding classification and determine the optimal treatment strategies.

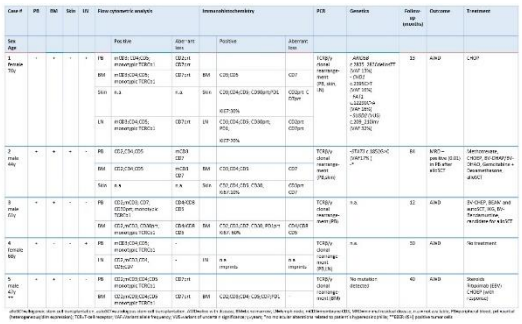

Table 1
Details of patients' immunophenotype, genetics, treatment and outcome.

EA4HP24-ABS-627

Enhancing Molecular Subclassification of B-Cell Lymphomas: Targeted Next Generation Sequencing and Immunohistochemistry versus Fluorescence in Situ Hybridization

PhD/MD Lorraine M. Treurniet-de Haan[1], PhD/MD student Fleur A. Groot[2], M.Sc./M.A. Ruben A. de Groen[2], Romée E. Jansen[2], Esther J. Kret[2], M.Sc./M.A. student Susan Blommers[2], Dr. Troy Noordenbos[1,8], Dr. Tom van Wezel[1], Dr. Dina Ruano[1], Dr. Ronald van Eijk[1], PhD/MD Alina Nicolae-Cristea[3], Dr. Valeska Terpstra[4], Dr. Els Ahsmann[5], PhD/MD Isabelle Focke-Snieders[6], PhD/MD Wietske C. den Hartog[7], Dr. Tim J. Dekker[2], Prof. Hendrik Veelken[2], Dr. Patty M. Jansen[1], Dr. Joost S. Vermaat[2]

[1] Leiden University Medical Center, Pathology, Leiden, Netherlands; [2] Leiden University Medical Center, Hematology, Leiden, Netherlands; [3] Haga Hospital, Pathology, Den Haag, Netherlands; [4] Haaglanden Medical Center, Pathology, Den Haag, Netherlands; [5] Pathan, Pathology, Rotterdam, Netherlands; [6] Reinier de Graaf Hospital, Pathology, Delft, Netherlands; [7] Alrijne Hospital, Pathology, Leiden, Netherlands; [8] Stanford University Medical Center, Department of Oncology, Stanford, USA

Background

The diagnostic evaluation of B-cell lymphomas (BCL) involves extensive immunohistochemistry (IHC) panels and molecular analyses. Fluorescence in situ hybridization (FISH) is considered the golden standard for assessing *MYC*, *BCL2* and *BCL6* rearrangements. At present, targeted Next Generation Sequencing (tNGS) is increasingly integrated into the standard diagnostic process. Studies suggest that *MYC/BCL2/BCL6* rearrangements often coincide with increased IHC expression. Accurate prediction of FISH outcome by tNGS and IHC could lead to a more time and cost-efficient diagnostic approach. This study assesses whether *MYC/BCL2/BCL6* mutational analysis and IHC can reliably predict FISH rearrangements in a large BCL cohort.

Principles/Methodology

This retrospective study included 645 BCL patients diagnosed between 2016-2024, including large B-cell lymphoma (n=462), high grade B-cell lymphoma (n=38), follicular lymphoma (n=118) and various indolent BCL (n=27). FISH analysis with break-apart probes assessed rearrangements, and an in-house developed diagnostic tNGS panel identified *MYC*, *BCL2* and *BCL6* variants.Positive MYC, BCL2 and BCL6 IHC staining was defined as ≥40% staining of tumor cells. As the reference standard, FISH results were compared to tNGS and IHC.

Results

In the *MYC* FISH vs tNGS analysis group (n=545), accuracy was 87% (95%CI 84-90%), with a positive predictive value (PPV) of 60% (95%CI 48-72%) and negative predictive value (NPV) of 90% (95%CI 87-93%). *MYC* FISH vs IHC (n=466) showed an accuracy of 71% (95%CI 67-75 %) with a low PPV 32% (95%CI 25-40%) and high NPV 93% (95%CI 90-96%).

BCL2 FISH vs tNGS (n=386) demonstrated an accuracy of 77% (95%CI 73-81 %) with PPV 83% (95%CI 75-90%) and NPV 75% (95%CI 70-80%). *BCL2* FISH vs IHC (n=384) showed low accuracy (56%, 95%CI 51-61%) with low PPV (49%,95% CI 43- 54%) and higher NPV (87%, 95%CI 77-93%). *BCL6* analysis had similar results to *BCL2*.

Conclusion

Our data suggest that *MYC* tNGS and IHC serve as good negative predictors, indicating a low likelihood of *MYC* rearrangement in the absence of *MYC* mutations or negative IHC expression. FISH confirmation could be omitted in these specific cases. However, both methods are poor positive predictors; presence of mutation or positive IHC expression does not accurately predict a rearrangement. For *BCL2* and *BCL6*, tNGS and IHC are insufficient predictors and FISH is indicated. The next steps involve exploring the combination of tNGS and IHC to improve prediction accuracy.

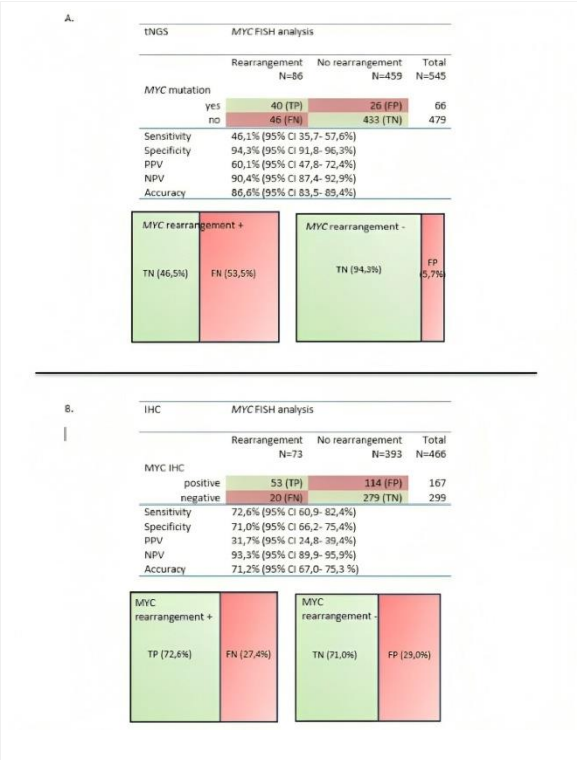

Correlation of MYC FISH with mutational analysis (A) and immunohistochemistry (B)

TP, true positive; FN, false negative; FP, false positive; TN, true negative; CI, confidence interval; IHC, immunohistochemistry

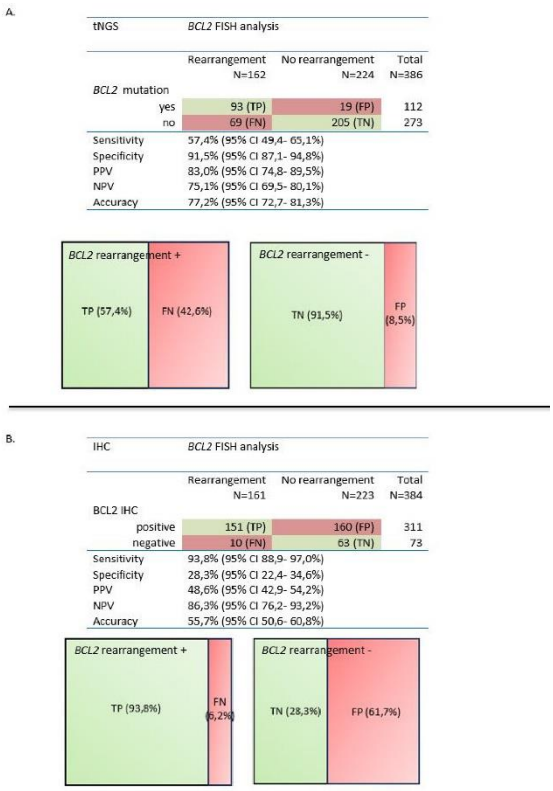

Correlation of BCL2 FISH with mutational analysis (A) and immunohistochemistry (B)
TP, true positive; FN, false negative; FP, false positive; TN, true negative; CI, confidence interval; IHC, immunohistochemistry

EA4HP24-ABS-630

Sellar solitary plasmacytoma with anaplastic features: rare presentation

Howayda S. ABD EL All[1,2]

[1] Suez Canal University, Pathology, Ismailia, Egypt; [2] Nasser Institute, IHC Lab, Oncolog Center, Cairo, Egypt

Background

Plasmacytoma, rarely located in brain, occurs usually in leptomeninges (1). Sellar plasmacytoma is rare as most of sellar neoplasms are of epithelial origin. Hematolymphoid tumors include primary CNS diffuse large B cell lymphoma, immunodeficiency associated CNS lymphom, lymphomatoid granulomatosis, intravascular large B cell lumphoma, low grade B cell lymphoma including MALT lymphoma of dura, anaplastic large cell lymphoma, T cell and NK/T cell lymphoma (1).

Principles/Methodology

We report a case of male patient 56 years old presenting with unexplained headache for one month. Brain MRI revealed large mass 3.4 x 3.6 x 3.8 cm at clivus and sellar floor with extensions into right and left cavernous sinuses, and sphenoidal sinus wall, without suprasellar extension, favoring pituitary adenoma. CBC has normal values. Initial pathology report of the excised mass concluded to invasive pituitary adenoma. Case was referred for slide revision and immmunostaining.

Results

Serial sections revealed atypical binucleated plasmacytoid cells with prominent nucleoli and increased mitotic activity (fig 1). The first panel showed negativity of neoplastic cells for pancytokeratin, chromogranin, and synaptophysin exluding epithelial or neuroendocrine neoplasms. Similarly, leucocyte common antigen was negative. The differential diagnosis was between plasmablastic lymphoma and plasma cell neoplasms. Further staining revealed positivity of all neoplastic cells for CD138 and Mum-1, 50% for CD38, kappa light chain restriction and negativity for CD56, IgA, EBV LMP-1 and HHV-8. Ki67 was expressed on 30% of neoplastic cells (fig 2). Further investigations for primary or secondary immunodeficiencies were negative, in addition to absence of monoclonal gammopathies or end organ damage. The final diagnosis was solitary plasmacytoma with anaplastic features.

Conclusion

Our case fulfill the WHO criteria for the diagnosis of solitary plasmacytoma (2). In addition, we report a case of solitary plasmacytoma with anaplastic features, an uncommon variant of plasma cell neoplasm specially in the sellar region. Plasmacytoma should be considered in the differential diagnosis of sellar neoplasms to avoid erroneous diagnosis.

References

1- WHO classification of CNS tumors, 2021, chapters 10 and 12.

2- WHO classification Hematolymphoid tumors, 2022, chapter 4.

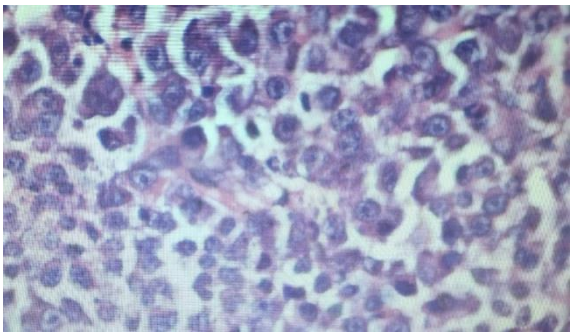

Fig 1
Plasmacytoid and plasma cells, HE staining X 40

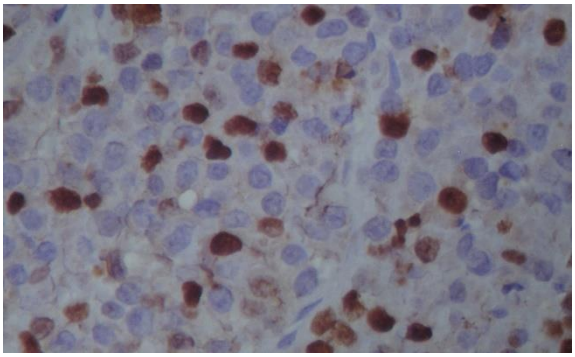

Fig 2
Ki67 clone MIB-1, DAB, x 40

EA4HP24-ABS-635

Protein Expression of the Novel Tumor Suppressor SAMHD1 is an Independent Prognostic Marker in ALK- Anaplastic Large Cell Lymphoma But Not in Other Peripheral T-Cell Lymphomas

Prof. George Z. Rassidakis[1,2], Dr. Vasiliki Leventaki[2], Prof. Elias Drakos[3], PhD/MD Nikolas Herold[4], Prof. Jeffrey L. Medeiros[2], Dr. Ioanna Xagoraris[1]

[1] Karolinska Institute, Department of Oncology-Pathology, Stockholm, Sweden; [2] The University of Texas MD Anderson Cancer Center, Department of Hematopathology, Houston, USA; [3] University of Crete, Medical School, Department of Pathology, Heraklion, Greece; [4] Karolinska Institute, Department of Women's and Children's Health, Stockholm, Sweden

Background

The SAM and HD domain 1 (SAMHD1) protein is a dNTP hydrolase that depletes the intracellular dNTPs. SAMHD1 gene mutations have been linked to Aicardi- Goutières syndrome and detected in chronic lymphocytic leukemia, mantle cell lymphoma and T- prolymphocytic leukemia. SAMHD1 operates as a restriction factor for HIV infection, is involved in DNA damage and anti-tumor immune responses, and confers resistance to cytarabine in acute myeloid leukemia. SAMHD1 may also play a role in oncogenesis as a tumor suppressor. However, the clinical significance of SAMHD1 protein expression in mature T-cell lymphoma types is yet unknown. The aim of this study was to investigate the prognostic value of SAMHD1 protein expression in common types of mature T-cell non-Hodgkin lymphomas (T-NHLs).

Principles/Methodology

The study group included 147 adult patients with PTCL: 48 ALK+ anaplastic large cell lymphoma (ALCL), 28 ALK- ALCL, 36 peripheral T-cell lymphoma, not otherwise specified (PTCL,NOS) and 35 with other T-NHLs with pre-treatment tumor tissue available for immunohistochemistry. Double immunostaining (SAMHD1/CD68), an autostainer and a previously validated antibody were utilized. The percentage of SAMHD1+ cells was calculated by counting 500 tumor cells and a 20% cutoff was used for positivity. Freedom from progression (FFP) and overall survival (OS) were the clinical endpoints. Survival analyses were performed using the Kaplan-Meier method (logrank test) and Cox regression models.

Results

The percentage of SAMHD1+ lymphoma cells varied significantly among mature T-cell lymphomas with PTCL-NOS showing the highest level as compared to ALK+ and ALK- ALCL groups (p=0.004, Kruskall-Wallis test). SAMHD1 was positive in 14/48 (29.2%) of ALK+ ALCL tumors; patients with SAMHD1+ tumors showed a 5-year FFP 89% compared to 57% for patients with SAMHD1- tumors (p= 0.003, logrank). Similarly, patients with SAMHD1+ tumors showed a 5-year OS 92% compared to 68% for patients with SAMHD1- tumors (p=0.002, logrank). Similarly significant differences in FFP and OS were obtained with Cox regression analysis (p=0.005 and p=0.003, respectively). Multivariable analysis confirmed the independent prognostic value of SAMHD1 expression in ALK+ ALCL. By contract, SAMHD1 expression was not associated with different FFP or OS in the groups of ALK- ALCL or PTCL, NOS.

Conclusion

Lack of SAMHD1 protein expression is strongly and independently associated with unfavourable clinical outcome in patients with ALK+ but not ALK- ALCL or PTCL, NOS.

EA4HP24-ABS-639

Dissecting CD47 expression in lymphoid neoplasms: implications for precise diagnosis and targeted immunotherapy

Dr. Andrea Marra[1], Dr. Alan Ramsay[2], Dr. Samuel Chamberlain-Keene[3], Dr. Ayse Akarca[3], Dr. Gabriela Soares[2], Prof. Maurilio Ponzoni[4], Dr. Manuel Rodriguez-Justo[2], Dr. Sabine Pomplun[2], Dr. Ian Proctor[2], Dr. Anna Childerhouse[2], Prof. German Ott[5], Prof. Miguel Piris[6], Prof. Brunangelo Falini[7], Prof. Teresa Marafioti[2]

[1] University Campus Bio-Medico of Rome, Department of Medicine and Surgery, Rome, Italy; [2] University College London, Department of Cellular Pathology, London, UK; [3] University College London, Department of Pathology, London, UK; [4] Università Vita-Salute San Raffaele, Department of Histopathology, Milan, Italy; [5] Robert Bosch Hospital, Department of Clinical Pathology, Stuttgart, Germany; [6] IIS Hospital Universitario Fundación Jiménez Díaz, Department of Pathology, Madrid, Spain; [7] University of Perugia, Department of Medicine and Surgery, Perugia, Italy

Background

CD47, a glycosylated cell surface molecule, inhibits phagocytosis by interacting with signal regulatory protein α (SIRPα) on macrophages. CD47 is overexpressed in solid tumors and hematologic malignancies, and is linked to aggressive disease and poor outcomes. Therapeutic agents targeting the CD47-SIRPα checkpoint show efficacy against lymphomas in preclinical models and clinical trials. However, a comprehensive characterization of CD47 expression across lymphoma histologies is needed to guide immunotherapy.

Principles/Methodology

Immunohistochemistry (IHC), using a recombinant rabbit monoclonal anti-CD47 antibody (EPR21794, Abcam), was performed on 336 lymphoma cases. Normal haematopoietic and lymphoid tissues were also stained for comparison.

Results

In normal lymphoid tissues (**fig.1**), CD47 marked mantle zone and was negative-to-weak in marginal zone B cells of the spleen, while T-cell areas showed strong positivity. In thymus, a subset of cortical thymocytes were positive, while medullary thymocytes were negative. In bone marrow, only megakaryocytes showed weak to moderate CD47 expression.

Among lymphoid neoplasms (**fig.2**), high-grade large B-cell lymphomas showed strong CD47 expression, particularly in Burkitt lymphoma (9/10) and non-GC DLBCL (9/13). Most small B-cell lymphomas were positive for CD47 (CLL 11/11; MCL 9/9; LPL 9/10). However, there was no expression of CD47 in HCL cases (10/10). 16/40 adult (classic) FL cases were positive for CD47 (most CD47+ cases were grade 1-2).Conversely, pediatric-type FL was CD47 negative (5/5). In MZL, the lymphoma cells exhibited strong positivity for CD47 (126/126), irrespective of nodal or extranodal localization. CD47 expression was detected on tumor cells with variable intensity in cHL (11/14), however, lymphoma cells were CD47 negative in NLPHL (0/20). In multiple myeloma, CD47 expression was strong positive in all examined cases (10/10). Among T-cell lymphomas, CD47 expression was found in all AITL cases (10/10), in 13/20 PTCL-NOS, and in 3/8 ALK+ and 3/10 ALK- ALCL cases, respectively.

Conclusion

We provide a comprehensive atlas of CD47 IHC expression across lymphoma histologies, offering potential insights for the rational usage of immunotherapeutic strategies targeting CD47/SIRPa. Further, we propose the practical utility of CD47 as a biomarker that can distinguish MZL from atypical

FL with marginal zone differentiation, or from higher-grade FL cases characterized by MUM-1/IRF4 expression and the absence of the prototypical *BCL2/IgH* translocation.

FIGURE 1

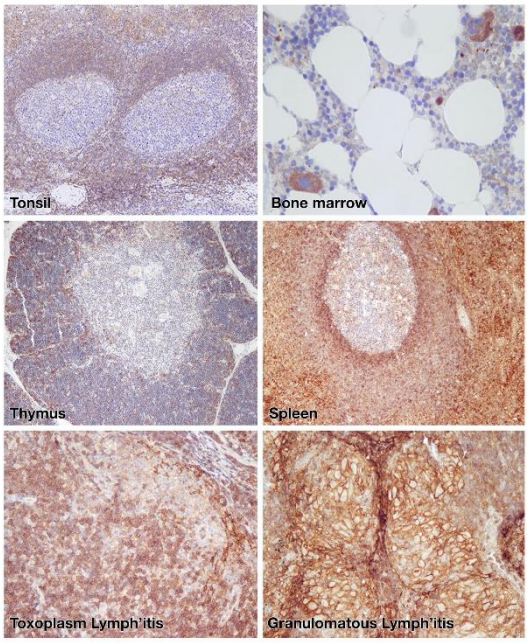

CD47 expression in normal and reactive lymphoid tissues.
In **lymphoid tissues**, CD47 marked mantle zone and was negative-to-weak in marginal zone B cells of the spleen, while T-cell areas showed strong positivity. In thymus, a subset of cortical thymocytes were positive, while medullary thymocytes were negative. In bone marrow, only megakaryocytes showed CD47 expression, erythroid cells were negative and myeloid cells showed non-specific staining.

In **reactive tissues**, monocytoid B cells in cases of Toxoplasma lymphadenitis were CD47 negative, and histiocytes in non-necrotizing granulomatous lymphadenitis were strongly positive for CD47.

FIGURE 2

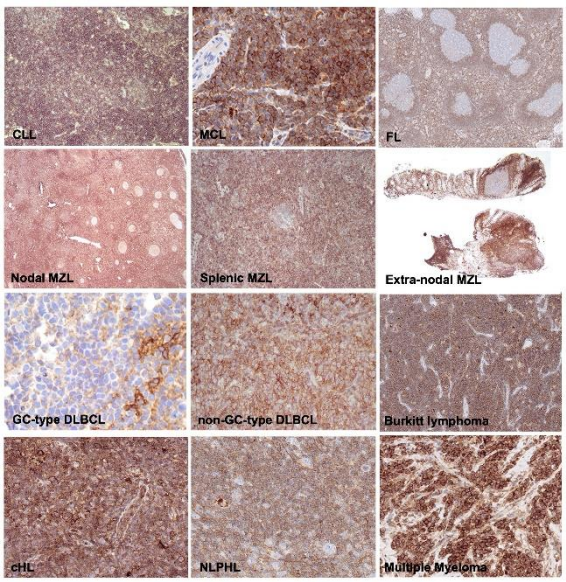

Immunohistochemical expression of CD47 immunoregulatory molecule in lymphoid neoplasms.
Most **small B-cell lymphoma** cases demonstrated positive staining for the CD47, as shown by representative cases of CLL and MCL. About 40% of adult (classic) FL cases were positive for CD47. In MZL, the lymphoma cells exhibited strong positivity for CD47, irrespective of nodal or extra-nodal involvement.

High-grade B-cell lymphomas showed strong CD47 expression, especially non-GC-type DLBCL and Burkitt lymphoma. CD47 was positive with variable intensity in **cHL**, while was negative on tumor cells in **NLPHL**.
Multiple myeloma showed strong positivity for CD47 on neoplastic plasma cells.

EA4HP24-ABS-641

Expression of TRBC1 and TRBC2 proteins in T- cell lymphomas: a new tool for detection of T cell clonality in routine diagnostics

Dr. Marie Therese Manipadam[1], Dr. Alan Ramsay[1], Sugerdana Padmasri[2], Dr. Andrea Marra[3], Dr. Margarida Neves[2], Dr. Hasan Rizvi[4], Dr. Sabine Pomplun[1], Dr. Paul Maciocia[5], Dr. Kate Cwynarski[6], Prof. Miguel Piris[7], Prof. Brunangelo Falini[8], Prof. Andreas Rosenwald[9], Prof. Martin Pule[6], Prof. Alberto Zamò[9], Prof. Teresa Marafioti[1]

[1] University College London, Department of Cellular Pathology, London, UK; [2] University College London, Department Research Pathology, London, UK; [3] University Campus Bio-Medico of Rome, Department of Medicine and Surgery, Rome, Italy; [4] Hamad Medical Corporation, Hamad Medical Corporation, Doha, Qatar; [5] University College London, Research Department of Haematology, London, UK; [6] University College London, Department of Clinical Haematology, London, UK; [7] Instituto de Investigacion Sanitaria Fundacion Jimenez Diaz, Pathology Department, Madrid, Spain; [8] University of Perugia, Department of Medicine and Surgery, Perugia, Italy; [9] University of Würzburg, Institute of Pathology, Wurzburg, Germany

Background

T cell malignancies account for 5-15% of non-Hodgkin's lymphoma and 15% of acute lymphoblastic leukaemia. Diagnosing T-cell neoplasms can be challenging due to their morphological heterogeneity and the similarity between malignant and benign reactive T cells. Assessment of T cell receptor (TCR) clonality, usually achieved through PCR or NGS analyses, can be critical due to assay complexity, accessibility and/or cost. Recently, we have demonstrated an alternative approach to assess TCR clonality by taking advantage of the mutually exclusive selection between two genes encoding the TCR β-chain constant region (TRBC1 and TRBC2). The pattern of TRBC1/2 immunohistochemical expression serves as surrogate for TCR clonality status demonstrating that a benign population of T cells consist of a mixture of TRBC1- and TRBC2-expressing cells, whereas neoplastic T cells exclusively express one or the other TRBCs.

Principles/Methodology

The study included 47 T cell neoplasms: T-ALL (n=4), PTCL-NOS (n=13), AITL (n=14), ALK+ ALCL (n=8), and ALK- ALCL (n=8). Immunohistochemistry (IHC) was conducted using a Bond-III Autostainer with anti-TRBC1 and anti-TRBC2 antibodies. Controls included human reactive tonsils and lymph node sections. Double immunofluorescence was performed on selected lymphoma cases using the Pheno-Imager platform.

Results

In normal reactive tissues, TRBC1 and TRBC2 staining was confined to T cells in the interfollicular area and some intra-germinal center T cells (fig.1). Among T cell lymphomas, 27.6% were TRBC1 positive and 36.2% were TRBC2 positive, with double negative and double positive cases observed in 23.4% and 12.8% of cases, respectively (fig.1). Double immunofluorescence (fig.2) revealed that, in the group of double positive cases, the predominant pattern was characterised by co-existence of non-overlapping populations (with the exception of one case that showed co-expression in a subset of tumour cells) of either TRBC1 or TRBC2 positive neoplastic cells, and, in only two cases, by co-expression of the two proteins in the same tumour cell population. Many double negative cases were found in ALK+ ALCL and T-ALL, likely due to decreased expression of multiple T cell antigens in these neoplasms.

Conclusion

TRBC1 and TRBC2 IHC detection in routine tissue sections proves useful for in situ T cell clonality assessment and offers rapid, universally applicable results compared to molecular testing, relevant for detecting neoplastic T cell populations in relapse settings and small biopsies.

FIGURE 1

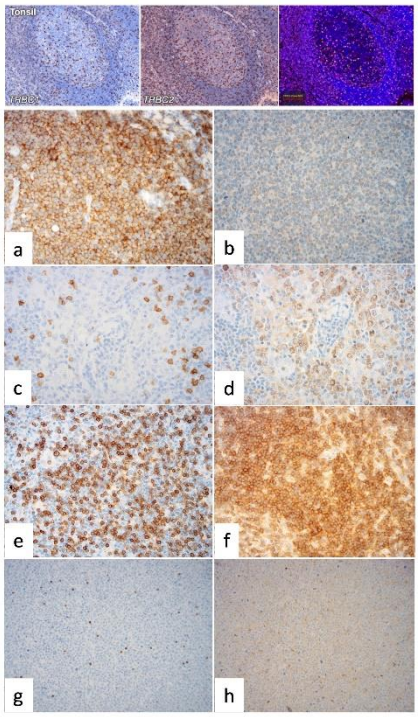

Expression of TCRβ1 (TRBC1) and TCRβ2 (TRBC2) in human tonsil and T cell neoplasms
Top lane) T cells within and outside the germinal centers express either TRBC1 or TRBC2. (IHC and Double-IF).

Panels a-b) PTCL-NOS. The neoplastic cells positive for TCRβ1 (a) and negative for TCRβ2 (b)
Panels c-d) ALK negative ALCL . The neoplastic cells negative for TCRβ1 (c) and positive for TCRβ2(d);
Panels e-f) AITL. The neoplastic cells are positive for TCRβ1 (e) and TCRβ2 (f);
Panels g-h) ALK negative ALCL. The neoplastic cells are negative for TCRβ1 (g) and TCRβ2 (h).

FIGURE 2

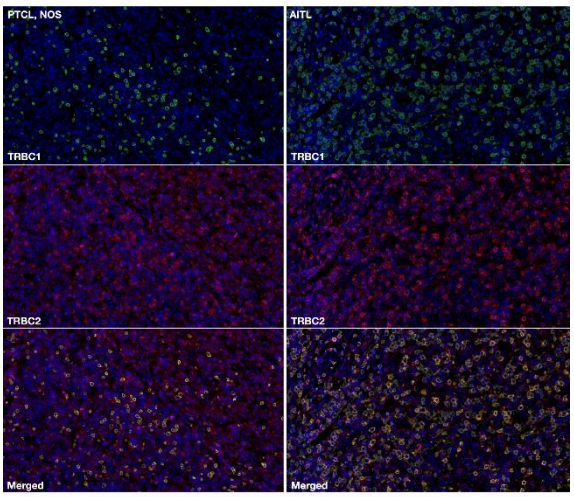

Double immunofluorescence for TCRβ1 and TCRβ2 in T cell lymphomas.
(*Left panels*) The case diagnosed with PTCL, NOS showed a proportion of tumour cells (~20%), which co-expressed TCRβ1 and TCRβ2. (*Right panels*) The case diagnosed with AITL displayed the majority of the tumour cells double positive for TCRβ1 and TCRβ2.

EA4HP24-ABS-642

Lymphadenopathy inActivated PI3-Kinase Delta Syndrome (APDS).

Dr. Malee Fernando[1], Dr. John Goodlad[3], Dr. Sophie Stenton[2], Dr. Michael Toss[1], Dr. Caroline Kerrison[2]

[1] Sheffield Teaching Hospitals NHS Trust/ HODS, Haemato-oncology Diagnostic Service, Sheffield, UK; [2] Sheffield Children's Hospital NHS Trust, Sheffield, UK; [3] Queen Elizabeth Hospital NHS Trust, Haematopathology, Glasgow, UK

Background

Activated PI3-Kinase Delta Syndrome (APDS) is a relatively recently reported primary Immunodeficiency caused by heterozygous gain-of-function mutations in PIK3CD gene. The phenotype is variable, ranging from asymptomatic adults to profound immunodeficiency causing early death in childhood.

We present the nodal features of a 2-year old male who was diagnosed with APDS during a workup for unexplained fluctuating cervical, epigastric and inguinal lymphadenopathy. There are 170 APDS patients on the ESID registry, but the exact numbers are unknown.

Principles/Methodology

In addition to the lymphadenopathy, our patient had recurrent respiratory infections since birth and chronic viral infection with slow clearance, mainly with cytomegalovirus (CMV) and Epstein–Barr virus (EBV). He had anaemia (87x10^9/L) and thrombocytopaenia (51x10^9/L) with atypical lymphocytes with granulated cytoplasm.

The axillary node excised to exclude a lymphoproliferative disorder showed follicles and reactive parocortex and without evidenceto suggest lymphoma. Singly scattered cells expressing CMV and EBV were thought to reflect previous infection. The posterior cervical node excised 3 months later showed intact lymph node architecture with large, irregular germinal centres, scattered immunoblasts and massive monocytoid B-cell hyperplasia, including activated lymphoid cells with intranuclear inclusions. The IHC did not show an obvious population of double negative (CD4-/CD8-) T-cells.
Many of the EBV-positive cells express LMP1 but they are negative for EBNA2 (type II latency). In addition, scattered activated lymphoid cells within the sinuses, including those with intranuclear inclusions, stained for CMV.

Results

The peripheral blood showed a low-normal lymphocyte count (6.12 x10^9/L) with a raised CD8+ T-cells (63.5%), normal expression of MHC class I & II and CD18, normal numbers of double negative T-cells and low NK cells %. He always had very high IgM, even in relation to high IgA and IgG. Germline testing identified a de novo heterozygous PIK3CD variant c.3061G>A p.(Glu1021Lys)mutation at Chr 1. He is currently 9 months post SCT with slow engraftment. He has no lymphadenopathy and does not have recurrent bacterial infections anymore though the respiratory viral infections take longer to clear on PCR testing.

Conclusion

We highlight the histopathology in a rare cause of unexplained lymphadenopathy in an infant with morphological features of delayed clearance of EBV and CMV infection, as is described in this disease.

EA4HP24-ABS-643

High-Grade B cell Lymphoma with MYC and BCL2 and/or BCL6 rearrangements : a genomic approach by targeted Next Generation Sequencing (NGS)

Dr. Catherine Chassagne-Clement[1], Dr. Emmanuel Beillard[1], Dr. Marie Donzel[2], Dr. Julie Gervasoni[1], Daniel Pissaloux[1], Dr. Yann Guillermin[3], Dr. Anne Sophie Michallet[3], Dr. Pierre Sesques[4], Prof. Emmanuel Bachy[4], Prof. Hervé Ghesquières[4], Claire Mauduit[2], Prof. Alexandra Traverse-Glehen[2]

[1] Centre Léon Bérard, Department of Biopathology, Lyon, France; [2] Hospices Civils de Lyon, Department of Biopathology, Lyon, France; [3] Centre Léon Bérard, Department of Hematology and Medical Oncology, Lyon, France; [4] Hospices Civils de Lyon, Department of Hematology, Lyon, France

Background

High-grade B-cell Lymphoma (HGBL) with MYC and BCL2 and/or BCL6 translocations appeared on the 4th revised edition WHO classification of lymphoid neoplasms as a new category for all “double/triple-hit” lymphomas. The 5th edition WHO classification recognized Diffuse Large B-cell Lymphoma (DLBCL) / HGBL with MYC and BCL2 rearrangements (DH2), but HGBL with MYC and BCL6 (DH6) should henceforth not be included in this entity. In the ICC 2022, HGBL DH2 appeared still as an entity, but HGBL DH6 was downgraded as a provisional entity.
Here we report a cohort of 50 HGBL with *MYC/BCL2* (DH2, n=24), *MYC/BCL6* (DH6, n=13) and *MYC/BCL2/BCL6* (TH, n=13) analyzed by targeted NGS technology.

Principles/Methodology

FISH status for *MYC*, *BCL2* and *BCL6* was screened with break-apart probes. MYC partners were unknown.

Targeted NGS analysis evaluating 47 genes was performed on formalin-fixed paraffin-embedded (FFPE) samples. Mutations retained were class 5 (pathogenic), class 4 (likely pathogenic) and class 3 (uncertain significance) only.

Results

By targeted NGS analysis, all cases carried alterations on 44 genes out of 47 (fig.1).

The six most frequently mutated genes were KMT2D (46%), BCL2 (46%) MYC (42%), TNFRSF14 (42%), EZH2 (40%) and CREBBP (40%) without significant difference between subgroups.

PIM1, SOCS1 and FOXO1 mutations frequencies were significantly higher in the DH6 group (fig.2). There were a non-significant trend towards alterations co-occurrence between PIM1 and SOCS1 and mutual exclusivity between FOXO1 and PIM1 and/or SOCS1.

NOTCH2 mutations were rare (6%) and only found in the DH6 group.

TP53 mutations were less frequently observed in DH6 (8%) than in DH2 (21%) and TH cases (38%) without significant difference.

Conclusion

Our results showed as expected that HGBL DH2/DH6/TH framed with EZB cluster according to Wright. However, we observed significant mutational differences between the DH6 group and the two other groups. Notably, PIM1 and SOCS1, affecting JAK/STAT signaling pathway, were the most frequently mutated genes in this group. The PI3K/AKT signaling pathway, with FOXO1 mutations, was the second most frequent altered pathway. Finally, NOTCH2 mutations could add one more signaling pathway.

This work brings to light a distinct mutational landscape among HGBL DH/TH. In agreement with the new classifications of lymphoid neoplasms, the DLBCL / HGBL DH6 could be considered as a different but non-homogeneous entity with potential oncogenic drivers associated with ST2 or BN2 Wright clusters.

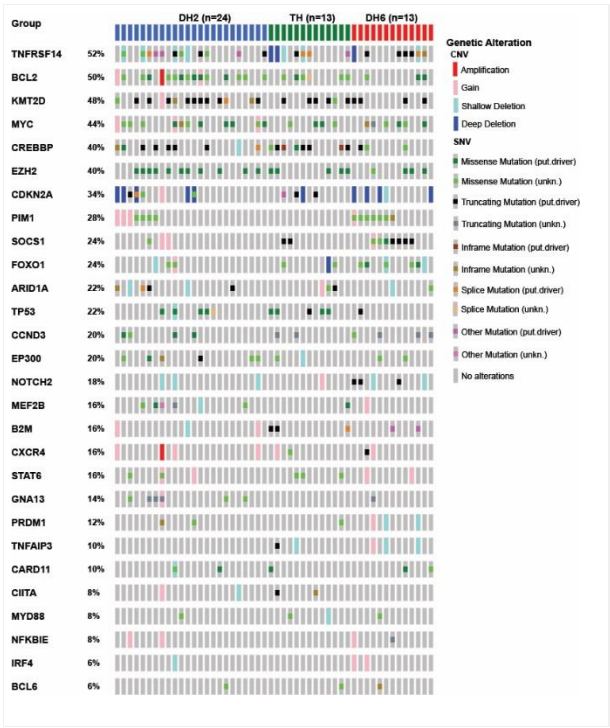

Figure 1 - Mutational landscape in HGBL DH2/DH6/TH

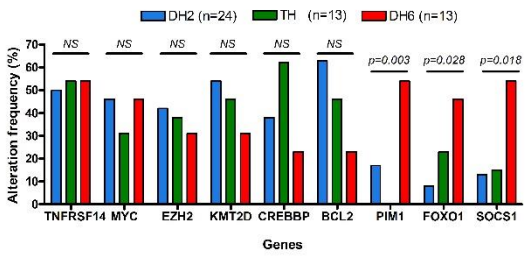

Figure 2 – Prevalence of the most frequent mutations in the three subgroups

EA4HP24-ABS-647

DNA methylation-based determination of tumor cell content in haematolymphoid neoplasms: fact or fiction?

Dr. Anja Fischer[1], Sara Hetzel[2], Luis Veloza[3], David Vallois[3], Edoardo Missiaglia[3], Raphael Koch[4], Alexander Pichler[5], Virginie Fataccioli[6], Laura Wiehle[1], Paurnima Patil[1], Cosima Drewes[1], Nadine Matscheko[1], Diana Laure Mboumba[7], Daphne de Jong[8], Ole Ammerpohl[1], Keisuke Kataoka[9], Seishi Ogawa[10], German Ott[11], Werner Kempf[12], Philipp Staber[5], Francois Lemonnier[7], Claudia Haferlach[13], Marco Herling[14], Stephan Stilgenbauer[15], Olivier Tournilhac[16], Lorenz Trümper[4], Philippe Gaulard[6], Helene Kretzmer[2], Laurence De Leval[3], Reiner Siebert[1]

[1] Ulm University and Ulm University Medical Center, Institute of Human Genetics, Ulm, Germany; [2] Max Planck Institute for Molecular Genetics, Department of Genome Regulation, Berlin, Germany; [3] Lausanne University Hospital, Institute of Pathology, Lausanne, Switzerland; [4] University Medical Center Goettingen, Department of Hematology and Medical Oncology, Goettingen, Germany; [5] Medical University of Vienna, Division of Hematology, Vienna, Austria; [6] Université Paris-Est, Département de Pathologie, Créteil, France; [7] Mondor Biomedical Research Institute, Team Ortonne, INSERM U955, Créteil, France; [8] Vrije Universiteit Amsterdam, Department of Pathology, Amsterdam, Netherlands; [9] National Cancer Center Research Institute Toyko, Division of Molecular Oncology, Tokyo, Japan; [10] Kyoto University, Department of Pathology and Tumour Biology, Kyoto, Japan; [11] Department of Clinical Pathology, Robert-Bosch-Krankenhaus, Stuttgart, Germany; [12] Kempf und Pfaltz Histologische Diagnostik Zurich, Zurich, Switzerland; [13] MLL Munich Leukaemia Laboratory, Munich, Germany; [14] University of Cologne, Department I of Internal Medicine, Cologne, Germany; [15] Ulm University Medical Center, Department of Internal Medicine III, Ulm, Germany; [16] Centres Hospitalier Universitaires Estaing, Service d'Hématologie Clinique et de Thérapie Cellulaire, Clermont-Ferrand, France

Background

DNA methylation-based tumor classification is an established diagnostic tool e.g. for brain tumors and sarcomas. Although various haematolymphoid tumors show distinct DNA methylation profiles, its potential to support the classification particularly of lymphoid neoplasms is unclear. The main reasons for this are (i) the long established, already highly detailed classification system of haematolymphoid neoplasms making further subtype classification a much more difficult task, (ii) the rather variable tumor cell content (TCC) and (iii) the same cell-of-origin derivation of tumor cells and non-neoplastic lymphoid bystander cells. As tumor purity potentially strongly confounds lymphoma subtype classification, assessment of TCC is a crucial step for DNA methylation-based classification. In light of the need for improved classification of T cell lymphomas (TCLs), we explored DNA methylation-based

subtyping by profiling a large cohort of TCLs covering the clinically most relevant subtypes and systematically compared their (predicted) TCC to that of other haematolymphoid malignancies.

Principles/Methodology

DNA methylation profiles of 318 T cell lymphomas were generated using the EPIC/450K array. Raw idat files were processed using the minfi R package and integrated with 1,844 in-house and publicly available haematopoietic healthy and tumor samples. TCC was calculated using the control-based R packages InfiniumPurify (Qin *et al.*, 2018) and PAMES (Benelli *et al.*, 2018) as well as the reference-free R package RF_Purify (Johann *et al.*, 2019).

Results

TCC estimation for mature T cell lymphomas based on DNA methylation led to strikingly differing results depending on the method. The widely used tool RF_Purify predicts values ranging from 39% – 83%. In contrast, PAMES and InfiniumPurify estimate TCC ranging from 4% - 86% and 0.8% – 94%, respectively, when using normal lymphatic FFPE tissue as a control. Of note, RF_Purify also places the TCC of non-neoplastic hematopoietic cells in the range of 29% – 80% while InfiniumPurify leads to 2.4% - 47% TCC. When comparing the estimated TCC values to pathological investigation in Enteropathy-associated T-cell lymphoma samples, InfiniumPurify shows the highest concordance ($p = 0.0016$).

Conclusion

Here, we show that commonly used tools to estimate tumor purity based on DNA methylation lead to very different results when applied to mature TCLs. In this analysis we show that InfiniumPurify might be the most suitable tool to assess TCC in haematolymphoid neoplasms.

EA4HP24-ABS-649

Molecular Insights of Lymphoma-Like Lesions of the Lower Genital Tract Support a Reactive Process.

Gabriela Caballero[1], Gerard Frigola[1,3], Fina Climent[2], Adela Saco[1], Montse Gomà[2], August Vidal[2], Elías Campo[1,3], Blanca Gonzalez-Farre[1,3]

[1] Hospital Clínic de Barcelona, University of Barcelona, Pathology Department, Barcelona, Spain; [2] Hospital Universitari de Bellvitge-IDIBELL, University of Barcelona, Pathology Department, L'Hospitalet de Llobregat, Spain; [3] Institut d'Investigacions Biomèdiques August Pi i Sunyer (IDIBAPS), Barcelona, Spain; [4] Centro de Investigación Biomédica en Red de Cáncer (CIBERONC), Madrid, Spain

Background

Florid lymphoid hyperplasia or lymphoma-like lesion (LLL) of the lower genital tract (LGT) is an uncommon benign condition with frequent large cell morphology, high proliferative index and occasional clonal IGH rearrangements that can mimic lymphoma. This study aims to provide molecular insights that may assist in the differential diagnosis of these lesions.

Principles/Methodology

Six cases of LLL of the LGT were examined with an immunohistochemical (IHC) lymphoid panel, Human Papilloma and Epstein Barr virus, fluorescence in situ hybridization (FISH) for *BCL2*, *BCL6* and *MYC* rearrangement, IG clonality, and next-generation-sequencing.

Results

The median age was 45 years (range: 32-61yr). Five patients had cervical polyps and one a clitoral lesion. Histologically, the lesions were composed of a diffuse (5 cases) or vaguely nodular infiltrate (1 case) of large cells with predominance of plasmablasts (2/6), centroblasts (2/6), anaplastic cells (1/6), or a mixture of large cells (1/6) in an inflammatory background. Frequent mitoses and high Ki67 index (60%-90%) were observed. Two cases showed lambda light chain restriction and two exhibited clonal IG rearrangement. However, no oncogenic rearrangements were detected by FISH, viruses were negative, and no mutations were observed in five cases studied, besides a *CREBBP* nonpathogenic germinal variant in one. Follow-up (18 to 157 months, median 94 months) showed no recurrences.

Conclusion

LLL of the LGT are highly proliferative lymphoid lesions mainly composed of large, atypical B cells that can resemble lymphomas. The absence of oncogenic alterations, even in cases with clonal IG or monotypic light chain expression, supports the diagnosis of reactive lesions.

EA4HP24-ABS-650

Composite and sequential Hodgkin and other lymphomas: B cell plasticity and immune dysregulation?

Dr. Domenico Ferrara[1], Dr. Massimo Granai[1], Dr. Maria Chiara Siciliano[1], Dr. Margherita Vannucchi[1], Dr. Raffaella Guazzo[1], Dr. Antonio De Nicola[1], Dr. Nicola Leone[1], Dr. Ledi Bardhi[1], Dr. Gioia Di Stefano[2], Anja Fisher[3], Reiner Siebert[3], Lorenzo Leoncini[1], Stefano Lazzi[1], Cristiana Bellan[1]

[1] University of Siena, Department of Medical Biotechnologies, Siena, Italy; [2] University of Florence, Department of Pathology, Florence, Italy; [3] Ulm University, Institute of Human Genetics, Ulm, Germany

Background

Clonally related morphologically distinct “composite” and “sequential” lymphomas are the result of B cell plasticity that can lead to the formation of two mature entities from the same origin. The transformation of a mature differentiated cell in another mature cell is known as transdifferentiation and can occur under physiological or pathologic conditions. Such phenomenon has been reported in cHL transforming to FL (or reverse) and less frequently in NLPHL to cHL. Interestingly, some authors demonstrated the presence of *EP300* mutations in cHL cases that transformed from another entity. It is still unclear whether EBV infection may be demonstrated and may contribute to the progression of these lymphomas

Principles/Methodology

Here we report 5 cases of “composite” and “sequential” lymphomas, including two cases of composite cHL and FL and three other combinations of sequential lymphomas. Among the latter cases one evolved from cHL to NLPHL and then to FL. The other two evolved from THRLBCL-like, pattern E of NLPHL to cHL. The different components or sequential samples have been analyzed for presence of EBV, for clonality (BIOMED primers) and by targeted NGS analysis using a 72 gene panel (Sophia Genetics)

Results

In all samples of a given case *IGH/IGK* rearrangements demonstrated a clonal relationship. EBV was detected in one case of composite lymphoma and one case of sequential lymphoma progressing from THRLBCL-like, pattern E of NLPHL to cHL. In addition, identical pathogenic variants, reinforcing the hypothesis of a "common clonal origin" were identified, but also additional mutations characterizing the specific entity, as TNFRSF14 and CREBBP mutations in FL. Among the identical pathogenetic variants, we identified mutations in genes involved in immunodeficiency and autoimmune disease in two cases requesting exclusion of germline variants which is currently ongoing

Conclusion

The identification of common mutations in genes primarily involved in allergic diseases, immunodeficiency and autoimmunity may suggest an underlying immune dysregulation in some of the studied patients. A more complete NGS analysis to detect additional predisposing germline mutations is ongoing in our cases but further studies are necessary to better assess the association of B cell plasticity and immune dysregulation

EA4HP24-ABS-651

Primary cutaneous epidermotropic, cytotoxic, ALK+ T-cell lymphoma: appraisal of a novel pattern of disease.

Dr. Giorgio A. Croci[1,2], Dr. Lorena Appio[3], Dr. Caterina Cecchetti[3], Prof. Silvia Tabano[1,4], Prof. Emilio Berti[5], Prof. Francesco Onida[6], Dr. Francesca Cavallaro[7], Dr. Daoud Rahal[9], Dr. Dario Tomasini[8], Dr. Elisabetta Todisco[3]

[1] University of Milan, Department of Pathophysiology and Transplantation, Milano, Italy; [2] Istituto di Ricovero e Cura a Carattere Scientifico (IRCCS) Ca' Granda Ospedale Maggiore Policlinico, Division of Pathology, Milano, Italy; [3] ASST ValleOlona Ospedale di Busto Arsizio, Division of Hematology, Busto Arsizio, Italy; [4] Istituto di Ricovero e Cura a Carattere Scientifico (IRCCS) Ca' Granda Ospedale Maggiore Policlinico, Medical Genetics Unit, Milano, Italy; [5] Istituto di Ricovero e Cura a Carattere Scientifico (IRCCS) Ca' Granda Ospedale Maggiore Policlinico, Dermatology Unit, Milano, Italy; [6] ASST-Fatebenefratelli-Sacco, University of Milan, Hematology Unit, Milano, Italy; [7] Istituto di Ricovero e Cura a Carattere Scientifico (IRCCS) MultiMedica Group, Hematology Unit, Milano, Italy; [8] ASST ValleOlona Ospedale di Busto Arsizio, Division of Dermatology, Busto Arsizio, Italy; [9] IRCCS Humanitas Research Hospital, Department of Pathology, Rozzano, Italy

Background

ALK-positive T-cell lymphoma is to be considered a nodal/systemic disease, until proven contrary

Principles/Methodology

Leading from 2 novel cases of primary cutaneous TCL (pcTCL), with a mycosis fungoides (MF)-like pattern and ALK expression and molecular alteration, we performed a critical appraisal of ALK+ pcTCL. PubMed database was queried for "ALK positive primary cutaneous", "ALK positive epidermotropic" and "ALK positive mycosis fungoides"

Results

Patients

Patient 1: 58-y.o. male, followed up for at least 3 years for a suspected erythrodermic psoriasis and featuring a widespread disease, with hyperkeratotic plaques and ulcerated lesions. Biopsy proved a superficial, epidermotropic infiltrate of pleomorphic cells, with a CD4+/perforin+/CD30dim/ALK1-/ALK-

D5F3+ phenotype and *ALK* rearrangement at FISH. Staging excluded an extracutaneous disease, but the patient experienced a cutaneous progression requiring hematologic management.
Patient 2: 62-y.o. female followed up since 2008 for a cutaneous manifestation akin to poikiloderma vasculare atrophicans; in 2014, diagnosed of nodal ALK+ ALCL (Lugano stage I), in complete remission. A patch was biopsied in 2023, consistent with early phase MF, but with scattered dermal and intraepidermal small, slightly pleomorphic cells, with a CD4+/perforin+/CD30-/ALK1-/ALK-D5F3+ phenotype. *TCRG* clonal identity between nodal and cutaneous biopsies was documented. Staging was negative and the patient is receiving PUVA therapy.
Literature review
A total of 32 ALK+ pcTCL cases was retrieved, 7 of which with a MF-like clinical picture over 4-to-20 years. Histology of MF-like cases included a predominantly epidermotropic pattern and morphology ranging from small, atypical to pleomorphic and anaplastic. Tested cases featured dim-to-intense CD30 expression, a CD4+/cytotoxic granule+ phenotype and cytoplasmic or nuclear/cytoplasmic ALK-positivity, best captured by D5F3 clone. In our cases, *ALK* breaks, in one published case, *ALK::ATIC* fusion ware detected. Therapeutic approach is detailed in Table.

Conclusion

Experience is limited, but data suggest the presence of a primary cutaneous epidermotropic, cytotoxic, ALK+ T-cell lymphoma pattern. The major challenges include the prodromal phases, misinterpreted as inflammatory dermatosis or parapsoriasis / early phase MF. Data on optimal management are far from being conclusive: a MF-like approach is currently chosen, but depending on CD30 and, most notably, ALK expression, a targeted therapy could be envisaged in advanced stages.

Epidermotropic / mycosis fungoides-like cases (n = 7, present included)
Clinical picture (follow up range 4-20 yrs) • 5 cases: disease presentation akin to parapsoriasis / early MF / poikilodermatous MF, ultimately with nodular / tumoral evolution • 2 cases: patches, keratotic plaques, nodules with ulceration
Histologic picture • epidermotropic, non-tumor forming proliferation of lymphoid cells • morphology from small atypical to anaplastic • detailed cases (n=4) report a CD4+/CD8-/cytotoxic granule+ phenotype, with dim to intense CD30 expression; • ALK+ cytoplasmic or nuclear / cytoplasmic • 1 case documented an *ATIC::ALK* fusion gene Histologic diagnosis comprised eczema, parapsoriasis, mycosis fungoides and PCTCL-NOS
Therapy and follow up *Published cases* • MF-type: PUVA, bexarotene, methotrexate, acitretin; one patient alive with disease[21] • Chemotherapy (BEAM-CAMPATH) and anti-CD30 immunotherapy, followed by allogenic stem cell transplant in one patient; patient died of septic complications post-alloHSCT[15] *Current case 1* • Receiving acitretin for (suspected) psoriaris • First line: gemcitabine (1000 mg/mq) → no response • Second line: brentixumab → complete response (4 doses) → relapse (few weeks) • Third line: CHOP-based → CR for few weeks • Fourth line: crizotinib → complete response → relapse after 2 months → died of disease *Current case 2* • PUVA
Legend: MF, mycosis fungoides; PTCL-NOS, peripheral T-cell lymphoma, not otherwise specified; PUVA, psoralen ultra-violet light A; BEAM-Campath, BiCNU (carmustine), etoposide, Ara-C, melphalan + Campath; CR, complete remission; CHOP, cyclophosphamide, doxorubicin (Adriamycin) vincristine (Oncovin)

Table
Clinic pathologic features of mycosis fungoides-like ALK+ primary cutaneous T-cell lymphoma.

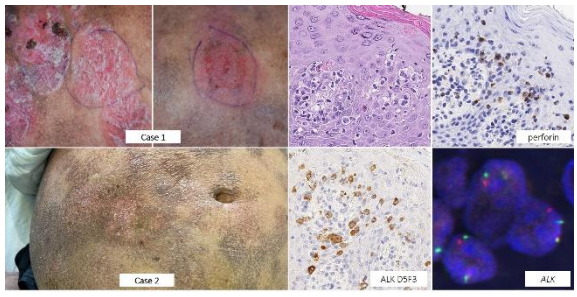

Image
Clinic-pathologic features of our cases.

EA4HP24-ABS-655

Burkitt-like lymphoma with 11q aberrations: systematic review

Dr. Timothy Onyuma[1], Dr. Noel Onyango[1,2]

[1] University of Siena, Department of Biotechnologies, Siena, Italy; [2] University of Nairobi, Department of Medical Microbiology and Immunology, Nairobi, Kenya

Background

The Burkitt-like lymphoma (HGBCL -11q) is a rare tumor that has been classified by the 5th edition of the WHO Classification of Tumours as a High grade mature B Cell lymphoma. It is similar to Burkitt Lymphoma (BL) morphologically and the characteristic aberration is loss in the 11q24.1 and gain in the 11q23.2-11q23.3 region. It also lacks the MYC translocation. The tumor morphologically exhibits a diffuse proliferation of medium-sized atypical lymphocytes with a background of apoptotic debris and tingible-body marcophages giving a “starry-sky” appearance akin to Burkitt Lymphoma (BL). It also shows similar immunophenotype to BL by expression of CD10, Bcl-2 and Ki67 index approaching 100%. It is important to distinguish this entity from BL because the clinical management should be tailored to the best available regimens and clinical trials.

Principles/Methodology

Databases such PubMed, Google scholar and Cochrane were searched for keywords, namely BL, Burkitt-like lymphoma, 11q using Boolean operators AND/OR in various combinations using the Preferred Reporting Items for Systematic Reviews and Meta-Analyses (PRISMA) guidelines.Case reports were extracted and duplicates were removed. Only case reports and case series were included, retrospective studies were excluded. Studies in language other than English were excluded.

Results

The age range was 13 to 73 years with median age 35.5 years. Most patients were adults with only 2 cases in the paediatric population. The M: F ratio was 5:1. Most cases occurred in the USA and Europe with fewer cases in Asia. No cases have been reported in Africa so far. Majority of the case 7 were located in the abdominal region with most cases seen in the ileocecal and appendiceal locations. The next most common location was in the cervical lymph nodes. In 3 patients the lymphoma was associated with immunosuppression (2 were HIV positive and 1 patient had history of renal transplantation). Paucity of clinical data in many cases was a limitation of this review. We also limited the search to English literature.

Conclusion

HGBCL -11q is a relatively rare tumor with clinically significant implication to the diagnosis. In most cases the tumor was previously described under the Burkitt-like group of lymphomas. No cases have been reported in the African setting to our knowledge. We postulate that there is a likelihood of misclassification of this lymphoma in the African setting and it would be worthwhile to explore this in future.

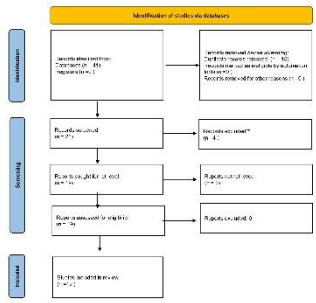

Figure 1
Flowchart

EA4HP24-ABS-659

Different molecular landscape among EBV/HHV8 negative effusion-based lymphomas and EBV or HHV8 positive ones?

PhD/MD Margherita Vannucchi[1], Dr. Maria Chiara Siciliano[1], Dr. Roberto Boccacci[1], Dr. Domenico Ferrara[1], Dr. Massimo Granai[1], Prof. Lori Soma[6], Prof. Stephan Dhirnofer[7], Prof. Leticia Quintanilla-Martinez[8], Prof. Cristiana Bellan[4], Prof. Lorenzo Leoncini[3], Prof. Stefano Lazzi[3], Prof. Arianna Di Napoli[12]

[1] University of Siena, Department of Medical Biotechnology, Siena, Italy; [2] University of Siena, Department of Medical Biotechnology, Siena, Italy; [3] University of Siena, Department of Medical Biotechnology, Siena, Italy; [4] University of Siena, Department of Medical Biotechnology, Siena, Italy; [5] University of Siena, Department of Medical Biotechnology, Siena, Italy; [6] City of Hope Medical Center, Duarte, CA, Department of Pathology, City of Hope Medical Center, Duarte, CA, Duarte, USA; [7] University Hospital Basel, Basel, Switzerland., Institute for Pathology & Medical Genetics, Basel, Switzerland; [8] University Hospital Tübingen, Tübingen, Germany, Institute of Pathology and Neuropathology, Tuebingen, Germany; [9] University of Siena, Department of Medical Biotechnology, Siena, Italy; [10] University of Siena, Department of Medical Biotechnology, Siena, Italy; [11] University of Siena, Department of Medical Biotechnology, Siena, Italy; [12] Sapienza University, Sant'Andrea University Hospital, Rome, Italy, Department of Clinical and Molecular Medicine, Roma, Italy

Background

The WHO-HAEM5 recognizes a new entity called Fluid-overloaded large B cell lymphoma (FO-LBCL) defined as a B-cell neoplasm presenting as serous effusions without detectable tumor masses, often in patients with fluid overload states. The International Consensus Classification (ICC), instead, reported the same entity as provisional but using more rigid criteria and excluding HHV8 and EBV positive cases. Recently, based on the revision of cases submitted to the last EAHP 2022, the panel suggested that HHV8 negative effusion-based lymphoma should be separated into three different groups: EBV-negative B-cell phenotype effusion only, EBV positive B-cell phenotype effusion only, associated with immune dysregulation, and cases with plasmacytic/plasmablastic phenotype, mostly EBV positive[1]. They recommend to follow these criteria until new studies are available.

Principles/Methodology

The present study was designed to better evaluate by target NGS analysis, using a 72 genes panel (Sophia Genetics), the similarities and differences among body cavity effusion lymphomas. We collected a total number of 16 cases for which the material was available. In particular, 7 cases were

HHV8/EBV negative effusion lymphomas and 9 cases, that showed a similar clinical presentation, were HHV8-/EBV+ (2 case), HHV8+/EBV- (3 cases) and HHV8+/EBV+ 4 cases.

Results

EBV/HHV8 negative effusion-based lymphoma showed previously described genetic alterations in *MYD88*, *IRF4*, and *CREBBP*, *PIM1* and *PRDM1*, but revealed also recurrent mutations in in *TBLXR1, KLHL6, EP300*. Collectively, EBV or HHV8 positive ones showed significantly lower number of pathogenetic mutations. Among HHV8+ cases, we did not find *PIM1* mutations, but demonstrated two nonsense mutations in *MFHAS1*, a gene primarily implicated in inflammatory response, as a regulator of the Toll-like receptors TLR2 and TLR4 signaling pathways, and in 2 cases, amplification in *MYC*, *STAT6* and *ETV6*.

Conclusion

Based on these very preliminary results we suggest a dual mechanism of lymphomagenesis (mutational *vs* viral-driven), as already reported in other EBV positive lymphomas. NGS analysis on more cases is ongoing to better define the mutational status of EBVpositive only cases and the role of genetic alterations in immunity-related genes in HHV8 positive effusions.

EA4HP24-ABS-660

Clinicopathological and Genetic Features of Nodal Marginal Zone Lymphoma and Lymphoplasmacytic Lymphoma: A Korean Multicenter Study Focusing on Differential Diagnosis

Dr. Sojung Lim[2], Dr. Bogyeong Han[3], Dr. Jeemin Yim[4], Dr. Young Keun Song[1], Dr. Jiwon Koh[1], Dr. Cheol Lee[1], Prof. Hee Jeong Cha[5], Prof. Hye Ra Jung[6], Prof. Uiju Cho[7], Prof. Wook Youn Kim[8], Prof. Ji Eun Kim[4,1], Prof. Jin Ho Paik[9,1], Dr. Hong Seok Yun[10], Prof. Yoon Kyung Jeon[1,11]

[1] Seoul National University College of Medicine, Department of Pathology, Seoul, South Korea; [2] Seoul National University College of Medicine, Department of Forensic Medicine, Seoul, South Korea; [3] Samsung Medical Center, Department of Pathology, Seoul, South Korea; [4] Seoul Metropolitan Government Seoul National University Boramae Medical Center, Department of Pathology, Seoul, South Korea; [5] Ulsan University Hospital, University of Ulsan College of Medicine, Department of Pathology, Ulsan, South Korea; [6] Keimyung University Dongsan Hospital, Department of Pathology, Daegu, South Korea; [7] St. Vincent's Hospital, The Catholic University College of Medicine, Department of Pathology, Suwon, South Korea; [8] Konkuk University Medical Center, Konkuk University School of Medicine, Department of Pathology, Seoul, South Korea; [9] Seoul National University Bundang Hospital, Department of Pathology, Seongnam, South Korea; [10] Seoul National University Hospital, Department of Genomic Medicine, Seoul, South Korea; [11] Seoul National University, Cancer Research Institute, Seoul, South Korea

Background

Nodal marginal zone lymphoma (NMZL) can be difficult to diagnose due to the lack of specific immunohistochemical markers or mutations. Differentiation from lymphoplasmacytic lymphoma (LPL) can be particularly challenging in cases with prominent plasma cell differentiation and IgM paraproteinemia. Detecting *MYD88* L265P or *CXCR4* mutations, which is characteristic of LPL, can be helpful in such instances.

Principles/Methodology

Seventy-one nodal lymphomas originally diagnosed as NMZL were analyzed. They were histologically classified as NMZL vs. LPL when showing diffuse lymphoplasma cells infiltration with lack of nodularity and marginal zone differentiation, or when showing dilated sinuses with eosinophilic material, prominent plasma cell differentiation, or amyloid deposition; otherwise, they were histologically classified as NMZL. Targeted next-generation sequencing (NGS) for 121 lymphoma-related genes or whole exome sequencing was performed. Cases were finally diagnosed as LPL if clinicopathological and genetic features (including the presence of *MYD88* L265P) were compatible

Results

Among the 71 cases, 40 (56%) were histologically classified as NMZL, and 31 (44%) as NMZL vs. LPL. After NGS, 51 (72%) were finally diagnosed as NMZL, 12 (17%) as LPL, and 8 (11%) were unclassified due to failure of genetic testing. All LPLs, but 37% of NMZLs, were histologically classified NMZL vs. LPL (p <0.001). Patients with LPLs showed more common bone marrow involvement (89% in LPLs vs. 40% in NMZL), advanced stage 3-4 (100% vs. 55%), anemia (75% vs. 42%), serum IgM elevation (100% vs. 32%) and M-spike (100% vs. 46%) than those with NMZLs (all, p <0.05). Progression-free survival was significantly shorter in LPLs (p = 0.004).The top five most frequently mutated genes in NMZLs were *KMT2C* (29%), *KMT2D* (24%), *TNFAIP3* (18%), *CD79B* (12%) and *B2M* (12%), whereas the top three most frequently mutated genes in LPLs were *MYD88* L265P (100%), *KMT2C* (17%) and *CD79B* (17%). *CXCR4* mutation was uncommon and detected in only one NMZL. Copy number (CN) gains of genes located in chromosome 6p (*IRF4*, *PIM1*, and *CCND3*) and CN losses of genes in 6q (*PHIP*, *PRDM1*, *TNFAIP3*, and *ARID1B*) and 11q (*ATM* and *CHEK1*) were significantly more frequent in LPLs

Conclusion

Differentiating NMZL from LPL based on clinicopathological findings alone can be misleading. Since LPLs have a poorer prognosis and may be treated differently, genetic analysis is highly recommended for accurate diagnosis.

EA4HP24-ABS-663

B-cell receptor immunogenetics in thyroid lymphomas

Dr. Maria Myrsini Tzioni[1], Dr. FangTian Wu[1], Dr. Natsuko Watanabe[2], Sarah Guo[1], Dr. Ewelina Madej[1], Alice Brown[1], Prof. Deborah Dunn-Walters[3], Dr. Ayoma Attygalle[4], Dr. Andrew Wotherspoon[4], Prof. Ming-Qing Du[1]

[1] University of Cambridge, Department of Pathology, Cambridge, UK; [2] Ito Hospital, Department of Internal Medicine, Tokyo, Japan; [3] University of Surrey, Department of Bioscience and Medicine, Guildford, UK; [4] The Royal Marsden Hospital, Department of Histopathology, London, UK

Background

Primary thyroid lymphomas are commonly derived from a background of Hashimoto's thyroiditis, an autoimmune disease. Patients with Hashimoto's thyroiditis typically have autoantibodies against thyroglobulin and thyroid peroxidase. Chronic antigenic stimulation is thought to drive the evolution of autoreactive B-cells and their clonal expansion, hence increased risk of genetic changes and malignant transformation. The present study aimed to gain molecular insights of B-cell receptors (BCRs) in primary thyroid lymphomas by analysis of their rearranged immunoglobulin heavy chain *(IGH)* genes.

Principles/Methodology

A total of 41 primary thyroid lymphomas, including 27 extranodal marginal zone lymphoma of mucosa-associated lymphoid tissue (EMZL), 8 follicular lymphoma (FL) and 6 diffuse large B-cell lymphoma (DLBCL) were successfully investigated. DNA was extracted from tumour rich areas microdissected from FFPE tissue biopsies and used for PCR and sequencing analysis of the rearranged *IGH* genes by adopting the BIOMED-2 primers, followed by Illumina Miseq sequencing. *IGH* gene usage and somatic mutations were analysed using the IMGT/V-QUEST tools. Additionally, the lymphoma derived *IGH* sequences were compared with those of auto-antibodies from patients with Hashimoto's thyroiditis, and also rheumatoid factors.

Results

There was a significant overrepresentation of several *IGHV* genes including *IGHV1-46, IGHV3-49, IGHV3-53, IGHV4-61* and *IGHV4-34* in these primary thyroid lymphomas in comparison with normal IgM memory B-cells. All cases showed significant somatic mutations in their rearranged *IGHV* genes, ranging from 73% to 96% identity to their corresponding germlines. A high proportion (7/10=70%) of *IGHV3-23* rearrangements in thyroid lymphoma had a short CDR3 sequence with a high homology to those of thyroid autoantibodies from patients with Hashimoto's thyroiditis. Additionally, the *IGH* rearrangements in all *BCL2* translocation positive thyroid FL (n=3) and the majority of thyroid DLBCL (83%) acquired a new *N*-glycosylation site, which may enable expression of mannosylated BCR and hence chronic BCR stimulation by lectins present in the tumour microenvironment.

Conclusion

The biased *IGHV* usage together with the high homology of lymphoma derived *IGH* CDR3 sequence to known thyroid autoantibodies indicate the selection of autoreactive B-cells in thyroid lymphomagenesis. These data provide further evidence supporting a pathogenic role of chronic BCR stimulation in the development of primary thyroid lymphoma.

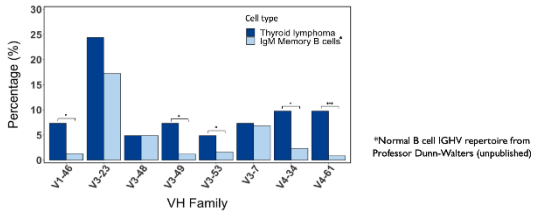

IGHV repertoire analysis
Distribution of *IGHV* gene usage in thyroid lymphoma and normal IgM B cells. Thyroid lymphomas showed bias *IGHV* usage in a number of *IGHV* genes including *IGHV1-46, IGHV3-49, IGHV3-53, IGHV4-61* and inately autoreactive *IGHV4-34*.

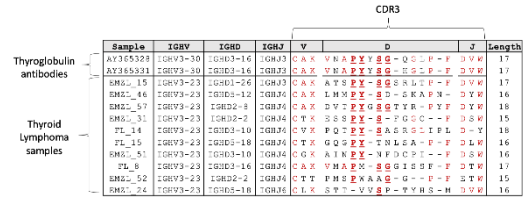

CDR3 analysis of thyroid lymphoma cohort
Complementary determining region (CDR3) analysis of *IGHV3-23* motif comparison to known anti-thyroglobulin *IGH* CDR3. *IGHV3-23* genes in thyroid lymphomas frequently harboured motifs in the D segment of CDR3 that have been identified in thyroglobulin antibodies of Hashimoto's thyroiditis patients.

EA4HP24-ABS-664

Primary thyroid B-cell lymphoma: molecular insights of its clonal evolution and relapse

Maria Myrsini Tzioni[1], Natsuko Watanabe[2], Fangtian Wu[1], Jasmine Makker[1], Ewelina Madej[1], Sarah Guo[1], Ayoma Attygalle[3], Andrew Wotherspoon[3], Ming-Qing Du[1]

[1] University of Cambridge, Department of Pathology, Cambridge, UK; [2] Ito Hospital, Department of Internal Medicine, Tokyo, Japan; [3] The Royal Marsden Hospital, Department of Histopathology, London, UK

Background

Primary thyroid lymphomas commonly arise from a background of Hashimoto's thyroiditis (HT) and comprise largely extranodal marginal zone lymphoma of mucosa-associated lymphoid tissue (EMZL) and diffuse large B-cell lymphoma (DLBCL), followed by follicular lymphoma (FL). Their development is a multistage process where dysregulated immune responses trigger autoreactive lymphoid cell infiltration and drive clonal B-cell evolution and malignant transformation. Although most thyroid lymphomas are amenable to treatments, local relapses occur. It remains to be investigated how the lymphoma clonally evolves and relapses at the molecular level.

Principles/Methodology

A total of 10 primary thyroid lymphoma cases were studied, including 5 cases with metachronous lymphomas [original lymphoma (EMZL=4, DLBCL=1) with local relapse occurring between 1-8 years later (EMZL=3, DLBCL=2)], 1 case of composite EMZL and EBV-positive DLBCL, and 4 cases of lymphoma (EMZL=3, FL=1) with prior or subsequent biopsy of HT. Genomic DNA from each specimen was investigated for mutations in 278 genes using the TWIST target enrichment protocol and the Illumina NextSeq platform. B-cell clonality was analysed using the BIOMED-2 PCR assay. *BCL2, BCL6* and *MYC* translocations were investigated by interphase FISH.

Results

In each of the 5 cases with metachronous lymphomas, the paired lesions shared common somatic variants and/or an identical *IG* gene rearrangement, confirming their clonal relationship. In 3 cases, distinct variants were also seen between the paired lymphomas, indicating divergent evolution from a clonally related common lymphoma precursor cells (CLP). In the remaining 2 cases, the relapsed lesion was a progression from the initial lymphoma. In the case with composite lymphoma, the EBV-positive DLBCL was transformed from EMZL.

Among the 4 cases with paired lymphoma and HT biopsies, 2 cases had common and distinct variants between the lymphoma and HT lesions, although few mutations were found in the latter. No somatic variants were detected in the HT lesion of the remaining 2 cases.

Conclusion

Relapsed thyroid lymphoma may progress from the original lymphoma or develop via divergent evolution from their clonally related CLP cell. This, together with the observation of somatic mutations in HT lesions, suggests that the lymphoma precursor clone may undergo perpetual evolution and acquire multiple malignant potential. These findings have important implications in the routine diagnosis and management of relapsed thyroid lymphoma.

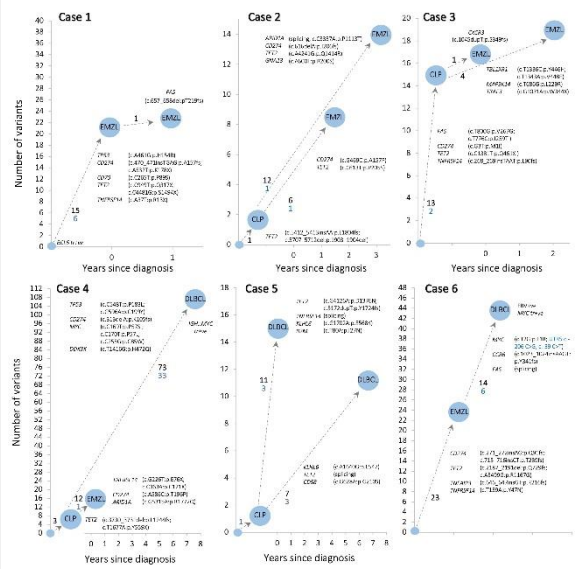

Phylogenetic Evolution of Metachronous and Composite Thyroid Lymphomas

Phylogenetic illustration of all metachronous thyroid lymphomas (cases 1-5) and the analysed composite lymphoma (case 6). The number of shared and distinct variants between paired lesions is indicated, along with the years between initial diagnosis and relapse for the metachronous lymphoma cases.